Cellobiose dehydrogenase on electrodes - an electrochemical biosensor for various analytes tunable by positive charges

Schulz, Christopher

2015

I was born in 1984 in Belzig, Germany. I grew up in Niemegk, a little town in the state of Brandenburg. When I was young, my favourite books were the "WAS IST WAS" series ("How and Why Wonder Books"), explaining things like sound, electricity, caves, the human body, trains, natural disasters and much more. Once, for Christmas my two brothers and I got a model railway. It was handmade with a lot of love by our grandparents and our parents. Every now and then some things broke, sometimes by chance and sometimes due to induced derailments. I especially enjoyed finding and fixing the electrical failures just by learning by doing.

Later on I discovered that the power transformer used to supply electricity to the model railway could be misused. I connected two pencil graphite rods to each pole and dipped them into the water filled leftover aluminium vessel usually housing tea candles. Interestingly, increasing the current at the power transformer, the water surrounding the graphite rods started to bubble. Without me and my family knowing it, I electrochemically produced pure oxygen and hydrogen. This time I did not blow up my room – that's another story. For this reason I was not allowed to get a chemistry set, which very much attracted me as well. So I got an electrical set instead and continued fiddling around but now with a bit more guidance by a book.

Then I came to secondary school with passionlessly taught electrical experiments and protocol writing killing all my childish enthusiasm. It was only during my bachelor and master studies in Wildau, Germany and Lund, Sweden that thanks to very engaged teachers I recovered my enthusiasm. So now, instead of only having the pencil graphite rods, I very much enjoy putting proteins onto them and send or take electrons to or from the protein. That is what this thesis is about. It is still amazing to me that one can do this, even after five years of research!

Printed by Media-Tryck, Lund University 2015

CHRISTOPHER SCHULZ

Cellobiose dehydrogenase on electrodes - an electrochemical biosensor for various analytes tunable by positive charges

LUND UNIVERSITY
Faculty of Science
Dept. of Chemistry
Biochemistry and Structural Biology
ISBN 978-91-7422-409-2

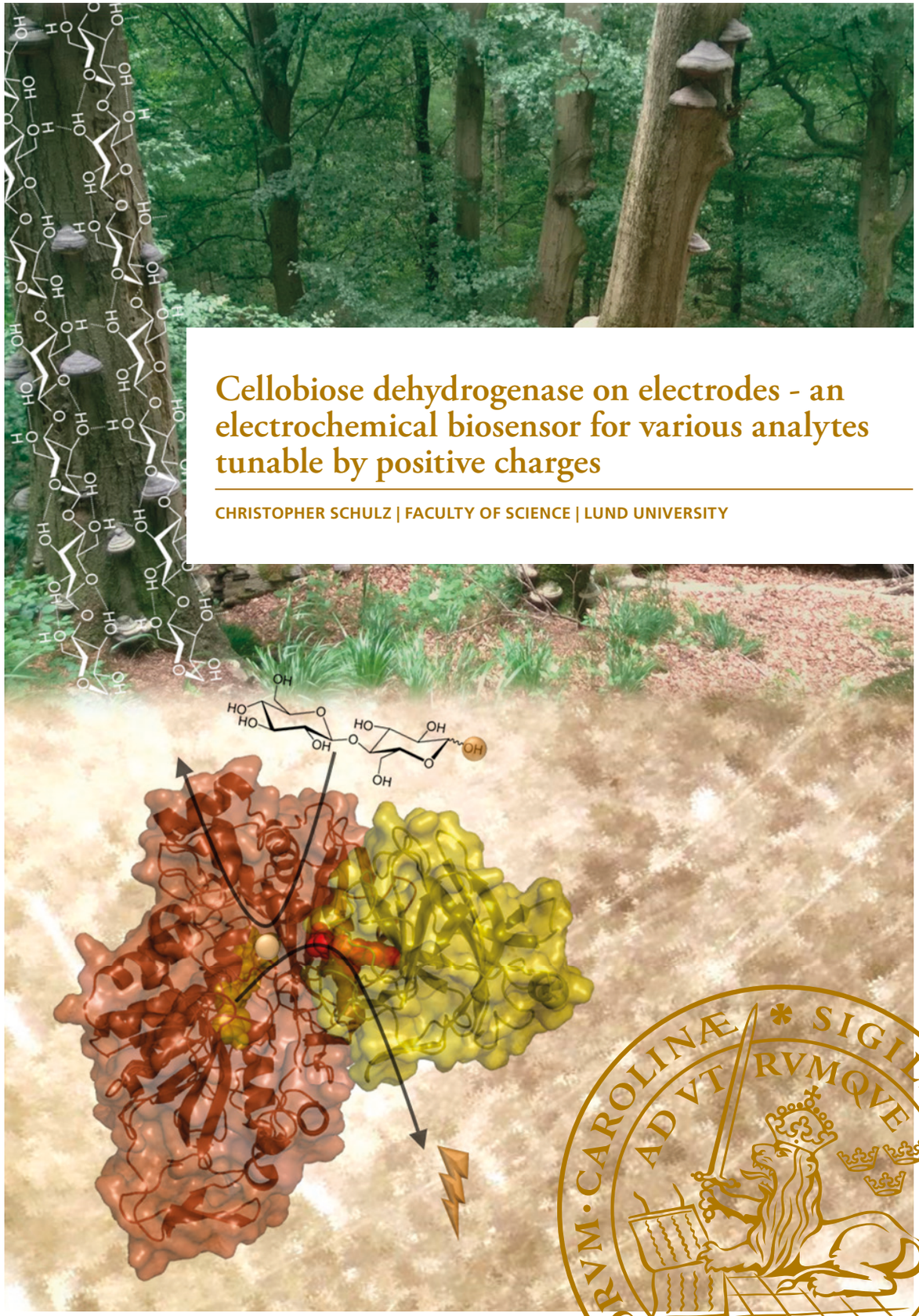

Cellobiose dehydrogenase on electrodes - an electrochemical biosensor for various analytes tunable by positive charges

CHRISTOPHER SCHULZ | FACULTY OF SCIENCE | LUND UNIVERSITY

Cellobiose dehydrogenase on electrodes - an electrochemical biosensor for various analytes tunable by positive charges

Christopher Schulz

LUNDS
UNIVERSITET

DOCTORAL DISSERTATION
by due permission of the Faculty of Science, Lund University, Sweden.

To be defended at Kemicentrum, lecture Hall A, Getingevägen 60 in Lund on Friday, the 25th of September 2015 at 13:15.

Faculty opponent

Dr. Elisabeth Lojou,

Centre national de la recherche scientifique (CNRS), Marseille, France

Organization:

Biochemistry and Structural Biology

Dept. of Chemistry,

Lund University

221 00 Lund, Sweden

Author: Christopher Schulz

Document name:

Doctoral Dissertation

Date of issue: September 2015

Sponsoring organization: European Commission ("Chebana", FP7-PEOPLE-2010-ITN-264772)

Title and subtitle: Cellobiose dehydrogenase on electrodes - an electrochemical biosensor for various analytes tunable by positive charges

Abstract

Cellobiose dehydrogenase (CDH) is a sugar oxidizing enzyme secreted by various species of wood degrading fungi to assist the process of wood degradation. It can oxidise analytically relevant sugars as cellobiose, lactose or glucose leading to a gain of two electrons per sugar molecule. CDH consists of a flavin containing catalytic domain (DH) and a haem containing electron mediating domain (CYT). CDH is able to directly communicate with electrode surfaces via the CYT delivering its gained electrons making it a suitable candidate for the construction of mediatorless biosensors and biofuel cell anodes being applicable either for the detection of sugars or for the generation of electricity out of sugar containing solutions.

In the present thesis the ability of CDH to electrically communicate with silver, gold and graphite electrode surfaces was investigated and employed mainly by electrochemical techniques as cyclic voltammetry and square wave voltammetry and was complemented by spectroscopic techniques.

The central finding is the ability of cations to enhance the electro-catalytic activity of CDH. Especially divalent cations as Ca^{2+} were found to increase the internal electron transfer (IET) from the DH to the electron mediating CYT leading to higher current outputs. The effect was ascribed to a yet unknown, transient, electrostatic interaction of Ca^{2+} with negative charges present on the DH and CYT decreasing their repulsion leading to a faster IET. Similar effects were observed for CDH electrodes premodified with immobilised polycations as polyethylenimine (PEI) or polydiallyldimethylammonium chloride (PDADMAC) or premodified with PEI covered gold nanoparticles. The polycations were found to enhance the enzyme load onto electrode surfaces by electrostatic interactions but were also suggested to increase the IET comparable to Ca^{2+}. The beneficial effect of cations and polycations on the electro-catalytic activity of CDH was employed to construct various biosensors to detect lactose, glucose, adenosine triphosphate and Ca^{2+} in various sensing schemes and analytes.

A further observation regarding the electrochemistry of CDH could be obtained only recently. We could finally prove unequivocally, after more than a decade of efforts, that a direct electronic communication is also possible between electrodes and the DH domain occurring at lower voltages than the DET with CYT. This potentially increases the voltage of biofuel cells and lowers the problematic oxidation of common interferents of biosensors pushing the commercial exploitation of CDH as a bioelectrocatalyst to a new level.

Key words: Cellobiose dehydrogenase, biosensor, cation, lactose, direct electron transfer, electrochemistry

Classification system and/or index terms (if any)

Supplementary bibliographical information | Language. English

ISSN and key title | ISBN: 978-91-7422-409-2

Recipient's notes | Number of pages: | Price

Security classification

Signature  Date 17.08.2015

Cellobiose dehydrogenase on electrodes - an electrochemical biosensor for various analytes tunable by positive charges

Christopher Schulz

LUNDS
UNIVERSITET

Front Cover, Upper part: Artwork derived from a picture of the cellobiose dehydrogenase producing fungus *Fomes fomentarius* growing on trees in the Söderåsen national park in Skåne, Sweden. Lower half: Crystal structure of cellobiose dehydrogenase from *Myriococcum thermophilum* with an artwork derived from a picture of a gold electrode surface in the background showing schematically substrate oxidation and electron transfer.

Supervisors:	Professor Lo Gorton (Lund University, Lund, Sweden) Professor Tautgirdas Ruzgas (Malmö University, Malmö, Sweden)
Examination Committee:	Professor Folke Tjerneld (Lund University, Lund, Sweden) Professor Sergey Shleev (Malmö University, Malmö, Sweden) Professor Elena E. Ferapontova (Aarhus University, Aarhus, Denmark)

Faculty of Science
Department of Chemistry
Center for Molecular Protein Science
ISBN 978-91-7422-409-2

Tryckt i Sverige av Media-Tryck, Lunds universitet
Lund 2015

Contents

Popular scientific summary

Enzymes are nanometer sized work units made up of proteins. Each of the thousands of the existing enzymes are produced by the cells of every living organism. They carry out certain functions as putting molecules together, e. g. connect sugar units to form cellulose for a growing tree or destroy molecules, e. g. degrade cellulose into its sugar units to eat and live on them. The latter is done by wood degrading fungi. One enzyme produced by such fungi and involved in the degradation process of wood is cellobiose dehydrogenase (CDH) – the main actor in this thesis, which is depicted on the cover of this thesis. The function of CDH is to substract electrons from cellobiose sugar units and deliver them to another enzyme, which makes highly reactive radicals with the help of those electrons and oxygen. Those oxygen radicals help to degrade the very stable wood. In this thesis CDH was put on electrode surfaces made of graphite and gold. Instead of delivering the electrons to the radical producing protein the electrons were delivered now to the electrode instead and the amount of gained electrons was counted by measuring the electrical current, which is nothing else than a flow of electrons. This is called a biosensor. Little amounts of sugar only give little currents and vice versa. So measuring the current one can calculate how much sugar is there. This is useful if one for example wants to know how much lactose is there in milk or how much sugar is there in blood. This is exactly how diabetric patients measure their blood sugar nowadays, only with a less fancy enzyme. In this thesis we found out that we can enhance the speed of how fast CDH can transport the electrons within the protein to the electrode by simply adding calcium ions, which are positively charged. That gave us more electric current so that we could measure sugar much more accurately. Also other positively charged compounds as long chained polymers gluing CDH to the electrode surface or to gold nanoparticles did the same effect. Our research showed that this effect depends on from which wood degrading fungus the enzyme was taken from, on the acidity of the measuring solution and on the calcium ion or polymer concentration. This is good to know because later sensors are supposed to only measure sugar units and should not be disturbed by calcium ions.

In this thesis we also managed to open up another electron transfer pathway from deep inside the enzyme to the electrode. This helped us to get the electrons with less of an applied force, which is beneficial for the CDH biosensor because the less force

we apply the smaller the chance of accidently substracting electrons from other molecules, which we don't want to measure, like vitamin C.

We also used a CDH biosensor to measure the release of lactose from ibuprofen tablets. Most tablets contain lactose as a filling material, only little of the tablet is the actual drug. So knowing how fast the lactose is released helps to understand how fast the tablet dissolves in the body.

Another biosensor was made to measure ATP, the common energy currency in your body. But this was only possible using two other enzymes working together with CDH in an assembly line like manner on the electrode surface.

The developed sensors are only prototypes – one cannot buy them. But in the near future CDH based biosensors are planned to be really used for measuring glucose in blood or lactose in dairy factories. And I look forward to participating in this.

List of publications

I. C. Schulz, R. Ludwig, P. O. Micheelsen, M. Silow, M. D. Toscano, L. Gorton, *Electrochem. Commun., 17 (2012) 71-74.*

Enhancement of enzymatic activity and catalytic current of cellobiose dehydrogenase by calcium ions.

II. R. Ludwig, R. Ortiz, C. Schulz, W. Harreither, C. Sygmund, L. Gorton, *Anal. Bioanal. Chem., 405 (2013) 3637–3658.*

Cellobiose dehydrogenase modified electrodes: advances by materials science and biochemical engineering.

III. P. Knöös, C. Schulz, L. Piculell, R. Ludwig L. Gorton, , M. Wahlgren, *Int. J. Pharm*., *468 (2014) 121-132.*

Quantifying the release of lactose from polymer matrix tablets with an amperometric biosensor utilizing cellobiose dehydrogenase.

IV. C. Schulz, R. Ludwig, L. Gorton, *Anal. Chem.*, *86 (2014) 4256-4263.*

Polyethylenimine as a promoter layer for the immobilization of cellobiose dehydrogenase from *Myriococcum thermophilum* on graphite electrodes.

V. A, Yarman, C. Schulz, C. Sygmund, R. Ludwig, L. Gorton, U. Wollenberger, F. W. Scheller, *Electroanalysis, 26 (2014) 2043 – 2048.*

Third generation ATP sensor with enzymatic analyte recycling.

VI. D. Kracher, K. Zahma, C. Schulz, C. Sygmund, L. Gorton, R. Ludwig, *FEBS J.*, *in press,* DOI: 10.1111/febs.13310.

Interdomain electron transfer in cellobiose dehydrogenase: modulation by pH and divalent cations

VII. P. Kielb, M. Sezer, S. Katz, F. Lopez, C. Schulz, L. Gorton, R. Ludwig, U. Wollenberger, I. Zebger, I. M. Weidinger, *ChemPhysChem, 16(9) (2015) 1960-1968*

Spectroscopic observation of calcium-induced reorientation of cellobiose dehydrogenase immobilized on electrodes and its effect on electrocatalytic activity.

VIII. M. Tavahodi, R. Ortiz, C. Schulz, A. Ekhtiari, R. Ludwig, B. Haghighi, L. Gorton, *Anal Chem, submitted*.

Direct electron transfer of cellobiose dehydrogenase on positively charged polyethyleneimine gold nanoparticles

IX. M. Tavahodi, A. Assarsson, C. Schulz, R. Ortiz, R. Ludwig, B. Haghighi, C. Cabaleiro-Lago, L. Gorton, *in manuscript.*

Interaction of polymer-coated gold nanoparticles with cellobiose dehydrogenase: The role of surface charges.

X. C. Schulz, R. Ludwig, L. Gorton, *in manuscript.*

Direct electron transfer from the FAD containing dehydrogenase domain of cellobiose dehydrogenase to electrodes.

XI. A. Cipri, C. Schulz, M. d. Valle, R. Ludwig, L Gorton, *in manuscript*

A novel bio-electronic tongue using cellobiose dehydrogenase from different origins to detect mixtures of various sugars and interfering analytes.

My contributions to the publications

I. L. Gorton and I designed the experiments. I conducted all experiments. All authors interpreted the experiments. I wrote the manuscript. All authors revised the manuscript.

II. I wrote parts of the review. All authors revised the manuscript.

III. I designed, conducted and interpreted all experiments related to the lactose biosensor and related to the removal procedure of SDS. I wrote the parts of the manuscript related to the lactose biosensor and the removal procedure of SDS. All authors revised the manuscript. The first authorship is shared by both, P. Knöös and me.

IV. I designed, conducted and interpreted all experiments. All authors took part in interpretation of the experiments. I wrote the manuscript. All authors revised the manuscript.

V. I designed, conducted and interpreted the initial experiments together with A. Yarman. I trained A. Yarman in conducting and interpreting the experiments. A. Yarman continued conducting experiments which were interpreted by A. Yarman, me and the co-authors. A. Yarman wrote the manuscript. All authors revised the manuscript.

VI. I designed and interpreted the initial experiments leading to this project. I took part in interpreting the experiments and revising the manuscript.

VII. I designed, conducted and interpreted the initial experiments related to the immobilisation procedure of CDH and the Ca^{2+} effect on the

electrochemistry of CDH. I trained F. Lopez in conducting and interpreting these experiments. Experimental work was continued by the co-authors. I took part in the interpretation of the experiments. All authors revised the manuscript.

VIII. I took part in designing, conducting and interpretation of the initial experiments. I took part in training M. Tavahodi in conducting and interpreting the experiments. M. Tavahodi continued conducting experiments which were interpreted by all co-authors including me. M. Tavahodi wrote the manuscript. All authors revised the manuscript.

IX. I took part in designing, conducting and interpretation of the initial experiments related to the electrochemistry part together with M. Tavahodi. I trained M. Tavahodi in conducting and interpreting the electrochemical experiments. M. Tavahodi continued conducting experiments which were interpreted by all co-authors including me. M. Tavahodi wrote the manuscript. All authors revised the manuscript.

X. I designed, conducted and interpreted all experiments. All co-authors took part in interpreting the experiments. I wrote the manuscript. All authors revised the manuscript.

XI. I designed, conducted and interpreted the experiments together with A. Cipri. I trained A Cipri in conducting and interpreting the experiments. I continued conducting experiments which were interpreted by both, me and A Cipri. A Cipri wrote the manuscript. All authors revised the manuscript. The first authorship will be shared by both, A. Cipri and me.

List of abbreviations

AA9	Auxillary active family 9
ADP	Adenosine diphosphate
ANN	Artificial neural network
ATP	Adenosine triphosphate
Cazy	Carbohydrate-active enzymes
CDH	Cellobiose dehydrogenase
COx	Cholesterol oxidase
Ct	*Corynascus thermophilus*
CYT	Cytochrome domain of CDH
Cyt c	Cytochrome *c*
DCIP	Dichlorindophenol
DET	Direct electron transfer
DH	Dehydrogenase domain of CDH
DOS	Density of states
EPR	Electron paramagnetic resonance
ET	Electron transfer
FAD	Flavin adenine dinucleotide (oxidised)
$FADH_2$	Flavin adenine dinucleotide (reduced)
FIA	Flow injection analysis
GDH	Glucose dehydrogenase
GOx	Glucose oxidase
Hi	*Humicola insolens*
HOPG	Highly oriented pyrolytic graphite

IEP	Isolelectric point
IET	Internal electron transfer
IR	Infrared
IRAS	Infrared absorption spectroscopy
IUPAC	International union of pure and applied chemistry
LPMO	Lytic polysaccharide monooxygenases
MET	Mediated electron transfer
Mt	*Myriococcum thermophilum*
NAD	Nicotinamide adenine dinucleotide
Nc	*Neurospora crassa*
Pc	*Phanerochaete chrysosporium*
PDADMAC	Polydiallyldimethylammonium chloride
PDH	Pyranose dehydrogenase
PEI	Polyethylenimine
PQQ	Pyrroloquinoline quinone
Ps	*Phanerochaete sordida*
RR	Resonance Raman
SAM	Self assembled monolayer
SAXS	Small angle x-ray scattering
SDS	Sodium dodecyl sulfate
SEIRA	Surface enhanced infrared absorption
SERR	Surface enhanced resonance Raman
SHE	Standard hydrogen electrode
SOx	Sulphite oxidase
St	*Sporotrichum thermophile*
Tv	*Trametes villosa*

1. Introduction

The present thesis is a result of a roughly five year period of experimental and theoretical work focused on the understanding and application of the sugar oxidising enzyme cellobiose dehydrogenase as a biocatalyst in electrochemical setups. The implications of the present work are broad. The present findings are not only of scientific interest but might also benefit medicinal and energy related aspects. The following chapters shall help you to understand why and how.

2. Enzymes and electrodes

2.1 Enzymes

The protein of interest here, CDH, is an enzyme. Enzymes are (mostly) proteins, which catalyse chemical reactions in biological systems. Proteins are polymers formed of up to 23 different amino acids. Each amino acid has different properties with respect to size, charge and hydrophilicity. The interactions of the amino acids within the protein polymer lead to a three dimensional structure. In an enzyme the three dimensional protein structure is evolutionary optimised in such a way that a catalytic site is formed into which the enzyme's substrate can specifically bind. The conversion from substrate to product is always exothermic, however, quite an activation energy leading to a transition state might be needed first to achieve the product state. Enzymes lower the activation energy necessary to achieve the product state by structurally facilitating the transition state of the substrate bound to the catalytic site. The facilitation of the transition state by enzymes can lead to enhancements of reaction rates of up to the factor of 10^{17} when compared to the uncatalysed reaction. In addition to the protein matrix many enzymes need cofactors in order to perform their catalytic activity. Those cofactors are either metal ions or small organic molecules. Depending on what kind of reaction is catalysed, enzymes can be classified into 6 classes: oxidoreductases, transferases, hydrolases, lyases, isomerases and ligases.[1] CDH belongs to the class of oxidoreductases and contains two cofactors, flavin adenine dinucleotide (FAD) and haem *b*.

A mathematical model describing the initial rate of reaction of an enzyme depending on the substrate concentration was developed by Michaelis and Menten leading to the so called Michaelis-Menten model. It describes a reaction, where one substrate molecule forms an enzyme-substrate complex with the enzyme, which is finally converted to one product molecule. A typical graph representing the dependence of the initial reaction speed V_0 of substrate conversion versus the investigated substrate concentration [S] is shown in Fig. 2.1.

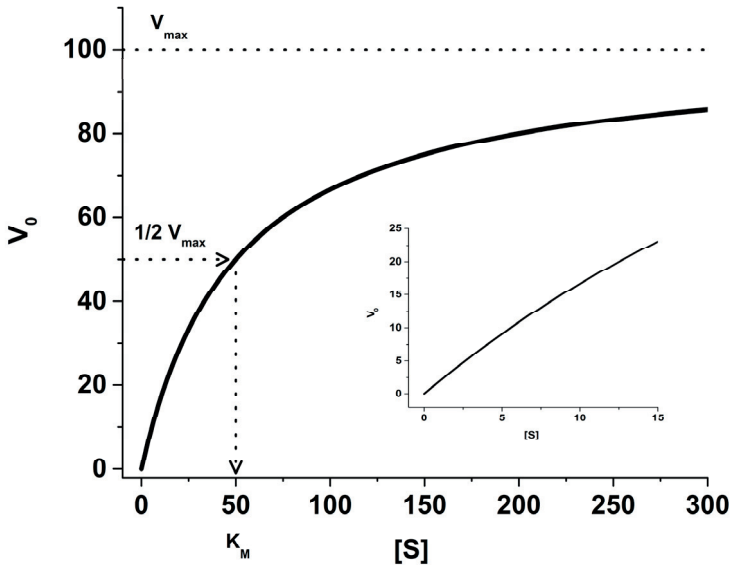

Fig 2.1 Michaelis Menten representation of an enzyme kinetics with a V_{max} of 100 and a K_m of 50 µM. The inset shows a zoom up of the substrate range, where there is a linear relationship between V_0 and [S].

Initially a linear dependence of V_0 on increasing [S] can be observed (see inset Fig. 2.1). However, increasing [S] further does not lead to equally increased V_0 values. At this point every new substrate molecule arriving at an active site of an enzyme is not converted into product immediately. Some active sites of some enzymes are still being occupied by substrate, since the rate of conversion into product is becoming rate limiting. Increasing the substrate concentration even further no increase in V_0 is observed since all enzymes are fully occupied with substrate working at its highest possible speed of conversion, V_{max}. The substrate concentration where half of the V_{max} value is reached is called the Michaelis constant (K_M) and reflects the state where 50% of all active sites of the enzyme molecules are occupied by substrate. The K_M is a characteristic parameter for an enzyme substrate pair and strongly depends on the experimental conditions as temperature and pH.[1]

To calculate how fast one single enzyme molecule converts one molecule of substrate into product V_{max} has to be divided (normalised) by the enzyme concentration. The result is a turnover number, k_{cat}, having the unit of frequency s^{-1}. Typical k_{cat} values range between 1 and 10^4 s^{-1}.

However, many enzymes do not physiologically work at a substrate saturation, where a V_{max} and its corresponding maximum turnover k_{cat} are reached. In biosensor applications enzymes as CDH are used to sense the analyte [S] far below the K_M ($[S] \leq 0.1 \times K_M$), where there is a linear relationship between analyte and V_0 (see inset Fig. 2.1) leading to turnover numbers below the theoretical achievable one. To calculate the efficiency of the enzymatic conversion at low substrate concentrations the calculated k_{cat} value can be divided by its K_M resulting in the catalytic efficiency k_{cat}/K_M with the unit s^{-1} M^{-1}. It is a measure for how good low substrate concentrations are converted and can help identify suitable substrates or analytes (when applied to the concept of biosensors as described below).

A few words should be mentioned about the enzyme of interest here, CDH. As described below, the catalytic mechanism of CDH is not represented by the simple Michaelis-Menten model having one substrate being converted into one product. As for all oxidoreductases, the catalytic mechanism of CDH is a ping-pong mechanism.[2] In CDH it involves two substrates (the oligosaccharide and the natural, oxidised electron acceptor protein LPMO) and two products (the oxidised substrate and the reduced electron acceptor protein LPMO). However, the Michaelis-Menten model is still sufficiently describing the enzyme kinetics of CDH and is consequently used in nearly all CDH related publications to calculate its kinetic parameters.

2.2 Electrodes

In the previous chapter a general introduction into enzymes and how they convert a substrate into a product was described. The present chapter will briefly introduce solid electrode materials and modifications, which were used to immobilise CDH to electrically communicate with it. Solid electrodes are of key interest in the field of electroanalytical chemistry. For a solid matter to be a suitable electrode it must have several characteristics as good conductivity, low double layer capacity, chemical and thermal stability, a suitable potential range, easy cleanability but it should also preferably be cheap and easy to handle, process and modify.[3] Many of the above factors strongly influence how fast electrons can be transferred between a redox enzyme as CDH and a solid electrode. The electrode materials mainly used in this thesis - graphite and gold – are quite different with respect to those parameters as highlighted below.

Electrode materials

Graphite electrodes

Carbon based electrodes are possibly the most widely used electrodes in the field of electroanalytical chemistry. Most common are materials based on sp^2 hybridised carbon atoms with a great variety of microstructures from highly ordered stacked graphene sheets in case of highly ordered pyrolytic graphite electrodes (HOPG) to pyrolysed, polymer like structures yielding interwoven ribbons in case of glassy carbon electrodes.[3-5] A schematic drawing of a graphene structure and how a graphene stack can be oriented is shown in Fig. 2.2. Certainly, any orientation is possible, but most pronounced are the basal plane and the edge plane. Basal plane electrodes have a graphene layer as their electrochemically active surface. Edge plane electrodes exhibit the edges of many graphene layers as their electrochemically active surface.

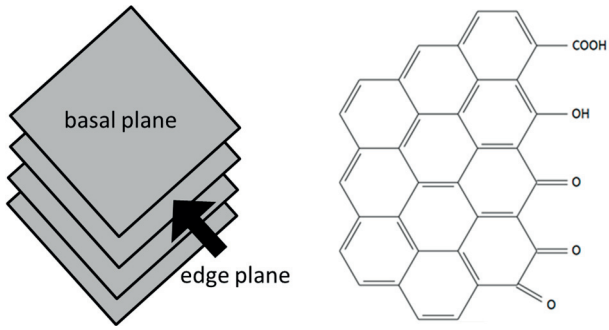

Fig. 2.2 Schematic representation of a carbon electrode showing the basal and the edge plane (left). Possibly oxygen functionalities present on the edge plane site are shown on the right.

The edge sites of graphene easily become oxidised already at ambient air and room temperature and can form various, oxygen based, functional groups as carbonyl, phenolic, hydroxyl, keto, quinone and carboxyl groups being then surface exposed (see Fig. 2.2).[3, 5] The same can happen to the basal plane when defect sites as steps occur as a result of damage due to wrong handling.[3] The introduced, oxygen based surface groups can tremendously affect the electrochemistry of redox compounds.[6-10] Rate constants for the oxidation and reduction are usually higher on oxidised edge plane sites, especially for redox probes reacting by an inner sphere electron transfer (see explanation below). It is suggested for oxidised edge plane site electrodes that a higher density of states (DOS) increases the probability of electron transfer[8] and that a mediation by carbonyl functionalities facilitates electron transfer[9]. The incorporation of oxygen leads to a more polar surface with better wettability, but also facilitates the adsorption of hydrophilic compounds.[3] The surface pk_a of graphite electrodes is acidic with values around pH 4 as found for glassy carbon electrodes.[11] Furthermore the oxygen functionalities can lead to interfering faradaic currents (from e. g. quinone oxidation/reduction)[3, 12-14] and can create additional pseudocapacitive charging currents on top of the normal charging current.[3, 15-16] Due to the rather uncontrolled oxidation, the reproducible preparation of graphite electrodes is usually worse than for noble metal electrodes as gold.[3, 5]

Carbon based electrodes can also be made of sp^3 hybridised carbon atoms leading to diamond like structures. However, doping (with most oftenly boron) is necessary to achieve conductivity and due to the high cost of diamond only thin film electrodes are manufactured.[17-19]

The electrode material used in this thesis is spectroscopic graphite. The name originates from its intended use in atomic spectroscopy, where it is applied for electrothermal atomisation of the sample.[20-21] It consists of graphene sheets, however, in a polycrystalline arrangement so that all kind of crystal orientations

including both planes, basal and edge plane sites are present on the electrode surface in a random mixture. Spectroscopic graphite is very pure (due to its intended use for spectroscopy), has a high porosity and a high charging current.[22] Also on spectroscopic graphite electrodes many oxygen functionalities are present on the electrode surface with the same implications as explained above. Easily detectable and very pronounced are the electrochemically active quinones[13, 23] which can also act as redox mediators for enzymes and catalyze the oxidation of e. g. NADH.[24]

Gold electrodes

Contrary to graphite electrodes, electrodes made of noble metals as gold, platinum or silver are a much more chemically defined. They can be used as bulk electrodes or as thin film electrodes where a thin gold layer of a few hundred nm thickness is deposited onto a suitable substrate.[3] Gold atoms form unit cells of face-centered cubic crystals leading to many possible crystal planes facing the electrode surface.[25] As described above for graphite also for gold the quality of the electrochemistry of redox active compounds depends on the crystal plane forming the electroactive surface.[26] Also the adsorption of anions as e. g. Cl^- onto the electrode surface of gold electrodes can alter the rate constants for the redox conversion of redox compounds. [3, 27] In this thesis polycrystalline gold electrodes containing a mixture of all possible crystal planes on the electrode surface have been used. The inert character of gold prevents the formation of heterogeneous, oxygen based surface groups as described for graphite leading to more defined surfaces with a lower charging current and a better reproducibility when comparing to spectroscopic graphite electrodes. Thus, for mechanistic studies of enzymes gold electrodes should rather be used (instead of graphite). However, the hydrophobic character of metal surfaces lead to a denaturation of most proteins when in direct contact with gold.[28] Thus gold electrodes have to be premodified when studying the electrochemistry of enzymes as described below.

Electrode modifications

In this thesis the electrochemistry of CDH was studied mainly on gold and graphite electrodes. When using graphite electrodes CDH can be directly immobilised onto the cleaned surface of the electrode resulting in a ready to use enzyme electrode. CDH and other proteins immobilise readily on graphite surfaces by physisorption.[29-30] However, chemisorption might also be possible through the reaction of surface aldehydes with amine residues of proteins forming spontaneously covalent bonds.[31] As described above gold electrodes have to be premodified since a direct enzyme contact would lead to irreversible denaturation of CDH.

Generally a premodification can increase the surface load of enzymes, the stability, the rate of electron transfer between enzyme and electrode and can help to control the orientation of the enzyme with respect to the electrode as discussed below in papers II, III, IV, VII, VIII and IX.

Even though graphite electrodes do not need to be premodified, various premodifications were applied for the above mentioned reasons.

One applied premodifier is the polycation polyethylenimine (PEI). It is a polymer based on amine groups connected by CH_2-CH_2 units as shown in Fig. 2.3. PEI exists as a linear or a branched polymer containing primary, secondary and tertiary amine functionalities.[32] In this thesis, branched PEI was used as a premodifier for graphite electrodes. At human physiological pH the polymer is positively charged[33-34] making it a suitable immobilization matrix for negatively charged proteins as shown by Lojou et al. for ferrodoxin and cytochrome c_3.[35] Also horseradish peroxidase[36], lactate oxidase[37], lactate dehydrogenase[38], glycerol dehydrogenase[39], glucose oxidase[40] and urease[41] were shown to be immobilised or stabilised via PEI. PEI readily adsorbs to graphite electrodes.[42] PEI is nonconductive, however, it does not necessarily prevent electron transfer between graphite electrodes and proteins as CDH as summarised below when discussing papers IV, VIII and IX.

Another investigated polycation used as electrode premodifier is the polymer polydiallyldimethylammonium chloride (PDADMAC, see Fig. 2.3). PDADMAC contains quaternary ammonium groups[43] making it positively charged independent on the solution pH enabling the immobilization of negatively charged proteins[44]. As PEI, PDADMAC is electrically insulating and readily binds to graphite and gold surfaces with a layer thickness of around 2 nm on gold.[45-49] Used as a thin immobilization matrix it enhances the enzyme load onto the electrode surface and does not prevent electron transfer between CDH and the electrode as shown below in papers III, V, and VII.

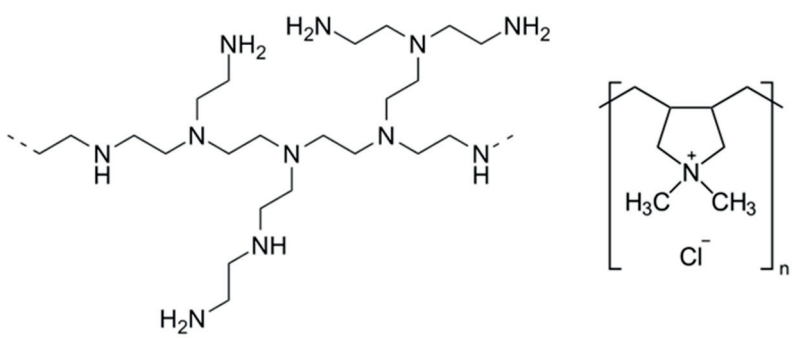

Fig 2.3 Structures of branched PEI (left) and PDADMAC (right).

The polycation PEI can also be used as a reducing and stabilizing agent for the formation of positively charged gold nanoparticles.[50] The effect of gold nanoparticles capped with PEI and other polyions on the electrochemistry of CDH was investigated in papers VIII and IX, where charged gold nanoparticles were used as a premodifier of spectroscopic graphite electrodes. Gold nanoparticles have the potential to increase the surface area of electrodes and enhance electron transfer kinetics[51-52] between enzymes and electrodes due to their size and electronic properties as reviewed in more detail in the following references[53-55].

A premodification procedure exclusively used for gold electrodes was the formation of self assembled monolayers of the alkanethiols mercaptohexanol and mercaptoundecanol forming densely packed layers protecting the enzyme from touching the electrode surface directly.[56] Alkanethiols have a sulphur head group, an alkane spacer of varying length and a variable functional headgroup with manifold applications as reviewed here.[28, 57-60] The sulphur headgroup chemisorbs to gold with a bond energy of around 40-50 kcal/mol[57-58, 61] being less strong than a covalent sulphur-sulphur bond (around 62 kcal/mol[61]) but stronger than any non-covalent interaction (1-5 kcal/mol[1]). The alkanethiols are not bound perpendicular to the surface but are slightly tilted from the axis perpendicular to the surface, depending on the alkanethiol by angles between 26[60] to 45 degrees[57-58]. The functional head group has a great influence on the quality of the electrochemistry of a redox compound or redox enzyme interacting with the SAM modified electrode. Common headgroups used for electrochemical investigations of CDH are hydroxyl, carboxyl, amino or quaternary amine functionalities leading to uncharged and depending on the pH negatively or positively charged surfaces respectively.[2, 62-63]

A further stabilisation of a formed alkanethiol layer comes from van der Waals interactions among the alkane spacers of each alkanethiol molecule. Longer spacers lead to more stable SAM layers, however, with the drawback of an increasing distance between electrode surface and solution.[58] The spacer length is of relevance when an electron transfer between electrode and enzyme as for CDH modified electrodes is of interest. The effect of spacer length on the electrochemistry of CDH is also highlighted in paper X and discussed below when addressing the Marcus theory.

2.3 Enzymes on electrodes - biosensors

Now as both entities of interest – enzymes and electrodes – have been introduced the present chapter will deal with the combination of both potentially leading to biosensors and biofuel cell anodes.

According to the IUPAC definition[64] a biosensor is "a device that uses specific biochemical reactions mediated by isolated enzymes, immunosystems, tissues, organelles or whole cells to detect chemical compounds usually by electrical, thermal or optical signals." The field of (electrochemical) biosensors is very versatile due to a vast amount of possible analytes, enzymes, electrodes and electrode modifications.[65-66] The present work focusses on the redox enzyme CDH catalysing the oxidation of analytically relevant sugars generating an electrical signal picked up by an electrode. The quantity of the electrical signal correlates with the analyte concentration and represents the analytical information obtained from a biosensor. The very first device which can be called a biosensor was developed by Clark in 1962. He used his previously developed oxygen sensitive electrode detecting oxygen by electrochemically reducing it to H_2O_2 and modified it with a membrane containing glucose oxidase (GOx). Glucose oxidase consumes oxygen during the oxidation of glucose leading to decreased O_2 concentrations with increasing glucose concentrations.[67] Such biosensors detecting changed levels of enzyme substrates or products are called first generation biosensors. If one of the enzyme's substrates or products is replaced by an artificial redox molecule being able to shuttle electrons between enzyme and electrode this type of electrochemical biosensor is called second generation biosensor. Most commercially available, electrochemical glucose biosensors used nowadays use such redox mediators, often in a polymeric, immobilised form as discussed below. One focus of this thesis lies in the complete avoidance of such mediators potentially leaching away, increasing the risk of false positive detection of interfering compounds and being potentially toxic.[68] The ability of an enzyme to directly communicate electrically with an electrode surface is called direct electron transfer (DET). As described below CDH is one of the few redox enzymes (and proteins) which are capable of DET.[65, 69-70] The first direct electric communication between a redox protein and an electrode was established in 1977 for cytochrome *c* independently by Yeh and Kuwana[71] and Eddowes and Hill[72]. Guo and Hill distinguished two classes of redox enzymes, intrinsic and extrinsic ones.[70] Extrinsic redox enzymes have built-in electron transfer pathways shuttling the electrons from the active site to the protein surface where they can be accepted by e. g. other proteins. For intrinsic redox enzymes the catalytic center is buried within the protein matrix and no built-in electron transfer pathway to the surface of the protein exist. The electron transfer from a donor to an acceptor molecule happens within the protein. For intrinsic redox enzymes a direct electric communication with an electrode surface might be hard to achieve due to

too high a distance between redox active site and the electrode surface.[69-70] According to this, CDH as a whole is an extrinsic redox enzyme. As described below, the CYT domain is the built-in electron transfer pathway to transfer the electrons from within the (intrinsic) catalytic DH domain closer to the protein surface. From there a DET with electrodes is much more facile than from within the protein due to distance reasons. The distance dependency of electron transfer from a donor to an acceptor molecule is described by a theory initially formulated by Marcus and is discussed below.

Electron transfer – between molecules, within proteins and to electrodes

A theory describing on a molecular level how an electron is transferred from a donor to an acceptor molecule was developed by Marcus in the 1950s[73-75]. Initially it was designed to describe the electron transfer from a donor to an acceptor molecule for homogenous, outer sphere reactions in a classical manner. Later on the theory was modified by quantum-mechanical terms[76] and was also extended to describe heterogeneous reactions at electrodes including applications to biology.[77-78] A homogeneous reaction is a reaction happening in the same phase (e. g. in solution), whereas a heterogeneous reaction occurs over phase boundaries (e. g. between a solution and a solid electrode). In outer sphere reactions donor and acceptor molecules do not form bonds or share ligands and do not lose their solvent shell when transferring an electron, whereas for inner sphere reactions the donor and acceptor molecule approach each other much closer so that bonds may be formed, ligands may be shared and parts of the solvent shell may be stripped for the reaction of transferring an electron.[64, 79]

The Marcus equation[75] *(Eq. 1)* describes the rate constant of electron transfer k_{et} being exponentially dependent on the standard free energy ΔG^0 of the reaction *(Eq. 2)*, whereas k_b is the Boltzmann constant and T the temperature.

$$k_{et} = A \exp(-\Delta G^* / k_b T) \qquad \text{(Eq. 1)}$$

$$\Delta G^* = \lambda/4 \, (1 + (\Delta G^0 / \lambda))^2 \qquad \text{(Eq. 2)}$$

The reorganization energy λ describes reorganizations processes (endothermic) regarding molecular vibrations and solvent molecules occurring in conjunction with an electron transfer, since for both, donor and acceptor the immediate molecular environment adapts to or compensates for the loss or gain of charge. A small λ

promotes a high rate of electron transfer. However, if the driving force of the reaction ΔG^0 (exothermic) exceeds the reorganization energy (endothermic), i. e. $\Delta G^0 > -\lambda$, a so called inverted region is observed, with a decreased rate of electron transfer in spite of an increased driving force. Too exothermic a reaction provides too much energy to be accepted in too short a time by the donor or acceptor molecules in vibrational modes leading to decreased values of k_{et}.[79-81]

The pre-exponential factor A summarises influences as the strength of the electronic coupling between donor and acceptor molecules. The electronic coupling decreases exponentially with the distance[82] leading to an exponential decrease in k_{et} with an increased distance between e.g. an electrode and an enzyme.[75, 78] The influence of the distance on the rate of electron transfer between the two domains of the enzyme CDH and to an electrode are discussed below in papers I, VI and VII.

The standard free energy ΔG^0 for the electron transfer from the donor to the acceptor molecule is inherent to the reaction itself. However, the introduction of a solid electrode as an electrode donor or acceptor allows the driving force for the electron transfer to be adjusted by varying the applied potential (*Eq*. 3).

$$\Delta G^0 = -n\,F\,E^0 \quad (Eq.\ 3)$$

A varied applied potential changes the standard electromotive force E^0 of the reaction, which can be converted to a standard free energy ΔG^0 (n is the amount of transferred electrons n and F the charge of one mole of electrons).[79] Thus by controlling the applied potential at an electrode one can control and study the rate of electron transfer k_{et} between e. g. an enzyme and an electrode. An inverted region as described above is not observed for metal or spectroscopic graphite electrodes. Those electrode materials always contain many electronic energy levels matching an energy level of the donor or acceptor molecule so that an electron transfer is not becoming limited by too high a driving force or applied potential.[56, 75, 77, 79]

The electron donor or acceptor molecules found in CDH are the redox active cofactors haem *b* and FAD. The haem *b* group is hexacoordinated by a methionine and a histidine residue and partly solvent exposed, whereas the FAD is completely buried within the protein shell.[2, 62, 83-84] Generally, the protein matrix surrounding the cofactors leads to an exclusion of solvent molecules and coordination of the cofactors with the protein matrix leads to a more constrained environment. Both factors decrease the reorganization energy λ connected to an electron transfer[78, 82, 85], thus increase the rate of electron transfer. The direct protein environment surrounding the redox active cofactor can also strongly modulate its redox potential with variations of several hundred of millivolts possible for the very same redox active group depending on its environment.[85] However, an additional protein matrix

also increases the distance between the cofactors thus decreasing the rate of electron transfer. In CDH the closest edge to edge distance between both cofactors involved in electron transfer is 9 Å[86] allowing for efficient electron transfer by electron tunneling.[82] Gray and Winkler put great effort in establishing tunneling timetables showing the dependence of tunneling speed on distance for various proteins and environments.[82, 85, 87] Electron tunneling occurs rather through the protein matrix than through water or solvent as it is faster.[82, 88] Tunneling is faster through β sheets than through α helices.[85] Aromatic amino acids were also shown to facilitate efficient electron tunneling.[88-90] This is also discussed below in paper X. If greater distances above 14-20 Å have to be overcome within proteins or protein complexes and functional units with a still sufficient rate of electron transfer, electron transfer occurs via electron hopping through several redox active groups arranged in an electron transfer chain by several electron tunneling steps[76, 82, 85, 88] as present in e. g. complex I and II in the respiratory chain[91] or in hydrogenases.[76]

3. Cellobiose dehydrogenase

3.1 *In vivo* function and electrochemical exploitation

Cellobiose dehydrogenase (CDH, EC number: 1.1.99.18) is an extracellular oxidoreductase secreted by wood degrading fungi.[2, 83] The degradation of wood supplies energy to the fungi living on it. Wood mainly consists of lignin, a phenol based polymer and the glucose based polymers hemicellulose and cellulose.[92] In the degradation process, the cellulose network of β-D-glucose molecules is hydrolysed into shorter polymers by endocellulases creating multiple reaction sites for exocellulases. Exocellulases hydrolyse cellulose into cellobiose and cellotriose units, consisting of two and three glucose molecules respectively.[93-94] The cellobi- and trioses are then hydrolysed by glycosidases into glucose monomers making them available for glycolysis. But cellobiose is also the natural substrate of CDH. CDH oxidises cellobiose to cellobionolactone and gains two electrons during this process. Those electrons are transferred by CDH to lytic polysaccharide monooxygenases (LPMOs, Cazy AA9) as found out recently.[95-99] The reduced LPMOs can further react with oxygen and form radicals, which attack the wood matrix to facilitate its decomposition and increase the supply of glucose for the fungus.

Instead of delivering the electrons to LPMOs, this thesis deals with how the electrons can be delivered to solid electrodes instead. This flow of electrons is nothing different than an electric current, which can be used as analytical information. The papers below deal with how a) we used different techniques to readout the current, b) we used different electrodes and electrode modifications to facilitate the electric communication with CDH and c) we used different variants of CDH to meet the analytical requirements of a certain problem. This allowed us to gain further insight into the mechanism of how CDH works and to construct analytical devices, called biosensors, to determine the level of relevant analytes as glucose, lactose, calcium chloride or adenosine triphosphate (ATP) in samples.

3.2 Structure of CDH

In 2015 Tan et al. succeeded to crystallise native, full length *Mt*CDH and determined its structure at 3.2 Å resolution (PDB accession code 4QI6). This was a major breakthrough since before 2015 only the crystal structures of the separately crystallised CYT[100] and DH[101] domains of *Pc*CDH were available impeding to elucidate the domain interaction hindering the understanding of the IET. In Fig. 3.1 the crystal structures of both domains of *Mt*CDH are shown. Depicted are the DH in dark grey, the CYT in light grey and the redox active cofactors FAD (yellow) and haem *b* (red). On the left a side view is shown, on the right a slightly tilted view to highlight the substrate tunnel leading to the FAD cofactor is shown. The structure of the linker region could not be sufficiently determined, however, the amino acid residues where the flexible linker attaches are highlighted with dotted circles.

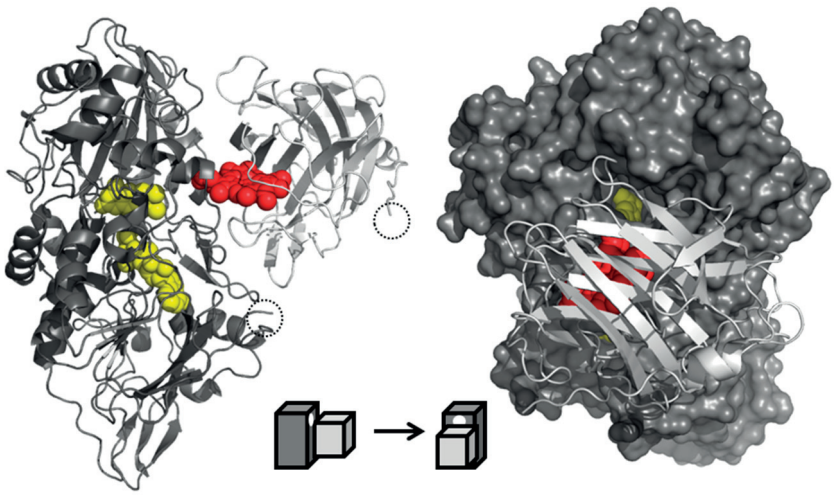

Fig. 3.1 Structure of the DH domain (dark grey) and the CYT domain (light grey) of *Mt*CDH. Highlighted are the FAD cofactor (yellow) and the haem b cofactor (red). Omitted is the linker region, but the locations of the amino acids connecting to the linker region are marked by dotted circles. On the left side a ribbon representation of both domains is shown. On the right side the DH is shown as a surface represenation instead to highlight the substrate tunnnel leading to the FAD cofactor (yellow). The boxes reflect the different view angles between the left and the right representation.

CDH is a monomeric enzyme composed of two domains. The catalytically active domain, DH is 589 residues long (in case of *Mt*CDH) and contains the redox active cofactor flavin adenine dinucleotide (FAD, see Fig. 3.1). The FAD cofactor is non-covalently bound to DH and is buried in the protein matrix. A funnel shaped tunnel

allows substrate and product to enter and leave the active site of DH.[86, 101] The active site has many similarities to glucose oxidase (GOx), pyranose dehydrogenase (PDH) and cholesterol oxidase (COx) as they all belong to the same family of glucose-methanol-choline oxidoreductases.[102-104] In CDH the natural substrate cellobiose can be easily modelled into the active site.[101] Two glucosyl binding sites were identified, one close to the flavin ring and one close to the substrate tunnel entrance.[86, 101] The presence of the two binding sites might explain the strong discrimination of CDH against glucose, which is a poor substrate as being a monosaccharide with only one possible glucosyl bond being formed.[101] During catalysis occurring at the *re* face of the isoalloxazine ring dehydrogenation of the substrate is believed to occur via a histidine acting as a base catalyst in a hydride transfer mechanism. An adjacent asparagine is believed to further support proton abstraction.[102, 105] The two protons and electrons gained from substrate oxidation fully reduce the FAD cofactor to $FADH_2$. *In-vivo* reoxidation of the $FADH_2$ occurs via the CYT, which is connected to the DH by a flexible linker region of around 20-30 amino acid length.[106] The linker can be cleaved by the proteolytic enzyme papain resulting in a separate CYT and a still catalytically active DH.[107-108] The DH of ascomycete CDHs can additionally contain a separate carbohydrate-binding module connected by a short long linker to the DH as found for *Mt*CDH[86] and *St*CDH[109] possibly allowing them to immobilise onto polysaccharides as cellulose.[103, 109]

The cytochrome domain, CYT, 208 residues long (in case of *Mt*CDH) is an electron mediating domain containing the redox active haem *b* moiety as prosthetic group (see Fig. 3.1). The haem *b* is hexacoordinated by a histidine and a methionine residue[100], which is a very rare arrangement.[110] The two propionate groups of the haem *b* are surface exposed (see Fig.1) and stretch into the active site pocket of the DH. One of the haem propionates interacts with a tryptophan and arginine residue of the DH as determined for *Mt*CDH.[86] These interactions are crucial for an efficient IET as shown by mutagenesis studies.[86] In a closed conformational state the CYT and DH domains are arranged with an edge-to-edge distance between haem *b* and FAD of 9 Å allowing for an efficient IET.[86] Even in the closed state there is the possibility for substrate and product to leave and enter the active site through an open path leading from the protein surface to the substrate tunnel.[86] Various conformational sub-states including open states, where both domains are not associated with each other were also observed for *Mt*CDH as determined by solution studies using small angle x-ray scattering (SAXS). An open state is crucial for the interaction of the CYT with the final electron acceptor protein, LPMO.[86]

A structurally similar enzyme, which helped us to understand CDH better is sulphite oxidase (SOx). It is part of the process to degrade the amino acids cysteine and methionine and catalyses the oxidation of sulphite to sulphate. It consists of a molybdenum containing, catalytic domain, Moco, which is connected by a flexible linker region to an electron mediating cytochrome *b5* domain.[111-112] The natural

electron acceptor is cyt *c*. Both domains are oppositely charged ensuring efficient IET. The study of the influence of the ionic strength[113] on the IET and on the domain flexibility and interaction[112] has triggered similar studies on CDH helping to understand its catalytic mechanism as shown in papers I, IV, VI and VII.

3.3 Classes of CDH and biochemical characteristics

CDH is produced and secreted by saprotrophic or phytopathogenic wood-degrading fungi produced by the phyla of Ascomycetes and Basidiomycetes. An example of a wood degrading, saprotrophic Basidiomycete, *Fomes fomentarius*, is shown in Fig. 3.2.

Figure 3.2 Fruit bodies of the Basidiomycete *Fomes fomentarius* (tinder fungus) growing on trees in the nationalpark Söderåsen in Scania, Sweden.

Based on their genetic sequences CDHs can be phylogenetically classified in class I and class II CDHs, coinciding with the genetic phyla of their producers Basidiomycetes and Ascomycetes respectively.[84] A third class of CDHs has been suggested based on CDH-like sequences found in genomes but no translated protein products were yet identified.[106, 114] The molecular weight ranges for all CDHs between 90 and 100 kDa with around 10% glycosylation.[2, 115] The experimentally determined isolelectric points (IEP) of CDH are below pH 5 for nearly all CDHs making them negatively charged under human physiological conditions.[2, 83-84] The IEP of the CYT is usually lower than the IEP of the DH.[84, 107, 116] The suggested

interface of the CYT and DH domains is also rich in charges, dominated by acidic amino acids as glutamic and aspartic acid as found for *Pc*CDH, *Mt*CDH and *Ct*CDH.[86, 116]

All CDHs have a rather broad substrate spectrum being able to oxidise lactose, cellobiose and other cellodextrins.[2, 83-84] A major difference between the CDH classes with respect to biosensing applications is the ability of class II CDHs to accept glucose as substrate, whereas class I, Basidiomycete CDHs do not. However, the catalytic efficiency of glucose oxidation is much lower compared to the natural substrate cellobiose.[84, 114, 117] Class I CDHs also have shorter sequences, usually pH optima in the acidic pH range whereas some class II CDHs also exhibit pH optima at neutral pH values[84, 114].

3.4 CDH - Electron acceptors and electron transfer

CDH contains two redox active cofactors, the FAD cofactor in the DH and the haem *b* cofactor in the CYT as depicted in Fig. 3.1. Both cofactors can interact with each other and with native and artificial electron acceptors as described below. In any case, the involved electrons move to the location with the higher, more positive redox potential.The redox potential of the FAD cofactor located in the DH was determined to be -132 mV vs. SHE at pH 7 and increased to 106 mV vs. SHE at pH 3 as determined spectrophotometrically for *Pc*CDH.[118] The change of the redox potential with the pH reflects protons being involved in the redox conversion of FAD. A slope of 59 mV/pH reflects the two proton/two electron conversion between FAD and $FADH_2$. For *Tv*CDH and *Ps*CDH comparable redox potentials for the FAD cofactor located in the DH between 82 mV and 108 mV vs. SHE were found as determined for the first time electrochemically as described in paper X. The redox potential of the CYT is more positive than the redox potential of the DH and was found to change between 130 mV at pH 7 to 190 mV at pH 3 as determined electrochemically for *Pc*CDH.[118-119]. The pH dependence of the redox potential of the CYT is confined to a narrower pH range and possibly reflects the titration of the haem *b* propionate groups by protons since the redox conversion of the haem *b* cofactor of the CYT itself involves no protons.[120-121] The redox potentials for the CYT of CDHs from different origins vary in a range between roughly 160 and 220 mV vs. SHE (at pH 3) as determined electrochemically (see paper X and reference[62]).

Comparing the redox potentials of both cofactors technically there is enough driving force to move electrons from the DH to the CYT via the IET step at any pH. However, the aspect of distance between electron donor and acceptor has to be kept in mind as described above by the Marcus theory and illustrated below in papers I,

VI and VII by a suggested, increased interdomain distance between CYT and DH with increased pH values limiting the IET.

In vivo electron transfer

As pointed out already above CDH can oxidise various substrates but it is also able to reduce various electron acceptors as described below. In the catalytic step, the oxidation of one molecule of cellobiose to cellobionolactone leads to a fully reduced FAD cofactor[122], $FADH_2$, located in the DH with two protons H^+ and two electrons e^- being gained from the oxidation of cellobiose as shown in *Eq. 4*.[2, 83, 122]

Catalytic step: FAD + cellobiose → $FADH_2$ + cellobionolactone (Eq. 4)

In vivo the fully reduced $FADH_2$ located in the DH is step-wise reoxidised by the CYT by two internal electron transfer steps (IET, see Fig 3.3) leading to a semiquinone radical, $FADH^{\bullet}$ after IET step one[118] (see *Eq. 5*) and the fully oxidised FAD after IET step 2 (see *Eq. 7*) and a reduced haem *b* moiety Fe^{2+} after each IET step.[2, 118, 122]

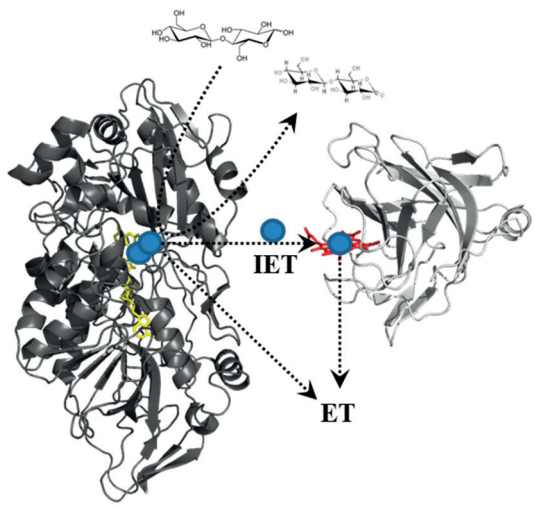

Fig. 3.3 Schematic representation of the possible electron electron transfer pathways of CDH after the oxidation of substrate leading to a reduced FAD cofactor (yellow). The electrons (blue) can be picked up directly from the DH domain (left, dark gray) via an electron transfer (ET) to electrodes, electron

mediators or oxygen. Alternatively the electrons can be transferred sequentially to the CYT (right, light grey) via an internal electron transfer step (IET) reducing the haem *b* cofactor (red) located in the CYT. From there, the electrons can be transferred to an electrode, to electron mediators or to the natural electron acceptor LPMOs.

After each IET step the haem *b* moiety in the CYT domain is reoxidised by its natural electron acceptor LPMO in a final, homogeneous ET step (see *Eq. 6* and *8*). LPMOs are copper dependent metalloenzymes that can be reduced amongst others by CDH. Reduced LPMOs are believed to insert oxygen into C-H bonds of cellulose leading to a break up of the carbohydrate units facilitating the decomposition of cellulose. [96-99, 123-124]

$$\textit{IET step 1: } FADH_2 + Fe^{3+} \rightarrow FADH^{\bullet} + Fe^{2+} \textit{ (Eq. 5)}$$

$$\textit{Final ET step1: } Fe^{2+} + LPMO_{ox} \rightarrow Fe^{3+} + LPMO_{red} \textit{ (Eq. 6)}$$

$$\textit{IET step 2: } FADH^{\bullet} + Fe^{3+} \rightarrow FAD + Fe^{2+} \textit{ (Eq. 7)}$$

$$\textit{Final ET step2: } Fe^{2+} + LPMO_{ox} \rightarrow Fe^{3+} + LPMO_{red} \textit{ (Eq. 8)}$$

To get an impression of the rate of the electron transfer steps (*Eq. 5-8*) an investigation on *Pc*CDH should be mentioned here.[118] The rate of the reduction (catalytic step, *Eq. 4*) of DH by cellobiose was found to exhibit a bell shaped dependence on the solution pH. It increased from 46 s^{-1} at pH 3 to a maximum of 71 s^{-1} at pH 4.5 and decreased to 30 s^{-1} at pH 6 and 15 s^{-1} at pH 7. The rate of IET (*Eq. 5* and *7*) had a similar, bell shaped dependence on the pH but with a maximum rate of reduction of 49 s^{-1} already at pH 3.5 and declined to 0.6 s^{-1} at pH 6. Most CDHs exhibit an acidic optimal pH for the IET. However, since the measurement of the IET is more advanced mostly the reduction rate of the artificial electron acceptor cyt *c* (described below) by the CYT is used as an estimation of the efficiency of the IET, since the IET is in most cases the rate limiting step.[2]

Homogeneous, *in vitro* electron transfer

In vitro the fully reduced $FADH_2$ located in the DH can be reoxidised by various artificial electron acceptors (see Fig. 3.3). The redox dye 2,6-dichlorophenol indophenol (DCIP) is effectively reduced by the DH and is widely used for

determining the activity of the DH photometrically in solution exhibiting a blue color when oxidised and no color when reduced.[125]

For electrochemical measurements also other, non-dye electron acceptors can be used. After being reduced by CDH the electron acceptors can be reoxidised at an electrode surface. They are also called mediators, since they mediate electrons between CDH and electrode. The main constraint when picking up charges from DH is not only a suitable redox potential (being higher than the redox potential of the FAD cofactor in the DH) but also their size, since the redox active cofactor FAD is buried in the protein shell of DH accessible only through a narrow substrate tunnel (see Fig. 3.1).[101] Charge plays an important role as well, since the entrance of the substrate tunnel is rich in acidic amino acid residues.[86, 116] Prominent mediators for DH are quinones and flexible, osmium containing redox polymers. Quinones as 1,4-benzoquinone are $2e^-/2H^+$ electron acceptors capable of fully oxidizing the reduced FAD cofactor in one step efficiently.[126] Quinones are efficient but freely diffusing mediators and potentially toxic, limiting them rather to *in vitro* applications. However, when attached to polymers, those drawbacks can be overcome.[127] Also toluidine blue based redox polymers were shown to efficiently mediate ET between CDH and electrodes.[128-130] More often applied in conjunction with CDH are osmium polymers. They are $1e^-$, non-H^+ electron acceptors which often contain a flexible polyvinyl based backbone and a redox active $Os^{2+/3+}$ group chelated by most oftenly bipyridyl groups when used in combination with CDH.[131-132] Redox polymers have the advantage to be immobilizable onto electrode surfaces preventing them from leaking away and to be tunable by synthesis with respect to flexibility, redox potential and solubility[131] making them applicable for *ex vitro* sensing applications. Contrary to quinones, which solely accept electrons only from the DH, osmium based redox polymers are able to accept electrons from both, DH and CYT.

Another potential electron acceptor is molecular oxygen being reduced to hydrogen peroxide by the DH of CDH.[133-136] In early days CDH was believed to be an oxidase and was also called cellobiose oxidase but was renamed to cellobiose dehydrogenase later.[2, 137] The rate of oxygen reduction by DH is rather low. For *Pc*CDH at pH 4 the rate of reduction of molecular oxygen by DH was found to be 0.15 s^{-1} [137]. Contrary, the rate of the IET from DH to CYT was found to be 300 times greater (45 s^{-1} at pH 4[118]) making CDH a dehydrogenase. Only at increased pH values the rate of the IET becomes slower (0.6 s^{-1} at pH 6[118]) and oxygen becomes a potential electron acceptor but only when compared to CYT as the competing electron acceptor. When more efficient DH electron acceptors as such as DCIP[132, 137], quinones[119, 132] or osmium redox polymers[132, 138-139] are used the reduction of molecular oxygen is negligible even at higher pHs.

A prominent 1 e^- acceptor picking up charges from the CYT of CDH (see Fig. 3.3) exclusively[126] is cyt *c*. It is too big in size to enter the DH and pick up charges from

there. Cyt *c* turns intensely red upon reduction by the CYT. Both DCIP and cyt *c* are widely used electron acceptors for determining the activity of CDH photometrically in solution.[125] Comparing the DCIP and cyt *c* activities of a certain CDH with each other, one gets information about the efficiency of the IET pathway.

Since the CYT of CDH is itself able to directly communicate with electrodes as discussed below, no great focus lies on the use of mediators shuttling electrons between CYT and electrode. However, as discussed above osmium redox polymers are electron mediators also for the CYT.

Heterogeneous, *in vitro* electron transfer

CDH can be immobilised onto various electrode surfaces and other electron transfer pathways than the natural ones are possible after the catalytic step. Technically the electrons could be directly donated from the DH to the electrode completely omitting the IET step (see *Eq. 9, 10* and Fig 3.3).

$$DET_1 \text{ from DH: } FADH_2 + Electrode \rightarrow FADH^{\bullet} + H^+ + Electrode + e^- \text{ (Eq. 9)}$$

$$DET_2 \text{ from DH: } FADH^{\bullet} + Electrode \rightarrow FAD + H^+ + Electrode + e^- \text{ (Eq. 10)}$$

Until recently the DET step from the DH was believed not to be feasible due to the deeply buried, hardly accessible FAD cofactor within the protein shell having too far a distance to an electrode surface. However, as discussed below and highlighted in paper X, today we are able to obtain DET from DH, however only at acidic pHs below pH 6 and only for class I CDHs.

Instead of a final ET step (see *Eq. 6* and *8*) the natural electron acceptor $LPMO_{ox}$ can also be replaced by an electrode and a heterogeneous, DET from CYT to the electrode can be accomplished (see *Eq. 11*) converting the haem *b* from its reduced state Fe^{2+} to its oxidised state Fe^{3+}.

$$DET_3: Fe^{2+} + Electrode \rightarrow Fe^{3+} + Electrode + e^- \text{ (Eq. 11)}$$

The capability of CDH for DET from CYT to electrodes was used manifold to construct biosensors and biofuel cell anodes and is described below.[2, 62]

Biosensors, biofuel cell anodes and other applications based on DET of CDH

The exploitation of the DET capabilities of CDH through the CYT are manifold. Summaries on the use of CDH modified electrodes as biofuel cell anodes and biosensors were given in the most recent reviews[2, 62] and in the papers discussed below.

As highlighted above, for biosensing applications a preferably low applied redox potential to avoid the oxidation of interfering species and high selectivity are desired. The complexity of CDH, having two domains, and having a rather broad substrate spectrum but also a rather broad spectrum of electron acceptors lead to many potential analytes to detect. Detecting substrates as analytes lead to a gain of electrons and an increase in catalytical current with increasing analyte concentration. Contrary, when detecting electron acceptors as analytes (in the presence of a suitable substrate) the catalytical currents decrease with increasing concentrations of electron acceptors.[140] Highly important analytes which are substrates for CDH are certainly the disaccharides lactose and cellobiose and the monosaccharide glucose.

The analytical detection of the natural substrate cellobiose with a CDH biosensor was used to measure the activity and elucidate the mechanism of cellulases depolymerizing cellulose in solution.[141]

Lactose is of interest with respect to a high amount of adults being intolerant to it with prevalences of around 2% in persons from Northern Europe to up to nearly 100% in persons from Asia.[142-143] Nearly all publications dealing with the electrochemistry of CDH use lactose as standard substrate, since for cellobiose substrate inhibition was observed (*Pc*CDH) when investigated electrochemically.[125, 144] The linear ranges for the detection of lactose in buffers depend on many factors as origin of CDH and the pH but range usually from one to a few hundred µM (in the absence of diffusion limitations of the substrate).[2, 62, 114] Amperometric biosensors based on *Tv*CDH and *Ps*CDH using its DET ability to detect lactose in real samples were shown to detect lactose in several dairy products as normal and lactose free milk with minimal requirements regarding sample preparation (only dilution necessary) achieving high recovery of lactose with minimal interference.[145-146] A combined biosensor using amperometry and thermometry based on *Pc*CDH and a mediated electron transfer approach with benzoquinone showed the ability to detect lactose reliably in real milk samples with only dilution being necessary as sample preparation step.[147] In 2012 a CDH based biosensor working in the DET mode was developed to detect lactose at-line in dairy processing plants.[148]

Lactose biosensors based on DET are also described in papers III and XI. Paper III describes a biosensor we have constructed to monitor the time dependent release of

lactose from ibuprofen containing tablets. Lactose is widely used as a filling material for tablets[149] but its release has not been studied intensely.[48] Investigating the time dependent release of lactose from tablets helps to understand and tune the kinetics of tablet decomposition and drug release. Paper XI describes a computational approach on how to detect lactose, glucose and $CaCl_2$ in parallel using the responses of three electrodes modified with different varieties of CDH applying artificial neural networks as described below.

Another interesting analyte is glucose. As mentioned above glucose can only be oxidised by ascomycete CDHs. The catalytic efficiencies of the oxidation of glucose are lower compared to the oxidation of the disaccharides lactose and cellobiose but are sufficient for the construction of glucose biosensors.[114, 150] Genetic modifications can further enhance the glucose turnover of CDH.[151] Glucose as analyte is certainly of main importance due to its relevance in the diabetes diagnostics. Diabetes has an estimated, global prevalence of around 9%.[152] Only a reliable measurement of the blood glucose level can enable an efficient treatment of the disease. There is a vast amount of commercially existing biosensors to detect glucose in blood samples electrochemically based on FAD dependent glucose oxidase[153-154] (GOx) and PQQ, FAD and NAD dependent glucose dehydrogenases[153-154] (GDH) but all rely on mediated electron transfer. CDH was shown to be a promising candidate for the construction of glucose biosensors, since it is advantageous due to its capability of DET at comparably low redox redox potentials[2, 62] minimizing the oxidation of interfering species.[154] GOx and all GDHs rely on electron mediators[154] making the sensor architecture more complex and increasing problems with interfering species[154]. A further advantage of CDH over GOx is its much lower or absent interference by oxygen[137]. Biosensors based on CDH were shown to detect glucose in buffers[155-157] with linear ranges of detection from 25 µM to 30 mM and in real samples as blood.[158]

However, in conjunction with glucose as substrate CDH was used more intensely in setups where it was the oxidising bioelement in biofuel cell anodes generating electricity in buffers[132, 159] and physiological solutions as blood[158, 160], serum[161], sweat[162], saliva[162] and tears[163]. Most of these fuel cell anodes were also tested with lactose as substrates, which usually lead to higher current densities, since it is the better substrate.[132, 158-161, 164] The developed fuel cells had open circuit voltages between 0.5 to 0.8 V and maximal power densities between 1 and 30 $\mu W/cm^2$ at operating voltages of around 0.5 V.

Next to the classical sensing approach using the substrate as the analyte also mediators can be detected by CDH based biosensors, however, in a mediated electron transfer approach with a higher required applied potential (compared to when using DET) and less selectivity compared to when detecting substrates as lactose, glucose or cellobiose. As described above quinones are potential electron

mediators shuttling the electrons from substrate oxidation from the DH to the electrode. Quinones and their reduced counterparts, phenols are used in industrial processes, occur as pollutants[165] or building units of lignin[92] or serve in biology as neurotransmitters or electron mediators in redox processes.[1, 166] The detection of quinones and phenols by CDH biosensors is reviewed in more detail in the following references.[2, 62]

Another interesting observation was made recently. Especially class II CDHs were found out to be tunable in their activity by cations, especially divalent cations as Ca^{2+}. Such cations were found to potentially increase the activity of CDH in solution and when immobilised on electrode surfaces. The relative increases in activity were highest for the Ascomycete *Mt*CDH[116, 167] and at neutral to basic pH[116]. The increases in activity were suggested to originate from a non-specific interaction of the divalent cations with both the negatively charged domains of CDH (at pHs above the isoelectric point).[167] An interaction of Ca^{2+} with negative surface residues present at the domain interfaces was supported experimentally and bioinformatically.[168] This interaction might decrease the interdomain distance between DH and CYT and might enhance the IET leading to increased activities when using cyt *c* as electron acceptor in solution and to increased catalytic currents when working in the DET mode with CDH immobilised on electrodes.[116, 167] This effect is described more in detail in papers I, IV, VI, VII and XI and is summarised below. The tunability of CDH by divalent cations is both – an advantage and a disadvantage. In various sugar sensing approaches Ca^{2+} clearly has to be seen as an interfering compound. However, this problem can be minimised by the choice of CDH to a CDH not or less tunable by divalent cations[116], by the use of permanently present polycations as a premodifier of electrode surface permanently mimicking the Ca^{2+} effect[14] (see paper IV) and by a smart sensing approach using sensor arrays of various CDHs responding differently to different analytes and interfering compounds (see paper XI). When used for biofuel cell anodes divalent cations are less of a problem, since they mostly increase the catalytic currents obtained by substrate oxidation potentially leading to beneficial, higher current densities. However, the positive effect of divalent cations on CDH was not yet applied to CDH modified biofuel cell anodes.

4. Techniques employed to investigate CDH

The electrochemical behaviour of CDH was mainly investigated by electrochemical techniques but was also complemented by spectroscopic techniques. The section below will only give a brief introduction into each technique, since they are described more in detail in the respective literature.

4.1 Electrochemical techniques

4.1.1Voltammetric techniques

In voltammetric techniques the potential applied at an electrode is changed and the resulting flow of current is detected. A widely used voltammetric technique to study the electrochemistry of redox proteins is cyclic voltammetry. In this method, the potential applied at an electrode is linearly varied over time (see Fig. 4.1, left) and the flowing current (see Fig. 4.1 right) is detected.

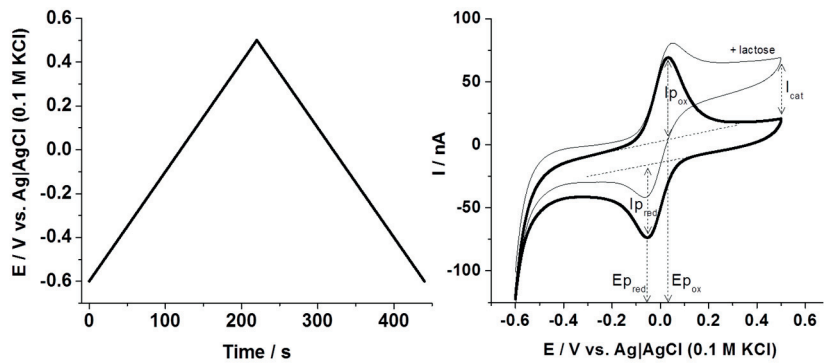

Fig. 4.1 (Left) Applied potential vs. time in a cyclic voltammetric scan with a scan rate of 5 mV/s. (Right) Corresponding cyclic voltammogram of *Mt*CDH entrapped under a dialysis membrane attached to a mercaptoundecanol modifed gold electrode at pH 3 in the absence (thick line) and in the presence of 5 mM lactose (thin line).

The speed with which the potential is changed over time can be varied between experiments. The protein of interest can be studied in solution or immobilised on the electrode surface. A typical voltammogram for CDH in solution is shown in Fig 4.1. The applied potential was changed from –600 to + 500 mV at a scan rate of 5 mV/s. Typical scan rates for the investigation of redox proteins lie in the range between 1 and 1000 mV/s. Scanning into the positive direction, a non-faradaic charging current is visible (dashed, nearly horizontal lines in Fig. 4.1, right). The charging current is attributed to the potential induced redistribution of charged ions at the electrode surface and across the electrochemical double layer. The charging current is present in the entire potential range and has to be substracted from the entire currents to obtain the faradaic currents originating from the redox conversion of the redox species of interest. Scanning further into the positive direction a positive, oxidative current from the oxidation of the haem *b* cofactor of CDH is visible. The current (corresponding to the transferred charges) increases with increasing potential (driving force) until at maximum current, the peak current Ip_{ox} has been reached at the oxidation peak potential Ep_{ox}. Increasing the applied potential any further leads to decreasing currents, since all CDH molecules in front of the electrode have been oxidised and diffusion of reduced (oxidizable) CDH present in the bulk to the electrode becomes rate limiting. This leads to a build-up of a diffusion layer in front of the electrode. On the reverse scan starting at the potential of +500 mV going to more negative potentials the oxidised CDH will be reduced with a maximum reduction current of Ip_{red} at the potential of Ep_{red}. As for the oxidation, more negative potentials than Ep_{red} lead to less reductive currents due to diffusion limitations of oxidised CDH to the electrode. When adding lactose to the measuring buffer (Fig. 4.1. right, thin line) there is no decrease in the oxidative currents at potentials more positive than Ep_{ox}, since electrons gained from the oxidation of lactose by CDH constantly reduce the haem *b* cofactor of CDH, which in turn can be constantly oxidised by the electrode.

The formal potential of the enzyme E^0_{pH3} corresponds to the midpoint potential calculated from the average of Ep_{ox} and Ep_{red} and is one key parameter in redox-protein electrochemistry. The parameters as peak positions, peak heights and shapes, ratio of peak heights, peak widths and scan rate dependencies can be used to discriminate surface confined processes from processes occurring in solution, to determine the reversibility of the redox conversion, to determine the amount of charges transferred or to calculate the speed of the redox conversion of the species of interest. The method of cyclic voltammetry was applied in papers II, V, VII, VIII, IX, X and XI. Detailed descriptions of this technique can be found here.[79, 169-170]

As mentioned above during the entire scan there is always a non-faradaic, charging current present. In the above case the signals of interest are high enough and well distinguishable from the charging current. If the faradaic currents originating from the electrochemistry of the enzyme molecules are too small or the charging currents

of the electrode is too big (as described above when using e. g. graphite electrodes instead of gold electrodes) one can use more sensitive techniques than cyclic voltammetry.

One of those techniques used in papers IV and X is called square wave voltammetry in which the applied potential is not changed linearly over time but rather step wise applying it for a longer time to let the charging current decay.[169, 171] Furthermore the current is not sampled immediately but slightly delayed. Both approaches enhance the visibility of the faradaic current originating from the redox conversion of the species of interest since the charging current decays much faster (over time) compared to the faradaic current. A detailed description of this technique can be found in the given references.[169, 171]

Both techniques, cyclic voltammetry and square wave voltammetry are commonly used as first methods to investigate the protein of interest to elucidate at which potentials the processes of interest are happening. This knowledge can then be applied when working at fixed potentials in case of e. g. amperometric biosensors as described below.

4.1.2 Chronoamperometry

In chronoamperometry a fixed potential is applied over time and the current response of the (modified) electrode is detected. The clear advantage here is the absence of the charging current after a very short time making the detection of the faradaic current much more sensitive compared to voltammetric techniques.[79] To identify the potential necessary to apply, typically a voltammetric experiment as described above can be used. In this thesis, amperometry was typically used in connection with a flow injection analysis (FIA) setup. The FIA setup consisted of a wall jet cell[172] housing the CDH modified electrode (and a reference and counter electrode) connected to a potentiostat, a six valve injector and a peristaltic pump. The pump constantly delivered buffer in a laminar flow to the modified electrode typically at flow rates of 0.5 ml/min. The injector was used to inject samples into the running buffer. Typically volumes of 50 µl of the substrate of CDH – e. g. lactose or glucose were injected into the running buffer and the resulting current due to substrate oxidation by the CDH modified electrode was detected. The advantage of a FIA setup compared to measuring in a batch is the easiness of change of the analyte of interest and the constant control of the background current. FIA in conjunction with amperometric detection was applied in papers I, III, IV, V, VIII and IX.

4.2 Spectroelectrochemical techniques

In combination with the above mentioned electrochemical techniques investigating the redox properties of the enzyme also spectroscopic techniques can be used. In principal any spectroscopic technique as e. g. UV, Vis, infrared (IR), Raman or resonance Raman (RR) or electron paramagnetic resonance spectroscopy (EPR) can be combined with electrochemistry spanning a wide range of investigated energies.[173] In paper VII, IR and RR absorption spectroscopy were applied in parallel to electrochemistry to investigate the influence of cations on CDH immobilised on gold and silver electrodes. IR and RR spectroscopy can give complementary information on the orientation, redox state, structural integrity and dynamics of the investigated enzyme, which otherwise cannot be obtained by electrochemical methods alone.[174]

Both IR and Raman spectroscopy detect molecular vibrations present in the molecule of interest. In infrared absorption spectroscopy (IRAS), light whose energy fits to a molecular vibration present in the molecule is adsorbed (e. g. by a chemical bond) and the absorption pattern dependent on the wavelength of the incident light can be seen as a fingerprint of the respective molecule.[175] Proteins are very complex in sequence and structure so that certainly not every possible bond can be readily identified or deduced from the obtained spectra – however, vibrational modes of secondary structures as α-helices or β-sheets can be identified and used to obtain information about the secondary structure of the protein of interest.[174, 176]

In Raman spectroscopy monochromatic light (e. g. a laser) is inelastically scattered and its energy (frequency) is shifted by the frequency of the molecular vibration (e. g. a chemical bond) it was interacting with.[175] In resonance Raman (RR) spectroscopy, the incident wavelength is chosen to be close to a molecular vibration of interest, e. g. of a certain chromophore (e. g. haem *b*) leading to an enhanced and more specific detection of the chromophore of interest.[175, 177] RR spectroscopy can readily detect the oxidation state of chromophores as haem *b*, the ligation and its orientation to the electrode surface and make it very suitable to study CDH.[174-175, 178-179]

The sensitivity of both techniques, IR and RR and be increased by factors of about 10^3 and 10^6 respectively by coupling the electric field of the incident light to a surface plasmon present on metal surfaces resulting in surface enhanced IRA (SEIRA) and surface enhanced RR (SERR) spectroscopy.[174-175] The use of metal surfaces as silver or gold not only has the advantage of surface enhancement of electric fields but also enables parallel, electrochemical studies of thin protein films as PDADMAC/CDH layers as shown in paper VII.[47] Any electrochemical technique can be applied in parallel. Commonly used are potential jump techniques to induce

changes of the redox state of the respective species while detecting spectroscopic changes in a time resolved manner.[179]

5. Summary of the research papers

In **paper II** (from 2013) the state of art of CDH used as a biocatalyst immobilised on electrode surfaces was summarised in a review. It focussed on increasing sensitivity, selectivity and current output by optimising the DET, MET and electrode surface by e. g. nanomaterials. Applications of CDH modified electrodes as biosensors for the detection of analytically relevant sugars as lactose and glucose and as biofuel cell anodes as a part of biofuel cells generating electricity from fuels (as e. g. blood) were addressed.

A topic which became a major part of this thesis is the influence of especially divalent cations on the catalytic activity of CDH. A first investigation highlighting the beneficial influence of NaCl on the turnover of *Pc*CDH was performed already in 2000 by Larsson et al.[180] Additional, 80 mM of NaCl present in the measuring buffer lead to increases in the catalytic currents of around 50%.

In **paper I** (from 2012) three CDHs, class I *Pc*CDH and class II *Mt*CDH and *Hi*CDH were investigated in solution and immobilised on graphite electrode surfaces with respect to their activity depending on additional KCl or $CaCl_2$ present in the measuring buffer. At optimal pH for DET, highest increases of catalytic activities in solution and catalytic currents when immobilised were found for class II *Mt*CDH and *Hi*CDH in the presence of 50 mM Ca^{2+}. The catalytic currents in the DET mode were increased about 5.1 times for *Mt*CDH and 4 times for *Hi*CDH, but only 2.4 times for *Pc*CDH. Monovalent K^+ present at comparable ionic strengths increased currents to a much less extend, pointing into a rather mechanistic involvement Ca^{2+}. Comparable increases were found for the enzyme's activities in solution when cyt *c* as electron acceptor was used monitoring also the IET pathway. The catalytic activity of the separately expressed DH domain of *Hi*CDH was not affected by additional monovalent or divalent cations. We suggested a Ca^{2+} induced complexation of negative charges present at the interfacing surfaces of both domains of CDH allowing a tighter interaction with an increased IET. In this context, CDHs as *Mt*CDH and *Hi*CDH with a less efficient IET pathway compared to *Pc*CDH are more tunable by additional Ca^{2+}.

The picture was further completed by an investigation published in 2015 in **paper VI** investigating the influence of $CaCl_2$ and KCl on *Mt*CDH and 10 further CDHs from different origins studied at different pHs in solution using spectroscopic kinetic techniques and docking studies. We confirmed that divalent cations as Ca^{2+} do tune

the IET pathway by a Ca^{2+} bridging effect decreasing electrostatic repulsions between the CYT and DH at elevated pHs. Neither the atomic radii nor the electronegativities of the chosen divalent cations were crucial. A weak, electrostatic, transient interaction between CDH and divalent cations was found. The Ca^{2+} induced increases of the IET were, as observed before, highest for class II *Mt*CDH. Docking studies using homology models based on structural data of *Pc*CDH revealed that the interfacing surfaces of the CYT and DH domains of CDH contain many negatively charged amino acid residues forming clusters. Especially for *Mt*CDH those clusters contained more negatively charged residues compared to class II *Ct*CDH and class I *Pc*CDH providing more interacting sites for Ca^{2+} possibly explaining why *Mt*CDH is most tunable by positive charges. The haem *b* propionate groups present on the CYT were found to be involved in the Ca^{2+} bridging. When studying the Ca^{2+} dependent behaviour of CDH using various electron acceptors as cyt *c*, ferrocenium, ferricyanide, DCIP or benzoquinone picking up charges from the DH and/or the CYT we found that the charge of the electron acceptor itself is crucial as well and can complicate the elucidation of the Ca^{2+} dependent behavior of CDH.

To mimic the beneficial effect of Ca^{2+} on CDH the influence of the polycation PEI used as a premodifier for graphite electrode surfaces on the electrochemistry of *Mt*CDH was investigated in **paper IV** (from 2014). Branched PEI contains primary, secondary and tertiary amino groups making it positively charged at human physiological pH and below. PEI was found to tremendously increase the catalytic currents obtained from lactose oxidation by *Mt*CDH in the DET mode, with increases of around 9 times at pH 5.5 (optimal pH for DET) and 150 times at pH 8 (pH optimum of the DH domain) compared to electrodes lacking the PEI layer. Furthermore the pH optimum for lactose oxidation was shifted from pH 5.5 to pH 8 when PEI was used as a premodifier. Since the pH optimum of the catalytically active DH domain is in the alkaline pH region but the IET is optimal at acidic pHs we concluded that PEI increased the rate limiting IET from the DH to the CYT allowing to exploit the inherently higher catalytic activity of the DH to a greater extend. The beneficial effect of Ca^{2+} on the catalytic currents of *Mt*CDH was observed, but decreased when PEI was used as premodifier layer, indicating that PEI partially mimics the Ca^{2+} bridging effect. PEI was also suggested to enhance the enzyme loading onto the electrode due to a tight electrostatic binding of negatively charged CDH molecules to the polycation. However, we also observed that the non-covalently bound FAD cofactor from the DH can leak out and become immobilised and oxidised to an unknown, redox active molecule. This process was facilitated by the PEI layer. The unknown, redox active molecule was shown to additionally mediate the electron transfer between CDH and the electrode and was partially responsible for the observed, increased catalytic currents at higher applied potentials.

In **paper IX (from 2015)** graphite electrodes were premodified with citrate capped gold nanoparticles optionally modified with positively and negatively charged polyions on their surface and their influence on the electrocatalytic response of negatively charged *Mt*CDH (above the pI of 3.8) was investigated. Only in the presence of the nanoparticles clear redox waves from the redox conversion of the CYT were observable using cyclic voltammetry. Nanoparticles covered with the positively charged PEI were shown to enhance the catalytic currents from lactose oxidation by *Mt*CDH by up to 66 times and shift the pH optimum for DET from pH 5.5 to pH 8 comparable to the findings of paper IV. Also here PEI was suggested to increase the surface load of *Mt*CDH by strong electrostatic interactions but also to increase the rate limiting IET mimicing the Ca^{2+} bridging effect as described in papers I, IV and VI.

Surprisingly also on negatively charged, poly(sodium-4-styrenesulphonate) or citrate covered nanoparticles increases of the catalytic currents were observed, however only by up to 3.7 times compared to electrodes lacking the nanoparticles indicating not only electrostatic interactions being responsible for the immobilization of *Mt*CDH onto the nanoparticles. In accordance with papers I, IV and VI, the addition of Ca^{2+} increased the catalytic currents further and was most pronounced when negatively charged nanoparticles were used as premodifier. The beneficial effect of the nanoparticles were also observed when the activity of *Mt*CDH was investigated in solution. In addition to the expected effect of the positively charged, PEI coated nanoparticles on the IET of *Mt*CDH also further, activity enhancing effects were seen for all nanoparticles and we suggested them to arise from the interactions of the soluble electron acceptors cytochrome *c*, DCIP and *Mt*CDH width the nanoparticles forming stable charge transfer complexes.

In **paper VIII** (from 2015) we used the polycation PEI as a reducing agent to form gold nanoparticles. The PEI capped nanoparticles had a diameter of 9 nm and a PEI shell thickness around of 2-3 nm. The PEI capped nanoparticles were used to increase the electrochemically active surface area of gold electrodes by around 30 times. We could successfully immobilise negatively charged *Ps*CDH onto the nanoparticle modified gold electrodes exhibiting clear and fast electrochemistry with a heterogeneous electron transfer constant of around 40 s^{-1}. The *Ps*CDH modified electrode was suggested to be used as a lactose biosensor exhibiting a linear measuring range between 1-100 µM for lactose and a high stability with signal decreases of only 5% in 24 h of continuous measurement.

Another polycation, PDADMAC was used in **paper VII** (from 2015) to immobilise CDH onto gold and silver electrodes and investigate the spectroelectrochemical response in the presence and in the absence of Ca^{2+}. PDADMAC contains quaternary ammonium groups being positively charged independently on the pH and electrostatically binds CDH. We successfully developed a procedure to

immobilise *Mt*CDH onto PDADMAC modified gold and silver electrodes. Using cyclic voltammetry, SEIRA and SERR spectroscopy we could prove that *Mt*CDH is immobilised, present in its native form and catalytically active. In the presence of Ca^{2+} we observed a negative shift of the onset of the catalytic current, whereas the midpoint potential of the CYT domain was shifted to more positive potentials in the presence of Ca^{2+} possibly due to binding of Ca^{2+} to propionate groups as also suggested in paper IV. The Ca^{2+} induced shifts resulted in apparent catalytic currents already visible below the midpoint potential of the CYT domain. From SERRS and SEIRA we concluded a slight reorientation of the CYT domain with respect to the electrode surface and possibly a closer conformation between CYT and DH. The Ca^{2+} induced reorientation and observed negative shifts of catalytic currents and positive shifts of the midpoint potential of the CYT made us suggest an alternative electron transfer pathway leading from the DH directly to the electrode, stabilised by the CYT, which serves as an anchor for the enzyme to the electrode surface.

More clear results proving a DET from the DH are presented in **paper X (**from 2015). Using cyclic voltammetry and mercaptoundecanol modified gold electrodes we could prove unequivocally that DET from the DH domain of CDH is possible. In addition to the established electrochemistry of CDH via the CYT domain we observed clear redox waves for the FAD located in the DH domain in the absence of substrate and a coinciding catalytic wave in the presence of substrate starting at the oxidation peak potential of the DH domain. The DET from DH was only possible at acidic pHs below pH 5 and only for the tested class I *Tv*CDH and *Ps*CDH but not for the tested class II *Ct*CDH and *Mt*CDH. We hypothesised that the amino acid composition around the substrate tunnel of the DH consisting of aromatic and acidic amino acid may be involved in the pH dependent DET from the DH.

The above described papers rather dealt with basic bioelectrochemical descriptions and findings regarding CDH. The following papers rather describe applications of CDH biosensors.

In **paper III** (from 2014) a graphite electrode modified with the polycation PDADMAC and *Ct*CDH was used as a lactose biosensor to detect lactose in samples obtained from dissolution experiments of ibuprofen containing tablets. Lactose is a common filling material for tablets and the study of its time dependent release gives information about the dissolution behavior of the tablet. As SDS was used for some dissolution experiments of tablets to mimic bile salts being present in the human intestine, a sample preparation procedure had to be established first to remove SDS from the samples, since it denaturises enzymes as CDH. A fast and easy procedure was developed using the polycation PEI to precipitate the negatively charged SDS. The formed precipitate readily adsorbed to the wall of the sample vial and the lactose containing supernatant could easily be measured without further treatment. The established lactose biosensor had a linear measuring range between 10 and 110 µM

lactose and was able to recover lactose in the real samples with a maximum error of 13%. The release profiles of lactose (hydrophilic) over time and in different media were compared to the release profiles of the drug ibuprofen (hydrophobic) released from the same tablet leading to a deeper understanding into the dissolution behavior of the tablet.

In **paper V** (from 2014) CDH was involved in an enzyme cascade to detect ATP at µmolar concentrations. A three enzyme biosensor operating in the DET mode containing the three enzymes hexokinase, pyruvate kinase and CDH was developed using the polycation PDADMAC as electrode premodifier. In the catalytic process hexokinase phosphorylated glucose, a process depending on the concentration of ATP present. A glucose mutant of *Ct*CDH with enhanced glucose turnover was used in parallel to compete with hexokinase for oxidizing glucose leading to a catalytic current, which decreased the more ATP was present. Pyruvate kinase was used to recycle ADP back to ATP using phosphoenol pyruvate as substrate so that the recycled ATP can enter the signaling cascade more often leading to an amplification of the ATP signal 220 fold. The biosensor was shown to operate at low potentials of 0 mV vs. Ag|AgCl avoiding false positive signals arising from the oxidation of common interferents in a biological fluid as ascorbic acid, dopamine, serotonin or L-DOPA.

Paper XI (from 2015) deals with the influence of divalent cations as Ca^{2+} on the activity of CDH being not only beneficial but also problematic behaving as an interfering compound when a CDH based biosensor is used for measuring sugar. In paper XI three different CDHs, *Mt*CDH, *Nc*CDH and *Ct*CDHC291Y (mutant of *Ct*CDH with enhanced glucose turnover) having different affinities for the analytes lactose, glucose and Ca^{2+} were used to construct an electrode tongue consisting of three electrodes to discriminate the three analytes. An electronic tongue consists of an array of rather unspecific, cross-responding sensors. However, the deconvolution of all cross-responses by mathematical treatment can enable a specific analyte determination. The cyclic voltammetric responses of gold electrodes modified with mercaptohexanol, CDH and a dialysis membrane to solutions containing the three analytes lactose, glucose and Ca^{2+} were analysed by an Artificial Neural Network (ANN). An ANN is a network of artificial neurons implemented in a software, which mimics biological neurons. After training (similar to calibrating) the ANN it is able to convert multidimensional input signals (as measurement data) into a desired output information (as concentration of analyte x, y or z). The ANN was used to discriminate the analytes lactose, glucose and Ca^{2+} in samples containing all three analytes at varying concentrations up to 500 µM, 260 µM and 10 mM respectively. Testing the trained network with samples of known compositions yielded deviations between true and measured concentrations of average only ±6.9% for lactose, ±4.8% for Ca^{2+} and ±12.3% for glucose. The electronic tongue

operated in the DET mode minimizing the oxidation of potential interferents and was suggested to e. g. detect levels of lactose, glucose and Ca^{2+} in milk.

Acknowledgements

This work is the scientific summary of my past five years of work. I have not done this entirely alone. My greatest acknowledgements go to Lo Gorton. It was a real joy working in your always international research group. Of course I very much thank you for all your scientific input. But at least as important were you as a person. I very much appreciated your easy going way of life, our discussions about music, language, having a few (or more) beers or just having a little gossip. Very much in hand with this goes my delight of having been a colleague and friend to all the permanent lab people as Roberto, Masha, Kamrul, Nadeem and Federico. But many thanks also to the numerous visiting students, PostDocs, Doctors and Professors coming from all over the world with all kind of knowledge, personalities and peculiarities – you guys always brought life to the lab!

I very much appreciated the collaborations with colleagues from BOKU University in Vienna, Austria, Potsdam University in Potsdam, Germany and University College Cork in Cork, Ireland. Staying at your places, discussing with you and getting new fresh insights were great!

Many thanks go to all the people from the department who made this place of work very enjoyable. Special thanks go to Gert and Magnus for being very helpful fixing anything broken and to Adine for handling orders and taking care of all those little things you usually don't notice.

Of course, I was not only working but also had a great time in Lund being entertained by a lot of people who became friends by now. As for many of us, it all started in Möllevångsvägen, moved to the great "German Embassy" and finally spread to little Rezidenturas scattered all over Lund. I very much enjoyed all the days and evenings and nights and mornings we had together discussing, dancing, making music, eating (only haute cuisine – thanks to Tobi), drinking lot of foreign delicacies, watching movies (*mostly* appreciable stuff – thanks to Mike), listening to music or to each other's complaints about supervisors, colleagues and other evil people. Dear Friends (Tobi, Sonja, Tim, Nata, Alexander, Basti, Irem, Janina, Juandiego, Mike, Miguel, Charlotte, Uta, Robert, Goran, Alak, Nawar, Eva, Hans and many more), it was a great time and I will miss it a lot!

I want to especially thank Jaha. I truly enjoyed your friendship and the time we spent together and I wish you a very bright future.

All the time being in Lund I was always supported by my friends in Germany. It is really nice to see that there is still a very strong bond among the old circle of friends (Loopi, Peter, Zelle, Katja, Stephan) and I hope it will stay like this, because it is just great!

Last but not least I want to thank my family. Es ist immer wieder wunderbar nach Hause zu kommen und zu merken, dass alles noch beim Alten ist. Mit Flo und Basti habe ich ziemlich relaxte Brüder erwischt – es ist herrlich mit Euch einen „fröhlichen“ Abend zu verbringen und den Weihnachtsbaum umzudekorieren! Auch Dir, liebste Oma, will ich von ganzem Herzen danken. Lustig, cool und weltoffen wie du bist, hast du mir gesagt, ich solle doch ins Ausland gehen! So eine Oma wünscht man sich! Mutti und Papa, Euch einen Riesendank für eure Liebe und nicht endende Unterstützung! Es ist beeindruckend zu sehen wie Ihr drei von unserer Sorte aufgezogen habt! Danke für alles!

References

1. J. M. Berg, J. L. Tymoczko, L. Stryer, *Biochemistry, 5th Edition*. W.H. Freeman: New York, 2002.

2. R. Ludwig, W. Harreither, F. Tasca, L. Gorton, *ChemPhysChem* 2010, *11*. 2674-2697.

3. G. M. Swain, in *Handbook of Electrochemistry*, ed. C. G. Zoski. Elsevier: Amsterdam, 2007, pp 111-V.

4. G. M. Jenkins, K. Kawamura, *Nature* 1971, *231*. 175-176.

5. R. L. McCreery, *Chemical Reviews* 2008, *108*. 2646-2687.

6. K. R. Kneten, R. L. McCreery, *Analytical Chemistry* 1992, *64*. 2518-2524.

7. P. Chen, M. A. Fryling, R. L. McCreery, *Analytical Chemistry* 1995, *67*. 3115-3122.

8. K. K. Cline, M. T. McDermott, R. L. McCreery, *The Journal of Physical Chemistry* 1994, *98*. 5314-5319.

9. P. Chen, R. L. McCreery, *Analytical Chemistry* 1996, *68*. 3958-3965.

10. R. Bowling, R. T. Packard, R. L. McCreery, *Langmuir* 1989, *5*. 683-688.

11. M. R. Deakin, K. J. Stutts, R. M. Wightman, *Journal of Electroanalytical Chemistry* 1985, *182*. 113-122.

12. C.-T. Hsieh, H. Teng, *Carbon* 2002, *40*. 667-674.

13. R. E. Panzer, P. J. Elving, *Electrochimica Acta* 1975, *20*. 635-647.

14. C. Schulz, R. Ludwig, L. Gorton, *Analytical Chemistry* 2014, *86*. 4256-4263.

15. H. Oda, A. Yamashita, S. Minoura, M. Okamoto, T. Morimoto, *Journal of Power Sources* 2006, *158*. 1510-1516.

16. K. Okajima, K. Ohta, M. Sudoh, *Electrochimica Acta* 2005, *50*. 2227-2231.

17. J. Xu, M. C. Granger, Q. Chen, J. W. Strojek, T. E. Lister, G. M. Swain, *Analytical Chemistry* 1997, *69*. 591A-597A.

18. A. Kraft, *International Journal of Electrochemistry* 2007, *2*. 355-385.

19. Y. V. Pelskov, A. Y. Sakharova, M. D. Krotova, L. L. Bouilov, B. V. Spitsyn, *Journal of Electroanalytical Chemistry and Interfacial Electrochemistry* 1987, *228*. 19-27.

20. J. E. Cantle, *Atomic Absorption Spectrometry. [Elektronisk resurs]*. Elsevier 1982: Amsterdam, 1982.

21. D. D. Miller, M. A. Rutzke, *Food Analysis* 2010. 421.

22. L. A. Coury Jr, W. R. Heineman, *Journal of Electroanalytical Chemistry and Interfacial Electrochemistry* 1988, *256*. 327-341.

23. J. F. Evans, T. Kuwana, *Analytical Chemistry* 1977, *49*. 1632-1635.

24. L. Gorton, P. N. Bartlett, in *Bioelectrochemistry*. John Wiley & Sons, Ltd: Chichester, 2008, pp 157-198.

25. D. M. P. Mingos, *Gold Clusters, Colloids and Nanoparticles I. [Elektronisk resurs]*. Cham : Springer International Publishing : Imprint: Springer, 2014.: Cham, 2014.

26. M. Hromadová, W. R. Fawcett, *The Journal of Physical Chemistry A* 2000, *104*. 4356-4363.

27. M. P. Soriaga, *Progress in Surface Science* 1992, *39*. 325-443.

28. E. Ostuni, L. Yan, G. M. Whitesides, *Colloids and Surfaces B: Biointerfaces* 1999, *15*. 3-30.

29. U. Hanefeld, L. Gardossi, E. Magner, *Chemical Society Reviews* 2009, *38*. 453-468.

30. S. D. Minteer, *Enzyme stabilization and immobilization : methods and protocols*. Humana Press: New York, 2011.

31. P. Jonkheijm, D. Weinrich, H. Schröder, C. M. Niemeyer, H. Waldmann, *Angewandte Chemie International Edition* 2008, *47*. 9618-9647.

32. R. Bahulekar, N. R. Ayyangar, S. Ponrathnam, *Enzyme and Microbial Technology* 1991, *13*. 858-868.

33. J. D. Ziebarth, Y. Wang, *Biomacromolecules* 2010, *11*. 29.

34. R. V. Benjaminsen, M. A. Mattebjerg, J. R. Henriksen, S. M. Moghimi, T. L. Andresen, *Molecular Therapy* 2013, *21*. 149-157.

35. E. Lojou, P. Bianco, *Electrochimica Acta* 2007, *52*. 7307-7314.

36. L. Gorton, G. Joensson-Pettersson, E. Csoregi, K. Johansson, E. Dominguez, G. Marko-Varga, *Analyst* 1992, *117*. 1235-41.

37. A. L. Hart, C. Matthews, W. A. Collier, *Analytica Chimica Acta* 1999, *386*. 7-12.

38. K. Watanabe, G. P. Royer, *Journal of Molecular Catalysis* 1983, *22*. 145-152.

39. X.-J. Tang, B. Xie, P.-O. Larsson, B. Danielsson, M. Khayyami, G. Johansson, *Analytica Chimica Acta* 1998, *374*. 185-190.

40. W. Zhang, Y. Huang, H. Dai, X. Wang, C. Fan, G. Li, *Analytical Biochemistry* 2004, *329*. 85-90.

41. B. Lakard, G. Herlem, S. Lakard, A. Antoniou, B. Fahys, *Biosensors and Bioelectronics* 2004, *19*. 1641-1647.

42. M. Schneider, M. Brinkmann, H. Möhwald, *Macromolecules* 2003, *36*. 9510-9518.

43. G. B. Butler, R. J. Angelo, *Journal of the American Chemical Society* 1957, *79*. 3128-3131.

44. K. D. Hildenbrand. Google Patents, 2005.

45. Y. Qi, H. Zhang, M. Yan, Z. Jiang, *Electrochemistry Communications* 2002, *4*. 431-435.

46. A. Yarman, C. Schulz, C. Sygmund, R. Ludwig, L. Gorton, U. Wollenberger, F. W. Scheller, *Electroanalysis* 2014, *26*. 2043-2048.

47. P. Kielb, M. Sezer, S. Katz, F. Lopez, C. Schulz, L. Gorton, R. Ludwig, U. Wollenberger, I. Zebger, I. M. Weidinger, *ChemPhysChem* 2015, *16*. 1960-1968.

48. P. Knöös, C. Schulz, L. Piculell, R. Ludwig, L. Gorton, M. Wahlgren, *International Journal of Pharmaceutics* 2014, *468*. 121-132.

49. N. A. Kotov, I. Dekany, J. H. Fendler, *The Journal of Physical Chemistry* 1995, *99*. 13065-13069.

50. C. Note, S. Kosmella, J. Koetz, *Colloids and Surfaces A: Physicochemical and Engineering Aspects* 2006, *290*. 150-156.

51. Y. Xiao, F. Patolsky, E. Katz, J. F. Hainfeld, I. Willner, *Science* 2003, *299*. 1877-1881.

52. N. D. Dimcheva, E. G. Horozova, *Chemical Papers* 2015, *69*. 17-26.

53. M.-C. Daniel, D. Astruc, *Chemical Reviews* 2004, *104*. 293-346.

54. S. Zeng, K.-T. Yong, I. Roy, X.-Q. Dinh, X. Yu, F. Luan, *Plasmonics* 2011, *6*. 491-506.

55. K. Saha, S. S. Agasti, C. Kim, X. Li, V. M. Rotello, *Chemical Reviews* 2012, *112*. 2739-2779.

56. S. Borgmann, G. Hartwich, A. Schulte, W. Schuhmann, in *Perspectives in Bioanalysis*, ed. E. Paleček, F. Scheller, J. Wang. Elsevier: Amsterdam, 2005, vol. 1, pp 599-655.

57. J. C. Love, L. A. Estroff, J. K. Kriebel, R. G. Nuzzo, G. M. Whitesides, *Chemical Reviews* 2005, *105*. 1103-1170.

58. A. Ulman, *Chemical Reviews* 1996, *96*. 1533-1554.

59. J. J. Gooding, F. Mearns, W. Yang, J. Liu, *Electroanalysis* 2003, *15*. 81-96.

60. S. Ferretti, S. Paynter, D. A. Russell, K. E. Sapsford, D. J. Richardson, *TrAC Trends in Analytical Chemistry* 2000, *19*. 530-540.

61. R. G. Nuzzo, B. R. Zegarski, L. H. Dubois, *Journal of the American Chemical Society* 1987, *109*. 733-740.

62. R. Ludwig, R. Ortiz, C. Schulz, W. Harreither, C. Sygmund, L. Gorton, *Analytical and Bioanalytical Chemistry* 2013, *405*. 3637-3658.

63. P. Lamberg, Malmö University, Malmö, 2014.

64. A. D. McNaught, A. Wilkinson, *IUPAC. Compendium of Chemical Terminology, 2nd Ed. (the "Gold Book")*. Wiley-Blackwell; 2nd Revised edition edition: Hoboken.

65. U. Wollenberger, R. Spricigo, S. Leimkühler, K. Schröder, *Advances in Biochemical Engineering/Biotechnology* 2008, *109*. 19-64.

66. A. P. F. Turner, *Chemical Society Reviews* 2013, *42*. 3184-3196.

67. L. C. Clark, C. Lyons, *Annals of the New York Academy of Sciences* 1962, *102*. 29-45.

68. X. Zhang, H. Ju, J. Wang, *Electrochemical sensors, biosensors and their biomedical applications*. Academic Press: San Diego, New York, London, Burlington, 2011.

69. J. E. Frew, H. A. O. Hill, *European Journal of Biochemistry* 1988, *172*. 261-269.

70. L.-H. Guo, H. A. O. Hill, *Advances in Inorganic Chemistry* 1991, *36*. 341-375.

71. P. Yeh, T. Kuwana, *Chemistry Letters* 1977. 1145-8.

72. M. J. Eddowes, H. A. O. Hill, *Journal of the Chemical Society, Chemical Communications* 1977. 771-2.

73. R. A. Marcus, *Journal of Chemical Physics* 1956, *24*. 979-989.

74. R. A. Marcus, *Journal of Chemical Physics* 1956, *24*. 966-978.

75. R. A. Marcus, *Angewandte Chemie International Edition* 1993, *32*. 1111-1121.

76. C. C. Page, C. C. Moser, X. Chen, P. L. Dutton, *Nature* 1999, *402*. 47-52.

77. R. A. Marcus, *The Journal of Chemical Physics* 1965, *43*. 679-701.

78. R. A. Marcus, N. Sutin, *Biochimica et Biophysica Acta* 1985, *811*. 265-322.

79. A. J. Bard, L. R. Faulkner, *Electrochemical methods: fundamentals and applications, 2nd Ed.* Wiley: New York, 2001; p 856.

80. O. Farver, P. Hosseinzadeh, N. M. Marshall, S. Wherland, Y. Lu, I. Pecht, *The Journal of Physical Chemistry Letters* 2015, *6*. 100-105.

81. J. R. Miller, L. T. Calcaterra, G. L. Closs, *Journal of the American Chemical Society* 1984, *106*. 3047-3049.

82. H. B. Gray, J. R. Winkler, J. Halpern, *Proceedings of the National Academy of Sciences* 2005, *102*. 3534-3539.

83. G. Henriksson, G. Johansson, G. Pettersson, *Journal of Biotechnology* 2000, *78*. 93-113.

84. M. Zamocky, R. Ludwig, C. Peterbauer, B. M. Hallberg, C. Divne, P. Nicholls, D. Haltrich, *Current Protein & Peptide Science* 2006, *7*. 255-280.

85. H. B. Gray, J. R. Winkler, *Quarterly Reviews of Biophysics* 2003, *36*. 341-372.

86. T.-C. Tan, D. Kracher, R. Gandini, C. Sygmund, R. Kittl, D. Haltrich, B. M. Hallberg, R. Ludwig, C. Divne, *Nature Communications* 2015, *6*.

87. H. B. Gray, J. R. Winkler, *Annual Review of Biochemistry* 1996, *65*. 537-561.

88. C. C. Page, C. C. Moser, P. L. Dutton, *Current Opinion in Chemical Biology* 2003, *7*. 551-556.

89. B. Giese, M. Wang, J. Gao, M. Stoltz, P. Müller, M. Graber, *The Journal of Organic Chemistry* 2009, *74*. 3621-3625.

90. B. Giese, M. Graber, M. Cordes, *Current Opinion in Chemical Biology* 2008, *12*. 755-759.

91. C. C. Moser, T. A. Farid, S. E. Chobot, P. L. Dutton, *Biochimica et Biophysica Acta (BBA) - Bioenergetics* 2006, *1757*. 1096-1109.

92. H. H. Nimz, U. Schmitt, E. Schwab, O. Wittmann, F. Wolf, in *Ullmann's Encyclopedia of Industrial Chemistry*. Wiley-VCH Verlag GmbH & Co. KGaA: Weinheim, 2000.

93. E. A. Bayer, H. Chanzy, R. Lamed, Y. Shoham, *Current Opinion in Structural Biology* 1998, *8*. 548-557.

94. M. K. Bhat, S. Bhat, *Biotechnology Advances* 1997, *15*. 583-620.

95. J. A. Langston, T. Shaghasi, E. Abbate, F. Xu, E. Vlasenko, M. D. Sweeney, *Applied and Environmental Microbiology* 2011, *77*. 7007-7015.

96. W. T. Beeson, C. M. Phillips, J. H. D. Cate, M. A. Marletta, *Journal of the American Chemical Society* 2011, *134*. 890-892.

97. C. M. Phillips, W. T. Beeson, J. H. Cate, M. A. Marletta, *ACS Chemical Biology* 2011.

98. M. Dimarogona, E. Topakas, P. Christakopoulos, *Applied Microbiology and Biotechnology* 2013, *97*. 8455-8465.

99. M. Eibinger, T. Ganner, P. Bubner, S. Rošker, D. Kracher, D. Haltrich, R. Ludwig, H. Plank, B. Nidetzky, *Journal of Biological Chemistry* 2014, *289*. 35929-35938.

100. B. M. Hallberg, T. Bergfors, K. Backbro, G. Pettersson, G. Henriksson, C. Divne, *Structure* 2000, *8*. 79-88.

101. M. B. Hallberg, G. Henriksson, G. Pettersson, C. Divne, *Journal of Molecular Biology* 2002, *315*. 421-434.

102. B. M. Hallberg, G. Henriksson, G. Pettersson, A. Vasella, C. Divne, *The Journal of Biological Chemistry* 2003, *278*. 7160-7166.

103. M. Zámocký, M. Hallberg, R. Ludwig, C. Divne, D. Haltrich, *Gene* 2004, *338*. 1-14.

104. M. E. Yakovleva, A. Killyéni, R. Ortiz, C. Schulz, D. MacAodha, P. Ó Conghaile, D. Leech, I. C. Popescu, C. Gonaus, C. K. Peterbauer, L. Gorton, *Electrochemistry Communications* 2012, *24*. 120-122.

105. F. A. J. Rotsaert, V. Renganathan, M. H. Gold, *Biochemistry* 2003, *42*. 4049-4056.

106. M. Zamocky, C. Schumann, C. Sygmund, J. O'Callaghan, A. D. W. Dobson, R. Ludwig, D. Haltrich, C. K. Peterbauer, *Protein Expression and Purification* 2008, *59*. 258-265.

107. G. Henriksson, G. Pettersson, G. Johansson, A. Ruiz, E. Uzcategui, *European Journal of Biochemistry* 1991, *196*. 101-6.

108. J. D. Cohen, W. Bao, V. Renganathan, S. S. Subramaniam, T. M. Loehr, *Archives of Biochemistry and Biophysics* 1997, *341*. 321-328.

109. S. S. Subramaniam, S. R. Nagalla, V. Renganathan, *Archives of Biochemistry and Biophysics* 1999, *365*. 223-230.

110. S. Schneider, J. Marles-Wright, K. H. Sharp, M. Paoli, *Natural Product Reports* 2007, *24*. 621-630.

111. C. Kisker, H. Schindelin, A. Pacheco, W. A. Wehbi, R. M. Garrett, K. V. Rajagopalan, J. H. Enemark, D. C. Rees, *Cell* 1997, *91*. 973-983.

112. M. Sezer, R. Spricigo, T. Utesch, D. Millo, S. Leimkühler, M. A. Mroginski, U. Wollenberger, P. Hildebrandt, I. M. Weidinger, *Physical Chemistry Chemical Physics* 2010, *12*. 7894-7903.

113. A. Pacheco, J. T. Hazzard, G. Tollin, J. H. Enemark, *Journal of Biological Inorganic Chemistry* 1999, *4*. 390-401.

114. W. Harreither, C. Sygmund, M. Augustin, M. Narciso, M. L. Rabinovich, L. Gorton, D. Haltrich, R. Ludwig, *Applied and Environmental Microbiology* 2011, *77*. 1804-1815.

115. R. Ortiz, H. Matsumura, F. Tasca, K. Zahma, M. Samejima, K. Igarashi, R. Ludwig, L. Gorton, *Analytical Chemistry* 2012, *84*. 10315-10323.

116. D. Kracher, K. Zahma, C. Schulz, C. Sygmund, L. Gorton, R. Ludwig, *Federation of the Societies of Biochemistry and Molecular Biology* 2015.

117. G. Henriksson, V. Sild, I. J. Szabo, G. Pettersson, G. Johansson, *Biochimica et Biophysica Acta* 1998, *1383*. 48-54.

118. K. Igarashi, I. Momohara, T. Nishino, M. Samejima, *Biochemical Journal* 2002, *365*. 521-526.

119. K. Igarashi, M. F. J. M. Verhagen, M. Samejima, M. Schülein, K.-E. L. Eriksson, T. Nishino, *The Journal of Biological Chemistry* 1999, *274*. 3338-3344.

120. D. K. Das, O. K. Medhi, *Journal of Inorganic Biochemistry* 1998, *70*. 83-90.

121. V. Guallar, B. Olsen, *Journal of Inorganic Biochemistry* 2006, *100*. 755-760.

122. G. D. Jones, M. T. Wilson, *Biochemical Journal* 1988, *256*. 713-718.

123. M. Bey, S. Zhou, L. Poidevin, B. Henrissat, P. M. Coutinho, J.-G. Berrin, J.-C. Sigoillot, *Applied and Environmental Microbiology* 2012.

124. F. L. Aachmann, G. Vaaje-Kolstad, Z. Forsberg, Å. Røhr, V. G. H. Eijsink, M. Sørlie, in *Encyclopedia of Inorganic and Bioinorganic Chemistry*. John Wiley & Sons, Ltd, 2011.

125. U. Baminger, S. S. Subramaniam, V. Renganathan, D. Haltrich, *Applied and Environmental Microbiology* 2001, *67*. 1766-1774.

126. G. Henriksson, G. Johansson, G. Pettersson, *Biochimica et Biophysica Acta (BBA) - Bioenergetics* 1993, *1144*. 184-190.

127. P. Hodge, J. E. Gautrot, *Polymer International* 2009, *58*. 261-266.

128. M. Shao, S. Pöller, C. Sygmund, R. Ludwig, W. Schuhmann, *Electrochemistry Communications* 2013, *29*. 59-62.

129. F. Conzuelo, J. Vivekananthan, S. Pöller, J. M. Pingarrón, W. Schuhmann, *ChemElectroChem* 2014, *1*. 1854-1858.

130. S. Pöller, M. Shao, C. Sygmund, R. Ludwig, W. Schuhmann, *Electrochimica Acta* 2013, *110*. 152-158.

131. D. Guschin, J. Castillo, N. Dimcheva, W. Schuhmann, *Analytical and Bioanalytical Chemistry* 2010, *398*. 1661-1673.

132. F. Tasca, L. Gorton, W. Harreither, D. Haltrich, R. Ludwig, G. Nöll, *Journal of Physical Chemistry C* 2008, *112*. 13668-13673.

133. M. G. Mason, M. T. Wilson, A. Ball, P. Nicholls, *FEBS Letters* 2002, *518*. 29-32.

134. S. Pricelius, R. Ludwig, N. J. Lant, D. Haltrich, G. M. Guebitz, *Biotechnology Journal* 2011, *6*. 224-230.

135. A. Flitsch, E. N. Prasetyo, C. Sygmund, R. Ludwig, G. S. Nyanhongo, G. M. Guebitz, *Enzyme and Microbial Technology* 2013, *52*. 60-67.

136. S. Pricelius, R. Ludwig, N. Lant, D. Haltrich, G. M. Guebitz, *Applied Microbiology and Biotechnology* 2009, *85*. 75-83.

137. M. Samejima, K.-E. L. Eriksson, *European Journal of Biochemistry* 1992, *207*. 103-107.

138. U. Salaj-Kosla, M. Scanlon, T. Baumeister, K. Zahma, R. Ludwig, P. Conghaile, D. MacAodha, D. Leech, E. Magner, *Analytical and Bioanalytical Chemistry* 2013, *405*. 3823-3830.

139. L. Stoica, N. Dimcheva, Y. Ackermann, K. Karnicka, D. A. Guschin, P. J. Kulesza, J. Rogalski, D. Haltrich, R. Ludwig, L. Gorton, W. Schuhmann, *Fuel Cells* 2009, *9*. 53-62.

140. L. Stoica, A. Lindgren-Sjölander, T. Ruzgas, L. Gorton, *Analytical Chemistry* 2004, *76*. 4690-4696.

141. N. Cruys-Bagger, G. Ren, H. Tatsumi, M. J. Baumann, N. Spodsberg, H. D. Andersen, L. Gorton, K. Borch, P. Westh, *Biotechnology and Bioengineering* 2012. 3199-3204.

142. F. J. Suchy, P. M. Brannon, T. O. Carpenter, J. R. Fernandez, V. Gilsanz, J. B. Gould, K. Hall, S. L. Hui, J. Lupton, J. Mennella, *Annals of internal medicine* 2010, *152*. 792-796.

143. D. L. Swagerty, Jr., A. D. Walling, R. M. Klein, *American Family Physician* 2002, *65*. 1845-50.

144. L. Stoica, T. Ruzgas, L. Gorton, *Bioelectrochemistry* 2009, *76*. 42-52.

145. G. Safina, R. Ludwig, L. Gorton, *Electrochimica Acta* 2010, *55*. 7690-7695.

146. L. Stoica, R. Ludwig, D. Haltrich, L. Gorton, *Analytical Chemistry* 2006, *78*. 393-398.

147. M. Yakovleva, O. Buzas, H. Matsumura, M. Samejima, K. Igarashi, P.-O. Larsson, L. Gorton, B. Danielsson, *Biosensors and Bioelectronics* 2012, *31*. 251-256.

148. N. Glithero, C. Clark, L. Gorton, W. Schuhmann, N. Pasco, *Analytical and Bioanalytical Chemistry* 2013, *405*. 3791-3799.

149. M. E. Aulton, *Pharmaceutics : the science of dosage form design*. Churchill Livingstone Elsevier: Edinburgh, 2002.

150. W. Harreither, V. Coman, R. Ludwig, D. Haltrich, L. Gorton, *Electroanalysis* 2007, *19*. 172-180.

151. 2013.

152. World Health Organization, *Global status report on noncommunicable diseases 2014*. World Health Organization, 2015: Geneva, 2014.

153. S. Ferri, K. Kojima, K. Sode, *Journal of diabetes science and technology* 2011, *5*. 1068-1076.

154. A. Heller, B. Feldman, *Chemical Reviews* 2008, *108*. 2482-2505.

155. F. Tasca, M. N. Zafar, W. Harreither, G. Nöll, R. Ludwig, L. Gorton, *Analyst* 2011, *136*. 2033-2036.

156. M. N. Zafar, G. Safina, R. Ludwig, L. Gorton, *Analytical Biochemistry* 2012, *425*. 36-42.

157. G. Kovacs, R. Ortiz, V. Coman, W. Harreither, I. C. Popescu, R. Ludwig, L. Gorton, *Bioelectrochemistry* 2012, *88*. 84-91.

158. M. Falk, M. Alcalde, P. N. Bartlett, A. L. De Lacey, L. Gorton, C. Gutierrez-Sanchez, R. Haddad, J. Kilburn, D. Leech, R. Ludwig, E. Magner, D. M. Mate, P. Ó Conghaile, R. Ortiz, M. Pita, S. Pöller, T. Ruzgas, U. Salaj-Kosla, W. Schuhmann, F. Sebelius, *Plos One* 2014, *9*. e109104.

159. V. Krikstolaityte, P. Lamberg, M. D. Toscano, M. Silow, O. Eicher-Lorka, A. Ramanavicius, G. Niaura, L. Abariute, T. Ruzgas, S. Shleev, *Fuel Cells* 2014, *14*. 792-800.

160. X. Wang, M. Falk, R. Ortiz, H. Matsumura, J. Bobacka, R. Ludwig, M. Bergelin, L. Gorton, S. Shleev, *Biosensors and Bioelectronics* 2012, *31*. 219-225.

161. V. Coman, R. Ludwig, W. Harreither, D. Haltrich, L. Gorton, T. Ruzgas, S. Shleev, *Fuel Cells* 2010, *10*. 9-16.

162. M. Falk, D. Pankratov, L. Lindh, T. Arnebrant, S. Shleev, *Fuel Cells* 2014, *14*. 1050-1056.

163. M. Falk, V. Andoralov, Z. Blum, J. Sotres, D. B. Suyatin, T. Ruzgas, T. Arnebrant, S. Shleev, *Biosensors and Bioelectronics* 2012, *37*. 38-45.

164. F. Tasca, L. Gorton, W. Harreither, D. Haltrich, R. Ludwig, G. Nöll, *Journal of Physical Chemistry C* 2008, *112*. 9956-9961.

165. C. Nistor, A. Rose, M. Farre, L. Stoica, U. Wollenberger, T. Ruzgas, D. Pfeiffer, D. Barceló, L. Gorton, J. Emnéus, *Analytica Chimica Acta* 2002, *456*. 3-17.

166. N. Balasundram, K. Sundram, S. Samman, *Food Chemistry* 2006, *99*. 191-203.

167. C. Schulz, R. Ludwig, P. O. Micheelsen, M. Silow, M. D. Toscano, L. Gorton, *Electrochemistry Communications* 2012, *17*. 71-74.

168. A. Kadek, D. Kavan, A. K. G. Felice, R. Ludwig, P. Halada, P. Man, *FEBS Letters* 2015.

169. R. G. Compton, C. E. Banks, *Understanding voltammetry*. World Scientific: London, 2010.

170. C. G. Zoski, *Handbook of Electrochemistry*. Elsevier: Amsterdam, 2007.

171. J. G. Osteryoung, R. A. Osteryoung, *Analytical Chemistry* 1985, *57*. 101-110.

172. R. Appelqvist, G. Marko-Varga, L. Gorton, A. Torstensson, G. Johansson, *Analytica Chimica Acta* 1985, *169*. 237-47.

173. W. Kaim, J. Fiedler, *Chemical Society Reviews* 2009, *38*. 3373-3382.

174. M. Sezer, D. Millo, I. M. Weidinger, I. Zebger, P. Hildebrandt, *IUBMB Life* 2012, *64*. 455-464.

175. F. Siebert, P. Hildebrandt, in *Vibrational Spectroscopy in Life Science*. Wiley-VCH Verlag GmbH & Co. KGaA: Weinheim, 2008, pp 11-61.

176. S. P. Best, S. J. Borg, K. A. Vincent, in *Spectroelectrochemistry*. The Royal Society of Chemistry: Cambridge, 2008, pp 1-30.

177. D. H. Murgida, P. Hildebrandt, *Chemical Society Reviews* 2008, *37*. 937-945.

178. A. Klein, in *Spectroelectrochemistry*. The Royal Society of Chemistry: Cambridge, 2008, pp 91-122.

179. H. Khoa Ly, M. Sezer, N. Wisitruangsakul, J.-J. Feng, A. Kranich, D. Millo, I. M. Weidinger, I. Zebger, D. H. Murgida, P. Hildebrandt, *Febs Journal* 2011, *278*. 1382-1390.

180. T. Larsson, A. Lindgren, T. Ruzgas, S. E. Lindquist, L. Gorton, *Journal of Electroanalytical Chemistry* 2000, *482*. 1-10.

Paper I

Electrochemistry Communications 17 (2012) 71–74

Contents lists available at SciVerse ScienceDirect

Electrochemistry Communications

journal homepage: www.elsevier.com/locate/elecom

Enhancement of enzymatic activity and catalytic current of cellobiose dehydrogenase by calcium ions

Christopher Schulz [a], Roland Ludwig [b], Pernille O. Micheelsen [c], Maria Silow [c], Miguel D. Toscano [c], Lo Gorton [a,*]

[a] Department of Biochemistry and Structural Biology, Lund University, SE-22100 Lund, Sweden
[b] Department of Food Sciences and Technology, Food Biotechnology Laboratory, BOKU-University of Natural Resources and Life Sciences, Muthgasse 18, A-1190 Vienna, Austria
[c] Novozymes A /S, Krogshøjvej 36, 2880 Bagsværd, Denmark

ARTICLE INFO

Article history:
Received 20 December 2011
Received in revised form 27 January 2012
Accepted 30 January 2012
Available online 4 February 2012

Keywords:
Activation
Cellobiose dehydrogenase
Catalytic activity
$CaCl_2$
KCl
Ionic strength

ABSTRACT

Cellobiose dehydrogenase (CDH) has recently become a redox enzyme at focus in bioelectrochemistry especially for the construction of sugar biosensors and biofuel cell anodes. The present study shows that an increase in the $CaCl_2$ concentration to up to 100 mM led to an increase in the maximal catalytic current generated by two different Ascomycete and one Basidiomycete CDH immobilised on a spectroscopic graphite electrode. For the Ascomycete *Myriococcum thermophilum* CDH the catalytic current was increased 5.1 fold, whereas Ascomycete *Humicola insolens* CDH showed a four-fold increase and Basidiomycete *Phanerochaete chrysosporium* CDH showed an increase by a factor of 2.4. On the other hand, the addition of a monovalent cation salt, KCl (up to 100 mM), to the buffers increased the catalytic currents only up to 2-fold for *Myriococcum thermophilum* CDH. Activity assays in solution with cyt *c* accepting solely the electrons from the CYT_{CDH} domain also revealed an increased activity in the presence of $CaCl_2$. Experiments with the isolated DH_{CDH} domain from *Humicola insolens* have shown that the catalytic turnover is totally independent on the addition of KCl or $CaCl_2$ to the solution. The results indicate a positive effect of metal cations, particularly Ca^{2+}, on the electron transfer between the DH_{CDH} and the CYT_{CDH} domains or between the CYT_{CDH} domain and the final electron acceptor, whereas the first hypothesis is favoured. These findings are of interest both for the construction of 3 rd generation biosensors and biofuel cell anodes, and also for a deeper understanding of the electron transfer mechanism in CDH.

1. Introduction

Cellobiose dehydrogenase (CDH, EC 1.1.99.18) is an extracellular monomeric redox enzyme consisting of a catalytically active, flavin adenine dinucleotide (FAD) containing dehydrogenase domain (DH_{CDH}), which is connected via a flexible linker region to a haem *b* containing cytochrome domain (CYT_{CDH}). During the catalytic cycle, two electrons from the oxidation of carbohydrates (e. g. cellobiose, lactose or glucose) reduce the FAD and can further be directly donated to soluble one- or two-electron acceptors. Alternatively, the electrons can be subsequently transferred from DH_{CDH} to CYT_{CDH} by an internal electron transfer process (IET). CYT_{CDH} further transfers the electrons to large soluble one-electron acceptors like cytochrome *c* (cyt *c*) or to a macroscopic electrode in a direct electron transfer (DET) reaction [1]. The natural electron acceptor of CYT_{CDH} was recently proposed to be copper-dependent monooxygenases of the glycoside hydrolase 61 (GH61) family [2].

The specific characteristics of CDH regarding substrate specificity, pH optima, sequence length, etc. depend on its origin. Basically class I CDHs produced by Basidiomycota and class II and class III CDHs produced by Ascomycota have been distinguished [3]. CDH can be immobilised in a stable manner on different electrode materials such as graphite or modified gold electrodes, where it can exhibit both DET and mediated electron transfer reactions (MET) [1,4–7]. This makes CDH an interesting enzyme for the construction of biosensors and biofuel cell anodes [8–12].

The influence of ionic strength as well as various cation and anion species on enzymes is known to modulate enzymatic activity or stability in numerous ways. For sulphite oxidase, SOx, an enzyme with two redox domains connected by a linker region, mechanistically similar to CDH [13], Sezer et al. showed that an increase in the catalytic current from a SAM modified electrode with immobilised human SOx was obtained when the ionic strength of the buffer was increased. This effect probably comes from a decreased contact time of the electron transferring domain with the electrode resulting in a higher flexibility [14]. The importance of protein flexibility was also pointed out by Feng et al., showing a decrease in the IET rate due to a higher viscosity [15]. Furthermore, sulphate anions were found to decrease the interaction

* Corresponding author. Fax: +46 46 222 4116.
E-mail addresses: lo.gorton@analykem.lu.se, lo.gorton@biochemistry.lu.se (L. Gorton).

1388-2481/$ – see front matter © 2012 Elsevier B.V. All rights reserved.
doi:10.1016/j.elecom.2012.01.031

of the two electron transferring domains of SOx due to electrostatic screening of the oppositely charged domains [16].

Previously it was shown for class I CDH from *Phanerochaete chrysosporium* immobilised on graphite electrodes that an increase in the catalytic current by 50% could be obtained when the concentration of sodium chloride in the electrolyte was increased from 0 to 80 mM [7]. As it is of prime importance to explore the catalytic activity of CDH in the presence of ions for biosensors and biofuel cell anodes, the present study investigates the influence of different concentrations of a monovalent (K^+) and a divalent (Ca^{2+}) cation on the performance of one class I and two class II CDHs of different origins in solution and immobilised on spectroscopic graphite electrodes.

2. Materials and methods

2.1. Enzymes

Phanerochaete chrysosporium CDH (*Pc*CDH, 2.6 mg/ml) (class I) was produced and purified according to [17]. *Myriococcum thermophilum* CDH (*Mt*CDH, 19.6 mg/ml, class II) was recombinantly overexpressed in *Pichia pastoris* [18]. *Humicola insolens* CDH (*Hi*CDH, 3.3 mg/ml, class II) and the single DH_{CDH} domain of *Humicola insolens* CDH (*Hi*DH_{CDH}, 9.05 mg/ml) were produced recombinantly in *Aspergillus oryzae*, following a standard method [19].

2.2. Buffers

As measuring buffers 50 mM sodium acetate, pH 5.5 for investigations of *Mt*CDH, 50 mM MOPS, pH 7.5 for *Hi*CDH, and 50 mM sodium acetate, pH 4.5 for *Pc*CDH were used. Optionally, the buffers contained KCl or $CaCl_2$ at various concentrations between 10 to 100 mM. The chosen pH values of the buffers represent the optimal pH for DET for each investigated CDH (data not shown) [4,5,20].

2.3. Activity assays in solution

Two spectrophotometric assays for measuring the activity of the CDHs were performed. In the first assay the two-electron/two-proton acceptor 2,6-dichloro-indophenol (DCIP) was used to monitor the activity of the DH_{CDH} domain [3] by measuring the time dependent change of absorption at 520 nm ($\varepsilon = 6.9\ mM^{-1}\ cm^{-1}$) of a mixture of 100 µl of 3 mM DCIP, 100 µl of 300 mM lactose, 780 µl of 50 mM buffer, and 20 µl of the enzyme solution [21]. In the second assay the one-electron acceptor cyt *c* is used, which communicates for steric reasons only with the CYT_{CDH} domains and consequently monitors the activity of intact CDH and the IET between the DH_{CDH} and CYT_{CDH} domain [3]. The absorption is followed at 550 nm ($\varepsilon = 19.6\ mM^{-1}cm^{-1}$) of a mixture of 20 µl of 1 mM cyt *c*, 100 µl of 300 mM lactose, 860 µl of 50 mM buffer, and 20 µl of the enzyme solution [21]. One unit of DCIP and cyt *c* activity was defined as the amount of CDH that reduces 1 µmol of DCIP or cyt *c*, respectively, per min under the applied conditions. All measured enzyme activities are the average of three measurements at 22 °C, whereas the average activity values in buffers without KCl or CaCl2 were set to 100% and the average activity values in the presence of KCl or $CaCl_2$ in the buffers were related to those.

2.4. Flow injection analysis (FIA)

Electrochemical measurements were performed amperometrically with CDH modified graphite electrodes mounted in a flow through electrochemical cell coupled to a single line flow injection system using different flow buffers (see buffer section) as described by Harreither et al. [4]. The applied potential for all CDH modified graphite electrodes was 250 mV versus a Ag|AgCl (0.1 M KCl) reference electrode. This potential guarantees a maximum DET current response. The catalytic currents of at least eight different concentrations of lactose solutions were measured for each buffer. I_{max} values were determined by non-

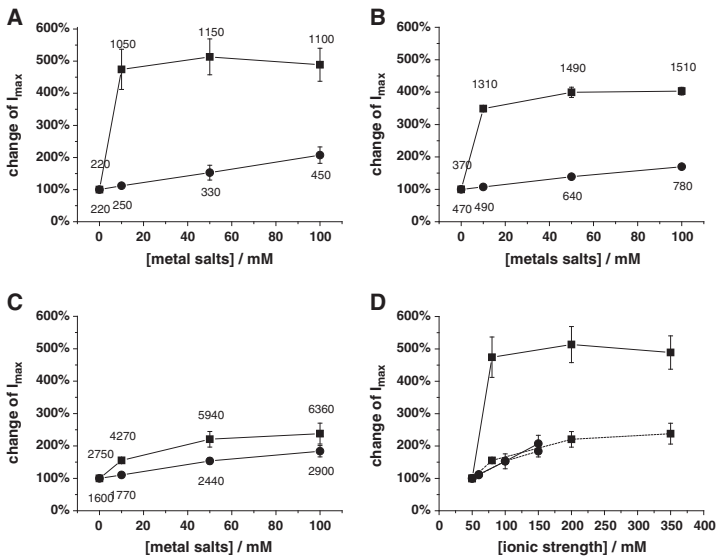

Fig. 1. Dependence of the relative maximal catalytic currents I_{max} on the concentration or on the ionic strength of buffers containing $CaCl_2$ (■) or KCl (●) determined amperometrically with CDH immobilised on spectroscopic graphite electrodes, mounted in a FIA system with lactose as substrate. A = *Mt*CDH, B = *Hi*CDH, C = *Pc*CDH, D = *Mt*CDH (solid line) and *Pc*CDH (dashed line). The error bars indicate the standard deviation of the relative maximal catalytic currents I_{max}. The numbers above and below the response curves represent the average of the absolute current density values in nA/cm^2.

linear curve fittings to the Michaelis-Menten equation.The maximal catalytic currents I_{max} detected in buffers without KCl or $CaCl_2$ were set to 100% for each electrode. The relative changes of I_{max} in the presence of additional KCl or $CaCl_2$ in the buffer were calculated individually for each electrode, whereas the averages and standard deviations of the relative I_{max} of three equally prepared electrodes were calculated and plotted in Fig. 1.

3. Results and discussion

All three CDHs were separately immobilised through simple adsorption onto the surface of spectroscopic graphite electrodes. Calibration curves with lactose as substrate in buffers with varying concentrations of $CaCl_2$ and KCl were then used to evaluate the maximal catalytic currents, I_{max}. Fig. 1 shows the dependencies of I_{max} on the concentration of $CaCl_2$ or KCl for *Mt*CDH, *Hi*CDH, and *Pc*CDH. Surprisingly, an increase in the concentration of $CaCl_2$ in the buffer drastically increased I_{max} for the Ascomycete CDHs with maximum increases of around 510% (corresponding to an average absolute current density value of 1150 nA/cm^2) for *Mt*CDH and 400% (corresponding to an average absolute current density value of 1510 nA/cm^2) for *Hi*CDH (see ■ in Fig. 1A and B). In contrast for the Basidiomycete *Pc*CDH, the I_{max} was also increased by the addition of $CaCl_2$ to the buffer, however, a maximal increase of only 240% (corresponding to an average absolute current density value of 6360 nA/cm^2) was obtained (see ■ in Fig. 1C). Addition of a salt of a monovalent metal cation, K^+, to the buffers instead, led to a linear increase in I_{max} for all investigated CDHs. However, the maximal increases produced by KCl were only between 170% for *Hi*CDH, 180% for *Pc*CDH, and 210% for *Mt*CDH (corresponding to average absolute current density values of 780, 2900 and 450 nA/cm^2 respectively). If I_{max} was instead plotted versus ionic strength for the two class II CDHs there was a substantial difference in the effect of addition of monovalent K^+ versus divalent Ca^{2+}. However, for class I *Pc*CDH the situation is different. Here there seems not to be any major difference in the effect of addition of monovalent K^+ versus divalent Ca^{2+} (see Fig. 1D).

In general, the observed drastic effects of especially divalent Ca^{2+} on the catalytic currents can be attributed to a modified interaction between CYT_{CDH} and the electrode and/or between CYT_{CDH} and DH_{CDH}. Taking into account that *Mt*CDH has a rather inefficient IET [4] between DH_{CDH} and CYT_{CDH} but shows the highest increase in I_{max} when increasing the concentration of $CaCl_2$ and that *Pc*CDH has a rather efficient IET [5] and shows the lowest increase in I_{max} when increasing the concentration of $CaCl_2$ favours the assumption that Ca^{2+} increases the interaction between DH_{CDH} and CYT_{CDH}. As a hypothesis, we propose a complexation of Ca^{2+} by the carboxy groups of aspartic and glutamic acid at the interface of the DH_{CDH} and CYT_{CDH} domains [5], which results in a closer domain interaction and a higher IET rate.

Similar dependencies of CDH activities on the addition of $CaCl_2$ to the buffer were observed in spectrophotometric activity assays performed with CDH in solution. As the electrons in the cyt *c* based assay are finally transferred from CYT_{CDH} to cyt *c*, the results are comparable to the ones with CDH immobilised on the electrodes. Fig. 2 reveals that when increasing the concentration of KCl or $CaCl_2$ in the buffer there is a relative increase in both the cyt *c* and DCIP activities of intact *Mt*CDH and *Hi*CDH (see Fig. 2A and B), whereas for the *Hi*DH_{CDH} there was no increase in either case (see Fig. 2C). As expected, for the case with the isolated *Hi*DH_{CDH} domain no cyt *c* activity was observed, since the presence of CYT_{CDH} is a prerequisite for a cyt *c* activity. The DCIP activity of *Hi*DH_{CDH}, monitoring only the activity of *Hi*DH_{CDH} was independent on additional KCl or $CaCl_2$ in the buffer (see Fig. 2C).

With intact CDHs, which contain both domains, the cyt *c* activities were increased up to around 500% for *Mt*CDH and 310% for *Hi*CDH by the addition of 17.2 mM or 43 mM $CaCl_2$ respectively to the buffer (see ■ in Fig. 2A and B). These increases in activity due to added $CaCl_2$ are comparable to the increased I_{max} values obtained with the same CDHs immobilised on graphite electrodes (see ■ in Fig. 1A and B).

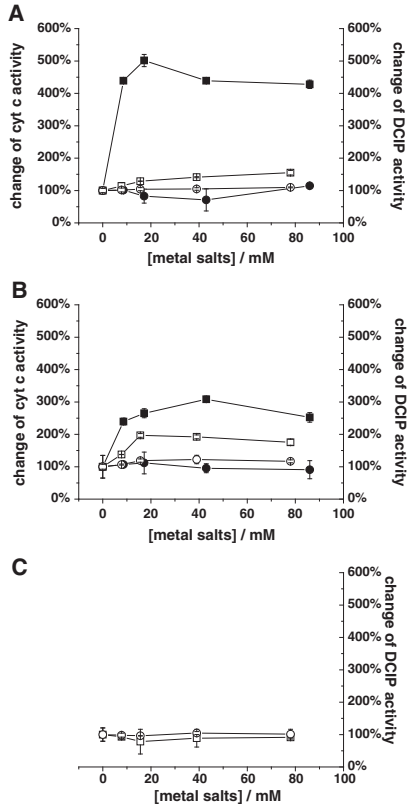

Fig. 2. Dependence of the relative cyt *c* (■,●) and DCIP (□, ○) activities of *Mt*CDH (A), *Hi*CDH (B) and *Hi*DH_{CDH} (C) on different concentrations of $CaCl_2$ (■,□) or KCl (●,○) in the measuring buffer determined with CDH in solution with 30 mM lactose as substrate. The error bars indicated the standard deviation of the relative changes of the enzyme activites.

The addition of 86 mM KCl to the buffers increased the cyt *c* activity up to around 110% for *Mt*CDH, whereas no significant increase was observed for *Hi*CDH (see ● in Fig. 2A and B). Unexpectedly, the DCIP activity of *Mt*CDH and *Hi*CDH was also slightly increased by the addition of $CaCl_2$ and KCl to the buffers but the effect was less pronounced than the increase in the cyt *c* activities (see □, ○ in Fig. 2A and B). As discussed above for *Hi*DH_{CDH} an increased turnover rate of DH_{CDH} due to increased concentrations of metal salts can be excluded as an explanation (see Fig. 2C) for increased DCIP activities. However, this effect has to be further investigated. Since in both experimental approaches with *different* large/macroscopic electron acceptors (cyt *c*/electrode) *comparable* increases in the catalytic signals after addition of especially $CaCl_2$ were obtained, the assumption that Ca^{2+} increases the interaction between DH_{CDH} and CYT_{CDH} is supported.

4. Conclusions

The activity of CDH in solution and on the electrode was increased to a maximum of around five-fold for *Mt*CDH, four-fold for *Hi*CDH, and two-fold for *Pc*CDH by addition of $CaCl_2$ to the buffer. The

enhanced activities of CDH were always higher with additional Ca^{2+} ions for the two class II CDHs but not for the class I, than with comparable concentrations of additional K^{+} ions in the buffer. It is assumed that the positively charged cations alter the interaction at the DH_{CDH} and CYT_{CDH} interface by complexation of negatively charged amino acid residues resulting in an increased IET and thus a higher measurable enzymatic activity through CYT_{CDH}. Further investigations should clarify whether the different dependence of I_{max} on the ionic strength of *Pc*CDH versus *Mt*CDH and *Hi*CDH is a general trait for class I CDHs.

These findings are no doubt of highest interest for studies of the mechanism of the IET between the DH_{CDH} and CYT_{CDH} domains, which might shed light into its physiological function [2], as well as for the construction of 3rd generation biosensors and biofuel cell anodes [7–10].

Acknowledgement

The authors thank the following agencies for financial support: The Swedish Research Council (Vetenskapsrådet, 2010-5031), the European Commission ("Chebana" FP7-PEOPLE-2010-ITN-264772, and "3D-Nanobiodevice" FP7-NMP4-2009-SL-229255), the Foundation for Research, Science and Technology, New Zealand, (LVLX0802), and the Austrian Academy of Science (APART project 11322 to R.L.).

References

[1] R. Ludwig, W. Harreither, F. Tasca, L. Gorton, ChemPhysChem 11 (2010) 2674–2697.
[2] C.M. Phillips, W.T. Beeson, J.H. Cate, M.A. Marletta, ACS Chemical Biology (2011).
[3] M. Zamocky, R. Ludwig, C. Peterbauer, B.M. Hallberg, C. Divne, P. Nicholls, D. Haltrich, Current Protein & Peptide Science 7 (2006) 255–280.
[4] W. Harreither, V. Coman, R. Ludwig, D. Haltrich, L. Gorton, Electroanalytical 19 (2007) 172–180.
[5] L. Stoica, T. Ruzgas, R. Ludwig, D. Haltrich, L. Gorton, Langmuir 22 (2006) 10801–10806.
[6] V. Coman, W. Harreither, R. Ludwig, D. Haltrich, L. Gorton, Chemia Analityczna Warsaw 52 (2007) 945–960.
[7] T. Larsson, A. Lindgren, T. Ruzgas, S.E. Lindquist, L. Gorton, Journal of Electroanalytical Chemistry 482 (2000) 1–10.
[8] L. Stoica, A. Lindgren-Sjoelander, T. Ruzgas, L. Gorton, Analytical Chemistry 76 (2004) 4690–4696.
[9] L. Stoica, N. Dimcheva, Y. Ackermann, K. Karnicka, D.A. Guschin, P.J. Kulesza, J. Rogalski, D. Haltrich, R. Ludwig, L. Gorton, W. Schuhmann, Fuel Cells 9 (2009) 53–62.
[10] G. Safina, R. Ludwig, L. Gorton, Electrochimica Acta 55 (2010) 7690–7695.
[11] F. Tasca, L. Gorton, W. Harreither, D. Haltrich, R. Ludwig, G. Noll, The Journal of Physical Chemistry. C 112 (2008) 13668–13673.
[12] L. Stoica, R. Ludwig, D. Haltrich, L. Gorton, Analytical Chemistry 78 (2006) 393–398.
[13] C. Kisker, H. Schindelin, A. Pacheco, W.A. Wehbi, R.M. Garrett, K.V. Rajagopalan, J.H. Enemark, D.C. Rees, Cell 91 (1997) 973–983.
[14] M. Sezer, R. Spricigo, T. Utesch, D. Millo, S. Leimkuehler, M.A. Mroginski, U. Wollenberger, P. Hildebrandt, I.M. Weidinger, Physical Chemistry Chemical Physics 12 (2010) 7894–7903.
[15] C.J. Feng, R.V. Kedia, J.T. Hazzard, J.K. Hurley, G. Tollin, J.H. Enemark, Biochemistry-Us 41 (2002) 5816–5821.
[16] A. Pacheco, J.T. Hazzard, G. Tollin, J.H. Enemark, Journal of Biological Inorganic Chemistry 4 (1999) 390–401.
[17] E. Uzcategui, M. Raices, R. Montesino, G. Johansson, G. Pettersson, K.E. Eriksson, Biotechnology and Applied Biochemistry 13 (1991) 323–334.
[18] M. Zamocky, C. Schumann, C. Sygmund, J. O'Callaghan, A.D.W. Dobson, R. Ludwig, D. Haltrich, C.K. Peterbauer, Protein Expression and Purification 59 (2008) 258–265.
[19] B. Huge-Jensen, F. Andreasen, T. Christensen, M. Christensen, L. Thim, E. Boel, Lipids 24 (1989) 781–785.
[20] A. Lindgren, L. Gorton, T. Ruzgas, U. Baminger, D. Haltrich, M. Schülein, Journal of Electroanalytical Chemistry 496 (2001) 76–81.
[21] U. Baminger, S.S. Subramaniam, V. Renganathan, D. Haltrich, Applied and Environmental Microbiology 67 (2001) 1766–1774.

Paper II

Anal Bioanal Chem
DOI 10.1007/s00216-012-6627-x

REVIEW

Cellobiose dehydrogenase modified electrodes: advances by materials science and biochemical engineering

Roland Ludwig · Roberto Ortiz · Christopher Schulz · Wolfgang Harreither · Christoph Sygmund · Lo Gorton

Received: 28 September 2012 / Revised: 27 November 2012 / Accepted: 3 December 2012

Abstract The flavocytochrome cellobiose dehydrogenase (CDH) is a versatile biorecognition element capable of detecting carbohydrates as well as quinones and catecholamines. In addition, it can be used as an anode biocatalyst for enzymatic biofuel cells to power miniaturised sensor–transmitter systems. Various electrode materials and designs have been tested in the past decade to utilize and enhance the direct electron transfer (DET) from the enzyme to the electrode. Additionally, mediated electron transfer (MET) approaches via soluble redox mediators and redox polymers have been pursued. Biosensors for cellobiose, lactose and glucose determination are based on CDH from different fungal producers, which show differences with respect to substrate specificity, pH optima, DET efficiency and surface binding affinity. Biosensors for the detection of quinones and catecholamines can use carbohydrates for analyte regeneration and signal amplification. This review discusses different approaches to enhance the sensitivity and selectivity of CDH-based biosensors, which focus on (1) more efficient DET on chemically modified or nanostructured electrodes, (2) the synthesis of custom-made redox polymers for higher MET currents and (3) the engineering of enzymes and reaction pathways. Combination of these strategies will enable the design of sensitive and selective CDH-based biosensors with reduced electrode size for the detection of analytes in continuous on-site and point-of-care applications.

Keywords Biosensors · Carbohydrates · Catecholamines · Cellobiose dehydrogenase · Electron transfer · Nanomaterials

Abbreviations

AuNP	gold nanoparticles
BQ	*p*-benzoquinone
BOx	bilirubin oxidase
CBM1	carbohydrate binding module (family 1)
CDH	cellobiose dehydrogenase
CNP	carbon nanoparticles
CNT	carbon nanotube
CV	cyclic voltammetry, cyclic voltammogram
cyt *c*	cytochrome *c* (from horse heart)
CYT_{CDH}	cytochrome domain of CDH
DCIP	2,6-dichloroindophenol
DET	direct electron transfer
DH_{CDH}	flavodehydrogenase domain of CDH
$E^{\circ\prime}$	formal potential
ET	electron transfer
GA	glutaraldehyde
IET	intramolecular electron transfer
LbL	layer by layer
MET	mediated electron transfer
MUA	mercapto-1-undecanoic acid
MUOH	mercapto-1-undecanol
MWCNT	multi-walled carbon nanotubes
NHE	normal hydrogen electrode
Os-EDP	osmium electrodeposition paint
PBS	phosphate buffered saline

Published in the topical collection *Bioelectroanalysis* with guest editors Nicolas Plumeré, Magdalena Gebala and Wolfgang Schuhmann.

R. Ludwig · W. Harreither · C. Sygmund
Food Biotechnology Laboratory, Department of Food Sciences and Technology, BOKU-University of Natural Resources and Life Sciences, Vienna, Muthgasse 18,
1190 Vienna, Austria

R. Ortiz · C. Schulz · L. Gorton (✉)
Department of Analytical Chemistry/Biochemistry and Structural Biology, Lund University, P.O. Box 124, 226 46 Lund, Sweden
e-mail: Lo.Gorton@biochemistry.lu.se

Published online: 18 January 2013

PEGDGE	polyethyleneglycol diglycidyl ether
PMO	polysaccharide monooxygenase
SAM	self-assembled monolayer
SiNP	silica nanoparticles
SPR	surface plasmon resonance
SWCNT	single-walled carbon nanotube

Introduction

The last few years have witnessed tremendous development in bioelectrochemistry largely owing to the increased knowledge of making nanostructured electrodes surfaces [1–4] in combination with the understanding of how to bring about controlled architectures/orientation of biomolecules on such surfaces [5–10] and also the closer collaboration between (bio)electrochemists and biochemists/molecular biologists [11–22]. Additionally, research on and the foreseen need for practical applications, e.g. in electrochemical biosensors [23], biofuel cells [24–26] and bioelectrosynthesis [27], have also speeded up the research activities in this area. The drive to make bioelectrochemical devices/systems as simple as possible has put a focus on how to bring about efficient electron transfer reactions between the biologically derived material and electrodes without the need for additional and possibly leaching (and toxic) chemicals [28–32].

Cellobiose dehydrogenase (CDH) is a flavocytochrome [33] belonging to the restricted number of oxidoreductases that in their native wild-type form show efficient direct electron transfer (DET) between the active site and an electrode surface. CDH does this because it consists of two separate domains with different structures and inherent properties joined together by a polypeptide linker region. The larger flavodehydrogenase domain (DH_{CDH}) is catalytically active, whereas the smaller cytochrome domain (CYT_{CDH}) contains haem *b* as a cofactor and acts as an electron transfer protein between DH_{CDH} and a terminal, macromolecular electron acceptor. By 1991 Hill and co-workers [34] had divided the oxidoreductases, from a bioelectrochemical point of view, into two different groups—intrinsic and extrinsic—and characterised them as follows [34]:

Catalytic reaction between an enzyme and its substrate takes place within a highly localised assembly of redox-active sites. There need be no electron transfer pathways from these sites to the surface of the enzyme, where, it is presumed, it would interact with an electrode. For such intrinsic redox enzymes, electrode reactions may require (1) that the sites of the catalytic reaction be close to the protein surface, (2) that the enzyme can deform without loss of activity, (3) that the electrode surface projects into the enzyme, (4) that electron pathways be introduced by modification of the enzyme. With the extrinsic redox enzymes, there is usually another protein involved in transporting electrons and therefore an electron transfer pathway exists within the enzyme connecting the active sites to an area on the surface where the ancillary protein binds. If this area could be disposed toward an electrode, it would be possible for the enzyme electrochemistry to be obtained.

From a structural point of view CDH [35, 36] is obviously an extrinsic redox enzyme, where the CYT_{CDH} acts as a built-in mediator [37]. What further supports this is that in several recent reports it has been shown that copper-dependent polysaccharide monooxygenase (PMO) is likely to be the physiological redox partner of CDH which can therefore explain the role of CYT_{CDH} (Fig. 1) [38–41].

In 2010 we reviewed the basic electrochemical properties of CDH [19]; however, since then, a series of investigations on the biochemistry and bioelectrochemistry of various CDHs [42–44] have been pursued as well as one on the fundamentals of the intramolecular electron transfer (IET) between the two domains of CDH [45]. Furthermore a series of genetic work has been done to improve the glucose-oxidising properties of CDH (Ortiz et al. submitted) [46], in particular, as well as nanostructuring of both carbon [47] and gold-based electrodes [48, 49] to improve the loading and orientation of CDH on the electrode surface and thus also current densities. Especially in the field of biofuel cells [49–51] great progress has been made on the spatial arrangement of CDH on electrodes (Ortiz et al. submitted) [47–49, 52, 53] and CDH-based biosensors [54–58]. Such progress has prompted this new review on the bioelectrochemistry of CDH. One should also note that CDH has been used to make gold nanoparticles (AuNPs) and with the use of scanning electrochemical microscopy it was possible also to localise such AuNPs on surfaces with the help of CDH [59].

Occurrence and classification of CDH

Cellobiose dehydrogenase is secreted by white- and brown-rot, phytopathogenic as well as composting fungi from the dikaryotic phyla Basidiomycota and Ascomycota under cellulolytic culture conditions [60]. The CDH enzyme family is a heterogenous group of proteins with protein sequences between 749 and 816 amino acids long and sequence identities as low as 35 %. Phylogenetic analyses of these sequences showed several well-supported branches. Basidiomycete CDH sequences (from the Atheliales, Corticiales and Polyporales) form the branch of class I CDHs. Class II consists only of sequences of ascomycete origin (Sordariales, Xylariales and Hypocreales). This class of CDHs partitions into two subclasses: class IIA CDHs and class IIB CDHs. For members of the Eurotiales, Helotiales and Pleosporales, CDH-encoding sequences of a separate phylogenetic branch were found in sequenced genomes. The secretion of these

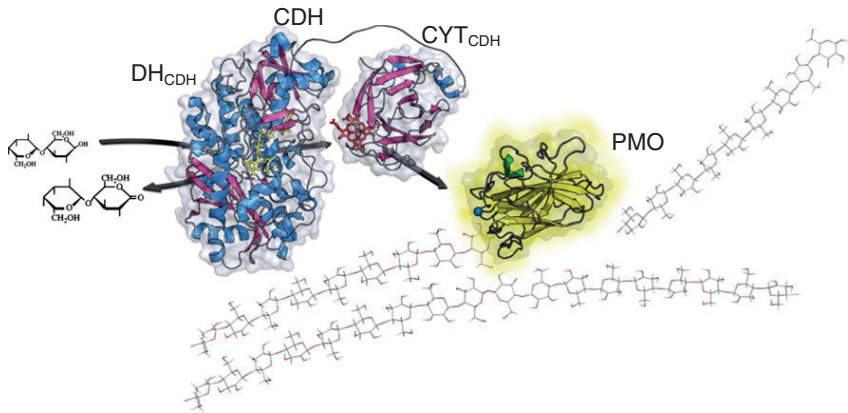

Fig. 1 Proposed in vivo function of CDH. Electrons from the oxidation of cellobiose or higher cellodextrins are acquired by CDH, which donates them to the surface-exposed type-2 copper centre of PMO to activate molecular oxygen for the cleavage of cellulose [38–41]. Initial studies show that the electron transfer via the CYT_{CDH} is quite efficient [62]

class III CDHs has not yet been confirmed [42, 60, 61]. The molecular architecture of CDHs from class I and II are slightly different. Whereas class I CDHs have supposedly a carbohydrate binding site on the DH_{CDH}, class IIA CDHs carry a small C-terminal family 1 carbohydrate binding module (CBM1), which is missing in class IIB CDHs.

The widespread appearance of CDH in fungi and the fact that it constitutes a considerable fraction of the lignocellulolytic enzymes secreted by these fungi (0.5–12 %) implies that CDH has an important function in wood degradation [62]. Recently the composition of lignocellulolytic enzyme cocktails and the up- and downregulation of single constituents were studied using transcriptomic and proteomic analyses [63–66]. Results from studies on the well-known ascomycete fungus *Neurospora crassa* and on the white-rot basidiomycete model organism *Phanerochaete chrysosporium* revealed that CDH genes are up-regulated during growth under cellulolytic conditions [66–68]. Important fungal producers of CDH are summarised in Table 1.

Structure and function

CDH is an extracellular fungal flavocytochrome (cellobiose:acceptor 1-oxidoreductase, EC 1.1.99.18) and is a monomeric protein consisting of two domains connected by a flexible linker of about 20 amino acids. The molecular mass ranges from 85 up to 101 kDa depending on the degree of glycosylation, which can account for up to 16 % of the molecular mass [19, 42, 69, 70]. The DH_{CDH} is a member of the glucose-methanol-choline oxidoreductase (GMC) family [61, 71]. The available structure of *P. chrysosporium* DH_{CDH} (PDB identifiers 1KDG and 1NNA [36]) is peanut shaped with dimensions of 72×57×45 Å. The average molecular mass of DH_{CDH} is ~60 kDa without glycosylation, which can contribute up to ~10 % of the total mass. The isoelectric point of DH_{CDH} is low and varies for different enzymes but is usually around 5 [60, 72, 73]. Oxidation of carbohydrates is catalysed by the non-covalently bound FAD cofactor in DH_{CDH}. The CYT_{CDH} structure available from *P. chrysosporium* (PDB identifiers 1D7B and 1D7C [35]) is formed by two ellipsoidal antiparallel β-sheets with dimensions of 47×36×47 Å. The average molecular mass is ~22 kDa without glycosylation and the isoelectric point of the CYT_{CDH} is very low, around 3. The haem cofactor is coordinated by Met 65 and His 163. This unusual ligation of haem *b* in CYT_{CDH} causes a relatively low redox potential, which is about 100–160 mV vs. normal hydrogen electrode (NHE) at pH 7.0 [62, 74, 75]. The N-terminal CYT_{CDH} is connected to DH_{CDH} via a flexible linker, which keeps the two domains in close contact and allows IET between them. Hence CDH can transfer reducing equivalents from an electron donor (e.g. cellobiose) via its two redox centres to different types of electron acceptors. Reoxidation of CDH can occur either directly at the (reduced) DH_{CDH} domain by transfer of reduction equivalents to a two-electron acceptor (e.g. quinones) or, alternatively, electrons can be sequentially shuttled from the reduced FAD to the haem *b* cofactor, followed by consecutive reduction of two one-electron acceptors (ferric iron complexes, cytochrome *c*) [60, 72, 73].

Recently a novel electron acceptor for CDH was identified. The PMOs are copper-dependent carbohydrate active enzymes (CAZy) of family GH61, which can receive

Table 1 Production of CDH by fungi

Fungal producer of CDH	Phylum	Volumetric activity (U L^{-1})	Activity assay[c]	Reference
Phanerochaete chrysosporium	B	66 (600[a])	Cellobiose, cyt *c*, pH 4.5	[139, 140]
Pycnoporus cinnabarinus	B	355	Cellobiose, DCIP, pH 4.5	[141]
Sclerotium rolfsii	B	7400 (15000[b])	Lactose, cyt *c*, pH 4.5	[69, 142]
Trametes villosa	B	580	Lactose, cyt *c*, pH 3.5	[142]
Trametes versicolor	B	2030	Cellobiose, cyt *c*, pH 3.5	[143]
Ceriporiopsis subvermispora	B	170	Lactose, DCIP, pH 6.0	[70]
Thielavia heterothallica	A	47	Cellobiose, cyt *c*, pH 4.5	[144, 145]
Corynascus thermophilus	A	4000	Lactose, DCIP, pH 5.0	[42]
Neurospora crassa	A	100	Lactose, DCIP, pH 5.5	[42]
Chaetomium sp. INBI 2-26(−)	A	190	Cellobiose, DCIP, pH 6.5	[146]

A ascomycete, *B* basidiomycete, *DCIP* 2,6-dichloroindophenol

[a] When supplemented with bovine calf serum

[b] When using increased concentrations of peptone or certain amino acids

[c] Activities can vary when using different assays based on other carbohydrate substrates (electron donors) and electron acceptors. The pH used in the assay is identical or close to the pH optimum

reducing equivalents from CDH and subsequently cleave cellulose by an oxidative mechanism. This interaction could be the key for the elucidation of the biological function of CDH and might end decades of speculation (Fig. 1) [38–41].

Catalytic properties of CDH

Preferred substrates of all CDHs are the β-1,4-linked di- and oligosaccharide breakdown products of cellulose—cellobiose or cellodextrins. Lactose has a very similar structure and is, although certainly not a natural substrate, also readily converted by CDHs [60]. A slight difference is observed between class I CDHs, which strongly discriminate glucose turnover, whereas some class II CDHs can also oxidise other mono- and disaccharides although with lower catalytic efficiencies. This difference might be an adaption to different fungal habitats and substrates [42, 45]. Catalysis takes place in the active site of DH_{CDH}, where two electrons and two protons are subtracted from the anomeric carbon atom of a substrate sugar residue in the reductive cycle, which results in a fully reduced FAD [76]. In the oxidative cycle the $FADH_2$ in the DH_{CDH} reduces electron acceptors such as 2,6-dichloroindophenol (DCIP), *o*- or *p*-benzoquinone and their derivatives, the 2,2′-azino-bis(3-ethylbenzothiazoline-6-sulfonate) (ABTS) cation radical, triiodide, strongly complexed iron ions, or oxygen. Alternatively, electrons can be donated to the haem *b*. Some electron acceptors like weakly complexed iron ions, cyt *c*, PMO and electrode surfaces depend on the action of the CYT_{CDH}. Cyt *c* is one of only a few one-electron acceptors which solely act with CYT_{CDH} and therefore is a good tool to estimate the IET (Fig. 2). The pH plays an important role in this reaction cascade. In class I CDHs the catalytic reaction at the active site and IET work only under acidic pH conditions. In class II CDHs three different groups of CDH with different IET behaviours were distinguished according to their pH-dependent interaction with cyt *c*: acidic, intermediate or neutral/alkaline IET optima [42] (Fig. 3). The same IET behaviour was found for these CDHs on polarised graphite electrodes [45].

Recombinant production of CDH

Although many lignocellulose-degrading fungi produce CDH in reasonable amounts their cultivation and subsequent protein purification are difficult and time consuming. Therefore, several *cdh* genes have been cloned and

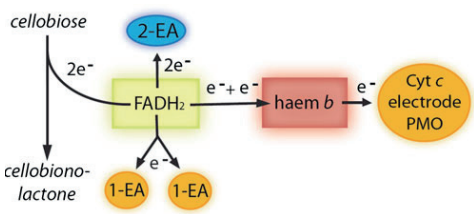

Fig. 2 Electron transfer in CDH from the substrate to various terminal electron acceptors. One- and two-electron acceptors (EA) can be reduced directly by the $FADH_2$ in the DH_{CDH}. Alternatively, electrons can be transferred by IET to the haem *b* in the CYT_{CDH}, which works as a relay for the reduction of macromolecular electron acceptors like PMO, cyt *c* or an electrode

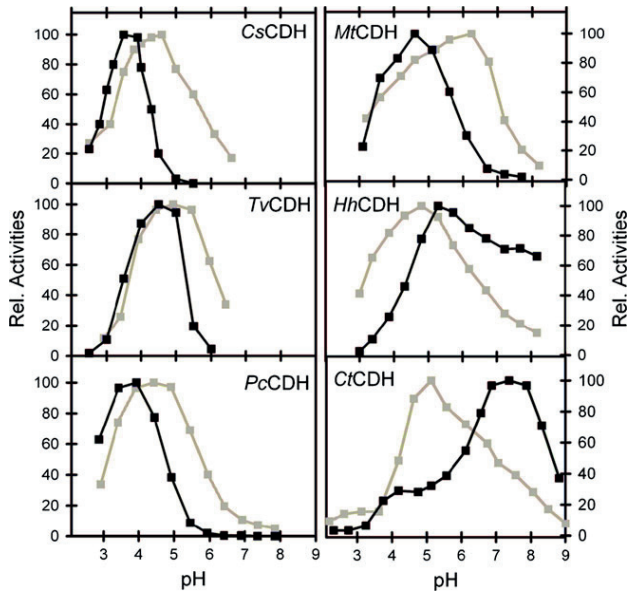

Fig. 3 Comparison of pH profiles of basidiomycetous class I and ascomycetous class II CDHs. In the *left column* acidic class I CDH from *Ceriporiopsis subvermispora* (*Cs*CDH) is shown above CDH from *Trametes villosa* (*Tv*CDH) and *Phanerochaete chrysosporium* (*Pc*CDH). The *right column* shows class II CDHs from *Myriococcum thermophilum* (*Mt*CDH), *Hypoxylon haematostroma* (*Hh*CDH) and *Corynascus thermophilus* (*Ct*CDH) with intermediate and neutral pH optima. DCIP (*grey lines*) indicates the activity of DH_{CDH}, whereas cyt *c* (*black lines*) is used to determine the pH dependency of the IET. For further information, see [42, 43, 45]

expressed in recombinant expression hosts. Li et al. [77] were the first to report recombinant expression of CDH by homologous overexpression of CDH in *P. chrysosporium*. The expression level was rather low (600 U L^{-1}), cultivation time was long (9 days) and genetic manipulation was difficult and time consuming. Therefore, Yoshida et al. [78] established the methylotrophic yeast *Pichia pastoris* as a heterologous expression system for *P. chrysosporium* CDH. Owing to the high reported expression levels, easy genetic manipulation and the ability of *Pichia* to perform eukaryotic post-translational modifications, it was used as an expression host for several basidiomyceteous and ascomeceteous CDHs during the following years (Table 2). Additionally, two ascomeceteous CDHs from *Thielavia terrestris* and *Humicola insolens* were recombinantly expressed in a fungal system, viz. *Aspergillus oryzae* [79, 80]. Several attempts to express CDH in the bacterial expression system *Escherichia coli* failed because of the different post-translational modifications of the two domains. However, the expression of the DH_{CDH} of *P. chrysosporium* was recently reported [81].

The advantages of recombinant protein expression are a fast, reliable and efficient enzyme production and the possibility to generate genetically engineered enzymes. However, some drawbacks have to be considered. A sub-stoichiometric occupation of the catalytic sites with the cofactor FAD in *C. thermophilus* CDH results in a generally lower specific activity of CDHs expressed in *P. pastoris* [75]. The fact that *Pichia* and *Aspergillus* produce several glycoforms of the recombinant protein results in an inhomogeneous enzyme preparation in respect to molecular mass and degree of glycosylation. Depending on the cultivation conditions and employed media a varying amount of proteolytically cleaved DH_{CDH} appears during purification [75, 82].

Direct electron transfer

The electron transfer pathways between the DH_{CDH} and an electrode can occur in principle along three different routes as illustrated in Figs. 2 and 4. In the first reaction the sugar substrate, an aldose, is oxidised at the C1 position (only the β-anomer is a substrate for CDH) into its corresponding lactone and concurrently the FAD in the active site of the DH_{CDH} is fully reduced to $FADH_2$-DH_{CDH}, reaction (1):

$$\text{aldose} + \text{FAD}-\text{DH}_{\text{CDH}} \rightarrow \text{lactone} + \text{FADH}_2-\text{DH}_{\text{CDH}} \quad (1)$$

The reoxidation of $FADH_2$-DH_{CDH} can be accomplished by a $2e^-$, $2H^+$ acceptor such as quinone (Q) or an equivalent aromatic redox compound according to reaction (2):

$$\text{FADH}_2-\text{DH}_{\text{CDH}} + \text{Q} \rightarrow \text{FAD}-\text{DH}_{\text{CDH}} + \text{QH}_2 \quad (2)$$

Table 2 Recombinant production of CDH and DH_{CDH} by recombinant expression hosts

Fungal producer of CDH	Expression host	Volumetric activity (U L^{-1})	Activity assay	Reference
Phanerochaete chrysosporium	*P. chrysospor.*[a]	600	Cellobiose, cyt *c*, pH 4.5	[77]
Phanerochaete chrysosporium	*P. pastoris*	1800	Cellobiose, cyt *c*, pH 4.5	[78]
P. chrysosporium DH_{CDH}	*E. coli*	733[b]	Cellobiose, DCIP, pH 5.0	[81]
Pycnoporus cinnabarinus	*P. pastoris*	7800	Cellobiose, DCIP, pH 5.0	[147]
Trametes versicolor	*P. pastoris*	5218	Cellobiose, cyt *c*, pH 4.2	[148]
Myriococcum thermophilum	*P. pastoris*	2150	Lactose, DCIP, pH 5.0	[82]
Neurospora crassa (CDH IIA)	*P. pastoris*	1700	Lactose, DCIP, pH 5.0	[62]
Neurospora crassa (CDH IIB)	*P. pastoris*	410	Lactose, DCIP, pH 5.0	[62]
Corynascus thermophilus	*P. pastoris*	376	Lactose, DCIP, pH 5.5	[75]
Thielavia terrestris	*A. oryzae*	NG	Cellobiose, DCIP, pH 6.0	[79]
Humicola insolens	*A. oryzae*	NG	Cellobiose, DCIP, pH 7.0	[80]

NG data not given

[a] Homologous overexpression

[b] Value refers to cell-free extract after cell disruption and not to cultivation volume

The reduced quinone, QH_2, will be reoxidised at the electrode if the applied potential (E_{app}) is set higher than the formal potential of the Q/QH_2 redox couple, $E^{o'}_{Q/QH_2}$, reaction (3):

$$QH_2 \xrightarrow{E_{app} > E^{o'}_{Q/QH_2}} Q + 2H^+ + 2e^- \quad (3)$$

Alternatively, a $1e^-$, non-H^+ acceptor, e.g. an Os^{3+} complex (Os^{3+}), accepts the electrons sequentially from the $FADH_2$-DH_{CDH}, whereby Os^{2+} complex (Os^{2+}) and the enzyme-stabilised semiquinone of the bound FAD, $FADH^{\bullet}$-DH_{CDH}, are formed in reaction (4):

$$FADH_2 - DH_{CDH} + Os^{3+} \rightarrow FADH^{\bullet} - DH_{CDH} + Os^{2+} + H^+ \quad (4)$$

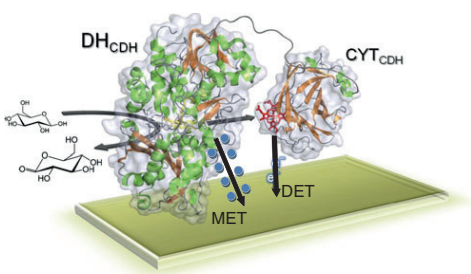

Fig. 4 Electron transfer between both CDH domains and the terminal electron acceptor. DET depends on CYT_{CDH} as an electron shuttle, whereas MET (*blue spheres* indicate soluble mediators or polymeric redox centres) transfers electrons directly from DH_{CDH} to the electrode surface

This reaction is then followed by the second electron transfer to a second Os^{3+}, whereby the fully oxidised DH_{CDH} is regained, reaction (5):

$$FADH^{\bullet} - DH_{CDH} + Os^{3+} \rightarrow FAD - DH_{CDH} + Os^{2+} + H^+ \quad (5)$$

The two Os^{2+} formed will be reoxidised at the electrode if E_{app} is set higher than the formal potential of the $Os^{3+/2+}$ redox couple, $E^{o'}_{Os^{3+/2+}}$, reaction (6):

$$2Os^{2+} \xrightarrow{E_{app} > E^{o'}_{Os^{3+/2+}}} 2Os^{3+} + 2e^- \quad (6)$$

The electrons can also be transferred from $FADH_2$-DH_{CDH} to the Fe^{3+}–CYT_{CDH} sequentially in an IET process according to reaction (7):

$$FADH_2 - DH_{CDH} - Fe^{3+} - CYT_{CDH} \xrightarrow{IET} FADH^{\bullet} - DH_{CDH} - Fe^{2+} - CYT_{CDH} + H^+ \quad (7)$$

This first electron transfer step is followed by reoxidation of the reduced CYT_{CDH}, Fe^{2+}–CYT_{CDH}, by an e^- acceptor such as Os^{3+} or cytochrome *c* (or by the electrode, see below); however, the second electron from the DH_{CDH} will then be subsequently transferred to the CYT_{CDH}, reaction (8):

$$FADH^{\bullet} - DH_{CDH} - Fe^{2+} - CYT_{CDH} + Os^{3+} \rightarrow FAD - DH_{CDH} - Fe^{2+} - CYT_{CDH} + Os^{2+} \quad (8)$$

Finally the last electron will be transferred from the CYT_{CDH} to a second $1e^-$ acceptor molecule, reaction (9):

$$FAD-DH_{CDH}-Fe^{2+}-CYT_{CDH}+Os^{3+} \rightarrow FAD-DH_{CDH}-Fe^{3+}-CYT_{CDH}+Os^{2+} \quad (9)$$

When CDH is immobilised on the electrode surface and in the absence of any competing e^- acceptors, the reoxidation of the reduced enzyme can be summarised as follows, reaction (10):

$$FADH_2-DH_{CDH}-Fe^{3+}-CYT_{CDH} \xrightarrow{\text{1st IET step}} FADH^{\bullet}{}^{-}DH_{CDH} - Fe^{2+}-CYT_{CDH}+H^+ \quad (10)$$

This step is followed by a first electron transfer (ET) step to the electrode, which is immediately followed by a second IET step delivering the second electron from the DH_{CDH} to the CYT_{CDH}, reaction (11):

$$FADH^{\bullet}{}^{-}DH_{CDH} - Fe^{2+}-CYT_{CDH} \xrightarrow{\text{1st ET to electrode and 2nd IET step}} FAD - DH_{CDH}-Fe^{2+}-CYT_{CDH}+H^++e^-(\text{electrode}) \quad (11)$$

Finally the second electron is then delivered to the electrode, reaction (12):

$$FAD-DH_{CDH} - Fe^{2+}-CYT_{CDH} \xrightarrow{\text{2nd ET to electrode}} FAD-DH_{CDH} - Fe^{3+}-CYT_{CDH}+e^-(\text{electrode}) \quad (12)$$

It is basically the DET properties of CDH that form the basis for the bioelectrochemical interest in this redox enzyme, ever since it was first documented [83]. The rather strict selectivity of the originally investigated class I basidiomycete CDHs for cellodextrins and lactose [60, 84] mainly found application in lactose biosensors for the dairy industry [55, 58, 85] or cellobiose biosensors that can be used to follow cellulose hydrolysis caused by cellulose-hydrolysing enzymes [54, 86]. However, when it was realised that the recently discovered ascomycete CDHs (class IIA and IIB) could also have high turnover rates for glucose (and a series of other mono- and oligosaccharides) and especially at neutral pH values (in contrast to class I CDHs that work best under slightly acidic conditions) an increased interest in CDH for application in biosensors and biofuel cells appeared [30, 42, 44, 49–51, 56, 57, 87–92].

Optimisation of direct electron transfer

Two approaches are used to optimise DET currents from CDH to electrodes. The first approach is based on new electrode materials, nanostructures and chemically modified electrode surfaces to either enhance the effective surface area available for CDH binding, or to increase the DET rate by suitable orientation of the enzyme on the surface. The second, biochemical approach uses modifications of the enzyme or the reaction cascade to increase the current of CDH-based electrodes. The following sections investigate the published work in the area of direct CDH/electrode interaction.

Novel nanostructures

The desire to increase the current density of bioelectrodes based on DET has led to the construction and use of nanostructured architectures so that a higher loading of the redox enzyme and a higher probability of correct orientation for DET can be obtained. Both the use of nanostructures based on the drop-casting deposition technique of nanomaterials such as single-walled carbon nanotubes (SWCNTs) [47, 89–91] (Ortiz et al. submitted) [93] or gold nanoparticles (AuNPs) [48, 49, 51] onto the electrode surface of Au, glassy carbon or graphite electrodes, as well as prefabricated carbon nanotube (CNT)-modified screen-printed electrodes [55, 57, 58] has been used and in all instances the use of nanomaterials resulted in an improved current density. An overview of the nanostructured materials used is presented in Table 3. For all the nanomaterials and immobilisation techniques tested only bioelectrocatalysis from CYT_{CDH} was observed.

Carbon-based nanomaterials

Initial investigations with various CDHs on SWCNT- or MWCNT-modified electrodes were based on direct adsorption of CDH on the nanomodified surface [55, 57, 89, 90, 93]. These studies used oxidatively shortened SWCNTs, kept as a suspension in water, without previous modification or commercially available screen-printed electrodes with MWCNT or SWCNT. No previous or further functionalisation of the nanomaterial was done and only in some of the studies was a cross-linker, i.e. polyethyleneglycol diglycidyl ether (PEGDGE) or glutaraldehyde (GA), was used in a following step to stabilise the enzyme–nanoparticle layer on the electrode surface. For screen-printed electrodes the use of a cross-linker increased the electrocatalytical currents in the presence of substrate by one order of magnitude for *T. villosa* and *Phanerochaete sordida* CDH-modified MWCNT screen-printed electrodes possibly owing to dissolution of certain components in the paste, thereby exposing a higher surface area for electric communication with the

Table 3 Nano- and surface modifications of CDH-based electrodes

Electrode nanomodification	Modification method	ET	Surface modification	Surface functionality	Measurement method	pH and substrate concentration	Current density ($\mu A cm^{-2}$)	Reference
GC+SWCNTs; *Ps*CDH	Drop-casting	DET	*p*-Phenylenediamine	NH_2	CV; 1 mV s^{-1}	3.5, 5 mM lactose	500	[47]
GC+SWCNTs; *Ps*CDH	Drop-casting	DET	*p*-Aminobenzoic acid	COOH	CV; 1 mV s^{-1}	4.5, 5 mM lactose	150	[47]
Au+AuNP; *Pc*CDH	Drop-casting	DET	ATP/MP+GA	OH	CV; 2 mV s^{-1}	4.5, 10 mM lactose	4.0	[48]
Au+AuNP; *Pc*CDH	Drop-casting	DET	ATP/MBA+GA	COOH	CV; 2 mV s^{-1}	4.5, 10 mM lactose	29.3	[48]
Au+AuNP; *Pc*CDH	Drop-casting	DET	$MUNH_2$/MUOH+GA	OH	CV; 2 mV s^{-1}	4.5, 10 mM lactose	11.6	[48]
Au+AuNP; *Pc*CDH	Drop-casting	DET	$MUNH_2$/MUA+GA	COOH	CV; 2 mV s^{-1}	4.5, 10 mM lactose	15.2	[48]
SPCE+MWCNT; *Tv*CDH	Drop-casting	DET	COOH-functionalised MWCNT	COOH	FIA	4.5, 0.1 mM lactose	0.08	[55]
SPCE+MWCNT; *Ps*CDH	Drop-casting	DET	COOH-functionalised MWCNT	COOH	FIA	4.5, 10 mM lactose	0.5	[55]
SPCE+MWCNT; *Ps*CDH	Drop-casting	DET	COOH-functionalised MWCNT and GA or PEDGDE	COOH	FIA	4.5, 10 mM lactose	5.6	[55]
GE+CNP; *CsCDH*	Drop-casting	DET	None	Not studied	CV; 2 mV s^{-1}	4.5, 50 mM lactose	297 deglycosylated enzyme ; 240 glycosylated enzyme	[94]
Au+SiNP+cyt *c*; *Tv*CDH	LbL (4 layers)	DET	COOH-functionalised SiNP	40 nm particles	CV; 5 mV s^{-1}	3.5, 5 mM lactose	4 nA[a] deglycosylated enzyme	[52]
Au+SiNP+cyt *c* *Tv*CDH	LbL (4 layers)	DET	COOH-functionalised SiNP	20 nm particles	CV; 5 mV s^{-1}	4.5, 5 mM lactose	28 nA[a] deglycosylated enzyme; 6 nA[a] g lycosylated enzyme	[52]
Au+SiNP+cyt *c*; *Tv*CDH	LbL (4 layers)	DET	COOH-functionalised SiNP	15 nm particles	CV; 5 mV s^{-1}	5.5, 5 mM lactose	9 nA[a] deglycosylated enzyme	[52]
Au+SiNP+cyt *c*; *Tv*CDH	LbL (4 layers)	DET	COOH-functionalised SiNP	5 nm particles	CV; 5 mV s^{-1}	6.5, 5 mM lactose	8 nA[a] deglycosylated enzyme	[52]
GE+SWCNT *Ps*CDH	Drop-casting	DET	PEGDGE	Not studied	FIA	5.3, 10 mM lactose	19.15	[90]
GE+SWCNT; *Ps*CDH	Drop-casting	DET	PEGDGE	Not studied	CV; 1 mV s^{-1}	4.5, 5 mM lactose	90	[90]
GE+SWCNT; *Pc*CDH	Drop-casting	DET	PEGDGE	Not studied	FIA	5.3, 10 mM lactose	6.84	[90]
GE+SWCNT; *Tv*CDH	Drop-casting	DET	PEGDGE	Not studied	FIA	5.3, 10 mM lactose	4.78	[90]
GE+SWCNT; *Sr*CDH	Drop-casting	DET	PEGDGE	Not studied	FIA	5.3, 10 mM lactose	1.36	[90]
GE+SWCNT+CDH; *Ps*CDH	Drop-casting	DET	Co-immobilisation with CNTs	Not studied	CV; 1 mV s^{-1}	3.5, 100 mM lactose	68	[93]
GE+SWCNT+CDH; *Ps*CDH	Drop-casting	DET	Co-immobilisation with CNTs	Not studied	LSV; 1 mV s^{-1}	4.0, 100 mM lactose	61.8	[93]
GE+SWCNT+CDH; *Ps*CDH	Drop-casting	DET	Co-immobilisation with CNTs	Not studied	LSV; 1 mV s^{-1}	4.5, 100 mM lactose	58	[93]

Table 3 (continued)

Electrode nanomodification	Modification method	ET	Surface modification	Surface functionality	Measurement method	pH and substrate concentration	Current density ($\mu A cm^{-2}$)	Reference
GE+SWCNT+CDH; *Ps*CDH	Drop-casting	DET	Co-immobilisation with CNTs	Not studied	LSV; 1 mV s^{-1}	5.0, 100 mM lactose	45	[93]
GE+SWCNT+CDH; *Ps*CDH	Drop-casting	DET	Co-immobilisation with CNTs	Not studied	LSV; 1 mV s^{-1}	5.5, 100 mM lactose	30	[93]
GE+SWCNT+CDH; *Ps*CDH	Drop-casting	DET	Co-immobilisation with CNTs	Not studied	LSV; 1 mV s^{-1}	6.0, 100 mM lactose	13	[93]
GE+SWCNT+CDH; *Ps*CDH	Drop-casting	MET	Co-immobilisation with CNTs+ PEGDGE	Not studied	LSV; 0.2 mV s^{-1}	3.5, 100 mM lactose	300	[93]
GE+SWCNT+CDH; *Ps*CDH	Drop-casting	MET	Co-immobilisation with CNTs+ PEGDGE	Not studied	LSV; 0.2 mV s^{-1}	4.0, 100 mM lactose	500	[93]
GE+SWCNT+CDH; *Ps*CDH	Drop-casting	MET	Co-immobilisation with CNTs+ PEGDGE	Not studied	LSV; 0.2 mV s^{-1}	4.5, 100 mM lactose	650	[93]
GE+SWCNT+CDH; *Ps*CDH	Drop-casting	MET	Co-immobilisation with CNTs+ PEGDGE	Not studied	LSV; 0.2 mV s^{-1}	5.0, 100 mM lactose	700	[93]
GE+SWCNT+CDH; *Ps*CDH	Drop-casting	MET	Co-immobilisation with CNTs+ PEGDGE	Not studied	LSV; 0.2 mV s^{-1}	6.0, 100 mM lactose	700	[93]
Au+AuNP; *Ct*CDH	Drop-casting	DET	ATP/MBA+GA	OH	LSV; 2 mV s^{-1}	7.4, 5 mM lactose; 100 mM glucose	40; 26	[49]
Au+AuNP; *Ct*CDH	Drop-casting	DET	ATP/MBA+GA	OH	LSV 2 mV s^{-1}	7.4, 5 mM glucose	7.5	[51]
SPCE+SWCNT; *Ct*CDH	Drop-casting	DET	PEDGDE	Not studied	FIA	7.4, 300 mM glucose	18.41	[57]
SPCE+MWCNT; *Ct*CDH	Drop-casting	DET	PEDGDE	Not studied	FIA	7.4, 300 mM glucose	15.58	[57]
GE+SWCNT; *Mt*CDH	Drop-casting	DET	PEGDGE	Not studied	FIA	5.3, 10 mM lactose	6.16	[89]
GE+SWCNT; *Mt*CDH	Drop-casting	DET	PEGDGE	Not studied	LSV; 1 mV s^{-1}	4.5, 100 mM lactose	5	[89]
GE+SWCNT; *Mt*CDH	Drop-casting	MET	Os-polymer+PEGDGE	Not studied	LSV; 1 mV s^{-1}	3.5, 100 mM lactose	68.4	[89]
GE+SWCNT; *Mt*CDH	Drop-casting	MET	Os-polymer+PEGDGE	Not studied	LSV; 1 mV s^{-1}	4.5, 100 mM lactose	102.6	[89]
GE+SWCNT; *Mt*CDH	Drop-casting	MET	Os-polymer+PEGDGE	Not studied	LSV; 1 mV s^{-1}	6.0, 100 mM lactose	205	[89]
GE+SWCNT	Drop-casting	MET	Os-polymer+PEGDGE	Not studied	LSV; 1 mV s^{-1}	7.0, 100 mM lactose	465	[89]
GE+SWCNT; *Mt*CDH	Drop-casting	MET	Os-polymer+PEGDGE	Not studied	CV; 1 mV s^{-1}	8.0, 100 mM lactose	800	[89]
GE+SWCNT; *Mt*CDH	Drop-casting	MET	Os-polymer+PEGDGE	Not studied	CV; 1 mV s^{-1}	7.4, 100 mM lactose; 50 mM glucose	450; 100	[89]
GC+SWCNTs; *Ct*CDH	Drop-casting	DET	*p*-Aminobenzoic acid	COOH	CV; 1 mV s^{-1}	7.4, 10 mM lactose; 50 mM glucose	30; 15	(Ortiz et al. submitted)
GC+SWCNTs; *Ct*CDH	Drop-casting	DET	Aniline	None	CV; 1 mV s^{-1}	7.4, 10 mM lactose; 50 mM glucose	21; 9	(Ortiz et al. submitted)
GC+SWCNTs; *Ct*CDH	Drop-casting	DET	*p*-Phenylenediamine	NH_2	CV; 1 mV s^{-1}	7.4, 10 mM lactose; 50 mM glucose	25; 13	(Ortiz et al. submitted)
GC+SWCNTs; *Ct*CDH	Drop-casting	DET	*p*-Phenylenediamine+GA	NH_2	CV; 1 mV s^{-1}	7.4, 10 mM lactose; 50 mM glucose	43; 21	(Ortiz et al. submitted)

Table 3 (continued)

Electrode nanomodification	Modification method	ET	Surface modification	Surface functionality	Measurement method	pH and substrate concentration	Current density ($\mu A cm^{-2}$)	Reference
GC+SWCNTs; *Ct*CDH	Drop-casting	DET	*N,N*-Diethyl-*p*-phenylenediamine	*N*-(*N,N*)-Diethyl	CV; 1 mV s^{-1}	7.4, 10 mM lactose; 50 mM glucose	16; 8	(Ortiz et al. submitted)
GC+SWCNTs; *Ct*CDH	Drop-casting	DET	*p*-Aminophenol	OH	CV; 1 mV s^{-1}	7.4, 10 mM lactose; 50 mM glucose	23; 14	(Ortiz et al. submitted)
GC+SWCNTs; *Ct*CDH	Drop-casting	DET	Not used	Not studied	CV; 1 mV s^{-1}	7.4, 10 mM lactose; 50 mM glucose	8; 4	(Ortiz et al. submitted)

GC glassy carbon, *GE* graphite electrode, *SPCE* screen-printed carbon electrodes, *SWCNT* single-walled carbon nanotubes, *MWCNT* multi-walled carbon nanotubes, *AuNP* gold nanoparticles, *SiNP* silica nanoparticles, *ET* electron transfer, *NA* not applicable, *LbL* layer by layer, *PEGDGE* polyethyleneglycol diglycidyl ether, *GA* glutaraldehyde, *CV* cyclic voltammetry, *MUOH* 11-mercapto-1-undecanol, *MUA* 11-mercapto-1-undecanoic acid, *MUNH*$_2$ mercapto-1-undecamine, *ATP* 4-aminothiophenol, *MP* 4-mercaptophenol, *MBA* 4-mercaptobenzoic acid

[a] Area of the electrode was not given

FIA results obtained through *flow injection analysis* with the CDH modified electrode mounted in a flow through amperometric cell and the maximum current response was followed after injection of a substrate containing sample volume

LSV results obtained with the CDH modified electrode investigated with *linear sweep voltammetry* taken the response value as the voltammetric peak current

immobilised CDH [55]. In the scope of this type of non-further functionalisation of the carbon nanomaterial, Ortiz et al. [94] increased the specific surface area by drop-casting carbon nanoparticles (CNPs) with a diameter of 27 nm onto graphite electrodes, which increased the electrocatalytical current by 350 times for deglycosylated *Ceriporiopsis subvermispora* CDH (297 $\mu A cm^{-2}$) and more than 500 times for glycosylated *C. subvermispora* CDH (240 $\mu A cm^{-2}$), see Table 3.

Gold nanoparticles and nanomaterials

Drop-casting of citrate-stabilised AuNPs with a diameter of 19 nm onto the surface of Au disk electrodes [95] was used in combination with mixed self-assembled thiol monolayers (SAMs), onto which *P. chrysosporium* CDH [48] or *C. thermophilus* CDH [49, 51] was covalently attached. The mixed SAM featured different thiols with amino, carboxy or hydroxyl head groups. The bifunctional cross-linker GA was used to form covalent bonds between the amino-terminated thiols and lysine residues on the enzyme. Cyclic voltammetry (CV) showed clear redox waves in the absence of substrate for all mixed SAMs tested and the heterogeneous electron transfer constant, k_s, could be calculated. An enhancement of the electrocatalytical activity of *P. chrysosporium* CDH of up to 75 times was achieved by this technique [48]. The procedure has been used further to prepare glucose/O_2 biofuel cell anodes using *C. thermophilus* CDH as the bioelement, in combination with cathodes based on adsorbed bilirubin oxidase (BOx) on AuNP-modified Au disks and nanowires [49, 51] (Table 3).

Layer-by-layer nanostructures

A different approach to achieve higher currents was taken by Lisdat et al., who, on the basis of previous work combining cyt *c* modified electrodes with CDH [96] and other redox enzymes [97–100], constructed a supramolecular structure using a layer-by-layer (LbL) immobilisation technique combining alternate layers of silica nanoparticles (SiNPs) and a mixture of *Tv*CDH and cyt *c* (Fig. 5) [52]. Various numbers of layers, i.e. 1, 2, 3 and 4, were investigated using both native glycosylated and also deglycosylated *Tv*CDH; the deglycosylated CDH yielded higher currents. The optimal SiNP particle size was 20 nm [52]. An LbL assembly technique was used. First a mixed SAM of MUA/MUOH was used to coat the Au surface and then SiNPs were adsorbed on the partially negatively charged surface, and finally a mixture containing *Tv*CDH and cyt *c* was added and the nanostructure was built up to four layers [52]. The same type of alkanethiol mixture was used to adsorb cyt *c* on a SAM of MUOH/MUA on gold wires. The bioelectrochemistry in the presence and the absence of

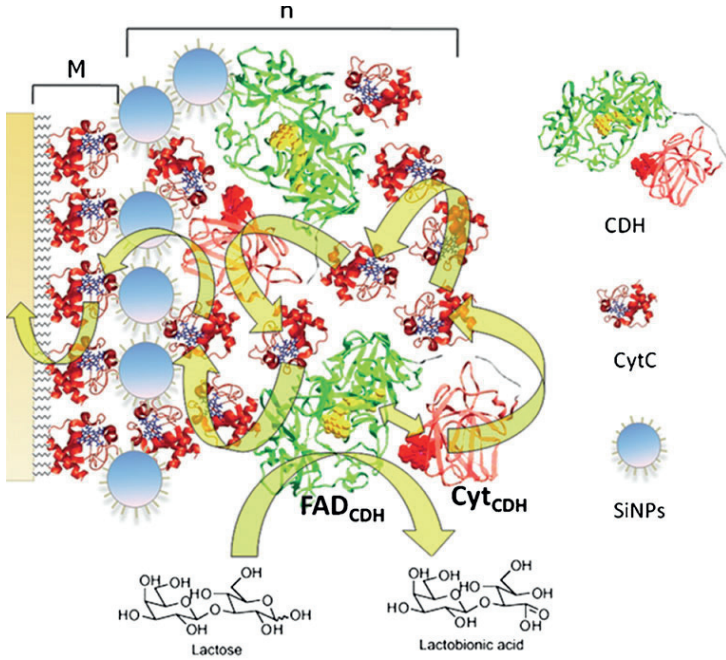

Fig. 5 Schematic representation of a supramolecular [SiNP/CDH·cyt *c*] architecture prepared on a cyt *c* monolayer electrode (M). The cyt *c* monolayer is assembled on a mixed thiol layer (MUOH/MUA). The layer by layer structure is [SiNPs/CDH·cyt *c*]$_n$ (*n*=1, 2, 3, 4), where *n* indicates the number of layers of SiNPs/CDH·cyt *c*. Reproduced from [52] with permission from The American Chemical Society

substrate was studied for solutions of *Tv*CDH and *Ct*CDH using this cyt *c* electrode; significantly, a shift of the optimal pH for electrocatalysis of cellobiose was observed using this approach [53].

Derivatisation of electrode surfaces

In the last few years functionalised SWCNTs have been tested in combination with CDH. It is established that the charge of the surface where CDH is immobilised has a strong effect on the electrochemistry of CDH. Investigations on different SAMs showed a strong effect of the functional group of the used thiol on the efficiency of the electrochemistry of CDH [44, 101–104]. Using the aryl amines *p*-phenylenediamine (NH_2-PD) or *p*-aminobenzoic acid (COOH-PD) for diazonium activation of the electrode surface, Tasca et al. [47] introduced amino or carboxylic groups, respectively, onto the SWCNTs previously drop-cast on glassy carbon electrodes. In the final step *Phanerochaete sordida* CDH, belonging to the class I CDHs, was adsorbed onto the modified electrode, where the positively charged $–NH_2$ functionalised surface or the negatively charged –COOH functionalised surface at the actual pH was used during CV measurements. For the $–NH_2$ functionalised surface a current density of 500 μA cm^{-2} was obtained in the presence of 5 mM lactose, which is the highest current density observed for any CDH-modified electrode based on DET (Fig. 6). For the –COOH functionalised SWCNTs a current density of ~150 μA cm^{-2} was obtained. The increased current density of the $–NH_2$ modified surface was attributed to a better orientation of the mainly negatively charged *P. sordida* CDH (isoelectric point=5.7) on the electrode. A similar modification procedure using a larger range of diazonium salts on SWCNTs drop-cast on GC was performed by (Ortiz et al. submitted), but in this case using the class II *C. thermophilus* CDH, which gave current densities of up to 25 μA cm^{-2} in the presence of 50 mM glucose.

Thiol-modified gold electrodes

Reports on facile electrochemistry of CDH trapped between a gold electrode modified with a thiol-based SAM and covered with a permselective membrane have appeared since the beginning of the 1990s [87, 101–104]. When such electrodes were investigated by CV they revealed clear non-turnover DET between the haem *b* cofactor of the CYT$_{CDH}$ in the absence of substrate, whereas in the presence of substrate a clear catalytic current was observed. The interaction between CDH and the thiol-based SAM-modified electrode results in facile electrochemistry which is

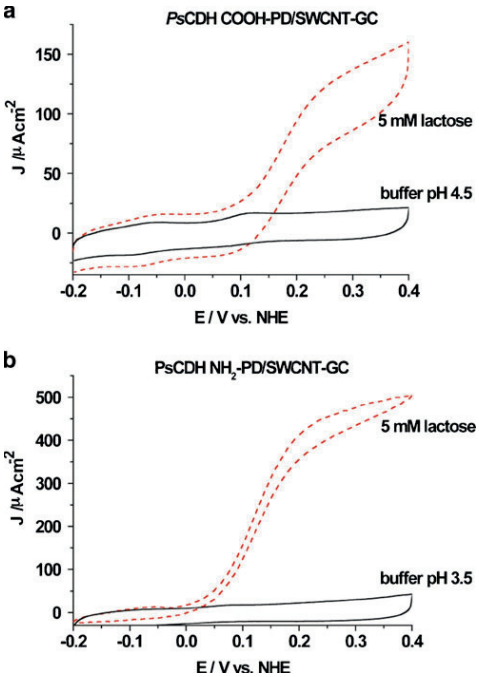

Fig. 6 **a** CV of a *P. sordida* CDH COOH-PD/SWCNT-GC electrode in the presence of 5 mM lactose (*red dashed line*) and in the absence of substrate (*black line*) at pH 4.5. **b** CV of a *P. sordida* CDH NH_2-PD/SWCNTs-GC electrode in the presence of 5 mM lactose (*red dashed line*) and in the absence of substrate (*black line*) at pH 3.5. Scan rate 1 mV s^{-1}. Reproduced from [47] with permission from The American Chemical Society

governed by a combination of different effects: (i) hydrophilic/hydrophobic interactions between the SAM and the enzyme that control the orientation on the electrode surface, e.g. interactions between the CDH cellulose binding domain with –OH terminated alkanethiols, as the cellulose binding domain has a strong affinity for naturally occurring hydroxyl groups present on cellulose [60], but also electrostatic interactions between oppositely charged SAMs and the surface of the enzyme; (ii) a dependency of the rate of ET on the distance between the electrode and the enzyme, described by the Marcus theory [105, 106]; and (iii) the compactness of the SAM, e.g. a densely packed SAM will slow down ET with the electrode.

Recently a series of investigations were performed on the interaction between various CDHs on gold and AuNP-modified solid gold electrodes [44, 48, 49, 51, 94]. In one study the effect of mutations close to the active site of study two different class II CDHs was investigated (Ortiz et al. submitted). In another study two class I CDHs were investigated [94], the focus being the effect of glycosylation/deglycosylation on the efficiency of DET. An exhaustive electrochemical investigation was performed on a number of class II CDHs (*Neurospora crassa*, *C. thermophilus*, *Humicola insolens*) and variants for improved glucose oxidation of *C. thermophilus* and *H. insolens* CDH using different aliphatic and aromatic thiols with varying head group functionalities (–NH_2, –COOH and –OH) and varying spacer lengths (2, 6 and 11 carbons) or a phenyl group [44] (Ortiz et al. submitted). For all CDHs tested electrodes with SAMs based on –OH functionalised thiols exhibited high electrocatalytical currents. In the case of *N. crassa* CDH the electrocatalytical currents became higher and the separation between the anodic and cathodic peak potentials (ΔE_p) of the CYT_{CDH} decreased when the –OH functionalised alkanethiol increased in length (Fig. 7) [44]. For *C. thermophilus* CDH the effect was the opposite and even more pronounced (Ortiz et al. submitted). *H. insolens* CDH showed in general small and poorly defined catalytical currents, but quasi-reversible CVs. The highest electrocatalytical responses for *H. insolens*, *N. crassa* and *C. thermophilus* CDH were found for mercaptohexanol, mercaptobenzoic acid and mercaptoethanol-based SAMs, respectively. *N. crassa* CDH also showed catalytic currents and a small ΔE_p for the thiols containing a phenyl group as spacer. On the other hand *C. thermophilus* CDH showed poor electrochemistry with such thiols. In another recent paper the electrochemistry of *P. chrysosporium* CDH was compared using four different thiols with –OH and –COOH head groups and different spacers [48]. In accordance with previous reports, the highest electrocatalytical currents for this class I CDH was found for mercaptoundecanol (MUOH). Interestingly, a lower current density was found for the equivalent thiol having a –COOH functionality (mercaptundecanoic acid, MUA). The reason could be electrostatic repulsion between the negatively charged CDH and the $–COO^-$ group. Harreither et al. [45] studied the $E^{\circ\prime}$ and the electrocatalytical activity of *C. thermophilus* CDH using thioglycerol at different pHs. The formal potential found, 100 mV vs. NHE, is the lowest reported so far for all investigated class II CDHs [45]. It can be concluded that the choice of the thiol is critical. Clear effects of the spacer length and the functional head group are observed.

When native, glycosylated, and deglycosylated CDH from *P. chrysosporium* and *C. subvermispora*, denoted *Pc*CDH, dg*Pc*CDH and *Cs*CDH, dg*Cs*CDH, respectively, were tested on an MUOH-based SAM, a higher current density was found for dg*Cs*CDH than for *Cs*CDH, but for dg*Pc*CDH and *Pc*CDH a similar current density was found [94]. The likely reason is that native *Cs*CDH is much more glycosylated than *Pc*CDH so that the effect of deglycosylation is more pronounced for *Cs*CDH.

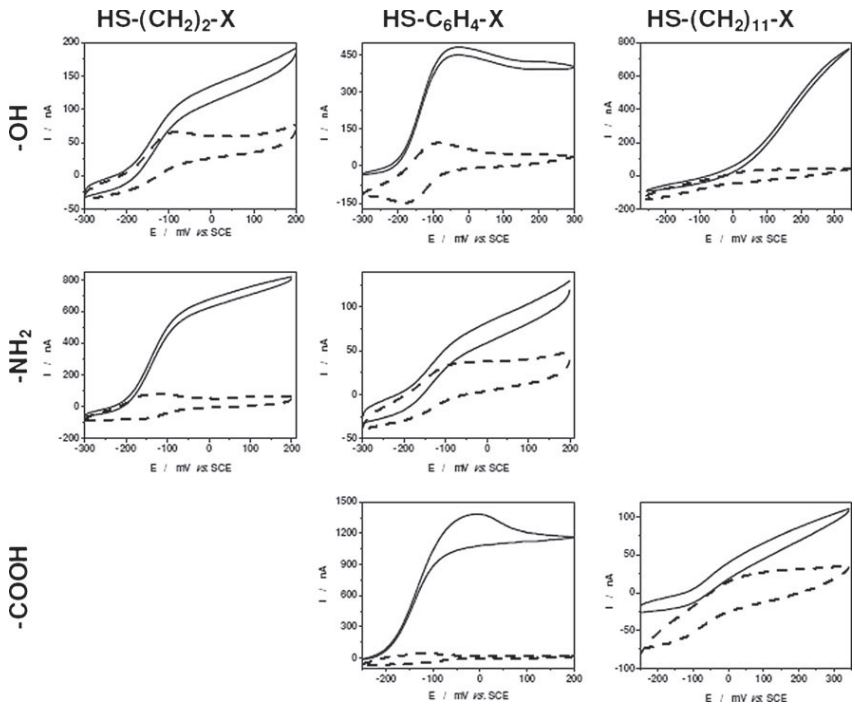

Fig. 7 Voltammetric responses of Au-mixed monolayer based SAM-*Neurospora crassa* CDH modified electrodes in absence (*dashed line*) and in presence (*solid line*) of 5 mM lactose. Experimental conditions: scan rate, 10 mV/s; supporting electrolyte, 50 mM citrate buffer pH 5.5. Reproduced from [44] with permission from Revue Roumaine de Chimie (Roumanian Journal of Chemistry)

Mixed thiol SAMs

Since the first bioelectrochemical studies on CDH in the late 1990s most studies have focused on the electrocatalytical activity. CV waves are not really observable on graphite electrodes modified with CDH owing to their high capacitive current. On the other hand, non-covalent interactions between CDH from different sources and gold electrodes or SAM-modified gold electrodes, and where the enzyme was retained behind a permselective membrane, has not shown stable electrochemical CV signals [102–104]. Efforts during recent years have focused on covalently immobilising CDH on alkanethiol-modified Au electrodes to avoid the usage of the permselective membrane [74, 102–104]. Matsumura et al. [48] compared immobilised CDH on four different SAMs based on two mixed thiols, where one of the head groups was $–NH_2$ and the other –COOH or –OH. GA was used to cross-link *P. chrysosporium* CDH to the amino group of the SAM. Matsumura et al. [48] used this approach to compare 11 different alkyl carbon chain based thiols as well as one incorporating a phenyl group as spacer and the head groups –OH with –COOH [48]. The ratio of the alkanethiol mixture (1:50 v/v) and GA (0.25 %) was optimised. The optimal ratio of the mixture for deglycosylated *P. chrysosporium* CDH, which has a smaller radius than its glycosylated form, was 1:40. This suggests that the surrounding glycosyl residues and the radius of the CDH have an effect [94]. This immobilisation protocol was also used in a 3D mesoporous structure created by drop-casting AuNPs on the surface of Au disk electrodes based on previous work by Murata et al. [95]. The k_s values for AuNP/SAM/GA/*Pc*CDH were lower for the mixture of thiols having a phenyl spacer than those based on the 11-carbon alkane spacer. The rate-limiting step of the overall ET was the DET between the CYT_{CDH} and the electrode instead of the IET from DH_{CDH} to CYT_{CDH} as measured by stoped-flow experiments. An overview of the current densities and k_s values is given in Table 4.

The same immobilisation procedure was applied for immobilising *C. thermophilu*s CDH on AuNP-modified

Table 4 Performance of *P. chrysosporium* CDH on mixed SAMs

Mixed SAMs	Polycrystalline gold	AuNPs				SPR
	J (μA cm^{-2})	J (μA cm^{-2})	$E^{\circ\prime}$ (mV)	ΔE (mV)	k_s (s^{-1})	Γ (pmol mm^{-2})
4-ATP/4-MP	0.26	4.0	161.7	14.7	59.8	5.79
4-ATP/4-MBA	0.40	29.3	161.5	14.6	52.1	5.71
$MUNH_2$/MUOH	0.34	11.6	161.8	14.7	154.0	5.67
$MUNH_2$/MUA	0.49	15.2	161.3	14.6	112.0	5.65

Current densities, J, surface coverage, Γ, k_s and $E^{\circ\prime}$ for covalently attached CDH onto mixed SAMs. J for polycrystalline gold and AuNPs were obtained at 300 mV vs. NHE. Formal potentials, $E^{\circ\prime}$, and peak separations, ΔE, at 0.2 V s^{-1}

ATP 4-aminothiophenol, *MP* 4-mercaptophenol, *MBA* 4-mercaptobenzoic acid, *$MUNH_2$* mercapto-1-undecamine, *MUOH* 11-mercapto-1-undecanol, *MUA* 11-mercapto-1-undecanoic acid, *SPR* surface plasmon resonance

Au disk and Au wire electrodes [49, 51]. The optimum GA amount (1 %) was higher than when using planar disk electrodes (0.25 %) [48], perhaps caused by the nanoparticle curvature but also because of using another CDH. A one-compartment mediator-less glucose/O_2 biofuel cell (BFC) working under physiological conditions was established using such a bioanode based on *C. thermophilus* CDH in combination with a biocathode based on BOx [49]. The BFC had an open-circuit voltage of 0.68 V and a maximum power density of 15 μW cm^{-2} at a cell voltage of 0.52 V in phosphate buffer and an open-circuit voltage of 0.65 V and a maximum power density of 3 μW cm^{-2} at a cell voltage of 0.45 V in human blood. The estimated half-lives of the biodevices were greater than 12, less than 8 and less than 2 h in a sugar-containing buffer, human plasma and blood, respectively. The basic characteristics of mediator-less sugar/oxygen BFCs were significantly improved compared with previously designed biodevices [50, 87], because of the usage of 3D AuNP-modified electrodes.

Influence of cations on the activity of CDH

A screening of the influence of various metal cations on the activity of CDH was done in 1999 for the basidiomycete *Schizophyllum commune* in solution [107]. The highest increase in cyt *c* activity by 8 % was caused by the presence of 2 mM Cu^{2+} and the highest decrease by 70 % was caused by the presence of 2 mM Ag^{+}, thereby showing the ability of cations to modulate the activity of CDH. A further study with immobilised *P. chrysosporium* CDH on a spectrographic graphite electrode showed a 50 % increase in the catalytic current for lactose and cellobiose following the addition of 80 mM NaCl to the buffer [108]. The molecular interactions behind this observation are unknown, but it was excluded that an increased CDH/electrode interaction was the reason.

Recently the influence of cations on the activity of two class II CDHs from *Myriococcum thermophilum* and *Humicola insolens* and one class I CDH from *P. chrysosporium* was investigated in more detail in solution and when immobilised on spectrographic graphite electrodes [109]. When immobilised on the graphite electrode the DET current for *M. thermophilum* CDH was most tunable by addition of $CaCl_2$ in the millimolar range and exhibited up to a fivefold increase in the catalytic currents (Fig. 8a). The DET current of *H. insolens* CDH-modified electrodes was enhanced fourfold, but for *P. chrysosporium* CDH only 2.4-fold. The exchange of $CaCl_2$ by $MgCl_2$ tuned the DET current in a similar manner. However, KCl had a much lower effect and enhanced DET currents by a maximum of twofold for *M. thermophilum* CDH. Activity assays based on cyt *c* were used to investigate the modulation of the IET of *M. thermophilum* and *H. insolens* CDH in solution. Similar dependencies of the cyt *c* activities on $CaCl_2$ were observed as for the immobilised CDHs. The separately expressed DH_{CDH} from *H. insolens* showed no cyt *c* activity and no dependency on any added cations. Similarly, the DCIP activity of *H. insolens* DH_{CDH} was completely independent of added $CaCl_2$ or KCl. It can be concluded that divalent cations increase either the interaction between the DH_{CDH} and CYT_{CDH} domains or between the CYT_{CDH} domain and the final electron acceptor, which can be cyt *c* or an electrode.

Polyethylenimine as a promoter layer

In analogy to the enhancing effect of $CaCl_2$, a current-increasing effect of the branched polycation polyethylenimine (PEI) as a promoter layer was anticipated for the construction of CDH-modified biosensors. Beneficial effects have been shown in several publications covering, for example, cyt *c* on carbon electrodes [110], the detection of NADH with phenoxazine derivative modified carbon paste electrodes [111, 112] and some other redox enzyme modified carbon paste electrodes [113–117] or improved electrochemistry of human sulfite oxidase on PEI-modified

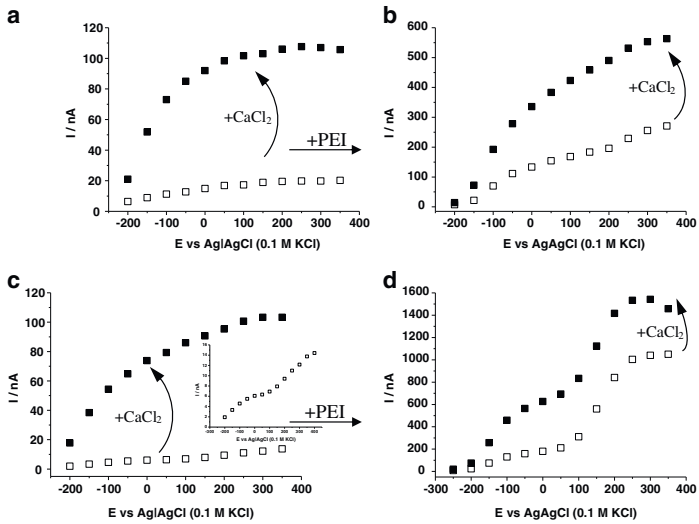

Fig. 8 Variation of response current (I) with the applied potential (E) of spectrographic graphite electrodes modified with *Myriococcum thermophilum* CDH (**a**, **c**) and optionally pre-modified with polyethylenimine (PEI) (**b**, **d**) in 50 mM sodium acetate buffer pH 5.5 (**a**, **b**) or 50 mM TRIS pH 8.0 (**c**, **d**) in the absence (*white squares*) or in the presence of 50 mM $CaCl_2$ (*black squares*) with 5 mM lactose as substrate. The *inset* in **c** shows a magnification of the response curve

gold nanoparticles [118]. In recent work the influence of PEI as a promoter layer on spectrographic graphite electrodes modified with *M. thermophilum* CDH was investigated. The pre-modification of a graphite electrode with PEI increased the maximal catalytic current from the oxidation of 3.75 mM lactose by around 13 times at pH 5.5 (pH optimum) and by around 87 times at pH 8.0 (Fig. 8). The modification with PEI also shifted the pH optimum from 5.5 to 8.0, which is interesting for biosensor applications measuring at human physiological pH (7.4). A further addition of 50 mM $CaCl_2$ still shows enhancing effects, but is less pronounced in the presence of PEI. This indicates that PEI acts similarly to $CaCl_2$. Another explanation would be an increased surface loading of *M. thermophilum* CDH on the PEI-modified electrode owing to strong electrostatic binding of CDH to PEI [19].

Besides the enhancing effect of PEI on the catalytic currents, the CVs unexpectedly revealed two catalytic redox waves. One starting at −100 mV vs. Ag|AgCl (0.1 M KCl) representing the expected ET from the CYT_{CDH} domain to the electrode [74] and a second catalytic wave, most pronounced at pH 8.0 and starting at around 100 mV, which is visible even in the absence of PEI (Fig. 8c, inset). The origin of the second catalytic wave is unknown, but has been observed before for *P. chrysosporium* CDH [108] and is currently under investigation. However, the enhancing effect of PEI is also clearly present at potentials below the second catalytic wave. Until now the beneficial effect of PEI was only observed for class II *M. thermophilum* CDH. The catalytic responses of class II *N. crassa* CDH and class I *P. chrysosporium* CDH could not be improved by the pre-modification of graphite electrodes with PEI. This is probably because the latter CDHs already have a more efficient DET and/or IET compared to that of *M. thermophilum* CDH [43, 88, 119].

Deglycosylation

Deglycosylation of enzymes has been used to facilitate the electron transfer and even to achieve DET from deeply buried prosthetic groups of redox enzymes, even from deeply buried FAD in e.g. *Aspergillus niger* glucose oxidase (GOx) [120–123]. CDH is a glycoprotein that shows a glycosylation between 8 and 16 % [19] depending on the organism used for expression. The carbohydrate chains are believed to stabilise the tertiary protein structure and increase the solubility of the protein molecule. A voluminous carbohydrate structure on the enzyme surface will act as an insulator for enzymes attached to electrodes [120]. Opposed to what was found for GOx and pyranose dehydrogenase, deglycosylation of CDH did not result in any DET between the FAD in the DH_{CDH} domain and an electrode. However, the catalytic current densities increased two- to threefold in the presence of lactose, for deglycosylated *P. chrysosporium* (9 % glycosylated) and *C. subvermispora* CDH (16 % glycosylated) compared with their glycosylated counterparts when adsorbed on spectrographic graphite electrodes (Fig. 9) [94]. The apparent Michaelis–Menten constant K_M^{app} for lactose was also found to decrease by two- to threefold for the deglycosylated CDHs compared to the glycosylated

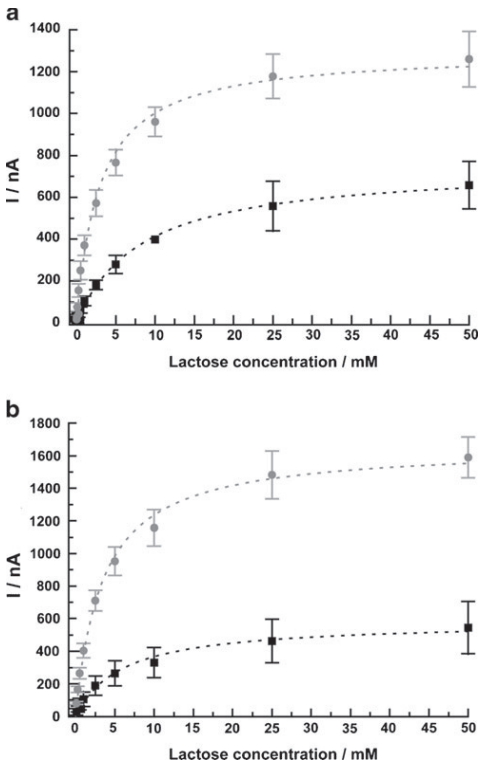

Fig. 9 Dependence of the amperometric response on lactose concentration of **a** glycosylated *Phanerochaete chrysosporium* CDH (*squares*) and deglycosylated *P. chrysosporium* CDH (*circles*) and **b** glycosylated *Ceriporiopsis subvermispora* CDH (*squares*) and deglycosylated *C. subvermispora* CDH (*circles*) in acetate buffer (pH 4.5). The applied potential was +150 mV vs. Ag|AgCl (0.1 M KCl) and the flow rate of the solution (pH 4.5) was 1 mL min^{-1}. The results were obtained in a flow-injection system. Reproduced from [94] with permission from The American Chemical Society

ones. When the enzymes were compared trapped under a permselective membrane and 11-mercaptoundecanol (MUOH) SAM-modified Au disk electrodes, glycosylated and deglycosylated *P. chrysosporium* CDH showed the same catalytic activity, whereas glycosylated and deglycosylated *C. subvermispora* CDH showed similar results to that obtained on spectrographic graphite electrodes, i.e. a much higher catalytic current was found when using the deglycosylated form. The $E^{\circ\prime}$ for the deglycosylated CDH was found to shift up by ~8 mV. In a different study glycosylated and deglycosylated *T. villosa* CDH were compared when immobilised on an LbL supramolecular architecture stabilised by electrostatic interaction between the layers. Au wire electrodes were first modified with a mixed monolayer of MUOH and MUA. Then successively alternating layers of carboxy-terminated SiNPs and a mixture of cyt *c* and *T. villosa* CDH were added and a supramolecular structure was built up to four bilayers. Using this technique, Feifel et al. [52] found a maximum increase of seven times higher faradaic currents in the presence of lactose as substrate for the deglycosylated variant. The results suggest that the increase in current density is attributed to an increase in the amount of molecules packed on the electrodes, i.e. to a more compact packing of CDH on the electrode surface and in the layers.

Mediated electron transfer

Even though a system based on DET is, from a fundamental point of view, more interesting than one based on MET, there are limitations to the current density that can be reached with DET. Even though it should be possible to immobilise multilayers of a redox enzyme with DET properties, it is expected that primarily only the innermost layer of enzyme molecules on the electrode surface will be able to electrochemically communicate with the electrode. However, through the use of nanostructured electrodes and with CDH oriented for improved DET [47–49] the current density can be largely increased compared with that obtained with conventional electrodes. Moreover, as DET between CDH and an electrode is obtained through the CYT_{CDH}, which has an $E^{\circ\prime}$ value much more positive than that of the FAD of the DH_{CDH} [74, 124], in a BFC anode based on MET using a mediator with an $E^{\circ\prime}$ much lower than that of the CYT_{CDH} (and close to that of the DH_{CDH}), both the power output and the current density can be largely improved [89, 91, 93, 125]. An overview of MET approaches with CDH was given in 2010 [19]. Since then mainly two directions have been followed. The first is the combination of CDH with cyt *c* as a mediator in an LbL approach, as discussed separately above. The second is the further development and application of osmium polymers, which were first applied together with CDH as early as 1992 [126] on the basis of the work by Heller and co-workers [127, 128]. Similar to the use of other sugar-oxidising redox enzymes in biosensors and biofuel cells [129–136], the "wiring" of various CDHs with Os-redox polymers accepting electrons direct from the DH_{CDH} is very promising for obtaining high current densities at low potentials [46, 90, 91, 93, 125]. During the last few years particular focus was given to electrodeposited Os-polymers (Os-EDPs), which contain, in addition to the polymeric backbone and the redox-active Os-complex, either one or more COO^- or NH_3^+ groups. Deposition of those

polymers is achieved by local changes of the pH at the electrode surface caused by either electrolysis or change of buffer, resulting in discharged and insoluble Os-polymers that precipitate on the electrode surface. Schuhmann and co-workers [125, 137] synthesised and investigated 50 different Os-EDPs having redox potentials ranging from −430 to +667 mV vs. Ag|AgCl. Os-polymer-mediated electron transfer was shown for CDH, glucose oxidase and PQQ-dependent glucose dehydrogenase suitable for biofuel cell anodes and for laccase and BOx suitable for corresponding cathodes [125, 137]. In a recent paper a bi-enzyme bioanode modified with an Os-DEP, the separate DH_{CDH} of *C. thermophilus* and pyranose dehydrogenase (PDH) from *Agaricus meleagris* were investigated for the multiple oxidation of glucose [46]. As CDH oxidises its substrate at the C1 it is only possible to gain two electrons per substrate molecule. However, if CDH is combined with PDH it is possible to obtain up to six electrons per substrate molecule, as PDH oxidises the sugar substrate at either C2 or C3 or both and the product when the substrate is oxidised by CDH is a substrate for PDH and vice versa. Figure 10 outlines how glucose can be oxidised at an anode where *C. thermophilus* CDH is co-immobilised with *Agaricus meleagris* PDH yielding six electrons instead of only two.

However, conventional mediators such as *p*-benzoquinone (BQ) are still in use as well. When comparing the efficiency of DET for a CDH-modified electrode in relation to MET it is quite convenient to use BQ dissolved in the buffer. This approach has been used previously [88] and was also used for the characterisation of various CDHs [45], especially for *N. crassa* CDH immobilised on spectrographic graphite electrodes with various substrates at pH 5.2 and 7 [43]. A biosensor for the real-time measurement of cellobiohydrolase activity was established by Cruys-Bagger and co-workers [54] using a BQ-containing carbon paste electrode modified with cross-linked *P. chrysosporium* CDH. The sensor detected cellobiose with a sensitivity of 87.7 μA

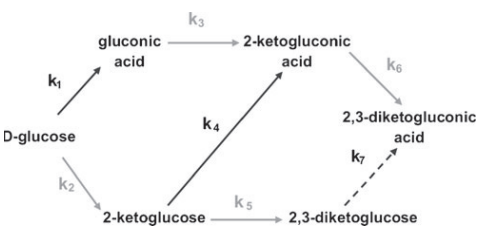

Fig. 10 Reaction pathway of glucose oxidation by a bi-enzymatic system consisting of CDH (C1 oxidation, *black arrows*) and *Agaricus meleagris* PDH (C2 and C3 oxidation, *grey arrows*). Reproduced from [46] with permission from Elsevier

mM^{-1} cm^{-2}, a low detection limit of 25 nM and a response time of ca. 3 s.

Application of CDH in biosensors

CDH was used in two ways in biosensors: either to detect the oxidation of carbohydrates or reduce quinones and catecholamines for signal amplification in an oxidative electrode setup. In a recent review the application of CDH in biosensors until 2010 is described in detail [19]; here we give an overview of developments in the few last years (Table 5). Depending on the source of CDH, specific catalytic properties allow the oxidation of different substrates by different CDHs and therefore different analytes in terms of biosensor applications. Class I CDHs show a very high specificity for β-1,4-linked substrates and are therefore ideal bioelements for the detection of cellobiose and lactose. But it has to be considered that these CDHs work only efficient under acidic pH conditions. Very sensitive lactose sensors based on class I CDH have been developed for use in the dairy industry; these have a detection limit down to 250 nM, which corresponds to 90 μg L^{-1} [55, 58, 85]. In a different approach a lactose biosensor was developed by the combination of the thermometric signal from lactose oxidation with the amperometric signal of the enzymatic reaction [138]. In contrast to the third-generation biosensor reported by Safina et al. [55], the amperometric signal was based on the reduction of hydroquinone, which is formed during the oxidation of lactose by CDH.

In another recent example, a CDH biosensor was designed to measure the cellobiohydrolase activity on insoluble cellulose [54]. The ability of CDH to oxidise cellobiose—the reaction product of cellobiohydrolase—was used to monitor the transient kinetics of cellobiohydrolase. The approach could be validation by HPLC analysis and represents an interesting real-time method to monitor cellulase activity. The discovery that class II CDHs are able to oxidise the monosaccharide glucose opened the door to designing a third-generation glucose biosensor [88]. Beside their altered substrate specificity, class II CDHs are not restricted to work under acidic pH conditions. Probably the most interesting candidate for a glucose biosensor is the CDH from *C. thermophilus* because the highest DET rates were found under human physiological pH conditions [45]. The third-generation glucose biosensor based on CDH showed a linear range between 0.1 and 30 mM, which makes it suitable for measuring blood glucose levels [47, 57]. This CDH should allow the construction of a simple glucose biosensor which does not depend on oxygen or any other artificial redox mediators and therefore represents an interesting alternative to established biosensors based on glucose

Table 5 CDH-based biosensors

Analyte	Detection limit	Sensitivity ($\mu A\ mM^{-1}\ cm^{-2}$)	Mediator/ enhancer[a]	Electrode modification	Electrode material	CDH	Reference
Noradrenaline	1 nM	15,800	Cellobiose	Adsorption	SG	*Pc*CDH	[85]
Catechol	1 nM	9,500	Cellobiose	Adsorption	SG	*Pc*CDH	[85]
Hydroquinone	0.75 nM	11,140	Cellobiose	Adsorption	SG	*Pc*CDH	[85]
L-Adrenaline	5 nM	1,140	Cellobiose	Adsorption	SG	*Pc*CDH	[85]
3-Hydroxylamine hydrochloride	2.5 nM	9,160	Cellobiose	Adsorption	SG	*Pc*CDH	[85]
3,4-Hydroxyphenylacetic acid	1 nM	13,440	Cellobiose	Adsorption	SG	*Pc*CDH	[85]
Lactose	1 μM	17.8	No	Adsorption	SG	*Tv*CDH	[85]
Lactose	1 μM	11.0	No	Adsorption	SG	*Ps*CDH	[85]
Lactose	1 μM	1.06	No	Adsorption	SG	*Mt*CDH	[88]
Lactose	1 μM	2.8	No	Adsorption	SCE	*Mt*CDH	[149]
Lactose	1 μM	0.38	No	PANI+adsorption	SCE	*Mt*CDH	[149]
Lactose	250 nM	NG	No	Cross-linked	SCE	*Ps*CDH	[55, 58]
Lactose	50 μM	NG	BQ	Covalent binding	CPG	*Rec. Pc*CDH	[138]
Cellobiose	25 μM	0.8	No	Adsorption	SG	*Pc*CDH	[150]
Cellobiose	25 μM	23	Os-polymer	Entrapment	SG	*Pc*CDH	[150]
Cellobiose	0.5 μM	1.85	No	Adsorption	SG	*Mt*CDH	[88]
Cellobiose	25 nM	87.7	Hydroquinone	Cross-linked	SG	*Rec. Pc*CDH	[54]
Glucose	1 mM	0.0068	No	Adsorption	SG	*Mt*CDH	[88]
Glucose	0.05 mM	0.22	No	Cross-linked+ SWCNTs	SG	*Ct*CDH	[56]
Glucose	0.01 mM	NG	No	Cross-linked+ SWCNTs	SCE	*Ct*CDH	[57]

SG spectroscopic graphite, *SCE* screen-printed carbon electrode, *PANI* polyaniline, *CPE* carbon paste electrode, *Rec.* recombinant, *NG* value not given

[a] To increase the signal of catecholamines the enzyme's carbohydrate substrate was applied for signal amplification by recycling of the analyte

oxidase and glucose dehydrogenase. The main targets for optimising CDH-based biosensors recently focused on the increase in current densities leading to higher sensitivities by designing the interface between the electrode and the enzyme.

Recent advances in CDH-based biofuel cell anode performance

The initial work on BFC applications was based on spectroscopic graphite electrodes modified with adsorbed CDH. The class I CDHs from *P. chrysosporium* [90, 93], *T. villosa* [125] and *Dichomera saubinetii* [87] and the class II CDHs from *M. thermophilum* [89, 90] and *C. thermophilus* [50] were used in these initial studies with lactose or glucose as the anodic fuel. In order to increase the current density in some of the studies, SWCNTs were also applied to increase the aspect ratio surface area to achieve higher loadings of adsorbed CDH [89, 90, 93]. Mediating Os-polymers were also applied to achieve a direct contact of the electrode with the DH_{CDH} domain aiming at higher power densities gained at lower potentials [89, 91, 93]. To maximise the open-circuit voltage, it is desirable to have enzyme molecules in

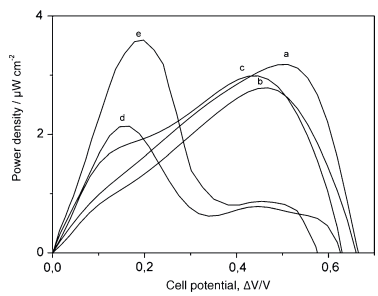

Fig. 11 Dependency of the power density on the operating voltage of a glucose/O_2 biofuel cell based on Au|AuNP|*Ct*CDH||bilirubin oxidase|AuNP|Au under air-saturated quiescent conditions in *a* PBS pH 7.4, 5 mM glucose; *b* human blood; *c* human plasma; *d* unstimulated human saliva; *e* human basal tears. Reproduced from [51] with permission from Elsevier

DET communication with the electrode, in the absence of redox mediators. Most recently the focus for BFC-based setups using CDH has been on the use of gold nanoparticles (AuNPs). On the basis of the work by Murata et al. [95] on nanomodification of polycrystalline Au electrodes with AuNPs, a covalent immobilisation technique for CDH was developed by Matsumura et al. [48] based on a SAM of mixed thiols, amino and hydroxyl or carboxylic acid terminated, and GA as a cross-linker. The technique was optimised and further used with a *C. thermophilus* CDH-based anode in combination with a BOx-based cathode to construct a one-compartment, mediator-less BFC working under human physiological conditions with glucose/O_2 as the fuel [49]. The performance of the biodevice was evaluated in blood and plasma. In buffer containing glucose, the open-circuit potential was 0.66 V with a maximum power density of 3.3 $\mu W\ cm^{-2}$ at a cell voltage of 0.52 V. The performance was only slightly reduced in the physiological fluids. The half-life was 30 h in buffer, 8 h in blood and 2 h in plasma. The same modification was used to fabricate a device tested in lachrymal fluid (tears) for possible future applications on non-invasive medical devices ex vivo [51]. The CDH/BOx/AuNP-based nanodevice had an open-circuit potential of 0.57 V with a maximum power density of 3.5 $\mu W\ cm^{-2}$ at a comparably low operational voltage of 0.2 V, probably owing to interferences with ascorbic acid and dopamine. At 0.5 V a maximum power density of only 0.8 $\mu W\ cm^{-2}$ was observed because of the low concentration of glucose in the lachrymal fluid. Figure 11 shows the performance of the BFC in the described buffers and physiological fluids.

Conclusions and outlook

CDH is an emerging biocatalyst for biosensors and biofuel cells. Its versatility originates from its unique molecular properties, but also from the catalytic heterogeneity of CDHs from different sources. Differences in the pH optima, the pH optima for IET, the substrate specificity, etc., span a wide range and provide a toolbox of CDHs for different tasks and applications. Over 20 CDHs from different fungi have been characterised so far and recombinant expression techniques guarantee access to these enzymes. An issue of importance with CDH is, however, the microheterogeneity of enzyme preparations, especially glycoforms. Glycosyl residues alter the IET, but also the binding to electrode surfaces and the orientation on the electrode and are therefore an important factor to watch in future experiments. Another critical factor is the loading of FAD in recombinantly produced ascomycete CDHs. The substochioimetric presence of FAD in the DH_{CDH} results in apparently lower turnover numbers and reduces the catalytic current. Alternative expression strategies or expression hosts should be tested for better results. The development of specifically modified electrode surfaces, either by chemical modification or by nanostructures, has tremendously increased the currents achievable with CDH-modified electrodes. A combination of the approaches from materials science and enzyme engineering will have great impact on the development of CDH-modified electrodes with high current densities in the milliampere per square centimetre range. Such high current densities will ultimately allow miniaturisation of CDH electrodes down to single carbon fibre electrodes, which can be used in miniaturised biosensors for continuous on-site or point-of-care measurements. Finally, one should mention the exciting use of ionic liquids in combination with CDH. Ionic liquids are potential candidates as non-aqueous solvents in this context and were shown to improve the shelf-life of CDH bound to AuNPs and carbon nanoparticles [151, 152].

Acknowledgments The authors thank the following agencies for financial support: the European Commission (project 3D-Nanobiodevice NMP4-SL-2009-229255, project Chebana FP7-PEOPLE-2010-ITN-264772), the nmC@LU, the Swedish Research Council (project 621-2010-5031), the Austrian Science Fund (translational project FWF L395-B11) and the Austrian Academy of Science (APART project 11322) and the New Zealand Ministry of Innovation, Business and Enterprise (formerly the Ministry of Science and Innovation).

References

1. Deepshikha, Basu T (2011) Anal Lett 44(6):1126–1171
2. Iost RM, Madurro JM, Brito-Madurro AG, Nantes IL, Caseli L, Crespilho FN (2011) Int J Electrochem Sci 6(7):2965–2997
3. Plowman BJ, Bhargava SK, O'Mullane AP (2011) Analyst 136 (24):5107–5119
4. Rahman MM, Ahammad AJS, Jin J-H, Ahn SJ, Lee J-J (2010) Sensors 10(5):4855–4886
5. Asefa T, Duncan CT, Sharma KK (2009) Analyst 134(10):1980–1990
6. Chen D, Wang G, Li JH (2007) J Phys Chem 111(6):2351–2367
7. Gooding JJ, Darwish N (2012) Chem Rec 12(1):92–105
8. Pingarron JM, Yanez-Sedeno P, Gonzalez-Cortes A (2008) Electrochim Acta 53(19):5848–5866
9. Shipway AN, Katz E, Willner I (2000) Chem Phys Chem 1(1):18–52
10. Xiao YH, Li CM (2008) Electroanalysis 20(6):648–662
11. Alferov S, Coman V, Gustavsson T, Reshetilov A, von Wachenfeldt C, Hägerhäll C, Gorton L (2009) Electrochim Acta 54(22):4979–4984
12. Baronian K, Downard A, Lowen R, Pasco N (2003) Appl Microbiol Biotechnol 60(1–2):108–113
13. Chelikani V, Downard AJ, Kunze G, Gooneratne R, Pasco N, Baronian KHR (2012) Electrochim Acta 73:136–140
14. Chelikani V, Rawson FJ, Downard AJ, Gooneratne R, Kunze G, Pasco N, Baronian KHR (2011) Biosens Bioelectron 26(9):3737–3741
15. Coman V, Gustavsson T, Finkelsteinas A, Von Wachenfeldt C, Hägerhäll C, Gorton L (2009) J Am Chem Soc 131(44):16171–16176

16. Durand F, Kjaergaard CH, Suraniti E, Gounel S, Hadt RG, Solomon EI, Mano N (2012) Biosens Bioelectron 35(1):140–146
17. Hasan K, Patil SA, Górecki K, Leech D, Hägerhäll C, Gorton L (2012) Bioelectrochemistry. doi:10.1016/j.bioelechem.2012.05.004
18. Kostesha NV, Almeida JRM, Heiskanen AR, Gorwa-Grauslund MF, Hahn-Hägerdahl B, Emnéus J (2009) Anal Chem 81 (24):9896–9901
19. Ludwig R, Harreither W, Tasca F, Gorton L (2010) Chem Phys Chem 11(13):2674–2697
20. Patil SA, Hasan K, Leech D, Hägerhäll C, Gorton L (2012) Chem Commun 48(82):10183–10185
21. Rawson FJ, Garrett DJ, Leech D, Downard AJ, Baronian KHR (2011) Biosens Bioelectron 26(5):2383–2389
22. Rawson FJ, Gross AJ, Garrett DJ, Downard AJ, Baronian KHR (2012) Electrochem Commun 15(1):85–87
23. Katz E, Willner I (2004) Chem Phys Chem 5(8):1085–1104
24. Meredith MT, Minteer SD (2012) Annu Rev Anal Chem 5 (1):157–179
25. Osman MH, Shah AA, Walsh FC (2011) Biosens Bioelectron 26 (7):3087–3102
26. Willner I, Yan YM, Willner B, Tel-Vered R (2009) Fuel Cells 9 (1):7–24
27. Rabaey K, Rozendal RA (2010) Nat Rev Microbiol 8(10):706–716
28. Barton SC, Gallaway J, Atanassov P (2004) Chem Rev 104 (10):4867–4886
29. Cracknell JA, Vincent KA, Armstrong FA (2008) Chem Rev 108 (7):2439–2461
30. Falk M, Blum Z, Shleev S (2012) Electrochim Acta 82:191–202
31. Leger C, Bertrand P (2008) Chem Rev 108(7):2379–2438
32. Woolerton TW, Sheard S, Chaudhary YS, Armstrong FA (2012) Energ Environ Sci 5(6):7470–7490
33. Mowat CG, Gazur B, Campbell LP, Chapman SK (2010) Arch Biochem Biophys 493(1):37–52
34. Guo LH, Hill HAO (1991) Adv Inorg Chem 36:341–376
35. Hallberg BM, Bergfors T, Baeckbro K, Pettersson G, Henriksson G, Divne C (2000) Structure 8(1):79–88
36. Hallberg MB, Henriksson G, Pettersson G, Divne C (2002) J Mol Biol 315(3):421–434
37. Ikeda T, Kobayashi D, Matsushita F, Sagara T, Niki K (1993) J Electroanal Chem 361(1–2):221–228
38. Beeson WT, Phillips CM, Cate JHD, Marletta MA (2012) J Am Chem Soc 134(2):890–892
39. Langston JA, Shaghasi T, Abbate E, Xu F, Vlasenko E, Sweeney MD (2011) Appl Environ Microbiol 77(19):7007–7015
40. Li X, Beeson WT, Phillips CM, Marletta MA, Cate JHD (2012) Structure 20(6):1051–1061
41. Phillips CM, Beeson WT, Cate JH, Marletta MA (2011) ACS Chem Biol 6(12):1399–1406
42. Harreither W, Sygmund C, Augustin M, Narciso M, Rabinovich ML, Gorton L, Haltrich D, Ludwig R (2011) Appl Environ Microbiol 77(5):1804–1815
43. Kovacs G, Ortiz R, Coman V, Harreither W, Popescu IC, Ludwig R, Gorton L (2012) Bioelectrochemistry 88:84–91
44. Kovacs G, Ortiz R, Coman V, Harreither W, Popescu IO, Ludwig R, Gorton L (2012) Rev Roum Chim 57:361–368
45. Harreither W, Nicholls P, Sygmund C, Gorton L, Ludwig R (2012) Langmuir 28(16):6714–6723
46. Shao M, Nadeem Zafar M, Sygmund C, Guschin DA, Ludwig R, Peterbauer CK, Schuhmann W, Gorton L (2013) Biosens Bioelectron 40:308–314
47. Tasca F, Harreither W, Ludwig R, Gooding JJ, Gorton L (2011) Anal Chem 83(8):3042–3049
48. Matsumura H, Ortiz R, Ludwig R, Igarashi K, Samejima M, Gorton L (2012) Langmuir 28(29):10925–10933
49. Wang X, Falk M, Ortiz R, Matsumura H, Bobacka J, Ludwig R, Bergelin M, Gorton L, Shleev S (2012) Biosens Bioelectron 31 (1):219–225
50. Coman V, Ludwig R, Harreither W, Haltrich D, Gorton L, Ruzgas T, Shleev S (2010) Fuel Cells 10(1):9–16
51. Falk M, Andoralov V, Blum Z, Sotres J, Suyatin DB, Ruzgas T, Arnebrant T, Shleev S (2012) Biosens Bioelectron 37(1):38–45
52. Feifel SC, Ludwig R, Gorton L, Lisdat F (2012) Langmuir 28:9189–9194
53. Sarauli D, Ludwig R, Haltrich D, Gorton L, Lisdat F (2012) Bioelectrochemistry 87:9–14
54. Cruys-Bagger N, Ren G, Tatsumi H, Baumann MJ, Spodsberg N, Andersen HD, Gorton L, Borch K, Westh P (2012) Biotechnol Bioeng 109:3199–3204
55. Safina G, Ludwig R, Gorton L (2010) Electrochim Acta 55:7690–7695
56. Tasca F, Zafar MN, Harreither W, Nöll G, Ludwig R, Gorton L (2011) Analyst 136(10):2033–2036
57. Zafar MN, Safina G, Ludwig R, Gorton L (2012) Anal Biochem 425(1):36–42
58. Glithero N, Clark C, Gorton L, Schuhmann W, Pasco N (2012) Anal Bioanal Chem (in press)
59. Malel E, Ludwig R, Gorton L, Mandler D (2010) Chem Eur J 16 (38):11697–11706
60. Zamocky M, Ludwig R, Peterbauer C, Hallberg BM, Divne C, Nicholls P, Haltrich D (2006) Curr Prot Pept Sci 7 (3):255–280
61. Zámocký M, Hallberg M, Ludwig R, Divne C, Haltrich D (2004) Gene 338(1):1–14
62. Sygmund C, Kracher D, Scheibelbrandner S, Zahma K, Felice AK, Kittl R, Harreither W, Ludwig R (2012) Appl Environ Microbiol 78(17):6161–6171
63. Phillips CM, Iavarone AT, Marletta MA (2011) J Proteome Res 10(9):4177–4185
64. Sun J, Glass NL (2011) PLoS One 6(9):1–14
65. Sun J, Tian C, Diamond S, Louise Glassa N (2012) Eukaryot Cell 11(4):482–493
66. Tian C, Beeson WT, Iavarone AT, Sun J, Marletta MA, Cate JHD, Glass NL (2009) Proc Natl Acad Sci U S A 106(52):22157–22162
67. MacDonald J, Doering M, Canam T, Gong Y, Guttman DS, Campbell MM, Master ER (2011) Appl Environ Microbiol 77 (10):3211–3218
68. Wymelenberg AV, Sabat G, Martinez D, Rajangam AS, Teeri TT, Gaskell J, Kersten PJ, Cullen D (2005) J Biotechnol 118(1):17–34
69. Baminger U, Subramaniam SS, Renganathan V, Haltrich D (2001) Appl Environ Microbiol 67(4):1766–1774
70. Harreither W, Sygmund C, Dünhofen E, Vicuña R, Haltrich D, Ludwig R (2009) Appl Environ Microbiol 75(9):2750–2757
71. Cavener DR (1992) J Mol Biol 223(3):811–814
72. Cameron MD, Aust SD (2001) Enzyme Microb Technol 28(2–3):129–138
73. Henriksson G, Johansson G, Pettersson G (2000) J Biotechnol 78 (2):93–113
74. Coman V, Harreither W, Ludwig R, Haltrich D, Gorton L (2007) Chem Anal (Warsaw) 52(6):945–960
75. Harreither W, Felice AKG, Paukner R, Gorton L, Ludwig R, Sygmund C (2012) Biotechnol J 7:1359–1366
76. Hallberg BM, Henriksson G, Pettersson G, Vasella A, Divne C (2003) J Biol Chem 278(9):7160–7166
77. Li B, Rotsaert FAJ, Gold MH, Renganathan V (2000) Biochem Biophys Res Commun 270(1):141–146

78. Yoshida M, Ohira T, Igarashi K, Nagasawa H, Aida K, Hallberg BM, Divne C, Nishino T, Samejima M (2001) Biosci Biotechnol Biochem 65(9):2050–2057
79. Langston JA, Brown K, Xu F, Borch K, Garner A, Sweeney MD (2012) Biochim Biophys Acta, Protein Proteom 1824 (6):802–812
80. Xu F, Golightly EJ, Duke KR, Lassen SF, Knusen B, Christensen S, Brown KM, Brown SH, Schülein M (2001) Enzyme Microb Technol 28(9–10):744–753
81. Desriani, Ferri S, Sode K (2010) Biotechnol Lett 32(6):855–859
82. Zámocký M, Schümann C, Sygmund C, O'Callaghan J, Dobson ADW, Ludwig R, Haltrich D, Peterbauer CK (2008) Protein Expr Purif 59(2):258–265
83. Larsson T, Elmgren M, Lindquist SE, Tessema M, Gorton L, Henriksson G (1996) Anal Chim Acta 331(3):207–215
84. Maischberger T, Nguyen TH, Sukyai P, Kittl R, Riva S, Ludwig R, Haltrich D (2008) Carbohydr Res 343(12):2140–2147
85. Stoica L, Ludwig R, Haltrich D, Gorton L (2006) Anal Chem 78 (2):393–398
86. Hildén L, Eng L, Johansson G, Lindqvist S-E, Pettersson G (2001) Anal Biochem 290(2):245–250
87. Coman V, Vaz-Dominguez C, Ludwig R, Herreither W, Haltrich D, De Lacey AL, Ruzgas T, Gorton L, Shleev S (2008) Phys Chem Chem Phys 10(40):6093–6096
88. Harreither W, Coman V, Ludwig R, Haltrich D, Gorton L (2007) Electroanalysis 19(2–3):172–180
89. Tasca F, Gorton L, Harreither W, Haltrich D, Ludwig R, Nöll G (2008) J Phys Chem 112(35):13668–13673
90. Tasca F, Gorton L, Harreither W, Haltrich D, Ludwig R, Nöll G (2008) J Phys Chem 112(26):9956–9961
91. Tasca F, Gorton L, Kujawa M, Patel I, Harreither W, Peterbauer CK, Ludwig R, Nöll G (2010) Biosens Bioelectron 25(7):1710–1716
92. Vasilchenko LG, Karapetyan KN, Yershevich OP, Ludwig R, Zamocky M, Peterbauer CK, Haltrich D, Rabinovich ML (2011) Biotechnol J 6(5):538–553
93. Tasca F, Gorton L, Harreither W, Haltrich D, Ludwig R, Nöll G (2009) Anal Chem 81(7):2791–2798
94. Ortiz R, Matsumura H, Tasca F, Zahma K, Samejima M, Igarashi K, Ludwig R, Gorton L (2012) Anal Chem 84:10315–10323
95. Murata K, Kajiya K, Nukaga M, Suga Y, Watanabe T, Nakamura N, Ohno H (2010) Electroanalysis 22:185–190
96. Fridman V, Wollenberger U, Bogdanovskaya V, Lisdat F, Ruzgas T, Lindgren A, Gorton L, Scheller FW (2000) Biochem Soc Trans 28(2):63–70
97. Dronov R, Kurth DG, Möhwald H, Spricigo R, Leimkühler S, Wollenberger U, Rajagopalan KV, Scheller FW, Lisdat F (2008) J Am Chem Soc 130(4):1122–1123
98. Lisdat F, Dronov R, Möhwald H, Scheller FW, Kurth DG (2009) Chem Commun (3):274–283
99. Spricigo R, Dronov R, Lisdat F, Leimkühler S, Scheller FW, Wollenberger U (2009) Anal Bioanal Chem 393(1):225–233
100. Spricigo R, Dronov R, Rajagopalan KV, Lisdat F, Leimkühler S, Scheller FW, Wollenberger U (2008) Soft Matter 4(5):972–978
101. Lindgren A (2000) Electrochemistry of heme containing enzymes - fundamentals and applications. Lund University, Lund, Doctoral dissertation
102. Lindgren A, Gorton L, Ruzgas T, Baminger U, Haltrich D, Schülein M (2001) J Electroanal Chem 496(1–2):76–81
103. Lindgren A, Larsson T, Ruzgas T, Gorton L (2000) J Electroanal Chem 494(2):105–113
104. Stoica L, Dimcheva N, Haltrich D, Ruzgas T, Gorton L (2005) Biosens Bioelectron 20(10):2010–2018
105. Marcus RA (1965) J Chem Phys 43(2):679–701
106. Marcus RA, Sutin N (1985) Biochim Biophys Acta Rev Bioenerg 811(3):265–322
107. Fang J, Huang F, Gao P (1999) Process Biochem 34(9):957–961
108. Larsson T, Lindgren A, Ruzgas T, Lindquist SE, Gorton L (2000) J Electroanal Chem 482(1):1–10
109. Schulz C, Ludwig R, Micheelsen PO, Silow M, Toscano MD, Gorton L (2012) Electrochem Commun 17:71–74
110. Lojou E, Bianco P (2007) Electrochim Acta 52(25):7307–7314
111. Domínguez E, Lan HL, Okamoto Y, Hale PD, Skotheim TA, Gorton L, Hahn-Hägerdal B (1993) Biosens Bioelectron 8(3–4):229–237
112. Ladiu CI, Popescu IC, Gorton L (2005) J Solid State Electrochem 9(5):296–303
113. Gorton L, Jönsson-Pettersson G, Csöregi E, Johansson K, Domínguez E, Marko-Varga G (1992) Analyst 117(8):1235–1241
114. Kacaniklic V, Johansson K, Marko-Varga G, Gorton L, Jönsson-Pettersson G, Csöregi E (1994) Electroanalysis 6(5–6):381–390
115. Lutz M, Burestedt E, Emnéus J, Lidén H, Gobhadi S, Gorton L, Marko-Varga G (1995) Anal Chim Acta 305(1–3):8–17
116. Spohn U, Narasaiah D, Gorton L, Pfeiffer D (1996) Anal Chim Acta 319(1–2):79–90
117. Vijayakumar AR, Csöregi E, Heller A, Gorton L (1996) Anal Chim Acta 327(3):223–234
118. Frasca S, Rojas O, Salewski J, Neumann B, Stiba K, Weidinger IM, Tiersch B, Leimkühler S, Koetz J, Wollenberger U (2012) Bioelectrochemistry 87:33–41
119. Stoica L, Ruzgas T, Ludwig R, Haltrich D, Gorton L (2006) Langmuir 22(25):10801–10806
120. Courjean O, Gao F, Mano N (2009) Angew Chem Int Ed Engl 48:5897–5899
121. Demin S, Hall EAH (2009) Bioelectrochemistry 76(1–2):19–27
122. Lindgren A, Tanaka M, Ruzgas T, Gorton L, Gazaryan I, Ishimori K, Morishima I (1999) Electrochem Commun 1 (5):171–175
123. Yakovleva M, Killyeni A, Popescu IO, Ortiz R, Schulz C, MacAodha D, Ó Conghaile P, Leech D, Peterbauer CK, Gorton L (2012) Electrochem Commun 24:120–122
124. Igarashi K, Verhagen M, Samejima M, Schülein M, Eriksson KEL, Nishino T (1999) J Biol Chem 274(6):3338–3344
125. Stoica L, Dimcheva N, Ackermann Y, Karnicka K, Guschin DA, Kulesza PJ, Rogalski J, Haltrich D, Ludwig R, Gorton L, Schuhmann W (2009) Fuel Cells 9(1):53–62
126. Elmgren M, Lindquist SE, Henriksson G (1992) J Electroanal Chem 341(1–2):257–273
127. Gregg BA, Heller A (1991) J Phys Chem 95(15):5970–5975
128. Heller A (1992) J Phys Chem 96(9):3579–3587
129. Heller A (2004) Phys Chem Chem Phys 6(2):209–216
130. Heller A (2006) Curr Opin Chem Biol 10(6):664–672
131. Heller A (2006) Anal Bioanal Chem 385(3):469–473
132. Heller A, Feldman B (2008) Chem Rev 108(7):2482–2505
133. Mano N, Mao F, Heller A (2004) ChemBioChem 5(12):1703–1705
134. Mano N, Mao F, Heller A (2004) Chem Commun (18):2116–2117
135. Mao F, Mano N, Heller A (2003) J Am Chem Soc 125(16):4951–4957
136. Pothukuchy A, Mano N, Georgiou G, Heller A (2006) Biosens Bioelectron 22(5):678–684
137. Guschin DA, Castillo J, Dimcheva N, Schuhmann W (2010) Anal Bioanal Chem 398(4):1661–1673
138. Yakovleva M, Buzas O, Matsumura H, Samejima M, Igarashi K, Larsson P-O, Gorton L, Danielsson B (2012) Biosens Bioelectron 31(1):251–256
139. Bao W, Usha SN, Renganathan V (1993) Arch Biochem Biophys 300(2):705–713

140. Habu N, Igarashi K, Samejima M, Pettersson B, Eriksson K-EL (1997) Biotechnol Appl Biochem 26(2):97–102
141. Temp U, Eggert C (1999) Appl Environ Microbiol 65(2):389–395
142. Ludwig R, Haltrich D (2003) Appl Microbiol Biotechnol 61 (1):32–39
143. Roy BP, Dumonceaux T, Koukoulas AA, Archibald FS (1996) Appl Environ Microbiol 62(12):4417–4427
144. Canevascini G, Borer P, Dreyer J-L (1991) Eur J Biochem 198(1):43–52
145. Subramaniam SS, Nagalla SR, Renganathan V (1999) Arch Biochem Biophys 365(2):223–230
146. Vasil'chenko LG, Khromonygina VV, Karapetyan KN, Vasilenko OV, Rabinovich ML (2005) J Biotechnol 119(1):44–59
147. Bey M, Berrin JG, Poidevin L, Sigoillot JC (2011) Microb Cell Fact 10:113
148. Stapleton PC, O'Brien MM, O'Callaghan J, Dobson ADW (2004) Enzyme Microb Technol 34(1):55–63
149. Trashin SA, Haltrich D, Ludwig R, Gorton L, Karyakin AA (2009) Bioelectrochemistry 76(1–2):87–92
150. Tessema M, Larsson T, Buttler T, Csöregi E, Ruzgas T, Nordling M, Lindquist SE, Pettersson G, Gorton L (1997) Anal Chim Acta 349(1–3):179–188
151. Fujita K, Nakamura N, Igarashi K, Samejima M, Ohno H (2009) Green Chem 11:351–354
152. Fujita K, Nakamura N, Murata K, Igarashi K, Samejima M, Ohno H (2011) Electrochim Acta 56:7224–7227

Paper III

International Journal of Pharmaceutics 468 (2014) xxx–xxx

Contents lists available at ScienceDirect

International Journal of Pharmaceutics

journal homepage: www.elsevier.com/locate/ijpharm

Quantifying the release of lactose from polymer matrix tablets with an amperometric biosensor utilizing cellobiose dehydrogenase

Patrik Knöös [a,1,*], Christopher Schulz [b,1,**], Lennart Piculell [a], Roland Ludwig [c], Lo Gorton [b], Marie Wahlgren [d,***]

[a] Division of Physical Chemistry, Lund University, Box 124, Lund SE-22100, Sweden
[b] Department of Biochemistry and Structural Biology, Lund University, Box 124, Lund SE-22100, Sweden
[c] Food Biotechnology Laboratory, Department of Food Sciences and Technology, BOKU University of Natural Resources and Life Sciences, Vienna, Austria
[d] Division of Food Technology, Lund University, Box 124, Lund SE-22100, Sweden

ARTICLE INFO

Article history:
Received 31 January 2014
Received in revised form 28 March 2014
Accepted 30 March 2014
Available online 12 April 2014

Keywords:
Controlled release
Polymer matrix
Biosensors
Cellobiose dehydrogenease
Lactose release
Release mechanisms

ABSTRACT

The release of lactose (hydrophilic) from polymer tablets made with hydrophobically modified poly (acrylic acid) (HMPAA) have been studied and compared to the release of ibuprofen, a hydrophobic active substance. Lactose is one of the most used excipients for tablets, but lactose release has not been widely studied. One reason could be a lack of good analytical tools. A novel biosensor with cellobiose dehydrogenase (CDH) was used to detect the lactose release, which has a polydiallyldimethylammonium chloride (PDADMAC) layer that increases the response. A sample treatment using polyethylenimine (PEI) was developed to eliminate possible denaturants. The developed methodology provided a good approach to detect and quantify the released lactose. The release was studied with or without the presence of a model amphiphilic substance, sodium dodecyl sulphate (SDS), in the release medium. Ibuprofen showed very different release rates in the different media, which was attributed to hydrophobic interactions between the drug, the HMPAA and the SDS in the release medium. The release of hydrophilic lactose, which did not associate to any of the other components, was rapid and showed only minor differences. The new methodology provides a useful tool to further evaluate tablet formulations by a relatively simple set of experiments.

1. Introduction

During pharmaceutical development of tablet formulations, emphasis is put on the release of the active substance. The information obtained by this strategy will in many cases not be sufficient to reveal the underlying mechanisms of the release under varying release conditions. If the release of other compounds in the formulation is investigated, additional information on the release mechanism can be obtained. In this work we present the investigation of a model polymer matrix tablet containing Pemulen™ TR2, lactose and ibuprofen. Pemulen™ TR2 is a commercially available cross-linked and hydrophobically modified poly(acrylic acid), henceforth referred to as HMPAA. We have previously studied the potential of HMPAA in tablet formulations, (Knöös et al., 2013a; Knöös et al., 2013b), where it has shown promising abilities to control the release of hydrophobic compounds. However the mechanism of release from these tablets is not yet fully understood.

Lactose is one of the most used excipients in the pharmaceutical industry (Aulton and Cooper, 1988). From a release point of view lactose can be regarded as a model hydrophilic substance and can thus be studied simultaneously with the active substance to give complementary information on the behavior of the formulation. In our case it provides an opportunity to compare the releases of a hydrophobic and a hydrophilic substance. To the authors' knowledge there are only few previous studies on the release of lactose in tablet formulations (Eadala et al., 2009; Gao et al., 1996). One reason could be that there is currently a lack of good analytical tools to study lactose release from pharmaceutical agents.

Various analytical methods are used to directly analyze lactose in dairy products, such as polarimetry, infrared absorption, gravimetry (Watson, 1994), HPLC, (Kwak and Jeon, 1988; West

* Corresponding author. Tel.: +46 46 222 81 63; fax: +46 46 222 44 13.
** Corresponding author. Tel.: +46 46 222 01 03; fax: +46 46 222 41 16.
*** Corresponding author. Tel.: +46 46 222 83 06; fax: +46 46 222 46 22.
E-mail addresses: patrik.knoos@fkem1.lu.se (P. Knöös), Christopher.Schulz@biochemistry.lu.se (C. Schulz), marie.wahlgren@food.lth.se (M. Wahlgren).
[1] These authors contributed equally and are listed alphabetically.

http://dx.doi.org/10.1016/j.ijpharm.2014.03.060
0378-5173/

and Llorente, 1981) or enzymatic assays (Essig and Kleyn, 1983; Kleyn, 1985; Watson, 1994). Those methods are inconvenient for the purposes in the present investigation due to the requirement of mercury (for polarimetry and infrared absorption), large sample volumes (10 or 25 g of milk sample for chromatography or gravimetry respectively) or expensive reagents (enzymatic assays utilizing NADH). Enzymes have also been used for the construction of biosensors allowing the direct or indirect conductometric (Marrakchi et al., 2008) or amperometric (Adányi et al., 1999; Eshkenazi et al., 2000; Ferreira et al., 2003) detection of lactose, however, these are not commercially available and not standardized yet.

Cellobiose dehydrogenase (CDH) has been shown to be a potential candidate for the construction of amperometric lactose biosensors with the advantages of only minimal sample preparation, higher specificity compared to non-enzymatic methods and the requirement of low sample volumes (Glithero et al., 2013; Safina et al., 2010; Stoica et al., 2006; Tasca et al., 2013; Yakovleva et al., 2012). CDH is an extracellular, two-domain, monomeric, enzyme expressed by saprophytic and by some pathogenic fungi (Zamocky et al., 2006). The enzyme consists of a catalytic dehydrogenase domain, DH_{CDH}, containing FAD as cofactor and a cytochrome domain, CYT_{CDH}, containing heme *b* as cofactor and a linker region connecting the two domains. CDH is able to oxidize various sugars including the natural substrate cellobiose, but also lactose, and depending on the phylum also glucose. During substrate oxidation at the DH_{CDH} the cofactor FAD is fully reduced. The electrons are then sequentially transferred to the CYT_{CDH} domain via an internal electron transfer step (IET) (Henriksson et al., 2000; Ludwig et al., 2010, 2013). In vivo the CYT_{CDH} is reoxidized possibly by a copper dependent lytic polysaccharide monooxygenase (CaZy auxilliary family AA9 (Cantarel et al., 2009)) (Beeson et al., 2011; Langston et al., 2011; Phillips et al., 2011). For the construction of a biosensor utilizing CDH the electrode can either reoxidize directly the reduced CYT_{CDH} domain in what is denoted a direct electron transfer (DET) step, as in the presented study or an additionally introduced redox mediator is used to shuttle electrons from the DH_{CDH} and/or CYT_{CDH} domain to the electrode (Ludwig et al., 2013).

In a previous investigation the polycation polyethylenimine (PEI) was found to enhance the analytical signal of a lactose biosensor constituted of a graphite electrode, the PEI promotor layer and the enzyme CDH from *Myriococcum thermophilum* (*Mt*CDH) (unpublished results). The PEI layer was suggested to increase the enzyme load onto the biosensor surface by electrostatic interactions between the polycation and the negatively charged enzyme. Also a possible increase in the electron transfer, either the IET and/or the DET was suggested due to the positive charges present in PEI based on earlier finding on the beneficial effect of Ca^{2+} on the activity of CDH (Schulz et al., 2012). In the present study, CDH from *Corynascus thermophilus* (*Ct*CDH) is used instead of *Mt*CDH due to its higher activity in the human physiological pH present in the samples to be measured. Furthermore, the applicability of the polycation polydiallyldimethylammonium chloride (PDADMAC) as a promotor layer for the construction of an amperometric lactose biosensor using CDH is investigated. In contrast to PEI, the quaternary amine containing PDADMAC is positively charged independent on the solution pH. This assures a tight electrostatic binding between *Ct*CDH (pI = 3.8 (Harreither et al., 2011)) and the promotor layer, even at basic or alkaline pH where PEI starts to be deprotonated. The combination of *Ct*CDH with PDADMAC has the potential to be used as a fast and sensitive lactose biosensor enabling the detection of lactose release from drug containing tablets.

The drug in a polymer matrix tablet can primarily be released via two mechanisms, either by diffusion through the swollen tablet or by erosion together with the polymer (Colombo et al., 2000; Maderuelo et al., 2011; Skoug et al., 1993; Tahara et al., 1995). The gelatinous semi-dilute polymer solution formed outside the dry tablet core, conventionally referred to as the "gel layer", is considered to determine the release and dissolution of the polymer tablets (Colombo et al., 2000). The properties of the gel layer are important for the performance of the tablet for controlled release and an increased strength (i.e., viscosity) of the gel layer leads to an increased thickness (Maderuelo et al., 2011). This results in a slower dissolution of the tablet and a longer way for the drug to diffuse in order to be released, thus a slower drug release (Colombo et al., 2000; Efentakis et al., 2007).

It has been shown that the diffusion of hydrophobic or amphiphilic substances can be affected by the addition of surfactant in a polymer matrix, especially for hydrophobically modified polymers (HM-polymers) (Bramer et al., 2009; Paulsson and Edsman, 2002). Moreover, owing to hydrophobic interactions, surfactants generally affect the viscosity of HM-polymer solutions (Dualeh and Steiner, 1990; Magny et al., 1992), and can also solubilize such HM-polymers that, owing to extensive hydrophobic association, are not soluble in water (Dualeh and Steiner, 1990; Piculell et al., 2001). Surfactant sensitivity could potentially affect the performance of tablets of HM-polymers in vivo, due to the varying composition of amphiphilic compounds in the intestine (Abrahamsson et al., 1999; Dressman et al., 1998).

Previous investigations have shown that the release of hydrophobic substances from HMPAA tablets can be manipulated by adding surfactants and/or changing the ionic strength in the surrounding medium (Knöös et al., 2013a). The behavior was further studied by NMR Chemical Shift Imaging, revealing clear differences in the concentration profiles of the polymer during dissolution that could be correlated to the polymer solubility and phase behavior (Knöös et al., 2013b). In pure water, the tablets showed only minor swelling and a rapid disintegration and release of non-soluble but swollen tablet/polymer particles were seen, which increased the release rate. Addition of buffer to the medium and/or surfactant at concentrations above the CMC increased the solubility of the HM-polymer and the tablets swelled indefinitely. A thicker gel layer was formed and the release of a model hydrophobic substance was slowed down. A hypothesis in these initial experiments with HMPAA was that not only the polymer solubility, but also interactions between a hydrophobic active substance and the hydrophobic substituents (hydrophobes) on the polymer played a major role for the drug release. Lactose is a hydrophilic substance and should not associate with either the hydrophobes or the surfactant. It is thus interesting to see how this molecule differs in its release behavior compared to a hydrophobic or amphiphilic drug.

This work evaluates the potential of a new analytical technique for lactose analysis that could be used within the pharmaceutical industry to quickly and easily quantify the release of lactose from pharmaceutical formulations. The technique is used to gain a better understanding of the dissolution of controlled release tablets based on HMPAA via studying the release of lactose and ibuprofen. Traditionally the sodium salt of ibuprofen is not considered to be poorly soluble as it has solubility above 100 mg/ml (Bustamante et al., 2000); in fact, it is often formulated as an immediate release tablet. However, the acid form has a much lower solubility, 55.4 μM (Yazdanian et al., 2004). Furthermore, ibuprofen has an amphiphilic character and will form mixed micelles with both cationic and anionic surfactants (Bramer et al., 2006; Stephenson et al., 2006). Thus, ibuprofen was chosen, as it will likely interact with the hydrophobic polymer matrix as compared to lactose that will not show such interactions. SDS is used to examine the effects of surface-active compounds. SDS is a well-studied anionic surfactant that is also approved for oral

formulation. It has been established that SDS has a similar effect as bile salts (50/50 mixture of sodium taurocholate and sodium deoxycholate) on the release from Pemulen™ TR2 tablets (Knöös et al., 2013a).

2. Materials and methods

2.1. Materials

Pemulen™ TR2 NF (lots no. CC11MCU893 and 0100834373) was kindly provided by Lubrizol Advanced Materials (Brussels, Belgium). According to the supplier, the polymer consists of poly (acrylic acid), cross-linked with allylpentaerytritol, and contains 52–62 wt% of COOH groups. Pemulen is also hydrophobically modified with grafted C10–C30 alkyl-chains via ester bonds.

Ibuprofen sodium salt (lots no. 038K0755 and 87H0764) was purchased from Sigma–Aldrich Chemicals (Steinheim, Germany) and used as delivered. Sodium dodecyl sulphate (SDS) was acquired from VWR International (Poole, England) and used as delivered. The critical micelle concentration (CMC) for SDS is 8.3 mM in pure water (Holmberg, 2003) and was determined to be 1.8 mM at 37 °C in 0.1 M phosphate buffered solution, pH 7.2 using a tensiometer and a de Noüy ring.

The following chemicals were used during the tablet production: lactose, talc and magnesium stearate, which were of analytical grade. A (70:30) mixture of ethanol (99.5%) and 0.001 M aqueous HCl was used as granulation fluid.

For the development and application of the lactose biosensor the following chemicals were used: branched polyethylenimine (M_w = 25,000 g/mol, M_n = 10,000 g/mol), polydiallyldimethylammonium chloride (20 wt% in H_2O, M_w = 100,000–200,000 g/mol), β-lactose, hydrochloric acid (37%) were purchased from Sigma–Aldrich Chemicals. Sodium 4-*n*-octylbenzenesulphonate (SOBS) was purchased from TCI Europe N.V. (Zwijndrecht, Belgium). Cellobiose dehydrogenase from *Corynascus thermophilus* (*Ct*CDH) was obtained following a published procedure (Harreither et al., 2012). The enzyme was stored in a 50 mM sodium acetate buffer at pH 5.5 at a concentration of 9.4 mg/ml (determined spectroscopically at 280 nm as in Ref. (Harreither et al., 2012)).

2.2. Dissolution experiments

2.2.1. Tablet preparation

Tablets with compositions as specified in Table 1 were prepared as described previously (Knöös et al., 2013a). First, the dry ingredients lactose, polymer and ibuprofen were mixed in an intensive mixer (Kitchen Aid, Model K5SS), for 5 min. The granulation process started with gently spraying granulation fluid over the powder, with interruptions to allow the fluid to absorb. The procedure was continued until the desired properties of the granulation were achieved. The granules were then sieved through a 2 mm sieve, and if the particle size was too large, a food-processer (Philips, Cucina) was used to reduce it. The granules were then dried in an oven at 50 °C over night and were sieved again through a 2 mm sieve. The dried granules were mixed with lubricants (talc and magnesium stearate) in a cone blender for 2 min after each addition.

The tablets were manufactured with a single-punch tableting machine (Diaf, Type TM 20, Denmark) to a weight of around 400 ± 20 mg (n = 10). Appropriate settings were applied to ensure a good hardness and weight of the tablets. Hardness and friability were measured according US Pharmacopeia methods. All tablets achieved a hardness above 5 kp and a friability less than 1%.

Table 1
Compositions of tablets used in this study. The amount of ibuprofen was chosen from an experimental perspective in order to the match detection levels of the analyses.

Ingredient	Amount (wt%)
Polymer	30
Ibuprofen	10
Lactose	58
Talc	1
Magnesium stearate	1

2.2.2. Release studies

Dissolution experiments were carried out at 37 °C in a USP dissolution apparatus II (Prolabo Intelligent dissolution tester, Novakemilab, Enskede, Sweden) with a paddle speed of 100 rpm. For experiments in buffered solution the fluid was continuously withdrawn and transferred by means of a pump to a spectrophotometer (Cary 50 Bio UV–visible, Varian, Belrose, Australia), which measured the ibuprofen concentration in the vessels at the absorption of λ = 222 nm. The spectrophotometer measured according to the following cycles; 1) every minute for 10 min 2) every 10 min until one hour 3) every 20 min until six hours 4) every hour until completed experiment. For all remaining experiments, aliquots (V_a = 1 ml) were manually withdrawn from the vessels. The release of lactose was measured for all cases in the aliquots and analyzed as described below. The released amount (%release), for lactose and ibuprofen was calculated according to

$$\%\text{release} = \frac{[c_s \times (V_o - V_a(n_a - 1))] + \sum_{n=0}^{n_a-1}(V_a \times c_{s,n})]}{m_s} \quad (1)$$

where the concentration of ibuprofen or lactose from the analyzed aliquots is given by c_s and the initial volume of the vessel is V_0 (=800 ml). V_a and $c_{s,n}$ denote the volume and the concentration in the aliquots and the number of aliquots is denoted n_a. The amount of ibuprofen or lactose in the tablets is given by m_s.

The media used were 0.1 M phosphate buffered solution, pH 7.2, or water deionized in a Milli-Q water apparatus. The pH was not monitored during dissolution in pure water. SDS was added in varying amounts, yielding concentrations between 0 and 10 mM (in phosphate buffered solution) and 0–20 mM (in water).

2.2.3. Gravimetric erosion and swelling studies

Experiments to determine the erosion and swelling of the polymer tablets were performed, where the tablets were removed from the vessels and weighed. The experiments were carried out under the same conditions as the release studies above and with the same apparatus. Triplicates of tablets were studied during specified time intervals and were at designated times picked up with a spoon and placed on a pre-weighed mesh. Care was taken to avoid excess fluid on the mesh and to ensure that the whole tablet was extracted. The diameter of the swollen tablet was measured at the same time, both the total diameter and the core diameter. The tablets were then dried at 55 °C until no further weight loss was seen. Furthermore, aliquots were withdrawn from the USP vessels, at the time of tablet removal, to determine the amount of released lactose and ibuprofen (according to Eq. (1)). Using the measured dried weights (W_d), the released amount of polymer from the tablets could be calculated from the following mass-balance

$$W_d = m_{pol} + m_{ibu} + m_{lactose} \quad (2)$$

Here the mass of ibuprofen and lactose in the tablets (m_{ibu} and $m_{lactose}$) are obtained as

$$m_{ibu} = 0.1 \times W_i - c_{ibu} \times V_0 \quad (3a)$$

$$m_{lactose} = 0.58 \times W_i - C_{lactose} \times V_0 \quad (3b)$$

and W_i is the initial weight, $c_{lactose}$ and c_{ibu} the concentrations of lactose and ibuprofen, respectively, in the vessels with a volume of V_0. Here, we assume that the added lubricants (talc and magnesium stearate), which were added in low amounts did not contribute significantly to the total tablet weight. The amount of polymer in the dried tablet can thus be written as

$$m_{pol} = W_d - (m_{ibu} + m_{lactose}) \quad (4)$$

and the released fraction of polymer (release (pol)) can be calculated from

$$\text{release(pol)} = \left[\frac{0.3 \times (W_t - (m_{ibu} + m_{lactose}))}{0.3 \times W_i}\right] \quad (5)$$

The data from the gravimetric experiments were further used to calculate the relative swelling (RS) and the release of total dry mass (RM), which were defined as

$$RS = \frac{W_w - W_d}{W_d} \quad (6)$$

$$RM = \left(\frac{W_i - W_d}{W_i}\right) \times 100 \quad (7)$$

2.3. Lactose analysis

2.3.1. Solutions

For the precipitation of SDS, a solution of 2.5 mM PEI in 0.1 M PBS was prepared. At this high concentration the activity of the hydronium ions does not equal to its concentration, so the pH was stepwise adjusted with HCl so that a final 50 times diluted PEI solution had a pH of 7.2.

2.3.2. Preparation of the lactose biosensor

Spectrographic graphite electrodes (d = 3.05 mm, Alfa Aesar GmbH & Co., KG, Karlsruhe, Germany) were polished on wet emery paper (P1200 from Norton, Saint-Gobain Abrasives AB, Sollentuna, Sweden) and cleaned with Milli-Q water and allowed to dry. If not differently stated, the electrodes were immersed for 10 min in a 4 wt% aqueous solution of PDADMAC for the immobilization of the polycation PDADMAC. The PDADMAC modified electrodes were rinsed with Milli-Q water and allowed to dry. Enzyme modification was done by adding a drop of 4 μl of a solution of 9.4 mg/ml *Ct*CDH. All prior steps were performed at room temperature. The electrodes were kept in the fridge at 4 °C between 0.5 and 3 h until use.

2.3.3. Sample preparation

The samples taken during tablet dissolution contained SDS of concentrations between 0 and 20 mM present in either water or 0.1 M PBS, pH 7.2. SDS is known to be a denaturant for proteins able to also irreversibly inactive CDH used for the construction of the lactose biosensor (Fang et al., 1998) and had to be removed or inactivated. Branched PEI was shown to be able to form hydrophobic, coagulating complexes with SDS (Mészáros et al., 2003). Depending on the pH the polycation-surfactant complex formation is driven by electrostatic and hydrophobic interactions

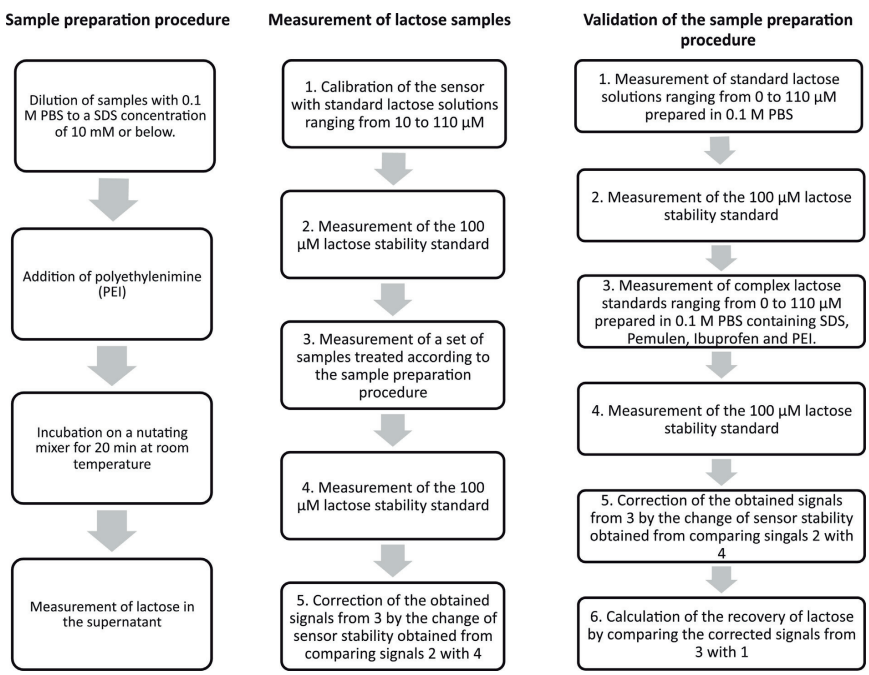

Fig. 1. Analytical flow chart describing the sample preparation procedure (left), the measurement of lactose samples (middle) and the validation of the sample preparation procedure (right).

(Li et al., 2000; Wang et al., 2006) partly accompanied by an uptake of protons (Bystryak et al., 1999; Mészáros et al., 2003). The ability of the PEI-SDS complex to form a hydrophobic coagulate is used for the establishment of a sample preparation procedure to diminish SDS present in the samples.

The SDS- and lactose-containing samples taken during tablet dissolution were diluted with 0.1 M PBS, pH 7.2 to an SDS concentration of ≤10 mM SDS and stored in a 1.5 ml polypropylene microtube. Twenty microliter of the 2.5 mM PEI solution was added to each 1 ml sample containing lactose and 10 mM SDS. If SDS concentrations were below 10 mM the volumes of the PEI solution added were adjusted accordingly. The samples containing PEI, SDS and lactose were incubated for 20 min on a nutating mixer (Gyromini, LabNet, Woodbridge, New Jersey, USA) at room temperature. A precipitate formed and adsorbed to the wall of the microtube. The supernatant was transferred into a new microtube and the lactose concentration was measured. Lactose samples in a 0.1 M PBS, pH 7.2 matrix, which did not contain SDS, were measured directly without a PEI treatment. Lactose samples in a H_2O matrix were diluted 1:5 with carrying buffer independently on their SDS content to adjust the matrix to the pH and the ionic strength of the carrying buffer (0.1 M PBS, pH 7.2). A flow chart of the sample preparation procedure is given in Fig. 1.

2.3.4. Measurement of lactose with flow injection analysis with amperometric detection

The lactose biosensors were rinsed with Milli-Q water prior to use to remove loosely adsorbed enzyme molecules. The biosensors were mounted into a flow-through, electrochemical wall-jet cell housing also an Ag|AgCl reference (0.1 M KCl) and a platinum wire counter electrode (Appelqvist et al., 1985). The electrodes were connected to an analogue potentiostat (Zäta Elektronik, Höör, Sweden) to control the applied potential and measure the currents obtained from the enzyme catalyzed lactose oxidation. The applied potential was 0 mV versus the Ag|AgCl (0.1 M KCl) reference electrode. The current signals were plotted on a strip chart recorder (Kipp & Zonen, Delft, The Netherlands). The flow cell was also connected to a six-valve injector (former Rheodyne, now IDEX Health & Science, Oak Harbor, USA) to control the injection of the samples. The samples were loaded into an injection loop with a volume of 20 μl. The injector was connected to a peristaltic pump (Gilson, Villier-le-Bel, France) pumping 0.1 M PBS, pH 7.2 carrying buffer at a speed of 0.5 ml/min to transport the samples from the injector to the flow cell containing the biosensor. Each sample or standard solution was injected at a rate of approximately one injection/min and at least three times and the average of the obtained signals was evaluated. Each newly mounted biosensor was calibrated with lactose standards with concentrations of 10, 30, 50, 70, 90 and 110 μM covering the linear range of the biosensor. It followed the injection of a lactose stability standard with a concentration of 100 μM to monitor and correct for changes in the biosensor response with time. Subsequently the supernatant of the samples, which have gone through the sample preparation procedure, were analyzed. In case the signals from the samples lay outside the linear range, they were further diluted with carrying buffer and measured again. The lactose stability standard was injected after each set of samples and the signals from the set of samples measured before were corrected by the possible deviation in sensor stability. A flow chart of the measurement of lactose samples is given in Fig. 1.

2.3.5. Validation of the sample preparation procedure

The lactose biosensor was calibrated using standard lactose solutions with concentrations of 10, 30, 50, 70 110, 500 and 5000 μM prepared in 0.1 M PBS, pH 7.2 according to the procedure described above. Complex standard lactose solutions containing equal concentrations of lactose (as above) prepared in 0.1 M PBS, pH 7.2 additionally containing 50 mM SDS and the tablet contents of 0.15 mg/ml Pemulen and 0.05 mg/ml Ibuprofen were treated according to the sample preparation procedure. Their analytical signals were measured and the recovery of lactose was calculated using the linear equation valid for the linear range of the biosensor. This was repeated independently from each other for 5 electrodes. A flow chart of the validation of the sample preparation procedure is given in Fig. 1.

3. Results

3.1. Lactose analysis

To detect lactose concentrations in samples taken during dissolution experiments of polymer matrix tablets also partly containing SDS, a sample preparation procedure to remove SDS and a lactose biosensor was developed to enable a fast, selective and sensitive detection of lactose in small sample volumes with minimal sample preparation. Therefore an amperometric measurement set-up was chosen utilizing graphite electrodes modified with the lactose oxidizing enzyme *Ct*CDH to gain selectivity and a PDADMAC promotor layer to the enhance sensitivity for the detection of lactose.

3.1.1. Signal enhancement of the lactose biosensor by a PDADMAC promoter layer

Based on previous findings on the beneficial effect of PEI on the response of *Mt*CDH modified biosensors (see Section 1), the applicability of the polycation PDADMAC as a promotor layer for the construction of *Ct*CDH modified biosensors was investigated. In Table 2 the apparent kinetic parameters for *Ct*CDH immobilized either on bare graphite or on PDADMAC modified graphite electrodes are summarized. The maximal catalytic current density J_{max} gained from lactose oxidation could be enhanced 120 times to 40.9 μA/cm^2 when PDADMAC was used as a promoter layer. Consequently for all lactose biosensors PDADMAC was used as a promotor layer. This increase in the maximal current density J_{max} can be attributed to a higher loading of enzyme onto the electrode surface, as suggested also for PEI/*Mt*CDH modified graphite electrodes (unpublished results). At the investigated pH of pH 7.2 *Ct*CDH is negatively charged (pI = 3.8 (Harreither et al., 2011)) allowing it to be bound electrostatically to the polycation PDADMAC. Also the IET within the enzyme or the final electron transfer from the enzyme to the electrode might be increased by PDADMAC due to a screening of repulsive, negative charges present on either the interface of the two domains of the enzyme or on the graphite electrode allowing a better electrical communication, as previously suggested for PEI (unpublished results) and $CaCl_2$ (Schulz et al., 2012).

The apparent K_M (K_M^{app}) was not changed significantly in the presence of PDADMAC indicating no mass transfer limitations of lactose to the immobilized enzyme through the PDADMAC layer.

Table 2
Calculated maximal current densities J_{max} and K_M^{app} obtained from the fitted response curves of SPG/*Ct*CDH lactose biosensors for lactose standard solutions without promotor layer (−PDADMAC), with promotor layer (+PDADMAC) and for complex lactose standard solutions treated with the sample preparation procedure (+SDS, +PEI) measured in a 0.1 M PBS, pH 7.2 buffer at an applied potential of 0 mV versus Ag|AgCl (0.1 M KCl). For each condition the response curves of three electrodes have been fitted individually and the averages and standard deviations of the obtained parameters have been calculated and are given in the table.

	−PDADMAC	+PDADMAC	+PDADMAC, +SDS, +PEI
J_{max}/nA cm^{-2}	340 ± 200	40,890 ± 8530	46,400 ± 7990
K_M^{app}/μM	760 ± 90	560 ± 100	600 ± 70

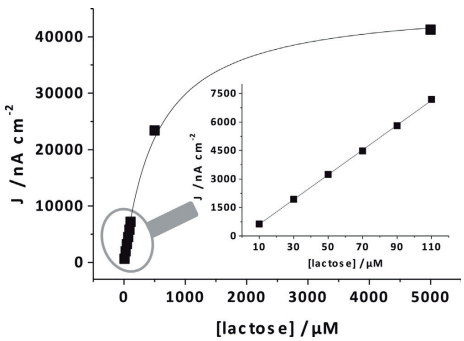

Fig. 2. Amperometric response of a SPG/PDADMAC/*Ct*CDH lactose biosensor to lactose standard solutions and linear range of the biosensor (inset) measured in a 0.1 M PBS, pH 7.2 buffer at an applied potential of 0 mV versus Ag|AgCl (0.1 M KCl).

The variations in the response between equally modified electrodes are rather high (see standard deviation in Table 2), so for the latter measurement of lactose in the samples, each used biosensor was calibrated using six standard lactose concentrations prior to use.

In Fig. 2 a typical response curve of a graphite/PDADMAC/*Ct*CDH lactose biosensor is shown. Since it is an enzymatic biosensor the signal gained from high substrate concentrations (here above 110 μM lactose) levels off as described by the Michaelis–Menten equation (Michaelis and Menten, 1913). The linear range of the biosensor response was between 1 and 110 μM using standard lactose solutions but only the range between 10 and 110 μM was used for the measurements of lactose in the samples, as discussed later (see inset Fig. 2).

3.2. Evaluation of removal of SDS by PEI

SDS present in the lactose containing samples, at concentrations between 0 and 20 mM, had to be removed or reasonably decreased to avoid the denaturation of *Ct*CDH used for the construction of the lactose biosensor. The measurement of untreated, 1 mM SDS, 100 μM lactose containing standards lead to irreproducible and rapid, irreversible decreases in the sensor response. Various methods were investigated to remove SDS from the lactose containing samples based on either ionic interactions (anion exchange chromatography) or hydrophobic interaction (incubation with commercially available polystyrene beads). Ion exchange chromatography was found to change the ionic strength/composition of the sample leading to additional, interfering electrochemical signals not related to the oxidation of lactose. The addition of the polystyrene beads to the SDS/lactose containing samples lead to a significant, apparent decrease in the lactose concentration in the samples. Possibly capillary liquid entrapped between the pre-soaked beads diluted the samples in an irreproducible manner. Disadvantageous was also the long incubation time necessary for SDS to bind to the polystyrene beads.

A method to precipitate the negatively charged SDS by the addition of branched PEI was developed. The precipitation of the PEI/SDS complex is due the formation of an uncharged complex between SDS and branched PEI (Mészáros et al., 2003; Wang et al., 2006). The amount and concentration of PEI necessary to be added to complex lactose standards (containing 10 mM SDS) were optimized with respect to a sufficient precipitation of SDS, high biosensor viability, minimal sample dilution and minimization of the sensor response to excess PEI. This led to the sample preparation procedure as described in Section 2.

To evaluate how much SDS could be removed by the sample preparation procedure the UV active anionic surfactant SOBS was used instead of SDS. It has a similar molecular weight, also a sulfate head group but shows UV absorption with an absorption maximum at 261 nm (experimentally determined). Applying the developed sample preparation procedure to a 10 mM SOBS solution 96 ± 1% ($n = 3$) of SOBS could be removed from the sample as determined photometrically. Assuming a comparable clearance by PEI for SDS as for SOBS, this means a residual leftover of SDS in PEI treated samples in the μM range. Furthermore, it was evident that the viability of the lactose biosensor was not decreased by the residual SDS. In fact the residual SDS seemed to affect the stability of the lactose biosensor positively, as indicated by an average 1.06 times higher response to the lactose stability standard after the measurement of PEI treated complex lactose standards (determined experimentally, see Section 2 or Fig. 1 Validation of the sample preparation procedure). A similar trend was observed for the measurement of PEI treated samples taken from the dissolution experiments. After an average of 80 measurements of PEI treated SDS/lactose samples the sensors responded in average 1.12 ± 0.08 ($n = 4$) higher to the lactose stability standard of 100 μM (determined experimentally, see Section 2 or Fig. 1). These sensor drifts were corrected as described in Section 2. There is possibly residual SDS binding to PDADMAC (Mukherjee et al., 2011) and/or CtCDH. How this might have altered the biosensor response was not further investigated. The dilution of the sample by the addition of PEI was only 2% and was neglected.

The injection of blank samples treated with the sample preparation procedure gave signals as high as a standard lactose solution with a concentration of average 6 ± 1.4 μM ($n = 5$). Excess PEI possibly changes the ionic strength of the sample, which creates a pseudo-response due to the recharge of the electrochemical double layer of the biosensor. Consequently only analytical signals higher or equal to the one of a 10 μM lactose standard solution were evaluated.

In Fig. 3 the average absolute recovery of lactose in complex lactose standard solutions treated with the sample preparation procedure is plotted versus the designated lactose concentration. The lactose concentrations of the complex, PEI treated standards are slightly overrated in their designated concentrations by

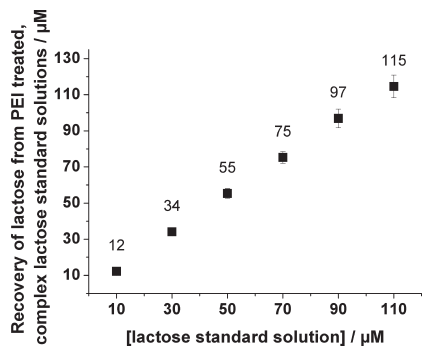

Fig. 3. Recalculated average recovery of lactose (see label) from complex lactose standard solutions containing lactose, 10 mM SDS, 0.03 mg/ml Pemulen and 0.01 mg/ml ibuprofen in 0.1 M PBS, pH 7.2 after treatment with the sample preparation procedure using PEI to precipitate SDS. The error bars indicate the standard deviation of five individually performed experiments.

maximum average +7 ± 5 μM for 90 μM lactose (n = 5). Thus, even if the sensor response was corrected by the response to the lactose stability standard the lactose concentrations in the complex lactose standards (containing 10 mM SDS) were still overrated, possibly caused by residual SDS and/or PEI with a standard deviation of ±5 μM (random error). However, the sensor responses were not corrected for the apparent systematic overrating of the real lactose concentrations, since the lactose samples were present in different matrices (PBS and H_2O), contained various concentrations of SDS (0 to 20 mM) and PEI and had to be diluted differently depending on their individual lactose concentration to end up in the linear measuring range of the biosensor. Consequently, the systematic error of maximum +7 μM was treated as a random error and all measured lactose concentrations in the samples are seen to have an overall random error of maximum ±13% ((±7 μM ± 5 μM)/90 μM).

3.3. Dissolution and release of HMPAA tablets

The release of ibuprofen and lactose for tablets dissolving in water and in buffered solutions are shown in Fig. 4, with and without SDS added to the surrounding media. Based on the behavior observed in previous work (Knöös et al., 2013a), the SDS concentration was chosen to be well above the CMC values of the surfactant (see Section 2) in water and buffer, respectively. The behavior of the tablets in pure water might seem irrelevant for pharmaceutical development of controlled release formulations. However, water was used for comparison with previous performed experiments in water, where the polymer showed very low swelling and differed in release characteristics compared to buffered solutions (Knöös et al., 2013a).

Fig. 4 reveals strong variations in the release patterns depending on the presence or absence of both buffer and surfactant. A rapid and, within error, simultaneous release of lactose and ibuprofen was seen in pure water. Here, it was also observed that the tablet had completely disintegrated after 24 h. In all other experiments, the dissolution of the tablets was more or less slow, and the release profiles differed between ibuprofen and lactose. For ibuprofen, the addition of surfactant to either water or buffer slowed down the release with a retained linear profile. In some cases the tablets appeared to release more than 100% when fully dissolved (see Fig. 4c). This is most likely due to accumulation of tablet particles in the flow cells of the UV/vis apparatus (see Section 2). Accumulated particles increase the background absorbance, affecting the calculated concentration of ibuprofen. As in our previous study (Knöös et al., 2013a), the tablets in this study show very long release times for ibuprofen, due to a high content of polymer. This tablet design was chosen in order to avoid possible experimental variations due to tablet inhomogeneities. However, the aim of the present study is to evaluate the release of lactose and possible effects of amphiphiles, not to optimize the release time. Preliminary results indicate that the dissolution times can be decreased by decreasing the polymer content.

The release of lactose from the tablets was more rapid than the ibuprofen release, except in pure water, and most of the lactose had been released already after 24 h in all media. In contrast to the results for ibuprofen, only minor effects on the lactose release were seen if buffer and/or SDS was added to the release medium. Tablets

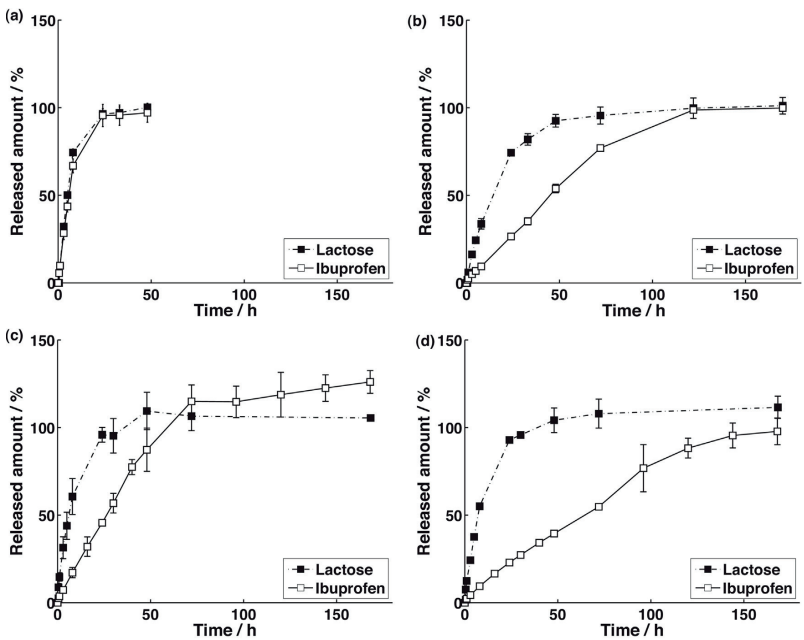

Fig. 4. The release of lactose (filled squares) and ibuprofen (open squares) from HMPAA tablets in water without (a) or with (b) 20 mM SDS, and in buffer solutions without (c) or with (d) 10 mM SDS. The released amount is calculated according to Eq. (1) and error bars indicate the standard deviation (n = 3).

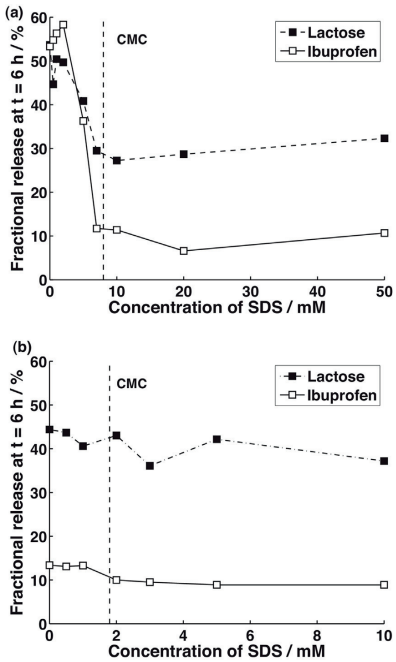

Fig. 5. Released fractions at t = 6 h in water (a) and buffer (b) solutions with varying concentration of SDS. The release for lactose is given by filled squares and ibuprofen by open squares. The values are an average of two tablets. The dashed vertical lines indicate the CMC values for SDS in the two solutions, water and buffer, respectively.

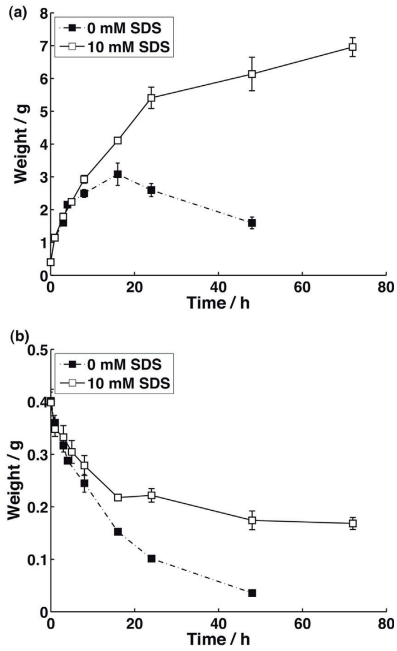

Fig. 6. Measured wet (a) and dry (b) weights of tablets dissolving in buffered solutions with (open symbols) and without (filled symbols) addition of 10 mM SDS. Error bars indicate the standard deviation ($n = 3$), except at zero hour which is the average value of all tablets where n is equal to 21 or 24 for pure buffer and buffer with surfactant, respectively.

dissolving in buffered solution showed almost no difference in lactose release rates with or without SDS in the bath, whereas the release in water was slowed down somewhat upon addition of 20 mM SDS.

To further compare the effects of the dissolution medium and surfactant concentration on the release of lactose and ibuprofen, the released fractions of the two compounds were evaluated at $t = 6$ h (Fig. 5) for a series of different surfactant concentrations (0–20 mM in water and 0–10 mM in buffer). The trends observed for ibuprofen have already been described in (Knöös et al., 2013a), but here we can compare with the behavior of lactose. For tablets dissolving in water the two model substances showed a qualitatively similar response to surfactant added to the medium (Fig. 5a). Here, a decrease in released amount with increasing surfactant concentration was observed below the CMC, followed by a leveling off at higher concentrations. The decrease in release rate below the CMC was quite steep for ibuprofen, but less pronounced for lactose. In buffered solution (Fig. 5b), the released amounts of the two substances differed at all surfactant concentrations. The release of ibuprofen was slightly, but significantly, affected by the addition of surfactant, again with a leveling off above the CMC. We note that the released amount of ibuprofen was similar in both media above the CMC. For lactose, the scatter in the data does not allow us to draw any conclusions regarding effects of surfactant addition. We note that the trends of Fig. 5 confirm the trends observed in the results of Fig. 4.

3.4. Water uptake, erosion and swelling

In order to further study the dissolution and release behavior of HMPAA tablets, gravimetric studies were performed, where tablets were, at designated times, picked up from the baths and the wet and dry weights were noted. For this purpose we chose to study the behavior only in buffered solution, which is more relevant for in vivo behavior. It was also possible to calculate the released amount of the polymer from the measured wet and dry weights.

The weights of the wet and dried tablets from the gravimetric studies are shown in Fig. 6 for tablets dissolving in buffered solution with and without 10 mM SDS added to the release media. In surfactant-free buffer the tablets showed a rapid increase in wet weight and a maximum was reached at 16 h. At later times the tablets started to decrease in size and at 48 h only small amounts of the tablets were left. For tablets dissolving in the presence of surfactant, the wet weight continued to increase throughout the duration of the experiment (72 h). In surfactant solution the tablets showed an initial rapid decrease of the dry weight, which leveled off at later times, and a large fraction of the dry tablet was still left at 72 h of dissolution. In the presence of surfactant the tablet erosion became slower and the initial decrease was most likely due to the rapid lactose release, as seen above.

The values for the relative swelling and release of total dry mass, calculated from Eqs. (6) and (7), respectively, are shown in

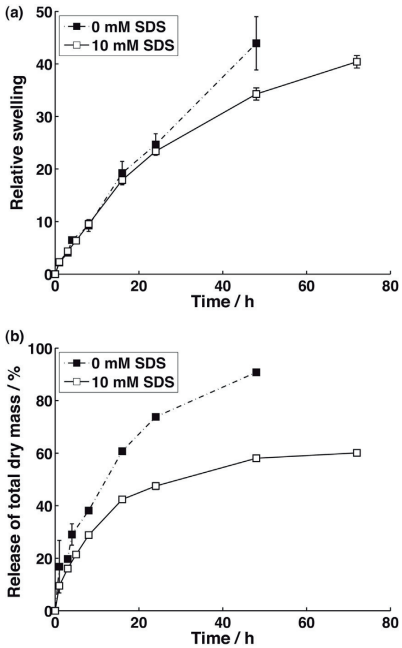

Fig. 7. The relative swelling (a) and release of total dry mass tablets (b) dissolving in pure buffer (filled symbols) and in 10 mM SDS buffer solution (open symbols). Error bars indicate the standard deviation ($n = 3$).

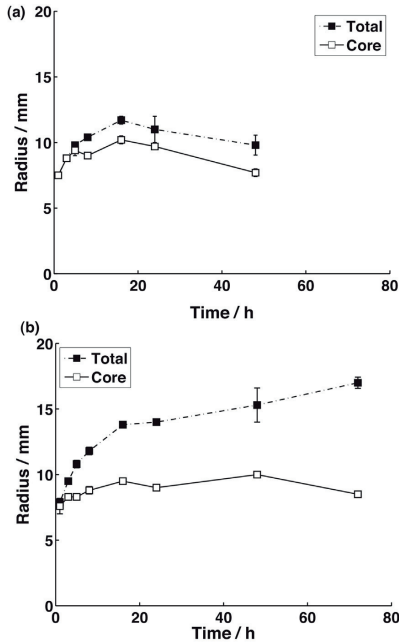

Fig. 8. Measured total (filled) and core (unfilled) radii of the swollen tablets at indicated times, dissolving in pure buffer (a) and in 10 mM SDS buffer solution (b). Error bars indicate the standard deviation ($n = 3$).

Fig. 7. The systems with and without SDS showed a similar swelling during the first hours of dissolution (Fig. 7a), however, after 24 h the data started to differ and the matrices in surfactant-free buffer were more swollen. It seems likely that the rapid initial solvent penetration was mainly driven by the osmotic pressure caused by the large fraction of lactose in the tablets. As the lactose content decreased due to the rapid lactose release, the differences caused by the presence or absence of surfactant in the medium became more obvious. At later stages the relative swelling slowed down in the surfactant solution, whereas the rate of relative swelling was similar throughout the dissolution period in surfactant-free buffer. The value for the relative swelling should at long times approach a value corresponding to the concentration of polymer present at the erosion front (Körner et al., 2005). However, even at the termination of the experiment this limiting case was presumably not reached, since the tablets were still far from complete dissolution – especially the tablets in surfactant solution.

The release of total dry mass (Fig. 7b) for the two systems differed more than the relative swelling. In surfactant-free buffer the tablets continued to erode throughout the dissolution time, but for tablets in buffer with surfactant the erosion seemed to slow down and at later times the rate of erosion was very slow. The results confirm the conclusions put forward above and show that the erosion of the tablets slowed down upon surfactant addition. Moreover, the results show that the initial decrease tablet mass is mostly due to the release of lactose. Once the lactose is released the tablet weight does not seem to decrease instead we are left with a swollen polymer matrix.

The swelling behavior of the tablets could be further established visually and via measuring the sizes of the extracted tablets (Fig. 8). All dissolving tablets were surrounded by transparent gel layers and in the middle of the tablet a white "core" could be seen, which at closer examination showed a sponge-like texture. Comparing the gel layer thickness (i.e., total radius – core radius) between the two media showed that the gel layers increased in thickness with added SDS. In surfactant-free buffer the tablets started to decrease in size after 16 h of dissolution, whereas the tablets in buffer with surfactant continued to grow throughout the experimental period. Moreover the gel layer increased in thickness throughout the dissolution time for both media and the tablet core started to decrease in size at later times. The results are quite consistent with the results above from the gravimetric studies. In the presence of surfactant, the tablets erode very slowly and seem to swell continuously. Furthermore, the results follow the previous observations that the largest effects on addition of surfactant was seen for the gel layer thickness (Knöös et al., 2013a; Knöös et al., 2013b).

The releases of all three major components (polymer, ibuprofen and lactose) of the tablets from the gravimetric studies are shown in Fig. 9. The releases of lactose and ibuprofen followed the patterns already seen in Fig. 4. Nonetheless, with some small differences, presumably due to the fact that all data points in Fig. 9 correspond to different tablets; each experiment was obviously terminated when the tablet was removed from the bath for gravimetric analysis. The release of the polymer with time in surfactant-free buffer was similar to that of ibuprofen, indicating

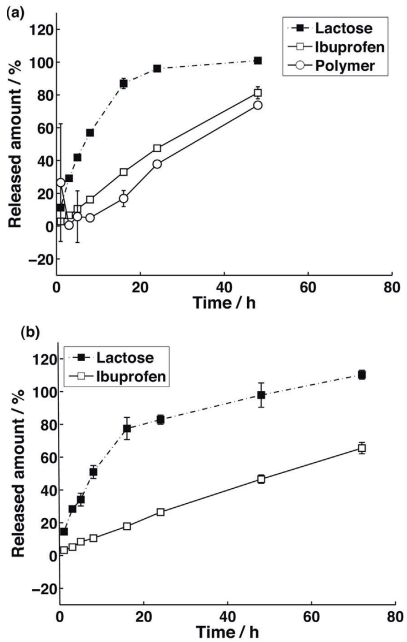

Fig. 9. Release of ibuprofen (filled squares), lactose (open squares) and polymer (open circles) from tablets dissolving in pure buffer (a) and in 10 mM SDS buffer solution (b). The polymer release is not shown for tablets dissolving in surfactant solution, for description of the release the reader is referred to the text. Error bars indicate the standard deviation ($n = 3$).

that the two releases were correlated (Skoug et al., 1993), as discussed above. The diffusional release of ibuprofen from the tablet was sufficiently slow so that the tablet erosion significantly contributed to the total release. When adding surfactant to the system the released amount of polymer was too small to be determined by our gravimetric approach. In fact the dry weight of the extracted tablets was higher than the initial polymer content, possibly due at least in part to the absorption of buffer and SDS from the medium (these contributions to the dry mass are neglected in Eq. (4) above). This indicates two things, a very slow release of the polymer and binding of SDS to the polymer matrix.

3.5. Drug release from polymer tablets

From the release and gravimetric studies, three distinct release scenarios for tablets containing the two compounds ibuprofen and lactose in different release media can be identified. In part, the differences are due to the interactions of the HMPAA polymer with both buffer and surfactant. In addition, lactose and ibuprofen interact very differently with the other components in the studied systems.

In the first scenario, for the release into water, both lactose and ibuprofen show a similar release patterns, indicating similar release mechanisms. In pure water, the tablets showed only a limited swelling and formed thin gel layers, as observed previously and confirmed here (Knöös et al., 2013a). Furthermore, eroded hydrated tablet particles were present in the bath that disintegrated from the tablet matrix. During our previous studies we have established that the polymer has poor water solubility and has a maximum swelling equal to ca. 25 wt% polymer content (Knöös et al., 2013b). This means that the polymer layer can only swell to this polymer concentration and the convection will shear off hydrated insoluble polymer/tablet particles (Knöös et al., 2013a; Knöös et al., 2013b). This leads to a rapid disintegration of the tablet that determines the release of both substances.

In the second scenario, for the release into phosphate buffer, the releases of lactose and ibuprofen differ. Lactose is released comparatively rapidly, whereas the releases of polymer and ibuprofen almost coincide, which indicates that ibuprofen is released mainly due to erosion of the tablet. In buffer, the carboxylic acid groups of HMPAA become partly charged (Laguecir et al., 2006; Mylonas et al., 1999). The tablet then swells more than in water and a thicker gel layer is formed that leads to slower erosion, thus a slower release of ibuprofen (compared to water). The release of lactose is marginally slower in surfactant-free buffer (compared to pure water), due to the decreased erosion of the tablets in buffer. The different release profiles for the polymer and lactose indicates that lactose is primarily released by a rapid diffusional transport, which is faster than the tablet erosion.

In the third scenario, for release into surfactant solutions, the releases of all three components differ. In the presence of surfactant (above CMC) the polymer is solubilized and the tablets can swell indefinitely (Knöös et al., 2013a). The thickness of the gel layer is then determined by the balance of the cohesive forces between the polymer molecules and the applied force from the convection (Borgquist et al., 2006; Körner et al., 2005). Furthermore, the surfactant most likely strengthens the polymer matrix by increasing the lifetime of the temporary cross-links formed by the hydrophobes (Magny et al., 1992). The tablets formed thick gel layers and showed a very slow dissolution/erosion. Lactose has about the same release rate as in surfactant-free media indicating that it is released through a rapid diffusion that is only slightly slowed down by the increased thickness of the swollen and stagnant polymer matrix. The effect of added surfactant on the lactose release is marginal in buffer, but significant in pure water (Figs. 4 and 5), where added surfactant also has the strongest effect on the swelling and disintegration of the polymer matrix and thus could effect the diffusion path of lactose. The release of ibuprofen is very slow but, nevertheless, faster than the polymer release.

It remains to discuss the interactions experienced by lactose and ibuprofen in the studied systems. Lactose is an uncharged hydrophilic substance that dissolves in water without associating with either the hydrophobes on the polymer or the surfactant. Ibuprofen, on the other hand, should have a quite complex behavior in the swollen HMPAA tablets. Although added in the salt form, ibuprofen can be partially protonated by proton exchange with the abundant acrylic acid groups' chain of the polymer. The studied system will thus be composed of a mixture of sodium salt and the acid form of ibuprofen, at varying water contents, depending on the degree of water penetration. Moreover, in the outermost part of the tablet, the ratios of the two forms will be affected by the penetrating phosphate buffer. (In the interior of the tablet, the carboxylate/carboxylic acid system will clearly be the dominating buffer system.) On top of this, ibuprofen will interact with the added surfactant and/or the hydrophobes and form mixed aggregates. A detailed modeling is clearly beyond the scope of this paper. However, hydrophobic interactions with the other components must decrease the concentration of molecularly dissolved ibuprofen in water. As stated above ibuprofen is known to form mixed micelles with SDS (Stephenson et al., 2006). We also know that the penetrating surfactant will form mixed micelles with the HMPAA hydrophobes (Piculell et al., 2001). It is therefore likely that a majority of the ibuprofen molecules will be associated with

the mixed aggregates formed by the hydrophobes and/or SDS. In media containing sufficient concentrations of SDS, the release of ibuprofen should thus depend on the diffusion through the gel layer of a small fraction of ibuprofen molecules molecularly dissolved in water; hence, it will be very slow (Bramer et al., 2009).

4. Conclusions

In the present study the release of lactose (hydrophilic) and ibuprofen (hydrophobic) from dissolving drug tablets containing lactose, ibuprofen and HMPAA were investigated in the presence or absence of the surfactant SDS in the dissolution bath. The lactose release was analyzed quantitatively by a novel lactose biosensor utilizing the sugar-oxidizing enzyme *Ct*CDH immobilized on a PDADMAC modified graphite electrode. The promotor layer PDADMAC increased the analytical signals by on average 120 times improving the sensitivity of the sensor possibly due to an increased loading of sensing *Ct*CDH molecules onto the biosensor and an increased interdomain or heterogeneous electron transfer from the enzyme to the electrode. The linear measuring range of lactose was between 10 and 110 μM lactose with a standard deviation of 13%. A fast and easy sample preparation procedure was developed to precipitate denaturating SDS from lactose containing samples by the addition of PEI forming a precipitate due to hydrophobic and electrostatic interactions. The addition of PEI diluted the samples by less than 2% and eliminated around 96% of the SDS within only 20 min enabling a fast and easy measurement of lactose present in samples taken during the dissolution of the tablets.

The release of lactose and ibuprofen differed vastly and the release of ibuprofen from tablets with HMPAA was greatly affected by the presence of surfactant and/or buffer, while the lactose release showed only minor differences. The release behavior of ibuprofen and lactose could be correlated to their different interactions with the polymer and/or the surfactant. A comparison of the release between these two tablet components, combined with studies on the swelling and disintegration of the polymer matrix, allowed us to identify and distinguish between diffusion and erosion controlled release mechanisms from the same tablet formulation. In principle three different scenarios for release could be deduced. For the first scenario, both substances showed similar release profiles and the releases were determined by the rapid tablet erosion. In the second scenario the substances differed, where lactose was mostly dependent on the transport and diffusion through the swollen tablets. Here, ibuprofen was primarily released with the polymer as the latter eroded. In the final scenario, the presence of surfactant slowed down the erosion of the tablets, and none of the three major components showed similar releases. The release of lactose was about the same as in surfactant-free buffer indicating that the rapid diffusion is only slightly slowed down. The release of ibuprofen was instead very slow, nevertheless faster than the polymer release, and the release became dependent on the slow diffusional transport of ibuprofen through the swollen tablets. The strategy and analyses used in this paper are able to further validate previous hypotheses (Knöös et al., 2013a; Wahlgren et al., 2009) and clearly show that the hydrophobic interactions between ibuprofen and the hydrophobically modified polymer are important for the release. By relatively simple dissolution tests and analyses, a deeper understanding of the system could be achieved.

Acknowledgements

The Research School in Pharmaceutical Sciences (FLÄK) is gratefully recognized for financial support (PK) as well as the European Commission ("Chebana" FP7-PEOPLE-2010-ITN-264772, CS, LG).

References

Abrahamsson, B., Roos, K., Sjogren, J., 1999. Investigation of prandial effects on hydrophilic matrix tablets. Drug Development and Industrial Pharmacy 25, 765–771.
Adányi, N., Szabó, E.E., Váradi, M., 1999. Multi-enzyme biosensors with amperometric detection for determination of lactose in milk and dairy products. European Food Research and Technology 209, 220–226.
Appelqvist, R., Marko-Varga, G., Gorton, L., Torstensson, A., Johansson, G., 1985. Enzymatic determination of glucose in a flow system by catalytic oxidation of the nicotinamide coenzyme at a modified electrode. Analytica Chimica Acta 169, 237–247.
Aulton, M.E., Cooper, J.W., 1988. Pharmaceutics: The Science of Dosage Form Design, first ed. Churchill Livingstone, Edinburgh, New York.
Beeson, W.T., Phillips, C.M., Cate, J.H.D., Marletta, M.A., 2011. Oxidative cleavage of cellulose by fungal copper-dependent polysaccharide monooxygenases. Journal of the American Chemical Society 134, 890–892.
Borgquist, P., Körner, A., Piculell, L., Larsson, A., Axelsson, A., 2006. A model for the drug release from a polymer matrix tablet – effects of swelling and dissolution. Journal of Controlled Release 113, 216–225.
Bramer, T., Dew, N., Edsman, K., 2006. Catanionic mixtures involving a drug: a rather general concept that can be utilized for prolonged drug release from gels. Journal of Pharmaceutical Sciences 95, 769–780.
Bramer, T., Frenning, G., Grasjo, J., Edsman, K., Hansson, P., 2009. Implications of regular solution theory on the release mechanism of catanionic mixtures from gels. Colloids and Surfaces B: Biointerfaces 71, 214–225.
Bustamante, P., Pena, M.A., Barra, J., 2000. The modified extended Hansen method to determine partial solubility parameters of drugs containing a single hydrogen bonding group and their sodium derivatives: benzoic acid/Na and ibuprofen/Na. International Journal of Pharmaceutics 194, 117–124.
Bystryak, S.M., Winnik, M.A., Siddiqui, J., 1999. Unusual conductivity changes for sodium dodecyl sulfate solutions in the presence of polyethyleneimine and polyvinylamine. Langmuir 15, 3748–3751.
Cantarel, B.L., Coutinho, P.M., Rancurel, C., Bernard, T., Lombard, V., Henrissat, B., 2009. The carbohydrate-active enzymes database (CAZy): an expert resource for glycogenomics. Nucleic Acids Research 37, D233–D238.
Colombo, P., Bettini, R., Santi, P., Peppas, N.A., 2000. Swellable matrices for controlled drug delivery: gel-layer behaviour, mechanisms and optimal performance. Pharmaceutical Science & Technology Today 3, 198–204.
Dressman, J.B., Amidon, G.L., Reppas, C., Shah, V.P., 1998. Dissolution testing as a prognostic tool for oral drug absorption: immediate release dosage forms. Pharmaceutical Research 15, 11–22.
Dualeh, A.J., Steiner, C.A., 1990. Hydrophobic microphase formation in surfactant solutions containing an amphiphilic graft copolymer. Macromolecules 23, 251–255.
Eadala, P., Waud, J.P., Matthews, S.B., Green, J.T., Campbell, A.K., 2009. Quantifying the 'hidden' lactose in drugs used for the treatment of gastrointestinal conditions. Alimentary Pharmacology & Therapeutics 29, 677–687.
Efentakis, M., Pagoni, I., Vlachou, M., Avgoustakis, K., 2007. Dimensional changes, gel layer evolution and drug release studies in hydrophilic matrices loaded with drugs of different solubility. International Journal of Pharmaceutics 339, 66–75.
Eshkenazi, I., Maltz, E., Zion, B., Rishpon, J., 2000. A three-cascaded-enzymes biosensor to determine lactose concentration in raw milk. Journal of Dairy Science 83, 1939–1945.
Essig, A.M., Kleyn, D.H., 1983. Determination of lactose in milk: comparison of methods. Journal: Association of Official Analytical Chemists 66, 1514–1516.
Fang, J., Liu, W., Gao, P.J., 1998. Cellobiose dehydrogenase from schizophyllum commune: purification and study of some catalytic, inactivation, and cellulose-binding properties. Archives of Biochemistry and Biophysics 353, 37–46.
Ferreira, L.S., Souza Jr, M.B., Trierweiler, J.O., Hitzmann, B., Folly, R.O.M., 2003. Analysis of experimental biosensor/FIA lactose measurements. Brazilian Journal of Chemical Engineering 20, 07–13.
Gao, P., Skoug, J.W., Nixon, P.R., Ju, T.R., Stemm, N.L., Sung, K.C., 1996. Swelling of hydroxypropyl methylcellulose matrix tablets. 2. Mechanistic study of the influence of formulation variables on matrix performance and drug release. Journal of Pharmaceutical Sciences 85, 732–740.
Glithero, N., Clark, C., Gorton, L., Schuhmann, W., Pasco, N., 2013. At-line measurement of lactose in dairy-processing plants. Analytical and Bioanalytical Chemistry 405, 3791–3799.
Harreither, W., Felice, A.K.G., Paukner, R., Gorton, L., Ludwig, R., Sygmund, C., 2012. Recombinantly produced cellobiose dehydrogenase from *Corynascus thermophilus* for glucose biosensors and biofuel cells. Biotechnology Journal 7, 1359–1366.
Harreither, W., Sygmund, C., Augustin, M., Narciso, M., Rabinovich, M.L., Gorton, L., Haltrich, D., Ludwig, R., 2011. Catalytic properties and classification of cellobiose dehydrogenases from ascomycetes. Applied and Environmental Microbiology 77, 1804–1815.
Henriksson, G., Johansson, G., Pettersson, G., 2000. A critical review of cellobiose dehydrogenases. Journal of Biotechnology 78, 93–113.
Holmberg, B.J., Kronberg, B., Lindman, B., 2003. Surfactants and Polymers Aqueous Solutions, second ed. John Wiley & Sons Ltd., Chichester.

Kleyn, D.H., 1985. Determination of lactose by an enzymatic method. Journal of Dairy Science 68, 2791–2798.
Kwak, H.S., Jeon, I.J., 1988. Comparison of high performance liquid chromatography and enzymatic method for the measurement of lactose in milk. Journal of Food Science 53, 975–976.
Körner, A., Larsson, A., Piculell, L., Wittgren, B., 2005. Molecular information on the dissolution of polydisperse polymers: mixtures of long and short poly(ethylene oxide). The Journal of Physical Chemistry B 109, 11530–11537.
Knöös, P., Onder, S., Pedersen, L., Piculell, L., Ulvenlund, S., Wahlgren, M., 2013a. Surfactants modify the release from tablets made of hydrophobically modified poly(acrylic acid). Results in Pharma Sciences 3, 7–14.
Knöös, P., Topgaard, D., Wahlgren, M., Ulvenlund, S., Piculell, L., 2013b. Using NMR chemical shift imaging to monitor swelling and molecular transport in drug-loaded tablets of hydrophobically modified poly(acrylic acid) – methodology and effects of polymer (in) solubility. Langmuir 29, 13898–13908.
Laguecir, A., Ulrich, S., Labille, J., Fatin-Rouge, N., Stoll, S., Buffle, J., 2006. Size and pH effect on electrical and conformational behavior of poly(acrylic acid): simulation and experiment. European Polymer Journal 42, 1135–1144.
Langston, J.A., Shaghasi, T., Abbate, E., Xu, F., Vlasenko, E., Sweeney, M.D., 2011. Oxidoreductive cellulose depolymerization by the enzymes cellobiose dehydrogenase and glycoside hydrolase 61. Applied and Environmental Microbiology 77, 7007–7015.
Li, Y., Ghoreishi, S.M., Warr, J., Bloor, D.M., Holzwarth, J.F., Wyn-Jones, E., 2000. Binding of sodium dodecyl sulfate to some polyethyleneimines and their ethoxylated derivatives at different pH values: electromotive force and microcalorimetry studies. Langmuir 16, 3093–3100.
Ludwig, R., Harreither, W., Tasca, F., Gorton, L., 2010. Cellobiose dehydrogenase: a versatile catalyst for electrochemical applications. ChemPhysChem 11, 2674–2697.
Ludwig, R., Ortiz, R., Schulz, C., Harreither, W., Sygmund, C., Gorton, L., 2013. Cellobiose dehydrogenase modified electrodes: advances by materials science and biochemical engineering. Analytical and Bioanalytical Chemistry 405, 3637–3658.
Magny, B., Iliopoulos, I., Audebert, R., Piculell, L., Lindman, B., 1992. Interactions between hydrophobically modified polymers and surfactants. Progress in Colloid and Polymer Science-Springer 89, 118–121.
Mylonas, Y., Staikos, G., Ullner, M., 1999. Chain conformation and intermolecular interaction of partially neutralized poly(acrylic acid) in dilute aqueous solutions. Polymer 40, 6841–6847.
Mészáros, R., Thompson, L., Bos, M., Varga, I., Gilányi, T., 2003. Interaction of sodium dodecyl sulfate with polyethyleneimine: surfactant-induced polymer solution colloid dispersion transition. Langmuir 19, 609–615.
Marrakchi, M., Dzyadevych, S.V., Lagarde, F., Martelet, C., Jaffrezic-Renault, N., 2008. Conductometric biosensor based on glucose oxidase and beta-galactosidase for specific lactose determination in milk. Materials Science and Engineering: C 28, 872–875.
Maderuelo, C., Zarzuelo, A., Lanao, J.M., 2011. Critical factors in the release of drugs from sustained release hydrophilic matrices. Journal of Controlled Release 154, 2–19.
Mukherjee, S., Dan, A., Bhattacharya, S.C., Panda, A.K., Moulik, S.P., 2011. Physicochemistry of interaction between the cationic polymer poly(diallyldimethylammonium chloride) and the anionic surfactants sodium dodecyl sulfate, sodium dodecylbenzenesulfonate, and sodium *N*-dodecanoylsarcosinate in water and isopropyl alcohol–water media. Langmuir 27, 5222–5233.
Michaelis, L., Menten l, M., 1913. Die kinetik der invertinwirkung. Biochemische Zeitschrift 49, 333–369.
Paulsson, M., Edsman, K., 2002. Controlled drug release from gels using lipophilic interactions of charged substances with surfactants and polymers. Journal of Colloid and Interface Science 248, 194–200.
Phillips, C.M., Beeson, W.T., Cate, J.H., Marletta, M.A., 2011. Cellobiose dehydrogenase and a copper-dependent polysaccharide monooxygenase potentiate cellulose degradation by neurospora crassa. ACS Chemical Biology .
Piculell, I., Thuresson, K., Lindman, B., 2001. Mixed solutions of surfactant and hydrophobically modified polymer. Polymers for Advanced Technologies 12, 44–69.
Safina, G., Ludwig, R., Gorton, L., 2010. A simple and sensitive method for lactose detection based on direct electron transfer between immobilised cellobiose dehydrogenase and screen-printed carbon electrodes. Electrochimica Acta 55, 7690–7695.
Schulz, C., Ludwig, R., Micheelsen, P.O., Silow, M., Toscano, M.D., Gorton, L., 2012. Enhancement of enzymatic activity and catalytic current of cellobiose dehydrogenase by calcium ions. Electrochemistry Communications 17, 71–74.
Skoug, J.W., Mikelsons, M.V., Vigneron, C.N., Stemm, N.L., 1993. Qualitative evaluation of the mechanism of release of matrix sustained-release dosage forms by measurement of polymer release. Journal of Controlled Release 27, 227–245.
Stephenson, B.C., Rangel-Yagui, C.O., Pessoa, A., Tavares, L.C., Beers, K., Blankschtein, D., 2006. Experimental and theoretical investigation of the micellar-assisted solubilization of ibuprofen in aqueous media. Langmuir 22, 1514–1525.
Stoica, L., Ludwig, R., Haltrich, D., Gorton, L., 2006. Third-generation biosensor for lactose based on newly discovered cellobiose dehydrogenase. Analytical Chemistry 78, 393–398.
Tahara, K., Yamamoto, K., Nishihata, T., 1995. Overall mechanism behind matrix sustained-release (sr) tablets prepared with hydroxypropyl methylcellulose-2910. Journal of Controlled Release 35, 59–66.
Tasca, F., Ludwig, R., Gorton, L., Antiochia, R., 2013. Determination of lactose by a novel third generation biosensor based on a cellobiose dehydrogenase and aryl diazonium modified single wall carbon nanotubes electrode. Sensors and Actuators B: Chemical 177, 64–69.
Watson, C.A., 1994. Official and Standardized Methods of Analysis, third ed. Royal Society of Chemistry, Cambridge.
West, L.G., Llorente, M.A., 1981. High performance liquid chromatographic determination of lactose in milk. Journal of the Association of Official Analytical Chemistry 64, 805–807.
Wang, H., Wang, Y., Yan, H., Zhang, J., Thomas, R.K., 2006. Binding of sodium dodecyl sulfate with linear and branched polyethyleneimines in aqueous solution at different pH values. Langmuir 22, 1526–1533.
Wahlgren, M., Christensen, K.L., Jorgensen, E.V., Svensson, A., Ulvenlund, S., 2009. Oral-based controlled release formulations using poly(acrylic acid) microgels. Drug Development and Industrial Pharmacy 35, 922–929.
Yakovleva, M., Buzas, O., Matsumura, H., Samejima, M., Igarashi, K., Larsson, P.-O., Gorton, L., Danielsson, B., 2012. A novel combined thermometric and amperometric biosensor for lactose determination based on immobilised cellobiose dehydrogenase. Biosensors and Bioelectronics 31, 251–256.
Zamocky, M., Ludwig, R., Peterbauer, C., Hallberg, B.M., Divne, C., Nicholls, P., Haltrich, D., 2006. Cellobiose dehydrogenase – a flavocytochrome from wood-degrading, phytopathogenic and saprotropic fungi. Current Protein Peptide Science 7, 255–280.

Paper IV

analytical chemistry

Article

pubs.acs.org/ac

Polyethyleneimine as a Promoter Layer for the Immobilization of Cellobiose Dehydrogenase from *Myriococcum thermophilum* on Graphite Electrodes

Christopher Schulz,[†] Roland Ludwig,[‡] and Lo Gorton*[,†]

[†]Department of Analytical Chemistry/Biochemistry and Structural Biology, Lund University, P.O. Box 124, Lund, Scania SE-22100, Sweden

[‡]Food Biotechnology Laboratory, Department of Food Sciences and Technology, BOKU University of Natural Resources and Life Sciences Vienna, Muthgasse 18, Wien A-1190, Austria

Supporting Information

ABSTRACT: Cellobiose dehydrogenase (CDH) is a promising enzyme for the construction of biofuel cell anodes and biosensors capable of oxidizing aldoses as well as lactose and glucose and with the ability to connect to an electrode through a direct electron transfer mechanism. In the present study, we point out the beneficial effect of a premodification of spectrographic graphite electrodes with the polycation polyethyleneimine (PEI) prior to adsorption of CDH from *Myriococcum thermophilum* (*Mt*CDH). The application of PEI shifts the pH optimum of the response of the *Mt*CDH modified electrode from pH 5.5 to 8. The catalytic currents to lactose were increased up to 140 times, and the K_M^{app} values were increased up to 9 times. The previously investigated, beneficial effect of divalent cations on the activity of CDH was also present for graphite/PEI/*Mt*CDH electrodes but was less pronounced. Polarization curves revealed a second unexpected catalytic wave for graphite/PEI/*Mt*CDH electrodes especially pronounced at pH 8. Square wave voltammetric studies revealed the presence of an unknown redox functionality present at 192 mV vs Ag|AgCl (0.1 M KCl) at pH 8, probably originating from an oxidized adenosine derivative. Adenosine is a structural part of the flavin adenine dinucleotide (FAD) cofactor of the dehydrogenase domain of CDH. It is suggested that for some enzyme molecules FAD leaks out from the active site, adsorbs onto graphite, and is oxidized on the electrode surface into a product able to mediate the electron transfer between CDH and the electrode. PEI is suggested and discussed to act in several manners by (a) increasing the surface loading of the enzyme, (b) possibly increasing the electron transfer rate between CDH and the electrode, and (c) facilitating the creation or immobilization of redox active adenosine derivatives able to additionally mediate the electron transfer between CDH and the electrode.

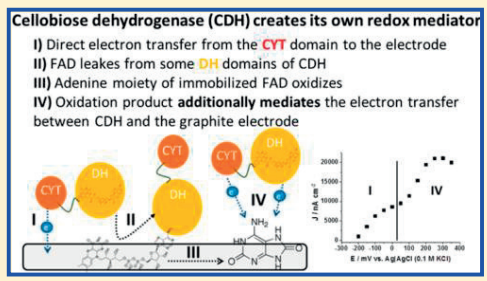

Cellobiose dehydrogenase (CDH, EC 1.1.99.18) is a promising enzyme for the development of biosensors[1,2] and biofuel cells[2,3] oxidizing aldoses including cellodextrins as well as lactose and glucose.[2,4,5] CDH is a monomeric, glycosylated, extracellular flavocytochrome secreted by wood degrading fungi within the phyla of Basidiomycota and Ascomycota. It consists of a catalytically active flavin adenine dinucleotide (FAD) containing dehydrogenase domain (DH_{CDH}) connected via a flexible linker region to an electron mediating, haem *b* containing cytochrome domain (CYT_{CDH}). During catalysis, the oxidation of the natural substrate cellobiose fully reduces FAD. Subsequently, the electrons are transferred by an internal electron transfer mechanism (IET) one by one to the CYT_{CDH} domain resulting in reduced haem *b*.[2,4] The final, natural electron acceptor was found to be copper dependent polysaccharide monooxygenases possibly forming radical adducts helping to degrade cellulose.[6]

Recently, especially divalent cations such as Ca^{2+} and Mg^{2+} were found to increase the activity of CDH both in solution as well as when adsorbed on graphite revealed by a drastic increase in the catalytic currents. Divalent cations were suggested either to increase the IET by complexing negatively charged, repulsing amino acid residues present on the interface of both domains or to increase the interaction between the CYT_{CDH} domain and the final electron acceptor, e.g., the electrode. The Ascomycete CDH from *Myriococcum thermophilum* (*Mt*CDH) was found to be most prone to enhancements of its activity or catalytic currents by divalent cations, probably due to a comparably inefficient IET capable of being improved to a greater extent.[7] In order to move from freely

Received: December 5, 2013
Accepted: April 8, 2014
Published: April 8, 2014

   dx.doi.org/10.1021/ac403957t | *Anal. Chem.* 2014, 86, 4256−4263

diffusive cationic charges as Ca^{2+} to immobilized charges on electrode surfaces, the applicability of polyethyleneimine (PEI) is investigated in the present study. PEI is a polycation consisting either of only primary amines for linear PEI or additionally secondary and tertiary amines for branched PEI, which makes branched PEI freely miscible with water at room temperature.[8] Due to its positive charges also at neutral pH,[9] PEI is a widely used agent for adhesion of cells or biocatalysts onto surfaces[8,10] and transfection of DNA into cells.[11] PEI has been applied for the construction of pH sensors utilizing the pH dependent swelling effect of PEI.[12] The adhesive properties of PEI were used for the construction of biosensors using, e.g., horseradish peroxidase,[13] lactate oxidase,[14] lactate dehydrogenase,[15] glycerol dehydrogenase,[16] glucose oxidase,[17] urease,[18] and cytochrome c_3,[19] mainly increasing stabilities but partly also electron transfer rates. Furthermore, PEI modified with electron transfer mediators, e.g., Meldola blue,[20] ferrocene,[21] or Prussian blue,[22] was also found to be beneficial for sensor construction. On the basis of these findings, the effect of branched PEI used as a premodifier of spectroscopic graphite electrodes on the electrochemistry of immobilized *Mt*CDH was investigated in the present study.

EXPERIMENTAL SECTION

Chemicals. Acetic acid (100%), sodium hydroxide solution (50%), and calcium chloride were purchased from Merck KGaA (Darmstadt, Germany). Sodium chloride, 4-morpholineethanesulfonic acid (MES), tris(hydroxymethyl)-aminomethane (TRIS), β-lactose, hydrochloric acid (37%) and polyethylenimine solution (50% w/v in H_2O, $M_n \sim 60\,000$, $M_w \sim 750\,000$), flavin adenine dinucleotide (FAD), and adenosine were purchased from Sigma-Aldrich Chemicals (Steinheim, Germany). All chemicals were of analytical grade.

Solutions and Enzymes. All buffer solutions had a concentration of 50 mM and were made of acetic acid for buffers covering pH 3−6, MES for buffers covering pH 5.5−7, and TRIS for buffers covering pH 6.5−9 by adjusting with diluted solutions of sodium hydroxide or hydrochloric acid. For the measurements of the pH profiles and long-term stabilities of the electrodes, sodium chloride was used where indicated to adjust the ionic strength of the buffers. An aqueous PEI stock solution of 50 mg/mL, adjusted with HCl to pH 7, was prepared and further diluted to 15, 12.5, 10, 7.5, 5, and 2.5 mg/mL. Four μL aliquots of those PEI solutions were used to modify the graphite electrodes as described in the section following below.

*Mt*CDH (GenBank identifier 164597964) was recombinantly expressed in *Pichia pastoris* and purified as described in ref 23. The truncated DH_{CDH} domain from *Myriococcum thermophilum* (DH_{MtCDH}, amino acids 251−828) was separately expressed in *P. pastoris* following the same protocol. A two-step purification was performed according to Harreither et al.[24] The protein concentrations were determined photometrically by using an extinction coefficient of $\varepsilon_{280} = 159\,063\ cm^{-1}\ M^{-1}$ for the full enzyme and $\varepsilon_{280} = 97\,018\ cm^{-1}\ M^{-1}$ for the separately expressed DH_{MtCDH} domain, which were calculated from the amino acid sequence. Enzyme dilutions of the enzyme stock solution (c = 37.9 mg/mL) were made with a 50 mM acetate buffer, pH 5.5.

Electrode Preparation. Spectrographic graphite electrodes (diameter = 3.05 mm, Ringsdorff Spektrahlkohlestäbe, SGL Carbon Group Ringsdorff-Werke GmbH, Bonn, Germany) were polished on wet emery paper (P1200 from Norton, Saint-Gobain Abrasives AB, Sollentuna, Sweden) and cleaned with Milli-Q water and ethanol and allowed to dry. Optionally, PEI modification was done by adding a drop of 4 μL of a PEI solution (2.5, 5, 7.5, 10, 12.5, 15 mg/mL) onto the surface of the graphite electrode, which was subsequently allowed to dry for around 30 min. Enzyme modification was done by adding a drop of 2 μL of a solution of *Mt*CDH (1, 5, 10, 20, or 25 mg/mL) onto the surface of the graphite electrode or onto the PEI modified graphite electrode and allowed to dry for around 20 min. For the modification of the electrode with FAD or adenosine, 2 μL of a 1 mM aqueous solution was added to the electrode surface and allowed to dry. The enzyme modified electrodes were stored in the refrigerator overnight at 8 °C. The FAD and adenosine modified electrodes were stored at room temperature overnight to facilitate degradation or oxidation (see Results and Discussion below). At least three equally prepared electrodes were measured for each tested condition. Presented error bars indicate the standard deviation of the measurement of three equally prepared electrodes.

Flow Injection Amperometry and Square Wave Voltammetry. The modified graphite electrodes were rinsed with deionized water prior to use to remove loosely bound molecules. For flow injection amperometry, the modified graphite electrodes were mounted into a flow through, 3-electrode electrochemical cell of the wall jet type[25] connected to a peristaltic pump (Gilson, Villier-le-Bel, France), an injector (former Rheodyne, now IDEX Health & Science, Oak Harbor, Washington, USA), a potentiostat (Zäta Elektronik, Höör, Sweden), and a strip chart recorder (Kipp & Zonen, Delft, The Netherlands) as described in ref 26. The reference electrode was an AglAgCl (0.1 M KCl) electrode, and the counter electrode was a platinum wire. The applied potential was, if not stated differently, 250 mV vs AglAgCl (0.1 M KCl). The flow rate was 0.5 mL/min, and the volume of the injection loop was 20 μL. For the measurements of the long-term stabilities of the electrodes, a lower flow rate of 0.16 mL/min was used. For calculations of the kinetic parameters of CDH, the injected substrate concentrations were corrected for the measured dispersion factor[27] equal to 1.33. For square wave voltammetry, the electrodes were mounted in a Teflon holder and measurements were performed in a glass vessel housing the working electrode, a platinum flag counter electrode, and a saturated calomel reference electrode (SCE, +244 mV vs SHE) in a 50 mM TRIS, pH 8 buffer, which was degassed with nitrogen for 20 min prior to measurements. Square wave voltammetry was performed with an EmStat2 potentiostat (PalmSens BV, Utrecht, The Netherlands) using a step potential of 1 mV, an amplitude of 20 mV, and a frequency of 8 Hz. All potentials were converted and refer to the AglAgCl (0.1 M KCl) reference electrode (+288 mV vs SHE).

RESULTS AND DISCUSSION

Spectrographic graphite electrodes were modified with varying amounts of PEI and *Mt*CDH, and the catalytic response of the electrodes to a 5 mM lactose solution containing 50 mM NaAc, pH 5.5, buffer solution was detected amperometrically in the flow injection analysis system. In Figure 1A, the dependence of the catalytic current densities is shown as a function of increasing amounts of PEI immobilized on the graphite electrodes before adsorbing a fixed amount of 410 $\mu g/cm^2$ of *Mt*CDH on top of the PEI layer. Increasing amounts of PEI increased the catalytic current densities linearly by more than 9 times from an average of 340 nA/cm^2 without PEI up to an

dx.doi.org/10.1021/ac403957t | *Anal. Chem.* 2014, 86, 4256−4263

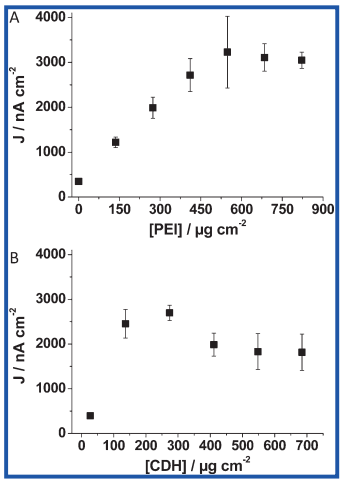

Figure 1. Optimization of the amount of PEI and *Mt*CDH immobilized on spectrographic graphite electrodes mounted in an electrochemical flow through cell connected to a FIA system. Influence of varying amounts of PEI immobilized on a graphite electrode modified followed by adsorption of 410 μg cm^{-2} *Mt*CDH (A) and varying amounts of *Mt*CDH immobilized on a graphite electrode modified with 550 μg cm^{-2} PEI (B). Catalytic currents gained from the oxidation of a 50 mM NaAc buffer, pH 5.5, containing 5 mM lactose were detected amperometrically at an applied potential of 250 mV vs Ag|AgCl (0.1 M KCl).

average of 3200 nA/cm^2 with 550 μg/cm^2 of PEI immobilized on the electrode surface. Amounts higher than 550 μg/cm^2 of PEI on the electrode surface caused a slight decrease in the current response. The linearly increasing current densities up to 550 μg/cm^2 of PEI could be explained by higher surface loadings of CDH achieved by higher loadings of PEI. Strong electrostatic interactions between *Mt*CDH (isoelectric point of 3.8[2]) and PEI (isoelectric point between pH 10 and 11[9]) at the investigated pH of 5.5 are expected to play a major role. The slightly decreasing catalytic currents of *Mt*CDH on electrodes with more than 550 μg/cm^2 of PEI could be explained by either hindered electron transfer between CDH and the electrode due to too thick of a layer of insulating PEI or by mass transfer limitations of the substrate to the enzyme entrapped in the PEI layer. Increased K_M^{app} values for *Mt*CDH in the presence of PEI, as presented in Table 1 and discussed below, support both hypotheses.

Subsequently, the amount of CDH on the electrode was varied while the amount of PEI was kept constant at 550 μg/cm^2 and the influence on the catalytic current densities was investigated, as shown in Figure 1B. Increasing the amount of CDH from 30 to 140 μg/cm^2 on a PEI modified electrode led to nearly equally increasing catalytic current densities, indicating a higher achieved loading of CDH onto the PEI modified electrode. A further increase in the amount of CDH up to 270 μg/cm^2 increased the catalytic current density only slightly to an optimum of around 2740 nA/cm^2. Further increases in PEI led to slightly decreasing currents. This could indicate mass transfer limitations of the substrate into the PEI/CDH layer. The optimal amounts of 550 μg/cm^2 of PEI and 270 μg/cm^2 were used for the further experiments.

In Figure 2, the pH profiles of *Mt*CDH immobilized directly on spectrographic graphite electrodes are compared to cases when the immobilization of *Mt*CDH on PEI modified spectrographic graphite electrodes was performed. In the absence of PEI, a pH optimum of pH 5.5 was found, which is identical to that found in a previous investigation of *Mt*CDH immobilized on graphite electrodes.[26] Interestingly, when *Mt*CDH was immobilized on a PEI modified graphite electrode, the pH optimum was found to shift to pH 8. Furthermore, the PEI modification of the graphite electrode leads to an increase in the catalytic current densities over the whole investigated pH range compared with the current response of graphite electrodes only modified with *Mt*CDH. The modification with PEI caused increases in the catalytic current densities by more than 10 times at pH 5.5 and more than 140 times at pH 8.

In cases where the pH profiles were done at a fixed ionic strength of 50 mM by adding sodium chloride to all used buffer solutions, the general finding was an increase in the catalytic currents and a shift of the pH optimum to an alkaline pH range in the presence of PEI (see Figure S1 in the Supporting Information). Hence, the pH optimum in the presence of NaCl was even higher than pH 8.

The general observed increase in catalytic current densities of CDH on PEI modified electrodes over the whole pH range can be explained by several effects. As discussed already above, a higher surface loading of CDH achieved by PEI contributes to higher catalytic currents in general. The fact that not only the catalytic currents were increased but also the pH optimum was

Table 1. Maximal Current Densities, J_{max}, and K_M^{app} Values for *Mt*CDH Immobilized Directly on Graphite Electrodes or on PEI Modified Graphite Electrodes with Lactose as Substrate at pH 5.5 and pH 8 in the Presence and in the Absence of 50 mM $CaCl_2$[a]

graphite electrode +	buffer: pH ± $CaCl_2$	J_{max} ± SD/nA cm^{-2}	K_M^{app} ± SD/μM	R^2 ± SD
*Mt*CDH	5.5	310 ± 80	55 ± 6	0.91 ± 0.03
	5.5 + $CaCl_2$	1430 ± 440	78 ± 19	0.99 ± 0.00
	8	160 ± 30	50 ± 19	0.93 ± 0.05
	8 + $CaCl_2$	1550 ± 560	96 ± 26	0.96 ± 0.02
PEI/*Mt*CDH	5.5	2890 ± 190	136 ± 84	1.00 ± 0.00
	5.5 + $CaCl_2$	8610 ± 730	185 ± 96	1.00 ± 0.00
	8	23430 ± 3530	490 ± 103	1.00 ± 0.00
	8 + $CaCl_2$	38780 ± 6790	476 ± 132	1.00 ± 0.00

[a]The running buffers were 50 mM NaAc, pH 5.5 or 50 mM TRIS, pH 8 optionally containing 50 mM $CaCl_2$. The applied potential was 250 mV vs. Ag|AgCl (0.1 M KCl).

dx.doi.org/10.1021/ac403957t | *Anal. Chem.* 2014, 86, 4256−4263

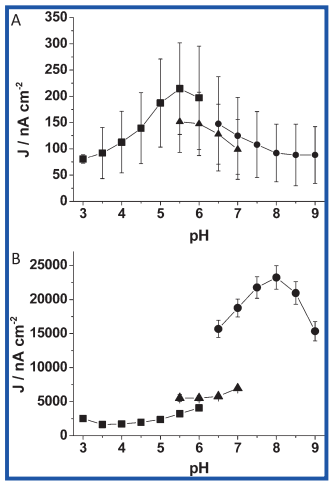

Figure 2. pH profiles of *Mt*CDH immobilized directly on spectrographic graphite electrodes (A) and on spectrographic graphite electrodes modified with 550 μg cm^{-2} PEI (B). The electrodes were mounted in an electrochemical flow through cell connected to a FIA system with 50 mM NaAc, MES, or TRIS of varying pH as a running buffer. The catalytic current responses to buffer solutions containing 5 mM lactose were detected at an applied potential of 250 mV vs AgI AgCl (0.1 M KCl).

shifted indicates further contributing factors. In a recent investigation, especially divalent cations, e.g., Ca^{2+}, but to a lower extent also monovalent cations as K^+ present in the measuring buffer were found to increase either the internal electron transfer between the DH_{CDH} and the CYT_{CDH} or the final electron transfer step from CYT_{CDH} to the graphite electrode leading to an increase in the response current by 5 times at pH 5.5.[7] A complexation of negative charges at the surfaces of DH_{CDH} and of CYT_{CDH} by Ca^{2+} was suggested as one possibility increasing the interaction and decreasing the distance between the domains and consequently increasing the rate of the IET. The protonated NH_2 groups of PEI might act in a similar manner by screening negative, repulsing charges present at the interface of both of the enzyme domains. This is supported by the shift in the pH optimum in the presence of PEI to pH 8, which is the pH optimum for the catalytic DH_{CDH} domain, as shown with *Mt*CDH immobilized on graphite electrodes in the presence of the mediator 1,4 benzoquinone, which is efficiently reduced by the DH_{CDH} domain.[26] Consequently, PEI might also increase the rate of the IET so that more of the catalytic turnover of the DH_{CDH} domain is "visible". The possible further shift of the pH optimum to values even higher than pH 8 in the presence of NaCl indicates a possible further screening of negative charges due to Na^+. The observed increases in the maximal current densities for PEI modified electrodes in the additional presence of Ca^{2+} as discussed below support this hypothesis.

To investigate the influence of PEI on the apparent enzyme characteristics, the maximal current density, J_{max}, and the apparent Michaelis–Menten constant, K_M^{app}, calibration graphs with *Mt*CDH modified graphite electrodes have been evaluated for electrodes with and without PEI modification and with lactose concentrations ranging from 3.75 μM to 37.5 mM. Since in a previous study the beneficial effect of Ca^{2+} on the catalytic response of *Mt*CDH has been discovered, identical

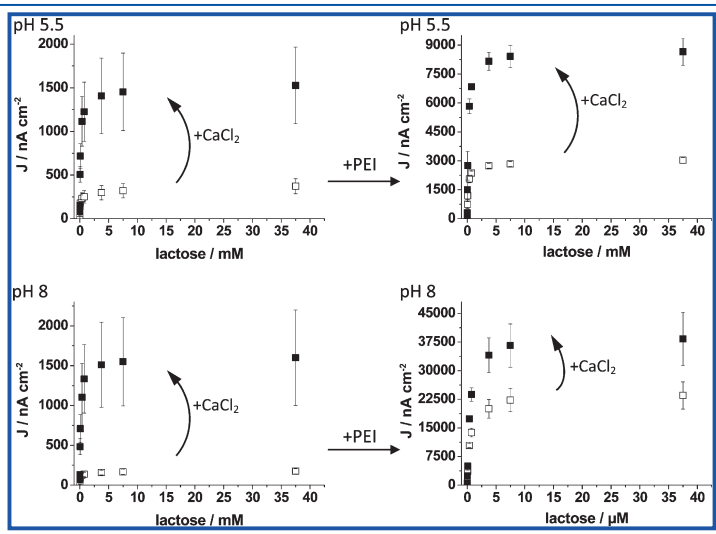

Figure 3. Calibration graphs of spectrographic graphite electrodes modified with (left column) *Mt*CDH only or with (right column) PEI and *Mt*CDH with lactose as substrate in the presence and in the absence of 50 mM $CaCl_2$ (as indicated by arrows) at (top row) pH 5.5 and (lower row) pH 8. The calibration graphs were obtained amperometrically with modified graphite electrodes mounted in a flow through cell connected to a FIA system. The running buffers were 50 mM NaAc, pH 5.5, or 50 mM TRIS, pH 8. The applied potential was 250 mV vs AgIAgCl (0.1 M KCl).

dx.doi.org/10.1021/ac403957t | *Anal. Chem.* 2014, 86, 4256–4263

calibration graphs in the presence of 50 mM $CaCl_2$ have been evaluated as well. The response curves are shown in Figure 3, and the kinetic data obtained from fitting the responses of each electrode to the Michaelis–Menten equation are summarized in Table 1. In the absence of PEI and $CaCl_2$, the catalytic currents are comparably low with a J_{max} of on average 310 nA/cm^2 at pH 5.5 (pH optimum for DET) and 160 nA/cm^2 at pH 8 (pH optimum for MET). The addition of 50 mM $CaCl_2$ to the measuring buffer increases J_{max} by around 5 times at pH 5.5 and 9 times at pH 8. When PEI premodified electrodes were used, the J_{max} could be increased by around 9 times at pH 5.5 and around 140 times at pH 8 compared to *Mt*CDH modified electrodes lacking PEI.

The huge increase in J_{max} in the presence of PEI at especially pH 8 is consistent with the observed shift of the pH optimum of *Mt*CDH from pH 5.5 to pH 8 due to the PEI premodification (see Figure 2) and might be partially explained by an increased DH_{CDH}-CYT_{CDH} domain interaction as suggested above. The premodification with PEI also leads to a 2-fold increase in the K_M^{app} value of *Mt*CDH at pH 5.5 and a 10 times increase at pH 8 compared to *Mt*CDH on bare graphite electrodes. This supports the hypothesis of a higher enzyme loading achieved with the PEI premodification leading to diffusion limitations of the substrate into the PEI/CDH layer.

The addition of 50 mM $CaCl_2$ to the measuring buffer was shown to still further increase the catalytic currents of *Mt*CDH immobilized on PEI premodified electrodes. Additional $CaCl_2$ increased J_{max} by around 3 times at pH 5.5 and 2 times at pH 8, indicating still a beneficial effect of $CaCl_2$ but to a smaller extent compared to the effect obtained when *Mt*CDH is immobilized on bare graphite electrodes without PEI premodification. This indicates that PEI not only might increase the DH_{CDH}–CYT_{CDH} domain interaction or the surface loading but also might act in another way.

Residual stabilities after 5 h were not significantly different (confidence level 95%) for *Mt*CDH modified electrodes modified with PEI (89 ± 6%) compared to electrodes lacking PEI (71 ± 7%) at an ionic strength of 50 mM. Increasing the ionic strength to 500 mM decreased the residual stabilities to significantly lower values (confidence level 95%) for PEI-*Mt*CDH modified electrodes (55 ± 1%) compared to electrodes lacking the PEI modification (84 ± 3%); see Table S1 in the Supporting Information. This indicates that the interaction between PEI and *Mt*CDH is more of an electrostatic nature compared to *Mt*CDH immobilized directly on graphite electrodes, which is due to physisorption.

The response times of the *Mt*CDH modified electrodes to 5 mM lactose were decreased from 22 ± 3 s in the absence to 10 ± 1s in the presence of the PEI layer. This is surprising at a first glance, since as discussed above, the PEI layer was suggested to limit the diffusion of the substrate to the enzyme as indicated by higher K_M^{app} values, theoretically resulting also in slower response times. However, as discussed below, in the presence of PEI, an additional electron transfer pathway from the DH_{CDH} to the electrode by an unknown mediator is suggested to be present. This additionally present, presumably fast, mediated electron transfer might be responsible for the decreased response times observed for PEI-*Mt*CDH electrodes.

In Figure 4, the polarization curves are shown of native *Mt*CDH containing both the DH_{CDH} and CYT_{CDH} domains and of the separately expressed DH_{CDH} domain immobilized on PEI modified graphite electrodes measured at pH 8 in the presence and absence of $CaCl_2$ in the flow buffer and with lactose as substrate. For native *Mt*CDH containing both domains, a catalytic wave between −200 and 50 mV can be observed in the absence and presence of $CaCl_2$ (Figure 4, □, ■). This first catalytic wave belongs to the expected ET from the CYT_{CDH}, which is reduced by the catalytically active DH_{CDH} domain.[26,28] Until today, no efficient direct communication with the DH_{CDH} has been shown,[28] which would have been expected if it occurred at redox potentials of around −480 mV vs Ag|AgCl (0.1 M KCl)[29] originating from the noncovalently bound FAD cofactor in the DH_{CDH}. As expected, the first catalytic wave originating from the CYT_{CDH} could not be observed for the separately expressed DH_{CDH}, which lacks the electron mediating CYT_{CDH} (see Figure 4, Δ). When comparing the catalytic current densities only in the region of the first and expected catalytic wave, the PEI modification increases the catalytic currents by around 30 times at pH 8 (data not shown).

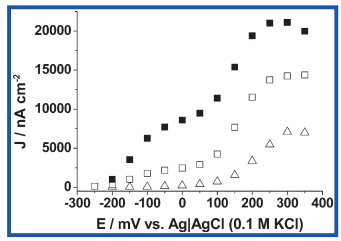

Figure 4. Polarization curves of PEI/graphite electrodes modified with *Mt*CDH containing both the CYT_{CDH} (squares □, ■) or only the DH_{CDH} domain (Δ) at pH 8 in the presence (filled symbol) or absence of 50 mM $CaCl_2$ (empty symbols). The responses of the modified graphite electrodes were investigated with flow injection analysis with 5 mM lactose as substrate.

Surprisingly, a further increase in the applied potential higher than +100 mV creates a second catalytic wave visible for electrodes modified with *Mt*CDH and also with the separate DH_{CDH}, which cannot be assigned to either the intact CYT_{CDH} or DH_{CDH}. The position of this second catalytic wave was pH dependent with a shift of around 40 mV/pH (data not shown), indicating protons being involved in the phenomenon of the second catalytic wave. The additional ET originating from the second catalytic wave seems to be responsible for a major part of the increase in the observed catalytic current densities in the presence of PEI.

As observed already for the calibration graphs (see Figure 3), the addition of $CaCl_2$ to the measuring buffer still increased the catalytic currents for intact *Mt*CDH immobilized on PEI premodified electrodes. From the polarization curves of intact *Mt*CDH (Figure 4, □, ■), it is visible that additional $CaCl_2$ only enhances the catalytic currents in the region of the first, expected catalytic wave originating from the ET between the CYT_{CDH} and the electrode, indicating a beneficial effect either on the IET between the DH_{CDH} and the CYT_{CDH} or on the final ET between CYT_{CDH} and the electrode. In the region of the second catalytic wave, additional $CaCl_2$ does not increase the catalytic currents, indicating that not only intact *Mt*CDH may be involved in this phenomenon.

The second catalytic wave could also be observed for *Mt*CDH immobilized on graphite electrodes lacking any PEI premodification but was much less pronounced (data not

dx.doi.org/10.1021/ac403957t | *Anal. Chem.* 2014, 86, 4256–4263

shown), indicating that it is not originating from the PEI modification itself. The second catalytic wave is also clearly visible for the separately expressed DH_{CDH} domain immobilized on PEI premodified graphite electrodes (see Figure 4, Δ), indicating that the CYT_{CDH} or haem *b* is not responsible for this phenomenon, but instead, it is due to DH_{CDH} or its cofactor FAD.

To further elucidate the origin of the second catalytic wave, square wave voltammetry was performed in order to investigate redox functionalities present on the surface of graphite electrodes modified with either only PEI or PEI and DH_{CDH} or PEI and adenosine, a structural part of the DH_{CDH} cofactor FAD. As shown in Figure 5, graphite electrodes modified only

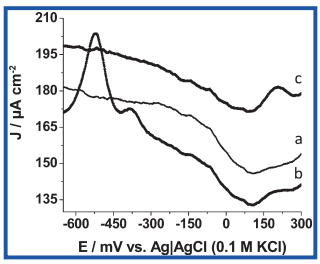

Figure 5. Square wave voltammograms of PEI modified graphite electrodes (a) additionally modified with the DH_{CDH} domain from *Myriococcum thermophilum* (b) or adenosine (c) measured at pH 8.

with PEI (a) show redox functionalities mainly in the region between 0 and −200 mV, probably originating from surface quinones naturally present on spectroscopic graphite electrodes.[30] A contribution of the surface quinones in ET from CYT_{CDH} to the electrode surface cannot be fully excluded. However, true and clear DET from CYT_{CDH} to, e.g., modified gold electrodes lacking any surface quinones is well established.[2,5,31] The response of the graphite/PEI/DH_{CDH} electrode (b) shows mainly three redox functionalities with $E^{\circ\prime}$ values of around −520, −376, and +192 mV. The first redox functionality present at −520 mV arises from the isoalloxazine ring of free FAD immobilized on the graphite/PEI electrode originating from DH_{CDH}.[32] FAD noncovalently bound to DH_{CDH} was reported to have a $E^{\circ\prime}$ of around −480 mV at pH 8.[29] Furthermore, no catalysis was observed in cyclic voltammetry studies starting at −520 mV (data not shown) supporting the assumption of free FAD adsorbed on the electrode surface and not FAD bound to the catalytically active DH_{CDH}. The redox functionality at −376 mV cannot be readily assigned yet, but as for the functionality present at −520 mV, it was observed exclusively for the graphite/PEI/DH_{CDH} electrode and is assumed to originate from the isoalloxazine moiety of the FAD.

The third redox functionality at +192 mV was observed for both the DH_{CDH} (b) and the adenosine modified graphite/PEI electrodes (c). Since adenosine is a structural part of FAD, this redox functionality can be assigned to originate from the adenosine part present in FAD. When comparing these findings with the polarization curves shown in Figure 4, one can conclude that the redox functionality with an $E^{\circ\prime}$ of +192 mV might be the responsible, surface immobilized mediator creating the second catalytic wave of unknown origin by mediating electrons from the CYT_{CDH} and/or the DH_{CDH} domain to the electrode at high potentials. It has to be mentioned that the redox functionality present at 192 mV for graphite/PEI/adenosine electrodes was not observed for freshly prepared electrodes. Only after 1 day of incubation, roughly 70% of the modified electrodes exhibited the additional redox functionality. This might indicate a degradation or oxidation process of the adenosine moiety responsible for the creation of the redox functionality with a formal potential of 192 mV. This process might be either facilitated by PEI or PEI increases the concentration of this species, since the additional catalytic wave observed in the polarization curves was also present in the absence of PEI, however, much less pronounced.

Adenosine or FAD added to the running buffers was not able to increase the catalytic currents obtained from the oxidation of lactose (see Figure S2 in the Supporting Information), indicating that they are not able to additionally mediate an electron transfer between enzyme and electrode but possibly only an oxidation product of them. To artificially create the unknown redox mediator from the precursor adenosine, graphite electrodes lacking PEI were first incubated overnight with adenosine at room temperature to facilitate its oxidation and afterward modified with *Mt*CDH. We observed increases in the catalytic currents for graphite-adenosine-*Mt*CDH electrodes compared to those lacking preadsorbed adenosine; hence, the increase was only on average 2-fold (see Figure S2 in the Supporting Information), whether or not those increases were due to an additionally mediated electron transfer or due to other effects, as changed enzyme orientation or loading of enzyme on the adenosine modified electrode is unclear. Assuming the presence of the unknown mediator formed from preadsorbed adenosine, still a correct orientation of the afterward immobilized enzyme toward this mediator cannot be readily assumed serving as one possible explanation for the only on average 2-fold increase in the catalytic current.

The redox functionality present at 192 mV was shown already in 2000 with square wave voltammetry to be present for CDH from *Phanerochaete chrysosporium* immobilized on the same graphite type electrodes as used here (without any PEI premodification) but has never been further investigated.[33] Also for gold electrodes modified with self-assembled monolayers and CDH, two catalytic waves have been observed sometimes in our laboratory but never in a reproducible manner. However, electrochemical oxidation of adenine derivatives and adenosine on various electrode surfaces was shown to be able to generate various redox active compounds prone to become immobilized on electrode surfaces.[34−36] Possible oxidation products of adenine at pyrolytic graphite electrodes were suggested to be 2-hydroxyadenine, 8-hydroxyadenine, 2,8-dihydroxyadenine, and further reaction products of them as allantoin exhibiting oxidation peak potentials between −250 and 360 mV at pH 8.[37] Tuñón-Blanco et al. described another, yet unknown, oxidation product of adenosine, which adsorbs at pyrolytic graphite electrodes and has an $E^{\circ\prime}$ of around −27 mV vs Ag|AgCl (0.1 M KCl) at pH 8 and is able to lower the overpotential for NADH oxidation.[36] However, the $E^{\circ\prime}$ is 200 mV more negative than the $E^{\circ\prime}$ of the species we observe. It was also pointed out that the electrode material itself strongly affects the oxidation potential of adenine[34] and that the way of oxidation, e.g., electrochemical or photochemical, also influences the nature of the oxidation products.[37] In our investigated electrode material, how the PEI premodification or the way of oxidation (incubation at room temperature or 8 °C)

dx.doi.org/10.1021/ac403957t | *Anal. Chem.* 2014, 86, 4256−4263

influences the creation of redox active adenosine derivatives has to be further investigated.

CONCLUSIONS

The catalytic currents from lactose oxidation by graphite electrodes modified with CDH from *Myriococcum thermophilum* could be greatly enhanced by a premodification of the electrodes with the polycation PEI. The optimal amount of PEI used for the premodification of the electrodes was found to be 550 $\mu g/cm^2$, and the optimal amount of *Mt*CDH was found to be 270 $\mu g/cm^2$. The utilization of PEI shifted the pH optimum of *Mt*CDH from pH 5.5 to pH 8, increased the catalytic currents up to 140 times at pH 8, and also increased the K_M^{app} of *Mt*CDH by maximally 9 times. The previously found enhancing influence of additionally present divalent cations as Ca^{2+} on the catalysis of CDH was observed also for graphite/PEI/*Mt*CDH electrodes but was less pronounced on PEI premodified electrodes. PEI is suggested to act in various manners. It increases the enzyme loading on the electrode surfaced due to strong electrostatic interactions between the negatively charged enzyme and the polycationic PEI. PEI may also increase the IET between DH_{CDH} and CYT_{CDH} or between CYT_{CDH} and the electrode by screening negative charges, comparable to the previously observed, beneficial effect of especially divalent cations on the activity of *Mt*CDH.[7] Polarization curves revealed the presence of an unexpected, second catalytic wave present for graphite/*Mt*CDH and was much more pronounced for graphite/PEI/*Mt*CDH electrodes and at pH 8. Using square wave voltammetry, adenosine, which is a structural part of DH_{CDH}'s cofactor FAD, was identified as a potential precursor for the formation of an immobilized, yet unknown, redox active compound able to mediate ET between CDH and the electrode. The findings are of importance for the construction of lactose or glucose biosensors and biofuel cells, especially working at a human physiological pH with high current densities but also for a deeper understanding of the catalytic mechanism of CDH.

ASSOCIATED CONTENT

Supporting Information

Two figures and one table, Figures S1 and S2 and Table S1. This material is available free of charge via the Internet at http://pubs.acs.org

AUTHOR INFORMATION

Corresponding Author

*E-mail: Lo.Gorton@biochemistry.lu.se.

Notes

The authors declare no competing financial interest.

ACKNOWLEDGMENTS

The authors thank the following agencies for financial support: The European Commission ("Chebana" FP7-PEOPLE-2010-ITN-264772) and The Swedish Research Council (Vetenskapsrådet, project 2010-5031).

REFERENCES

(1) Feifel, S. C.; Ludwig, R.; Gorton, L.; Lisdat, F. *Langmuir* **2012**, *28*, 9189−9194. Sarauli, D.; Ludwig, R.; Haltrich, D.; Gorton, L.; Lisdat, F. *Bioelectrochemistry* **2012**, *87*, 9−14. Cruys-Bagger, N.; Ren, G.; Tatsumi, H.; Baumann, M. J.; Spodsberg, N.; Andersen, H. D.; Gorton, L.; Borch, K.; Westh, P. *Biotechnol. Bioeng.* **2012**, *109*, 3199−3204.

(2) Ludwig, R.; Harreither, W.; Tasca, F.; Gorton, L. *ChemPhysChem* **2010**, *11*, 2674−2697.

(3) Tasca, F.; Harreither, W.; Ludwig, R.; Gooding, J. J.; Gorton, L. *Anal. Chem.* **2011**, *83*, 3042−3049. Matsumura, H.; Ortiz, R.; Ludwig, R.; Igarashi, K.; Samejima, M.; Gorton, L. *Langmuir* **2012**, *28*, 10925−10933. Wang, X.; Falk, M.; Ortiz, R.; Matsumura, H.; Bobacka, J.; Ludwig, R.; Bergelin, M.; Gorton, L.; Shleev, S. *Biosens. Bioelectron.* **2012**, *31*, 219−225.

(4) Henriksson, G.; Johansson, G.; Pettersson, G. *J. Biotechnol.* **2000**, *78*, 93−113.

(5) Ludwig, R.; Ortiz, R.; Schulz, C.; Harreither, W.; Sygmund, C.; Gorton, L. *Anal. Bioanal. Chem.* **2013**, *405*, 3637−3658.

(6) Beeson, W. T.; Phillips, C. M.; Cate, J. H. D.; Marletta, M. A. *J. Am. Chem. Soc.* **2011**, *134*, 890−892. Phillips, C. M.; Beeson, W. T.; Cate, J. H.; Marletta, M. A. *ACS Chem. Biol.* **2011**, *6*, 1399−1406. Langston, J. A.; Shaghasi, T.; Abbate, E.; Xu, F.; Vlasenko, E.; Sweeney, M. D. *Appl. Environ. Microbiol.* **2011**, *77*, 7007−7015.

(7) Schulz, C.; Ludwig, R.; Micheelsen, P. O.; Silow, M.; Toscano, M. D.; Gorton, L. *Electrochem. Commun.* **2012**, *17*, 71−74.

(8) Bahulekar, R.; Ayyangar, N. R.; Ponrathnam, S. *Enzyme Microb. Technol.* **1991**, *13*, 858−868.

(9) Burgess, R. R. *Methods Enzymol.* **1991**, *208*, 3−10.

(10) Vancha, A.; Govindaraju, S.; Parsa, K.; Jasti, M.; Gonzalez-Garcia, M.; Ballestero, R. *BMC Biotechnol.* **2004**, *4*, 23.

(11) Boussif, O.; Lezoualc'h, F.; Zanta, M. A.; Mergny, M. D.; Scherman, D.; Demeneix, B.; Behr, J. P. *Proc. Natl. Acad. Sci. U. S. A.* **1995**, *92*, 7297−7301.

(12) Mandler, D.; Kaminski, A.; Willner, I. *Electrochim. Acta* **1992**, *37*, 2765−2767. Lakard, B.; Herlem, G.; de Labachelerie, M.; Daniau, W.; Martin, G.; Jeannot, J.-C.; Robert, L.; Fahys, B. *Biosens. Bioelectron.* **2004**, *19*, 595−606.

(13) Gorton, L.; Jonsson-Pettersson, G.; Csöregi, E.; Johansson, K.; Domínguez, E.; Marko-Varga, G. *Analyst* **1992**, *117*, 1235−1241.

(14) Hart, A. L.; Matthews, C.; Collier, W. A. *Anal. Chim. Acta* **1999**, *386*, 7−12.

(15) Watanabe, K.; Royer, G. P. *J. Mol. Catal.* **1983**, *22*, 145−152.

(16) Tang, X.-J.; Xie, B.; Larsson, P.-O.; Danielsson, B.; Khayyami, M.; Johansson, G. *Anal. Chim. Acta* **1998**, *374*, 185−190.

(17) Zhang, W.; Huang, Y.; Dai, H.; Wang, X.; Fan, C.; Li, G. *Anal. Biochem.* **2004**, *329*, 85−90.

(18) Lakard, B.; Herlem, G.; Lakard, S.; Antoniou, A.; Fahys, B. *Biosens. Bioelectron.* **2004**, *19*, 1641−1647.

(19) Lojou, E.; Bianco, P. *Electrochim. Acta* **2007**, *52*, 7307−7314.

(20) Ladiu, C. I.; Popescu, I. C.; Gorton, L. *J. Solid State Electrochem.* **2005**, *9*, 296−303.

(21) Tran, T. O.; Lammert, E. G.; Chen, J.; Merchant, S. A.; Brunski, D. B.; Keay, J. C.; Johnson, M. B.; Glatzhofer, D. T.; Schmidtke, D. W. *Langmuir* **2011**, *27*, 6201−6210. Chuang, C. L.; Wang, Y. J.; Lan, H. L. *Anal. Chim. Acta* **1997**, *353*, 37−44. Merchant, S. A.; Glatzhofer, D. T.; Schmidtke, D. W. *Langmuir* **2007**, *23*, 11295−11302. Merchant, S. A.; Tran, T. O.; Meredith, M. T.; Cline, T. C.; Glatzhofer, D. T.; Schmidtke, D. W. *Langmuir* **2009**, *25*, 7736−7742.

(22) Pchelintsev, N. A.; Vakurov, A.; Millner, P. A. *Sens. Actuators, B: Chem.* **2009**, *138*, 461−466.

(23) Flitsch, A.; Prasetyo, E. N.; Sygmund, C.; Ludwig, R.; Nyanhongo, G. S.; Guebitz, G. M. *Enzyme Microb. Technol.* **2013**, *52*, 60−67.

(24) Harreither, W.; Felice, A. K. G.; Paukner, R.; Gorton, L.; Ludwig, R.; Sygmund, C. *Biotechnol. J.* **2012**, *7*, 1359−1366.

(25) Appelqvist, R.; Marko-Varga, G.; Gorton, L.; Torstensson, A.; Johansson, G. *Anal. Chim. Acta* **1985**, *169*, 237−247.

(26) Harreither, W.; Coman, V.; Ludwig, R.; Haltrich, D.; Gorton, L. *Electroanalysis* **2007**, *19*, 172−180.

(27) Růžička, J.; Hansen, E. H. *Anal. Chim. Acta* **1975**, *78*, 145−157.

(28) Coman, V.; Harreither, W.; Ludwig, R.; Haltrich, D.; Gorton, L. *Chem. Anal. (Warsaw)* **2007**, *52*, 945−960.

(29) Igarashi, K. Function of cellobiose dehydrogenase in cellulose biodegradation by the white-rot fungus Phanerochaete chrysosporium. Doctoral Thesis, University of Tokyo, Tokyo, Japan, 1999.

(30) Panzer, R. E.; Elving, P. J. *Electrochim. Acta* **1975**, *20*, 635−647. Thorogood, C. A.; Wildgoose, G. G.; Jones, J. H.; Compton, R. G. *New J. Chem.* **2007**, *31*, 958−965.
(31) Larsson, T.; Lindgren, A.; Ruzgas, T. *Bioelectrochemistry* **2001**, *53*, 243−249. Lindgren, A.; Larsson, T.; Ruzgas, T.; Gorton, L. *J. Electroanal. Chem.* **2000**, *494*, 105−113.
(32) Gorton, L.; Johansson, G. *J. Electroanal. Chem.* **1980**, *113*, 151−158.
(33) Larsson, T.; Lindgren, A.; Ruzgas, T.; Lindquist, S. E.; Gorton, L. *J. Electroanal. Chem.* **2000**, *482*, 1−10.
(34) Gonçalves, L. s. M.; Batchelor-McAuley, C.; Barros, A. A.; Compton, R. G. *J. Phys. Chem. C* **2010**, *114*, 14213−14219.
(35) Tao, N. J.; DeRose, J. A.; Lindsay, S. M. *J. Phys. Chem.* **1993**, *97*, 910−919. Martins, A.; Queirós, A.; Silva, F. *ChemPhysChem* **2005**, *6*, 1056−1060. Prieto, F.; Rueda, M.; Prado, C.; Feliu, J. M.; Aldaz, A. *Electrochim. Acta* **2010**, *55*, 3301−3306. de-los-Santos-Álvarez, N.; de-los-Santos-Álvarez, P.; Lobo-Castañón, M. J.; López, R.; Miranda-Ordieres, A. J.; Tuñón-Blanco, P. *Electrochem. Commun.* **2007**, *9*, 1862−1866. Dryhurst, G.; Elving, P. J. *J. Electrochem. Soc.* **1968**, *115*, 1014−1020.
(36) de los Santos Álvarez, N.; Ortea, P. M.; Pañeda, A. M.; Castañón, M. J. L.; Ordieres, A. J. M.; Blanco, P. T. *J. Electroanal. Chem.* **2001**, *502*, 109−117.
(37) Goyal, R. N.; Kumar, A.; Mittal, A. *J. Chem. Soc., Perkin Trans. 2* **1991**, 1369−1375.

Paper V

Full Paper Wiley Online Library ELECTROANALYSIS

DOI: 10.1002/elan.201400231

Third Generation ATP Sensor with Enzymatic Analyte Recycling

Aysu Yarman,*[a, b] Christopher Schulz,[c] Cristoph Sygmund,[d] Roland Ludwig,[d] Lo Gorton,[c] Ulla Wollenberger,[b] and Frieder W. Scheller*[a, b]

Abstract: For the first time the direct electron transfer of an enzyme - cellobiose dehydrogenase, CDH - has been coupled with the hexokinase catalyzed competition for glucose in a sensor for ATP. To enhance the signal output for ATP, pyruvate kinase was coimmobilized to recycle ADP by the phosphoenolpyruvate driven reaction. The new sensor overcomes the limit of 1:1 stoichiometry of the sequential or competitive conversion of ATP by effective enzymatic recycling of the analyte. The anodic oxidation of the glucose converting CDH proceeds at electrode potentials below 0 mV vs. Ag|AgCl thus potentially interfering substances like ascorbic acid or catecholamines do not influence the measuring signal. The combination of direct electron transfer of CDH with the enzymatic recycling results in an interference-free and oxygen-independent measurement of ATP in the lower μmolar concentration range with a lower limit of detection of 63.3 nM ($S/N=3$).

Keywords: ATP · Third generation sensor · Enzymatic recycling · Cellobiose dehydrogenase · Hexokinase · Pyruvate kinase

1 Introduction

Adenosine-5′-triphosphate (ATP) is the main intracellular energy source. It is involved in different signaling processes and released into the extracellular surrounding after various mechanical and chemical stimuli. Luciferase-based bioluminescence is the gold standard for in situ ATP measurement even in the subnanomolar concentration range [1]. On the other hand the nondestructive, online measurement of ATP in the lower μM range is still a challenge [2,3].

Amperometric enzyme electrodes have the potential for in vivo measurements of metabolites in the millimolar range e.g., for glucose and lactate [4,5]. For ATP measurement multi-enzyme systems have been developed since ATP conversion by a single enzyme does not generate an electric signal and additionally enzymatic signal amplification is necessary to reach the low physiological concentration range.

In an early attempt a two-enzyme sensor was constructed, in which ATP was converted in the hexokinase (HK)/glucose-6-phosphate dehydrogenase sequence and the formation of NADPH was indicated at the electrode [6]. The majority of ATP sensors use HK in combination with glucose oxidase (GOx) [7] or PQQ-glucose dehydrogenase [8] and are based on evaluating the decrease in the glucose signal in the presence of ATP. For signal generation either the anodic oxidation of hydrogen peroxide (with GOx) or the electrochemical conversion of mediators or redox polymers [8] have been applied. Evaluation of the glucose consumption is influenced by changes in the glucose concentration in the solution thus it requires an independent glucose measurement by a second electrode. As an alternative to the HK based measurement of ATP the enzyme pair glycerokinase/glycerol-3-phosphate oxidase has been suggested and applied in a microelectrode format [2].

Signal amplification by enzymatic recycling of ADP back to ATP has allowed increasing the sensitivity for ATP measurements by several orders of magnitude [9]. The most frequently applied recycling pair is HK in combination with pyruvate kinase (PK).

In this paper for the first time the response signal was generated by a direct electron transfer (DET) reaction between a glucose-converting enzyme – a mutated cellobiose dehydrogenase (CDH) from the ascomycete *Corynascus thermophilus* – and an electrode, which was coupled with the HK catalyzed competition for glucose in presence of ATP. To enhance the signal output for ATP, pyruvate kinase (PK) was coimmobilized to recycle ADP by the phosphoenolpyruvate (PEP) driven reaction.

[a] A. Yarman, F. W. Scheller
Fraunhofer Institute for Cell Therapy and Immunology (IZI), Branch Bioanalytics and Bioprocesses (IZI-BB)
Am Mühlenberg 13, 14476 Potsdam, Germany
*e-mail: fschell@uni-potsdam.de
aysu.yarman@yahoo.de

[b] A. Yarman, U. Wollenberger, F. W. Scheller
Institute for Biochemistry and Biology, University of Potsdam
Karl-Liebknecht Strasse 24–25, 14476 Potsdam, Germany

[c] C. Schulz, L. Gorton
Department of Analytical Chemistry/Biochemistry and Structural Biology, Lund University
P.O. Box 124, 226 46, Lund, Sweden

[d] C. Sygmund, R. Ludwig
Department of Food Science and Technology, BOKU – University of Natural Resources and Life Sciences, Vienna
Muthgasse 18, 1190, Vienna, Austria

2 Experimental

2.1 Chemicals

Pyruvate kinase from rabbit muscle (Type III, lyophilized powder), hexokinase from *Saccharomyces cerevisiae* (lyophilized powder), adenosine 5-triphosphate disodium salt hydrate, adenosine 5-diphosphate disodium salt hydrate, phospho(enol)pyruvic acid monopotassium salt, L-dopa, serotonin hydrochloride, dopamine hydrochloride, poly(diallyldimethylammonium chloride) (PDADMAC , average Mw:100 000–200 000 mol, 20 wt.% in H_2O), and ascorbic acid were purchased from Sigma-Aldrich (Steinheim, Germany).

2.2 Enzyme Preparation

Cellobiose dehydrogenase from *Corynascus thermophilus* [10] was mutated at position 310 to generate the variant C310Y featuring an increased glucose turnover over the wild-type enzyme [11]. The variant was recombinantly produced in *Pichia pastoris* X-33 (Invitrogen) using a 7 L bioreactor (MBR) filled with 4 L of Basal Salts Medium. After sterilization, the pH of the medium was adjusted to pH 5.0 with 28% ammonium hydroxide and maintained at this level throughout the whole fermentation process. Cultivation was started by adding 0.4 L (9% (v/v) of preculture grown on YPD medium in 1 L baffled shaking flasks at 125 rpm and 30 °C overnight. The cultivation was performed according to the Pichia Fermentation Process Guidelines of Invitrogen and the expression of recombinant protein was induced with methanol. The cultivation temperature was 30 °C, the airflow rate was 6 L/min, and the stirrer speed 800 rpm. CDH was homogeneously purified according to a previously reported protocol [12]. The purified CDH had a protein concentration of 8.6 mg/mL. The specific activity measured at pH 7.5 was 9.1 U/mg when using 2,6-dichloroindophenol as two-electron acceptor and was 1.4 U/mg when using the one-electron acceptor cytochrome *c*.

2.3 Enzyme and Protein Assays

Cellobiose dehydrogenase activity was determined by two assays in the presence of 100 mM glucose. The reduction of cytochrome *c* ($\varepsilon_{550}=19.6\ mM^{-1}cm^{-1}$, 20 μM final concentration) occurs exclusively at the *b*-type heme cofactor in the cytochrome domain (CYT_{CDH}), whereas the reduction of 2,6-dichlorindophenol ($\varepsilon_{520}=6.8\ mM^{-1}\ cm^{-1}$, 300 μM final concentration) is catalyzed by the FAD cofactor of the dehydrogenase domain (DH_{CDH}). Reactions were followed for 180 s at 30 °C in a Lambda 35 UV/Vis spectrophotometer featuring a temperature controlled 8-cell changer (Perkin Elmer). All assays were measured in McIlvaine buffer, pH 7.5. One unit of CDH activity was defined as the amount of enzyme that oxidizes 1 μmol of glucose per min under the assay conditions. Protein concentrations were determined by the method of Bradford using a prefabricated assay from Bio-Rad Laboratories and bovine serum albumin as calibration standard.

2.4 Electrode Preparation

Graphite electrodes ($d=3.05$ mm, from Alfa Aesar, Ward Hill, MA, USA) were polished on wet emery paper (P1200 from Norton, Saint-Gobain Abrasives AB, Sollentuna, Sweden) and cleaned with Milli-Q water and dried at room temperature. CDH/HK/PK modified graphite electrodes were prepared in two steps. At first, freshly cleaned graphite electrodes were immersed in a PDADMAC solution (4 wt.% in H_2O) for 10 min [13]. After rinsing with water, 5 μL of a 1:1:1 mixture of CDH (8.6 mg/mL), HK (10 mg/mL) and PK (10 mg/mL) were dropped onto the PDADMAC modified graphite electrodes. All modified electrodes were dried at 4 °C overnight and rinsed thoroughly with the measuring buffer.

2.5 Methods

Electrochemical measurements were performed in a stirred electrochemical cell with a three-electrode configuration by using a PALMSENS potentiostat (Utrecht, The Netherlands). A graphite electrode was used as the working electrode, an Ag|AgCl (in 3 M KCl solution) electrode was the reference electrode, and a platinum wire served as the counter electrode.

Cyclic voltammograms were recorded in 50 mM TRIS/HCl buffer, pH 7.2 (containing 5 mM magnesium chloride and 5 mM potassium chloride) and scanned from −0.3 V to +0.4 V with a scan rate of 50 mV/s.

Amperometric measurements were performed in 50 mM phosphate TRIS/HCl, pH 7.2, containing 5 mM magnesium chloride and 5 mM potassium chloride. A working potential of −100 mV vs. Ag|AgCl (in 3 M KCl) was chosen for ATP determination. The current was recorded after the addition of substances into the reaction chamber as a function of time.

3 Results and Discussions

3.1 Measuring Principles

The signal generation by the DET reaction between CDH and the electrode has been coupled with the HK catalyzed competition for glucose in presence of ATP. To enhance the signal output for ATP, pyruvate kinase (PK) was coimmobilized to recycle ADP by the phosphoenolpyruvate (PEP) driven reaction (Scheme 1).

3.2 Immobilization of the Enzymes

The three enzymes CDH ($pI=4.6$), HK (isoforms:$pI_I=5.25$ and $pI_{II}=4.93$) and PK ($pI=7.6$) have been successfully coimmobilized by adsorption to the PDADMAC modified graphite electrodes. After optimization of the amount and the ratio of the 3 enzymes, the catalytic cur-

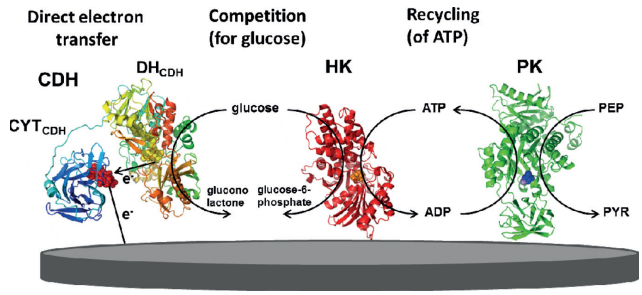

Scheme 1. Schematic representation of the sensor.

rent for glucose was comparable to that of a sensor based on CDH alone. Obviously, the negatively charged CDH is not markedly displaced by the presence of the two other enzymes. Both CDH and HK will be bound to the positively charged PDADMAC surface by electrostatic forces. On the other hand, the positively charged PK may be trapped by the interaction with the two other oppositely charged proteins as the signal amplification on addition of PEP indicates. The simple adsorption of the three enzymes onto the PDADMAC modified surface is surprisingly effective as it is indicated by only a 30% signal decrease within 5 h incubation in the measuring buffer.

3.3 The Sensor Performance for Glucose

As shown in Scheme 1, the glucose signal of the three-enzyme electrode is based on the oxidation of glucose by the DH_{CDH}, containing FAD in the active site, yielding δ-gluconolactone and $FADH_2$. The charge is then transferred to the CYT_{CDH}, which in turn is electrochemically reoxidized by the electrode through DET resulting in the registered current [14]. When running cyclic voltammetry in the absence of glucose (non-turn over conditions) no redox waves are visible exhibiting DET between CDH and the electrode. However, addition of glucose generates an anodic current starting at −200 mV revealing DET under turn over conditions. The non-turn over electrochemistry of CDH has only been clearly seen on SAM modified Au electrodes and on diazonium activated CNT modified glassy carbon [15]. On these kinds of electrode materials CDH can be oriented for DET. Using graphite electrodes, the charging current is too high to reveal non-turn over electrochemistry of CDH.

When the electrode is placed in the electrochemical flow through cell the electrocatalytic current reaches an almost potential-independent value above −100 mV (Figures 1 and 2). The three-enzyme electrode shows a linear measuring range for glucose between 0.125 mM and 1 mM ($R^2 = 0.9954$) with a response time of 180 s. The

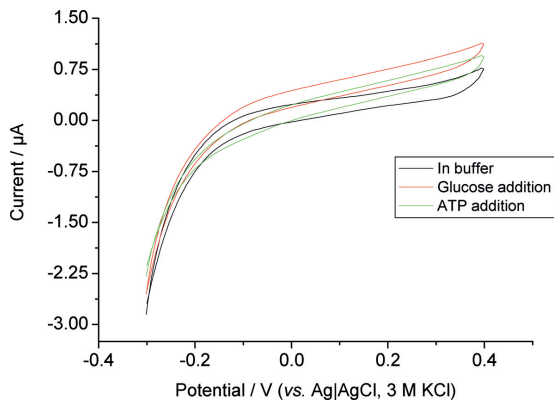

Fig. 1. CVs showing the influence of 0.1 mM ATP (green curve) on the catalytic current for 1 mM glucose in 50 mM TRIS/HCl buffer containing 5 mM $MgCl_2$ and 5 mM KCl, pH 7.2 (in the absence of PEP).

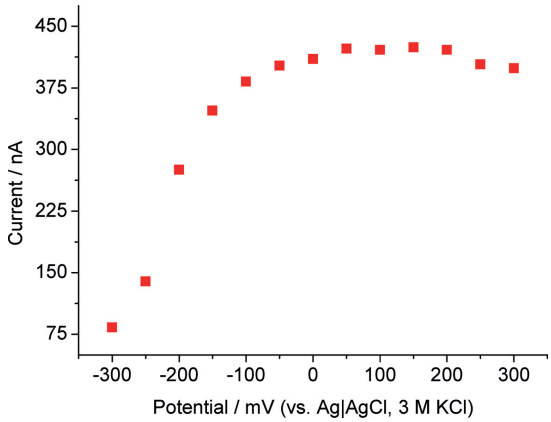

Fig. 2. Potential dependence of the catalytic current for a 1 mM glucose solution (in 50 mM TRIS buffer containing 5 mM $MgCl_2$ and 5 mM KCl, pH 7.2) measured with a CDH/HK/PK electrode ($n=3$).

low electrode potential for the glucose measurement (−100 mV) is a clear advantage as compared with the peroxide indication of GOx based electrodes [16] because the co-oxidation of interfering sample constituents like ascorbic acid is avoided. Furthermore, the glucose signal of the DET is almost independent of oxygen, thus allowing for the measurement under anaerobic conditions [17,18].

3.4 ATP Measurement

Without enzymatic signal amplification a measurable decrease in the glucose signal was obtained at an ATP concentration above 100 μM (Figure 1). The current decrease at −100 mV depends linearly on the ATP concentration between 0.1 and 1 mM ($R^2=0.9991$) and it reaches a saturation above 1.5 mM (Figure 3). As expected, addition of ADP did not influence the glucose signal.

GOx/HK based electrodes described in the literature allowed quantitative glucose measurements down to 1 μM. Because one glucose molecule is consumed for each ATP molecule and its diffusion is slower, the sensitivity for ATP can only approach that for glucose under optimal conditions. Reports describing higher sensitivities for ATP than for glucose seem questionable for these enzyme combinations [19,20].

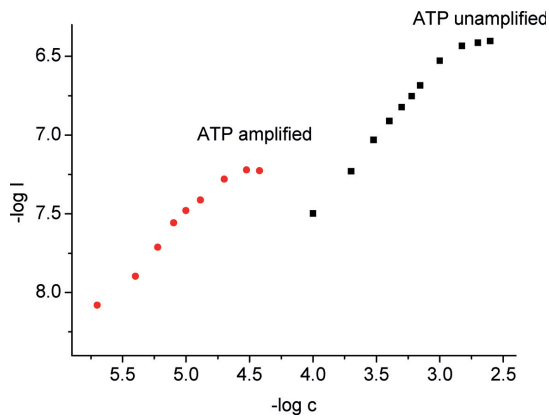

Fig. 3. Unamplified and amplified calibration curves of the three enzyme electrode for ATP at −100 mV: in the absence of PEP (black squares) and in the presence of 2.5 mM PEP (red circles) ($n=3$).

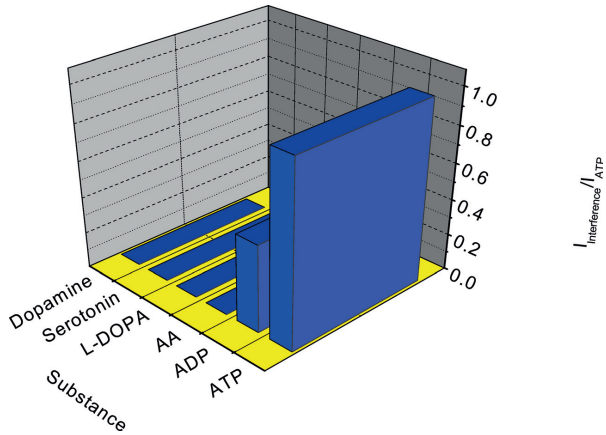

Fig. 4. Comparison of the signal for ATP with that for possible electroactive interfering substances at −100 mV (2 μM concentration of each substance was used).

A disadvantage of the competition sensors for ATP is the evaluation of small decreases in the large glucose signal. Thus the imprecision of both signals is summed up. This problem has been circumvented by measuring the formation of pyruvate from PEP in the HK/PK system [9].

3.5 ATP Measurement with Enzymatic Recycling

As shown in Scheme 1 ATP is regenerated by the action of PK. Therefore, each molecule of the analyte is recycled several times between HK and PK. This results in an overstoichiometric consumption of glucose. The ratio of sensitivities for ATP to glucose is expressed by the amplification factor.

The sensor reaches a steady state signal since the concentration of ATP approaches a constant value in the enzyme layer due to its regeneration by PK. Stationary signals for a given ATP concentration have been reported in earlier publications on recycling sensors [9,21,25]. This finding is in accordance with mathematical models of the recycling sensors [16].

Signal amplification by recycling of ADP after the addition of 2.5 mM PEP results in a linear measuring range between 2 and 10 μM ATP (R^2=0.9941) with a lower limit of detection of 63.3 nM (S/N=3) (Figure 3). The enzymatic recycling results in an almost 30-fold amplification of the response signal for ATP.

Coupling the HK/PK system with the detection of pyruvate resulted in a 220-fold amplification of the ATP signal [9]. The sensitivity for ATP detection has been further amplified by accumulation of an intermediate [21] and recycling of pyruvate in the pyruvate oxidase/lactate dehydrogenase enzyme pair respectively [9]. This "double amplification" resulted in a subnanomolar limit of detection of ATP. Recycling of ATP between PK and myokinase resulted in an "exponential" amplification because in each reaction cycle one additional ADP molecule is formed from AMP [22,23]. These sensors are able to measure ATP in the lower nanomolar range, however, on the expense of expensive reagents. In an alternative amplification system ATP has been recycled by the enzyme pair glycerokinase/creatine kinase in combination with glycerol-3-phosphate oxidase. Addition of phosphocreatine amplified the ATP signal almost five times and made the sensor sensitive to ADP [2].

In general sensors in which the signal is amplified by recycling, ATP cannot be discriminated from ADP because both ATP and ADP enter the reaction cycle. For these sensors the sensitivities for both substances are slightly different due to the different permeabilities [9]. We obtained for ADP a response signal almost 48% of that of the signal for ATP with our sensor (Figure 4). In order to exclude the influence of ADP, the signal amplification should use a recycling system for the phosphorylated product, e.g. for glucose-6-phosphate in the HK reaction.

For electrochemical ATP measurements in physiological media the working potential of the enzyme electrode is crucial. The CDH based sensor allows the measurement of glucose at −100 mV, thus the presence of neurotransmitters like dopamine, L-dopa or serotonin but also ascorbic acid does not contribute to the anodic response signal. The same property has been found for the amplified ATP signal of the CDH/HK/PK sensor. Equal concentrations of the neurotransmitter or ascorbic acid generate only a negligible current signal in comparison to that of ATP (Figure 4). The high sensitivity, the independence of oxygen content and the absence of electrochemical interferences are advantages of this new sensor.

3.6 The Bioelectronic Aspect

In our earlier work [24,25] we emphasized the potential of coupled enzyme reactions in the internal signal processing in biosensors. The rational coupling of enzyme catalyzed reactions increases not only the spectrum of measurable substances but it performs also mathematical operations.

In this respect enzyme sequences sum up the concentrations of all substrates. For example the enzyme sequence of invertase and glucose oxidase "sums up" the concentrations of sucrose and glucose. The cofactor-dependent competition of e.g. the conversion of glucose by GOx and HK in the presence of ATP, represents the difference in the signals of a GOx sensor and that of a GOx/HK-bienzyme electrode. Recycling of ADP/ATP by the HK/PK couple (on addition of PEP) multiplies the current decrease. Recently, Katz and coworkers [26,27] interpreted the signal processing by coupled enzyme reactions on the basis of logic gates. The output of an enzyme sequence sensor represents AND. On the other hand, parallel reactions which generate the same electroactive species reflect the logic operation OR.

4 Conclusions

The new sensor proposed here overcomes the border of a 1:1 stoichiometry of the sequential or competitive conversion of ATP by effective enzymatic recycling of the analyte. Because the anodic oxidation of glucose converting CDH proceeds at electrode potentials below 0 mV potentially interfering substances like ascorbic acid do not influence the measuring signal. This is a remarkable advantage as compared with the peroxide indication of the GOx based sensors. Thus the combination of DET properties of CDH with the enzymatic recycling by HK and PK results in an interference-free measurement of ATP in the lower μmolar concentration range.

Acknowledgements

The authors gratefully acknowledge the financial support of *Deutsche Forschungsgemeinschaft* (*DFG*) within the framework of the *German Excellence Initiative* (EXC 314), the *BMBF* in *TERA-Sens* (93719903), *The Swedish Research Council* (Project 2010-5031), and the *European Commission* ("Chebana" FP7-PEOPLE-2010-ITN-264772). This work is a part of *UniCat, the Cluster of Excellence* in the field of catalysis coordinated by *the Technical University of Berlin*.

References

[1] F. McCapra, in *Biosensors. Fundementals and Applications*, 1st ed., Oxford University Press, New York **1987**, pp. 617–637.
[2] E. Llaudet, S. Hatz, M. Droniou, N. Dale, *Anal. Chem.* **2005**, *77*, 3267–3273.
[3] E. Hecht, A. Liedert, A. Ignatius, B. Mizaikoff, C. Kranz, *Biosens. Bioelectron.* **2013**, *44*, 27–33.
[4] G. S. Wilson, Y. Hu, *Chem. Rev.* **2000**, *100*, 2693–2704.
[5] A. Heller, B. Feldman, *Chem. Rev.* **2008**, *108*, 2482–2505.
[6] F. Schubert, D. Kirstein, F. Scheller, M. Abraham, L. Boross, *Anal. Lett.* **1986**, *19*, 2155–2167.
[7] D. Compagnone, G. Guilbault, *Anal. Chim. Acta* **1997**, *340*, 109–113.
[8] C. Weber, E. Gauda, B. Mizaikoff, C. Kranz, *Anal. Bioanal. Chem.* **2009**, *395*, 1729–1735.
[9] U. Wollenberger, F. Schubert, F. Scheller, B. Danielsson, K. Mosbach, *Anal. Lett.* **1987**, *20*, 657–668.
[10] W. Harreither, C. Sygmund, M. Augustin, M. Narciso, M. L. Rabinovich, L. Gorton, D. Haltrich, R. Ludwig , *Appl. Environ. Microbiol.* **2011**, *77*, 1804–1815.
[11] Patent *Cellobiose dehydrogenase*, *WO 2010/097462*.
[12] W. Harreither, A. K. G. Felice, R. Paukner, L. Gorton, R. Ludwig, C. Sygmund, *Biotechnol. J.* **2012**, *7*, 1359–1366.
[13] P. Knöös, C. Schulz, L. Piculell, R. Ludwig, L. Gorton, M. Wahlgren, *Int. J. Pharm.* **2014**, *468*, 121–132.
[14] R. Ludwig, R. Ortiz, C. Schulz, W. Harreither, C. Sygmund, L. Gorton, *Anal. Bioanal. Chem.* **2013**, *405*, 3637–3658.
[15] F. Tasca, W. Harreither, R. Ludwig, J. J. Gooding, L. Gorton, *Anal. Chem.* **2011**, *83*, 3042–3049.
[16] F. Scheller, F. Schubert, in *Techniques and Instrumentation in Analytical Chemistry: Biosensors*, vol 11, Elsevier, Amsterdam, The Netherlands **1992**, pp. 98–106.
[17] F. Tasca, L. Gorton, W. Harreither, D. Haltrich, R. Ludwig, G. Nöll, *J. Phys. Chem.* C **2008**, *112*, 13668–13673.
[18] M. Zamock, R. Ludwig, C. Peterbauer, B. M. Hallberg, C. Divne, P. Nicholls, D. Haltrich, *Curr. Protein Pept. Sci.* **2006**, *7*, 255–280.
[19] B. A. Patel, M. Rogers, T. Wieder, D. O'Hare, M. G. Boutelle, *Biosens. Biolectron.* **2011**, *26*, 2890–2896.
[20] A. Kueng, C. Kranz, B. Mizaikoff, *Biosens. Biolectron.* **2004**, *19*, 1301–1307.
[21] X. Yang, G. Johansson, D. Pfeiffer, F. Scheller, *Electroanalysis* **1991**, *3*, 659–663.
[22] D. Pfeiffer, F. W. Scheller, C. J. McNeil, T. Schulmeister, *Biosens. Bioelectron.* **1995**, *10*, 169–180.
[23] D. Okamura, K. Machida, T. Kawahara, K. Kojima, W. Tsugawa, *Electrochemistry* **2012**, 3, 80(5), 334–336.
[24] F. W. Scheller, F. Schubert, R. Renneberg, H. G. Müller, M. Jänchen, H. Weise, *Biosens. Bioelectron.* **1985**, *1*, 135–160.
[25] U. Wollenberger, F. Schubert, D. Pfeiffer, F. W. Scheller, *Trends Biotechnol.* **1993**, *11*, 255–262.
[26] K. M. Manesh, J. Halámek, M. Pita, J. Zhou, T. K. Tam, P. Santhosh, M. C. Chuang, J. R. Windmiller, D. Abidin, E. Katz, J. Wang, *Biosens. Bioelectron* **2009**, *24*, 3569–3574.
[27] E. Katz, S. Minko, J. Halámek, K. MacVittie, K. Yancey, *Anal. Bioanal. Chem.* **2013**, *405*, 3659–3672.

Received: May 9, 2014
Accepted: July 6, 2014
Published online: August 12, 2014

Paper VI

the FEBS Journal

Inter-domain electron transfer in cellobiose dehydrogenase: modulation by pH and divalent cations

Daniel Kracher[1,†], Kawah Zahma[1,†], Christopher Schulz[2], Christoph Sygmund[1], Lo Gorton[2] and Roland Ludwig[1]

1 Department of Food Sciences and Technology, Food Biotechnology Laboratory, University of Natural Resources and Life Sciences, Vienna, Austria

2 Department of Analytical Chemistry, Biochemistry and Structural Biology, Lund University, Sweden

Keywords
cellobiose dehydrogenase; divalent cation bridging effect; domain docking; inter-domain electron transfer; oxidative cellulose degradation

Correspondence
R. Ludwig, Department für Lebensmittelwissenschaften und -technologie, Universität für Bodenkultur, Muthgasse 18/2, A-1190 Wien, Austria
Fax: +431 47654 6199
Tel: +431 47654 6149
E-mail: roland.ludwig@boku.ac.at

†These authors contributed equally to this work.

(Received 31 October 2014, revised 2 April 2015, accepted 22 April 2015)

doi:10.1111/febs.13310

The flavocytochrome cellobiose dehydrogenase (CDH) is secreted by wood-decomposing fungi, and is the only known extracellular enzyme with the characteristics of an electron transfer protein. Its proposed function is reduction of lytic polysaccharide mono-oxygenase for subsequent cellulose depolymerization. Electrons are transferred from $FADH_2$ in the catalytic flavodehydrogenase domain of CDH to haem *b* in a mobile cytochrome domain, which acts as a mediator and transfers electrons towards the active site of lytic polysaccharide mono-oxygenase to activate oxygen. This vital role of the cytochrome domain is little understood, e.g. why do CDHs exhibit different pH optima and rates for inter-domain electron transfer (IET)? This study uses kinetic techniques and docking to assess the interaction of both domains and the resulting IET with regard to pH and ions. The results show that the reported elimination of IET at neutral or alkaline pH is caused by electrostatic repulsion, which prevents adoption of the closed conformation of CDH. Divalent alkali earth metal cations are shown to exert a bridging effect between the domains at concentrations of > 3 mM, thereby neutralizing electrostatic repulsion and increasing IET rates. The necessary high ion concentration, together with the docking results, show that this effect is not caused by specific cation binding sites, but by various clusters of Asp, Glu, Asn, Gln and the haem *b* propionate group at the domain interface. The results show that a closed conformation of both CDH domains is necessary for IET, but the closed conformation also increases the FAD reduction rate by an electron pulling effect.

Introduction

Cellobiose dehydrogenase (CDH; EC 1.1.99.18; CAZy database ID AA3-1) is detected in the secretome of wood-degrading, composting and plant pathogenic fungi. The results of recent studies support a role in the oxidative breakdown of crystalline cellulose or other polymeric, carbohydrate constituents of plant biomass in combination with lytic polysaccharide monooxygenase (CAZy database ID AA9) [1–5]. As a flavocytochrome, CDH exhibits a unique architecture for a secreted enzyme. It features an N-terminal electron-transferring cytochrome domain (CYT) that is bound to a carbohydrate-oxidizing dehydrogenase domain (DH). Electrons obtained from carbohydrate oxidation are transferred from the DH to the CYT by inter-domain electron transfer (IET). The proposed function of the CYT is to donate electrons to the

Abbreviations
BQ, 1,4-benzoquinone; CDH, cellobiose dehydrogenase; CYT, cytochrome domain; DCIP, 2,6-dichloroindophenol; DH, dehydrogenase domain; IET, inter-domain electron transfer.

copper centre of lytic polysaccharide mono-oxygenase to activate oxygen [2,6]. IET from $FADH_2$ to the *b*-type haem in the CYT is therefore an important step towards oxidative cellulose depolymerization.

Various pH optima for the IET have been reported in the literature. Usually, the activity with the *in vitro* electron acceptor cytochrome *c* (cyt *c*), which only interacts with the CYT [6–8], is used to approximately determine the IET. Direct observation of IET requires stopped-flow spectrophotometry, which has been performed for *Phanerochaete chrysosporium* CDH [9]. These studies show that CDHs from basidiomycetes (class I) have acidic pH optima, and IET ceases at approximately pH 6. The reported reason is electrostatic repulsion between the domains [10]. Ascomycetous CDHs (class II) are more diverse, and some of them exhibit less acidic or even alkaline IET pH optima [10,11]. This is remarkable because the reported isoelectric points for these CDHs do not differ from those of basidiomycetous CDHs with acidic pH optima. A possible explanation is that the DH and the CYT exhibit different patches of charged or non-charged amino acid residues.

The structure of full-length CDH is unknown, but structures for the isolated DH (PDB ID 1KDG) and CYT (PDB ID 1D7C) from *P. chrysosporium* are available [12,13]. Docking of the two domains has been reported, whereby a haem propionyl group was found to protrude into the substrate channel of the DH and come into close contact with the FAD [10]. The modelling is based on structural complementarity, and it is unclear whether this closed conformation is energetically favoured or whether the CYT is mobile and moves freely between a closed and an open conformation. The long linker (15 amino acids) between the domains suggests that the CYT has a high degree of freedom to move when not in contact with the DH. This appears to be necessary on order to transfer electrons to proteins such as cyt *c* or lytic polysaccharide mono-oxygenase. In previous stopped-flow measurements [9], no IET above pH 6 was observed for *P. chrysosporium* CDH, but the dehydrogenase domain was highly active at alkaline pH. One of two explanations may apply: (i) the domains separate because of electrostatic repulsion, and the increased distance between the domains prevents IET, or (ii) the closed conformation is stable and the domains are kept together, but IET is disrupted by structural and protonation changes along the electron transfer pathway. The possibility of reversal of the electron transfer by shifting the FAD redox potential to above the haem *b* potential has been excluded by Igarashi *et al.* [9].

A recent study revealed a way to investigate the pH dependency of the IET in more detail. It reported that calcium ions increased the enzymatic activity and catalytic current of three CDHs from *Myriococcum thermophilum*, *Humicola insolens* and *Phanerochaete sordida* [14]. Addition of a millimolar concentration of calcium ions to the buffer solution increased the catalytic current of CDH-modified spectroscopic graphite electrodes and also the turnover of cyt *c*. It was speculated that calcium ions modulate the domain interaction, and thereby enhance the IET between FAD and haem *b* cofactors. Here, we study the effect of the calcium concentration on twelve CDHs from various fungi to determine whether the effect is ubiquitous among CDH. We also investigate whether CDH is only IET-competent when both domains are in the closed conformation, and whether electrostatic repulsion above a certain pH prevents the closed state and therefore IET. *M. thermophilum* CDH was used to investigate the domain interaction and IET using spectroscopic, steady-state, pre-steady-state and calorimetric techniques. To elucidate the charges at the domain interfaces of three CDHs, comparative modelling and docking were performed.

Results and Discussion

Modulation of CDH activity by pH ions

CDH from *M. thermophilum* (*Mt*CDH), was previously reported to be responsive to calcium ions [14]. A millimolar concentration of calcium ions increased the activity of the enzyme fivefold. Using a screening approach based on artificial electron acceptors for *Mt*CDH, we also observed such enhancement when using other divalent earth alkaline metals such as Mg^{2+}, Sr^{2+}, Ba^{2+} and Cd^{2+} (Fig. 1), but not when using monovalent cations or anionic species (Table S1). The effect is stronger at alkaline pH, and is only observed for CDH activity towards cyt *c*, and to a much lesser extent for reduction of the two-electron acceptor 2,6-dichloroindophenol (DCIP). Reduction of the two-electron acceptor 1,4-benzoquinone (BQ) was not affected at all. Cyt *c* is solely reduced by the haem *b* of CDH and requires IET. The two-electron acceptors DCIP and BQ are reduced directly by $FADH_2$ and do not require IET and the cytochrome domain. The increase in electron acceptor turnover in the presence of divalent cations depends on their concentration. Below a 3 mM concentration, only a small increase in cyt *c* turnover by CDH was detected. The maximal effect was found at concentrations between 30 and 60 mM, while higher concentrations also

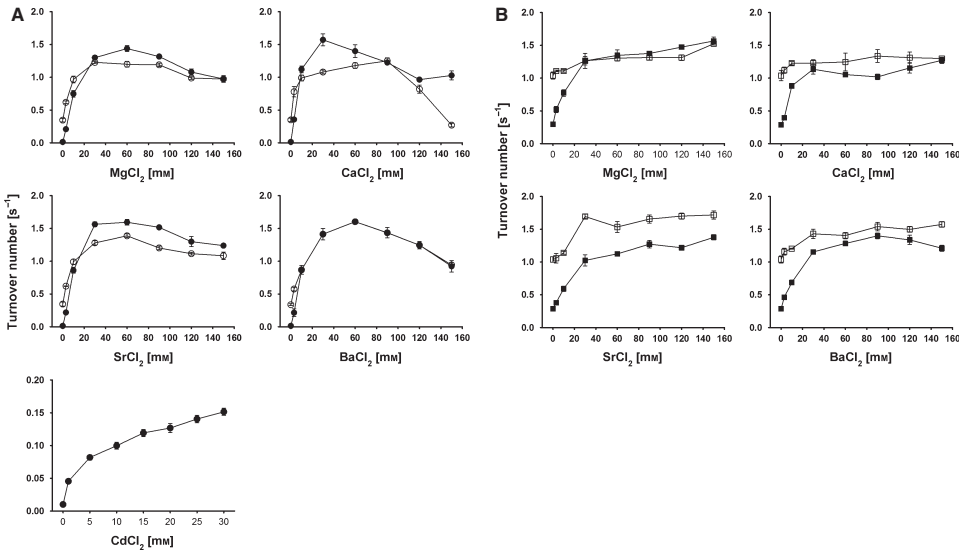

Fig. 1. (A) Effect of divalent cation concentration on cyt *c* turnover for *Mt*CDH measured at pH 5.5 (open circles) and pH 7.5 (closed circles). (B) Effect of divalent cation concentration on turnover of the two-electron acceptor DCIP for *Mt*CDH at pH 5.5 (open squares) and pH 7.5 (closed squares).

decreased the turnover of cyt *c* (Fig. 1A). A smaller increase was found for DCIP turnover, where the optimum cation concentration was also 30–60 mM, but no decrease at higher concentrations was observed (Fig. 1B). Apparent catalytic constants of *Mt*CDH for cyt *c* in the presence of 30 mM of divalent cations were measured at pH 5.5 and 7.5, and compared to a 30 mM concentration of Na^+ (Table 1). The increase in k_{cat} caused by divalent cations was 3.5–4-fold at pH 5.5, but 160–200-fold at pH 7.5. The huge enhancement at pH 7.5 is only partly attributable to an increase in the absolute turnover of cyt *c* by CDH (1.2–1.4-fold higher compared to pH 5.5), and is mostly due to a reduced of cyt *c* turnover in the absence of Ca^{2+}. At pH 7.5 and in the absence of divalent cations (Na^+ was used as substitute), cyt *c* turnover is negligible. In the presence of divalent cations, the catalytic efficiency for cyt *c* is very similar at pH 5.5 (mean of ~ 2.8×10^5 $M^{-1}{\cdot}s^{-1}$) and pH 7.5 (mean of ~ 3.2×10^5 $M^{-1}{\cdot}s^{-1}$). This indicates that divalent cations strongly counteract the shutdown of the IET at neutral/alkaline pH, and do not influence electron transfer from the CYT to cyt *c*. Apparently, neither the atomic radius ($Ba^{2+} > Sr^{2+} > Ca^{2+} > Mg^{2+}$) nor the electronegativity ($Mg^{2+} > Ca^{2+} > Sr^{2+} > Ba^{2+}$) of the earth alkali metal ions significantly modulate the observed enhancing effect. A lower enhancing effect was found for Cd^{2+}, which increases cyt *c* turnover at pH 7.5 to 0.15 s^{-1}, compared with a turnover of 1.3 s^{-1} observed in the presence of Ca^{2+} (Fig. 1A).

Table 1. Catalytic constants of *Mt*CDH for cyt *c* measured in the presence of cations at a concentration of 30 mM.

Salt/pH	K_M (μM)	k_{cat} (s^{-1})	k_{cat}/K_M ($M^{-1}{\cdot}s^{-1}$)
NaCl, pH 5.5	2.8 ± 0.5	0.4 ± 0.1	1.43×10^5
NaCl, pH 7.5	0.5 ± 0.1	0.010 ± 0.003	0.20×10^5
$MgCl_2$, pH 5.5	5.6 ± 0.2	1.6 ± 0.1	2.86×10^5
$MgCl_2$, pH 7.5	6.1 ± 0.1	2.1 ± 0.1	3.44×10^5
$CaCl_2$, pH 5.5	5.6 ± 0.1	1.4 ± 0.1	2.50×10^5
$CaCl_2$, pH 7.5	6.0 ± 0.4	1.6 ± 0.2	2.67×10^5
$SrCl_2$, pH 5.5	4.3 ± 0.1	1.4 ± 0.4	3.26×10^5
$SrCl_2$, pH 7.5	5.8 ± 0.1	2.0 ± 0.1	3.45×10^5
$BaCl_2$, pH 5.5	5.5 ± 0.2	1.5 ± 0.1	2.73×10^5
$BaCl_2$, pH 7.5	6.5 ± 0.2	2.0 ± 0.1	3.08×10^5

Modulation of activity in CDH from other sources

Twelve CDHs from 11 fungi were subjected to screening using the three electron acceptors cyt *c*, DCIP and BQ at three pH values in the presence or absence of

30 mM Ca^{2+} (Tables 2 and 3). None of the investigated enzymes showed activation of BQ turnover in the presence of Ca^{2+}. DCIP turnover was slightly increased for some class II CDHs at pH 7.5. However, the turnover of cyt *c* was increased for both CDH classes, typically 1.4-fold for class I and between 1.3- and 4.2-fold for class II. At higher pH, the observed increase was most often higher, ~ 2–4-fold for class I CDHs and 3–5-fold for class II CDHs. In contrast to ascomycetous class II CDHs, which show higher pH optima, the measured pH for class I CDHs was pH 6.5, and no activity for cyt *c* was detected at pH 7.5. Interestingly, there are exceptions from the observed increase in activity: The class I CDH from *Sclerotium rolfsii* showed a decreased cyt *c* turnover at pH 6.5, and the class II *Neurospora crassa* CDH IIA showed a decreased cyt *c* turnover at pH 5.5 and 7.5 in the presence of Ca^{2+}. Whether these enzymes are inert to the presence of divalent cations, or the pH chosen was not suitable, cannot currently be determined. The 125-fold activation of *Mt*CDH activity at pH 7.5 in the presence of Ca^{2+} is very high compared to the other investigated CDHs. Despite these exceptions, the enhancement effect of divalent metal cations was observed for all tested CDH enzymes.

Modulation of electron acceptor pH profiles by Ca^{2+}

The observed pH dependency of the electron acceptor turnover in the presence of divalent cations was studied in detail using *Mt*CDH and Ca^{2+} *partes pro toto* (Fig. 2). The turnover rate of the positively charged one-electron acceptor cyt *c* by the CYT depends on the IET, and is optimum at pH 5. Above this pH, the turnover of cyt *c* decreases rapidly, and disappears at pH 6.5. As the charge of cyt *c* (pI 10.0–10.4) is not altered at this pH, the change in turnover is probably attributable to reduction of the IET between the DH and the CYT. At pH 5, the side-chain carboxy functions of surface-exposed aspartic acid (pK_a = 3.86) and glutamic acid (pK_a = 4.07) are ~ 90% deprotonated, creating a strong electrostatic repulsion between both domains. In the presence of Ca^{2+}, this reduction of turnover above pH 5 is not observed, indicating that the electrostatic repulsion is neutralized. The increasing turnover of cyt *c*

Table 2. Effect of 30 mM $CaCl_2$ on CDHs from Ascomycota.

		Activation (fold)								
		DCIP		BQ		Cyt *c*		pH optimum		
	Source	pH 5.5	pH 7.5	pH 5.5	pH 7.5	pH 5.5	pH 7.5	DCIP	Cyt *c*	pI
Myriococcum thermophilum IIA CBS 208.89	Recombinant	1.2	3.8	1.1	1.1	4.2	125	5.5	5.0	3.8
Neurospora crassa IIA CBS 232.56	Recombinant	1.1	1.1	1.0	0.9	0.5	0.7	5.0	6.0	4.9
Neurospora crassa IIB CBS 232.56	Recombinant	1.0	1.8	1.0	1.0	1.3	4.5	5.0	5.5	5.1
Corynascus thermophilus IIB CBS 174.70	Wild-type	1.4	4.0	1.0	1.1	2.6	3.0	5.0	7.5	3.8
Chaetomium atrobrunneum IIA CBS 238.71	Wild-type	1.1	3.2	0.9	0.9	1.0	5.2	6.0	5.0	4.1
Hypoxolon haematostroma IIB CBS 255.63	Wild-type	0.9	0.8	1.1	1.1	0.8	3.2	5.0	5.5	4.3
Dichomera saubinetii IIA CBS 990.7	Wild-type	1.0	0.9	1.0	1.2	1.4	4.7	5.5	5.5	4.2

Table 3. Effect of 30 mM $CaCl_2$ on CDHs from Basidiomycota.

		'Activation' (fold)								
		DCIP		BQ		Cyt *c*		pH optimum		
	Source	pH 4.5	pH 6.5	pH 4.5	pH 6.5	pH 4.5	pH 6.5	DCIP	cyt *c*	pI
Trametes villosa CBS 334.49	Wild-type	0.9	0.8	1.0	0.8	1.0	2.9	5.0	3.5	4.4
Phanerochaete chrysosporium K3	Wild-type	0.8	1.0	1.0	0.9	1.4	2.9	4.0	4.0	4.2
Phanerochaete sordida MB 66	Wild-type	0.9	0.9	0.9	0.9	1.4	2.2	4.0	4.0	4.1
Sclerotium rolfisii CBS 191.62	Wild-type	0.9	0.9	1.0	0.9	1.5	0.7	4.0	3.5	4.2
Ceriporiopsis subvermispora FP-90031	Wild-type	0.9	0.9	1.0	0.9	1.4	3.8	4.5	3.5	3.0

Values are means from three replicates; errors are below 10%.

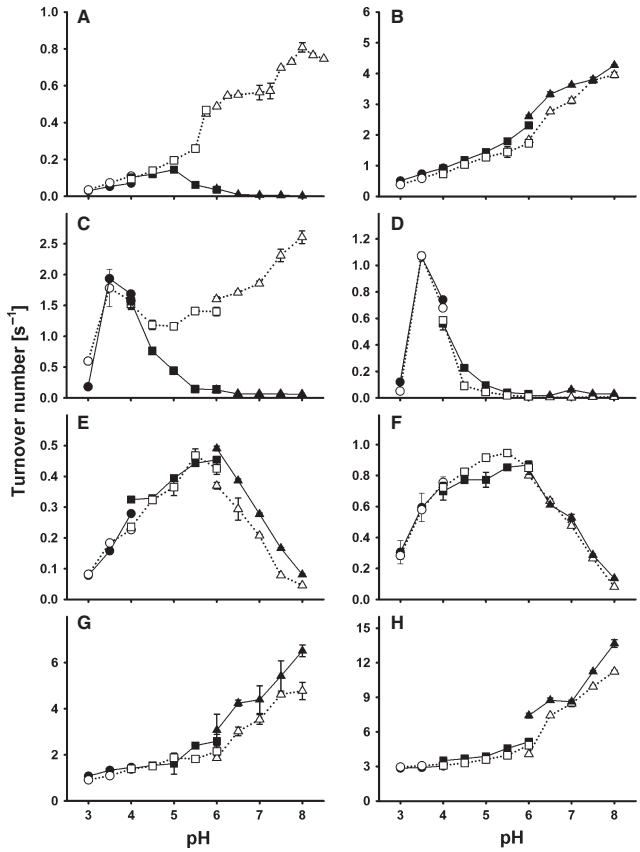

Fig. 2. pH-dependent activities of *Mt*CDH (A–C, E, G) and the dehydrogenase domain *Mt*DH (D, F, H) towards the electron acceptors cyt *c* (A), ferrocenium (B), ferricyanide (C, D), DCIP (E, F) and 1,4-benzoquinone (G, H) measured in the absence of $CaCl_2$ (open symbols) and upon addition of 30 mM $CaCl_2$ (closed symbols). The buffers used were 50 mM sodium formiate (pH 3–4, circles), 50 mM sodium acetate (pH 4–6, squares) and 50 mM MOPS (pH 6–8, triangles). Error bars represent the standard deviation from three independent repeats.

at increasing pH shows that the reductive cycle at the FAD has an alkaline pH optimum.

The positively charged electron acceptor ferrocenium showed similar behaviour in the absence or presence of Ca^{2+} Increasing turnover at alkaline pH indicates that this one-electron acceptor does not depend on IET, but is reduced by the $FADH_2$ directly. The activity of CDH towards the two-electron acceptors DCIP (with a strong negative partial charge) and BQ (with weak negative partial charge) was slightly increased in the presence of Ca^{2+} at pH values above 6. Interestingly, this activation was not observed for the single DH, which indicates that not only do the negative charges around the substrate channel reduce the accessibility for electron acceptors, but that the proximity of the haem *b* also affects electron acceptor-mediated oxidation of FAD.

The most interesting behaviour was observed for the ferricyanide anion. This one-electron acceptor may be directly reduced by $FADH_2$ in the DH, but only at pH values below 5.0. Such behaviour was also observed for glucose oxidase [15]. For CDH, ferricyanide reduction may be observed up to pH 6.0, demonstrating that the proximity of the CYT to the DH influences ferricyanide reduction more strongly than it influences DCIP or BQ reduction. The pH profiles of the DH in the presence and absence of Ca^{2+} reveal that the charge-induced reduced accessibility of the ferricyanide anion to the active site is a minor factor. The increasing ferricyanide turnover by CDH at alkaline pH in the presence of Ca^{2+} may be explained by two models. In model 1, the close proximity of the haem *b* to the FAD increases ferricyanide turnover at FAD. In model 2, the reduction of ferricyanide

occurs at the CYT above pH 5. The two pH optima observed in the pH profile promote the second mechanism.

The breakdown of ferricyanide and cyt *c* reduction above pH 6.0–6.5 provides a measure for shutdown of the IET. If the pH increases above pH 6.5, the CYT of *Mt*CDH no longer interacts with the DH, because electrostatic repulsion of the negatively charged domains prevents adoption of a closed-state conformation (Table 2, pI values). In the presence of Ca^{2+}, the ferricyanide turnover of CDH shows a monotonic increase from pH 5–8. The pH profiles of ferricyanide and cyt *c* therefore give a clear indication that divalent cations support adoption of a closed conformation by the DH and the CYT when the domain interface becomes negatively charged at neutral/alkaline pH. This effect is not caused by the presence of distinct binding sites for divalent cations, as these were not found in our docking models of the DH and the CYT, and the 30–60 mM concentration of dications required to achieve the optimal effect is magnitudes higher than the reported affinities for Ca^{2+} specific EF-hand binding sites, for example (2.1 μM [16] or 0.49 μM [17]). The high concentration required suggests unspecific shielding of close opposing charges at both sides of the domain interface. Similar behaviour has been reported for surfactants, DNA and hyaluronan in the presence of Ca^{2+}, and was termed the 'divalent cation bridging effect' [18–22].

Spectral features of *Mt*CDH

Electron absorption spectra of oxidized *Mt*CDH in the presence of NaCl or $CaCl_2$ were recorded at pH 7.5, and showed the typical Soret-band maximum at 421 nm for haem *b* (Fig. 3A). Upon reduction, the

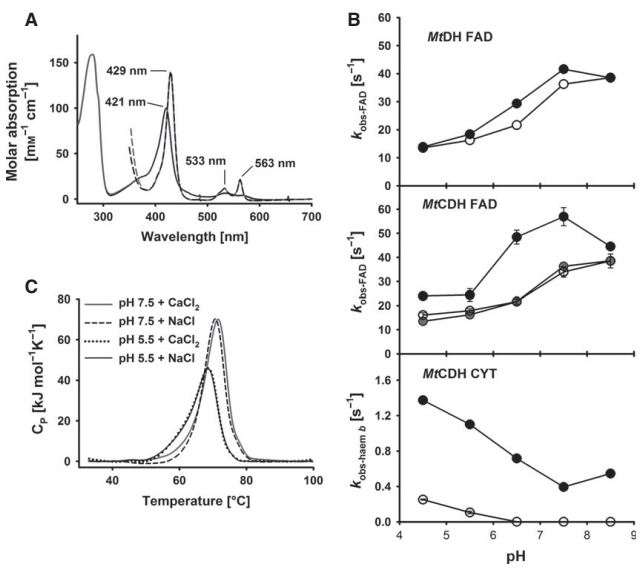

Fig. 3. (A) Spectra of oxidized *Mt*CDH at pH 7.5 (50 mM MOPS) in the presence of 30 mM NaCl (black line) and 30 mM $CaCl_2$ (grey line). Spectra of reduced MtCDH in the presence of NaCl (black dashed line) and $CaCl_2$ (grey dashed line) were obtained upon addition of a 2000-fold excess of sodium dithionite. Under these conditions, the experimentally determined molar absorption coefficient of oxidized *Mt*CDH at 421 nm is 99.4 mM^{-1} cm^{-1}. The absorbance ratio (A_{420}/A_{280}) is 0.62. (B) pH dependency of apparent reduction rate constants of the isolated *Mt*DH fragment and the *Mt*CDH holoenzyme in the presence of 30 mM NaCl (open circles) and 30 mM $CaCl_2$ (closed circles). For comparison, the apparent reduction rate constants of *Mt*DH in the presence of 30 mM NaCl are shown (grey circles). Traces for FAD reduction were recorded at 449 nm; haem *b* reduction was followed at 563 nm. *Mt*CDH or *Mt*DH (5 μM) were mixed with 3 mM cellobiose, in a stopped-flow spectrometer at a temperature of 30 °C. Indicated concentrations are those after mixing. Values represent means of five independent replicates; error bars are given for all experiments but in many cases are smaller than the data points. (C) Differential scanning calorimetry performed with *Mt*CDH in the presence of 30 mM NaCl or 30 mM $CaCl_2$ at pH 5.5 and 7.5. The thermal ramp speed is 1 K min^{-1}.

absorbance of the haem α and β peaks at 533 and 563 nm increased, the Soret band shifted from 421 to 429 nm, and the FAD absorbance at 450 nm decreased. Addition of calcium chloride to a final concentration of 30 mM had no effect on the spectra of the oxidized and reduced enzyme. Measurements at pH 5.5 showed the same result. No indications of Ca^{2+}-induced changes in the coordination environment of the haem *b* cofactor were found.

Inter-domain electron transfer of *Mt*CDH in the presence of $CaCl_2$

Based on the spectral characteristics of CDH, stopped-flow spectroscopy was used to monitor reduction of the FAD and haem *b* cofactors of CDH. Rapid mixing of *Mt*CDH (5 μM final concentration) with an excess of cellobiose (3 mM) results in fast FAD reduction, followed by IET and one-electron reduction of the haem *b*. For comparison, the dehydrogenase domain from *M. thermophilum* (*Mt*DH) was also analysed. Figure 3B shows apparent pseudo first-order rate constants (k_{obs}) for both reduction steps between pH 4.5 and 8.5. The FAD reduction changes with pH, and shows a maximum of 38.5 s^{-1} at pH 8.5 in the presence of 30 mM NaCl. In the presence of 30 mM $CaCl_2$, k_{obs} is only slightly higher and reaches a maximum of 41.6 s^{-1} at pH 7.5. These differences are negligible compared to the changes Ca^{2+} exerts on full-length CDH. The FAD reduction rate in the absence of the dication is almost identical to that in the DH, but in the presence of Ca^{2+}, the k_{obs} increases 1.3–1.7-fold. The close proximity of the haem *b* appears to exert a pull effect on the FAD, resulting in a faster FAD reduction rate. From docking experiments, a mean edge-to-edge distance of 8 ± 2 Å between FAD and the haem *b* proprionate chain was calculated, which is close enough for fast electron transfer. Modulation of the FAD redox potential by electronic coupling through the bridging Trp295 residue may explain the increased steady-state turnover of DCIP and BQ in the presence of Ca^{2+} (Fig. 2E,G and Table 2). Both pre-steady-state and steady-state experiments indicate an alkaline pH optimum of approximately pH 8 for the reductive half-reaction at the FAD, which differs greatly from the acidic pH optimum (4.5–5.0) observed for *P. chrysosporium* CDH [9].

The pH-dependent interaction of both CDH domains shows maximal reduction of haem *b* and therefore IET at pH 4.5 (Fig. 3B). The pH optimum of *Pc*CDH is slightly lower (pH 3.5 [9]). In agreement with the steady-state measurements using cyt *c*, an effect of calcium ions was also observed here. Apparent haem reduction rates at pH 4.5 increased from 0.25 to 1.37 s^{-1} upon addition of $CaCl_2$. At pH 6.5 and above, the haem reduction became extremely slow. At pH 7.5, only ~ 5% of haem *b* cofactors was reduced within the observed time span of 30 s, but haem reduction was recovered by addition of Ca^{2+}. In the presence of Ca^{2+}, k_{obs} decreases monotonically from pH 4.5 to 7.5, but the rate is always higher compared to the rates measured in the absence of Ca^{2+}. This decrease indicates that, with increasing pH, the cation-bridging effect is overcome by electrostatic repulsion. A comparison with the steady-state cyt *c* pH profile shows that the positive charges of this proteinogenic electron acceptor strongly influence the IET. Turnover maxima of *Mt*CDH for cyt *c* are found at pH 5 in the absence of Ca^{2+} and at pH 8 in the presence of Ca^{2+}, whereas the IET measured by stopped-flow in the absence of cyt *c* continuously decreases from its maximum at pH 4.5, in either the presence or absence of Ca^{2+}. These results indicate the limits of the use of cyt *c* to measure IET.

Effect of calcium chloride on the thermostability of *Mt*CDH

Transition mid-point temperatures (T_M) of *Mt*CDH in the presence of 30 mM NaCl or 30 mM $CaCl_2$ were recorded at pH 5.5 and pH 7.5. At pH 5.5, overlapping peaks were observed, with a maximum (T_M) at 68.5 °C (Fig. 3C and Table 4). At pH 7.5, the presence of $CaCl_2$ shifted the thermostability only slightly by 0.7 °C (from 70.7 to 71.4 °C). The observation of a slightly higher T_M at pH 7.5 shows that the closed conformation at pH 5.5 does not lead to higher thermal stability of the enzyme, which suggests that no strong interactions are involved in forming the closed structure. It also confirms that stabilization of the closed conformation of CDH in the presence of Ca^{2+} is achieved by weak forces rather than strong binding. To further test whether divalent ions exert a permanent interaction with *Mt*CDH, the enzyme was incubated in 30 mM $CaCl_2$ at 22 °C for 2 h. Dilution in a buffer containing 30 mM NaCl showed that the activity-

Table 4. Effect of 30 mM $CaCl_2$ and 30 mM NaCl on the stability of *Mt*CDH at pH 5.5 and 7.5 measured by differential scanning calorimetry.

	pH 5.5			pH 7.5		
	Buffer	NaCl	$CaCl_2$	Buffer	NaCl	$CaCl_2$
T_M (°C)	67.3	68.5	68.5	70.4	70.7	71.4
ΔH (kJ·molL^{-1})	393	454	473	847	565	634

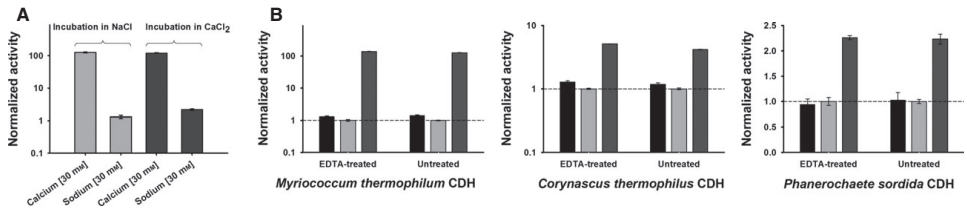

Fig. 4. (A) Cyt *c*-dependent activity of *Mt*CDH at pH 7.5 in the presence and absence of 30 mM calcium. The *x* axis indicates the ion concentration in the assay mixture. *Mt*CDH activity was measured before and after incubation in the salt containing solutions at pH 7.5 and room temperature. Error bars indicate the standard deviation of three independent replicates. (B) Comparison of cyt *c* activities of untreated and EDTA-treated CDHs. Black bars, salt-free buffer; light grey bars, addition of 30 mM sodium chloride; dark grey bars, addition of 30 mM calcium chloride. Error bars indicate the standard deviation of three independent measurements. Activities of *Mt*CDH and *Ct*CDH were measured at pH 7.5 (MOPS, 50 mM), whereas that of *Pc*CDH was measured at pH 6.5 (MOPS, 50 mM).

enhancing effect disappeared and the activity became similar to that of the negative control incubated in buffer containing 30 mM NaCl (Fig. 4A). Incubation of the enzyme in 30 mM NaCl and subsequent measurement of cyt *c* activity in the presence of 30 mM $CaCl_2$, resulted in the same enhancement of activity. Based on the results of these experiments, it may be concluded that the nature of the interaction is transient and does not increase the stability of CDH. To exclude potential interferences from residual divalent metal ions in the CDH preparations, CDHs from *Phanerochaete sordida*, *Corynascus thermophilus* and *Myriococcum thermophilum* (0.2 $mg \cdot mL^{-1}$) were incubated with 5 mM EDTA for 1 h at 22 °C. After incubation, enzymes were extensively diafiltered using EDTA-free buffer. The same procedure was applied to cyt *c*. The cyt *c* activities of the EDTA-treated and untreated enzymes were measured, and no difference was observed (Fig. 4B), indicating that no interfering ions were present.

Structure analysis and docking of CDH domains

The characterized *Mt*CDH, together with CDH from *P. chrysosporium* (*Pc*CDH) and *C. thermophilus* (*Ct*CDH), as examples of class I and class II CDHs, were used for modelling and docking studies. To analyse the DH/CYT interface of the CDHs, homology models of *Mt*DH, *Mt*CYT, *Ct*DH and *Ct*CYT were generated, and, together with the crystal structures of *Pc*DH and *Pc*CYT, were subjected to docking. The opposing domain surfaces of each CDH are shown in Fig. 5, which highlights charged Asp, Glu, Lys and Arg residues at the domain interface or in its vicinity. *Pc*CDH and *Mt*CDH show the highest number of negatively charged amino acid residues in the interfacial area (five for *Pc*CYT, ten for *Pc*DH, seven for *Mt*CYT and eight for *Mt*DH), whereas *Ct*CDH has fewer charges (five for *Ct*CYT and seven for *Ct*DH). However, the number of charged amino acids alone does little to explain the domain behaviour and IET of the selected CDHs. Therefore, titration plots of the surface-exposed amino acids in the interfacial area were created (Fig. 5). The calculated isoelectric points are similar for *Pc*CDH and *Mt*CDH (~ 4.0 for the CYT, ~ 4.5 for the DH), consistent with experimental data that show the same upper pH limit of IET for both enzymes (6). The titration plots also correctly predict a higher pH for electrostatic repulsion of the domains for *Ct*CDH (pI of ~ 5.0 for the CYT and ~ 6.2 for the DH), which does indeed show a higher pH for its IET optimum. However, the two-dimensional view does not give information on the divalent cation-bridging effect. Therefore, the interface of the docking models was investigated. The obtained docking positions do not differ by much, but all models were evaluated, and the best was selected on the basis of (i) a close haem *b* to FAD distance, and (ii) a suitable length and orientation of the linker peptide. Interestingly, the distance between the haem *b* propionate

Fig. 5. (A–C) Surface charge at pH 7.0, docking models and calculated titration plots of the amino acids located at the interface of *Pc*CDH (A) *Mt*CDH (B) and *Ct*CDH (C). Residues considered for calculation of titration plots are those within circles. *Mt*CDH and *Ct*CDH are homology models based on separately crystallized *Pc*CDH sub-domains (PDB IDs 1NAA and 1D7C). The docking models show the DH in yellow and the CYT in orange. Distances between clusters are used to indicate their position (black lines). (D) Crystal structure of the CYT fragment of *P. chrysosporium*, including the coordination of co-crystallized cadmium atoms (pink).

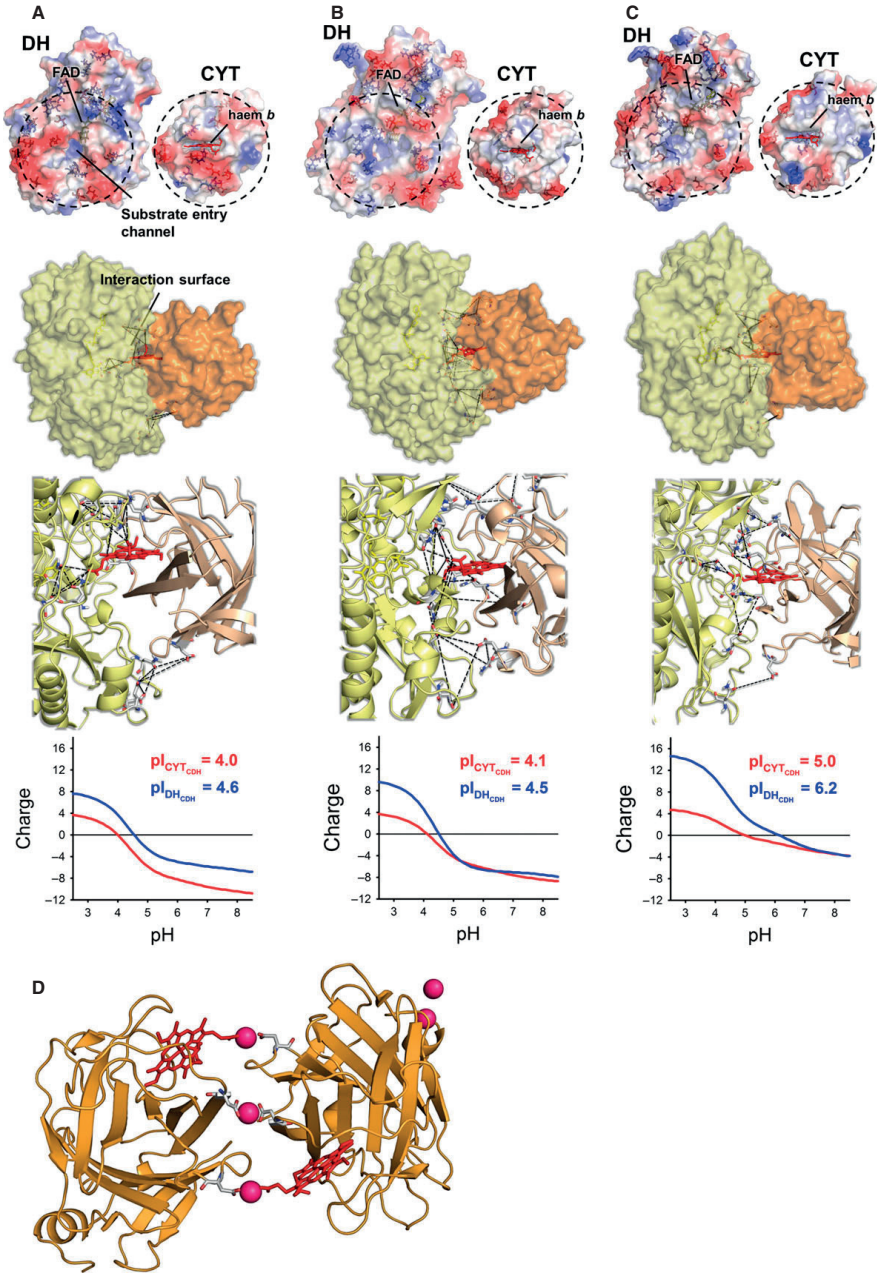
A
DH
FAD
CYT
haem *b*
Substrate entry channel
B
DH
FAD
CYT
haem *b*
C
DH
FAD
CYT
haem *b*
Interaction surface
Charge
pH
$pI_{CYT_{CDH}}$ = 4.0
$pI_{DH_{CDH}}$ = 4.6
$pI_{CYT_{CDH}}$ = 4.1
$pI_{DH_{CDH}}$ = 4.5
$pI_{CYT_{CDH}}$ = 5.0
$pI_{DH_{CDH}}$ = 6.2
D

group reaching into the substrate channel and the FAD isoalloxazine ring (edge-to-edge distance) was shortest for *Ct*CDH (5.6 ± 0.6 Å) compared to *Mt*CDH and *Pc*CDH (8 ± 2 and 8.6 ± 2 Å, respectively). A closer distance between the cofactors in the closed confirmation may additionally support the occurrence of IET at an increased pH under which the domains begin to separate. The mean calculated interfacial area between the DH and the CYT for the three CDHs differs by a maximum of 16% (*Mt*CDH 2270 ± 280 $Å^2$, *Ct*CDH 2090 ± 70 $Å^2$, *Pc*CDH 1910 ± 250 $Å^2$). Docked structures with highlighted cofactors and distances below 13 Å between opposing Asp, Glu, Asn and Gln residues are shown in Fig. 5. Such clusters, which inadequately mimic the structurally well-defined Ca-binding sites in calmodulin, for example, allow weak electrostatic interactions between Ca^{2+} and negatively charged amino acid side chains. It is obvious that, in *Mt*CDH, these clusters contain many residues, but in *Pc*CDH and *Ct*CDH, they contain only a few. Four clusters were found in *Mt*CDH and *Pc*CDH, and three in *Ct*CDH (Table S2). For all enzymes, at least one cluster involves one or both haem propionate groups. The much higher number of potential dication ligands in *Mt*CDH provides an explanation for the high increase of IET at alkaline pH. The presence of more sites for Ca^{2+} binding more efficiently counteracts electrostatic repulsion of the domains. Interestingly, for a number of proteins crystallized in the presence of cadmium ions, it has been observed that Cd^{2+} is positioned at the interface between two neighboring protein molecules and coordinated by two carboxyl groups of glutamic or aspartic acid side chains each belonging to one of the two molecules [23–25]. This coordination may be supplemented by interactions with carbonyl groups of the polypeptide backbone. Such complexation was also observed in the structure of *P. chrysosporium* CYT (PDB ID 1D7C [13]). Either one or both of the Cd^{2+} -complexing sites known for dimers of *P. chrysosporium* CYT (Fig. 5D) were found in the predictions for *Pc*CDH, *Mt*CDH and *Ct*CDH.

Conclusions

Steady-state and pre-steady-state measurements in combination with homology models show that the pH dependence of IET and the reduction of cyt *c* may be explained by the presence of negatively charged amino acids at the interface of the DH and CYT, preventing formation of a closed conformation of the DH and the CYT. Calculated titration plots of these interfaces demonstrate that the CYT has a lower pI than the DH; the same trend was also observed for the isoelectric points of the domains [10]. Below, or a little above these pIs, the domains do not repulse each other, and thus allow electron transfer between the domains.

In the present work, we also unequivocally demonstrate that dications enhance the IET reaction in cellobiose dehydrogenase, as first suggested by Schulz *et al.* [14]. Catalytic constants for cyt *c* at pH 7.5 measured in the presence of calcium ions indicate that the presence of divalent cations supports a closed conformation of both domains at neutral and alkaline pH. The reduction state of the cofactors during catalysis, monitored by stopped-flow spectroscopy, reveals that Ca^{2+} affects the IET most strongly. Less prominent, but clearly observable, is the coupling of both cofactors in close proximity of the domains, which increases the reduction rate of FAD. This effect occurs either at low pH or in the presence of Ca^{2+}. Currently, we have no supported explanation for this phenomenon, which was observed in steady-state and pre-steady-state kinetic measurements, but the observed pull effect on the FAD may originate from a modified redox potential of the FAD via an intermediary Trp295 side chain.

It has been reported [18–22] that divalent cations potentially form a bridge between oppositely charged carboxylate groups on polyelectrolytes, DNA or hyaluronic acid. Based on our data, this effect also influences domain interaction in CDH, and presumably also applies to other proteins, given that a number of negatively charged amino acid residues are present in close proximity at domain interfaces. In addition to providing an explanation for the observed pH-dependent IET of CDH and the Ca^{2+} ion effect, these findings may also have practical relevance, e.g. for increasing the current output of CDH-based biosensors or biofuel cells. Also, in accordance with the results of a previous study [26], a CDH-based bioelectrochemical switch may be accomplished at neutral/alkaline pH using divalent cations to switch the IET and hence direct electron transfer on and off. The high millimolar dication concentrations required for such an effect are rarely encountered in nature, but may provide ways to stabilize or regulate enzymes in biocatalytic and biomedical applications.

Experimental procedures

Chemicals and enzymes

Chemicals were purchased from commercial suppliers at the highest purity available. The CDHs used in this study are from the fungi *Corynascus thermophilus* CBS 174.70 (*Ct*CDH, [11]), *Chaetomium atrobrunneum* CBS 238.71 [11],

Hypoxylon haematostroma CBS 255.63 [11], *Dichomera saubinetii* CBS 990.7 [11], *Trametes villosa* CBS 334.49 [27], *Phanerochaete chrysosporium* K3 (*Pc*CDH [28]), *Phanerochaete sordida* MB66 (R. Ludwig, unpublished data), *Sclerotium rolfsii* CBS 191.62 [29] and *Ceriporiopsis subvermispora* FP-90031 [30]. CDHs were isolated and purified as described [11] previously. CDH IIA and IIB from *Neurospora crassa* CBS 232.56 [6] and CDH IIA from *Myriococcum thermophilum* CBS 208.89 (*Mt*CDH [31]) were recombinantly produced in *Pichia pastoris* X-33 cells, and purified as described [6] previously. The recombinant dehydrogenase domain of *Mt*CDH (*Mt*DH) was produced in *P. pastoris* X-33 and purified as described previously [6].

Steady-state kinetics

CDH activities were assayed spectrophotometrically based on the cellobiose-dependent reduction of the two-electron acceptors DCIP (0.3 mM, ε_{520} = 6.9 $mM^{-1}\cdot cm^{-1}$) and BQ (1 mM, ε_{290} = 2.24 $mM^{-1}\cdot cm^{-1}$) and the one-electron acceptors cyt *c* (0.02 mM, ε_{550} = 19.6 $mM^{-1}\cdot cm^{-1}$), potassium ferricyanide (1 mM, ε_{420} = 0.98 $mM^{-1}\cdot cm^{-1}$) and ferrocenium hexafluorophosphate (0.1 mM, ε_{300} = 4.3 $mM^{-1}\cdot cm^{-1}$). All assays contained 3 mM cellobiose, and were performed in 50 mM sodium formiate buffer (pH 3–4), 50 mM sodium acetate buffer (pH 4–6) or 50 mM MOPS buffer (pH 6–8.5). Reactions were started by mixing 20 μL of enzyme solution (0.05–0.2 $U\cdot mL^{-1}$) with 980 μL of a pre-warmed reaction mix containing the electron acceptors and cellobiose. Reduction of electron acceptors was followed for 180 s at 30 °C in a Lambda 35 spectrophotometer (Perkin Elmer, Waltham, MA, USA) with a thermo-controlled eight-cell changer. Enzyme activity is defined as the amount of enzyme that reduces 1 μmol of the respective electron acceptor per minute under the specified conditions. Catalytic constants were calculated from initial rates by using non-linear least-squares regression to fit the observed data to the Michaelis–Menten equation using SIGMA PLOT 11 (Systat Software, San Jose, CA, USA). The influence of various anions and cations on CDH activity was measured in 96-well plates in an EnSpire multimode plate reader (Perkin Elmer). For measurements below 340 nm, UV-transparent 96-well-plates or UV-transparent cuvettes were used. Protein concentrations were determined by the dye-binding method [32] using a pre-fabricated assay (Bio-Rad, Hercules, CA, USA) with BSA as the calibration standard. Concentrations of *Mt*CDH used for stopped-flow spectroscopy were determined based on the enzyme's absorption coefficient at 421 nm (ε_{420} = 99.4 $mM^{-1}\cdot cm^{-1}$).

Pre-steady-state kinetics

Fast kinetic studies were performed on a SX-18MV spectrophotometer (Applied Photophysics, Leatherhead, UK). The cellobiose-dependent reduction of CDH was monitored in single mixing mode using a SX/PDA photodiode array detector or a SX/PMT photomultiplier tube. The reduction of FAD was followed at 449 nm and the reduction of haem *b* was followed at 563 nm. Concentrations of CDH and cellobiose after mixing were 5 μM and 3 mM, respectively. All measurements were performed at 30 °C with at least five repeats for each investigated condition. Observed rate constants (k_{obs}) were calculated by fitting the absorbance changes to a double exponential curve using PRODATA software (Applied Photophysics).

Differential scanning calorimetry

The transition mid-point temperature (T_M) of *Mt*CDH in the presence of $CaCl_2$ and NaCl was determined using a MicroCal VP-DSC calorimeter equipped with an autosampler (MicroCal, Northampton, MA, USA). *Mt*CDH was adjusted to a concentration of 1 $mg\cdot mL^{-1}$ based on its molar absorption at 421 nm. Thermograms were obtained at pH 4.5 (100 mM sodium acetate buffer) and pH 7.5 (100 mM MOPS buffer) between 30 °C and 100 °C at a scan speed of 1 °C min^{-1}. Heat-inactivated enzymes were re-scanned as a control, and their values were subtracted from the experimental thermograms. Data were evaluated using ORIGIN 7.5 software (Origin Lab Corporation, Northampton, MA, USA).

Comparative modelling and docking

Structure-guided homology models of the individual DH and CYT of *Mt*CDH (GenBank accession number ABS45567.2) and *Ct*CDH (GenBank accession number ADT70772.1) were generated using the SWISS-MODEL server (http://swissmodel.expasy.org/) [33] with the individually crystallized DH of *P. chrysosporium* CDH (PDB ID 1KDG [12]) and the CYT of *P. chrysosporium* CDH (PDB ID 1D7C [13]) as templates. The HADDOCK webserver (http://haddock.science.uu.nl/) was used for protein–protein docking of the individual CDH domains [34]. To roughly pre-define the docking position, residues located within 4 Å of the haem *b* CYT (Pro72, Tyr98, M100, Gln173, Gln174, His175 and Met179) and residues in proximity to the substrate channel in the DH (Met80, Ala81 and Val91) were selected as initial docking sites. In total, 12 models from three clusters per enzyme were evaluated. Models with a haem *b* to FAD distance of more than 10 Å were not considered for further analysis. Structures were visualized using the PyMOL MOLECULAR GRAPHICS SYSTEM, version 1.4 (Schrödinger, New York, NY, USA).

Acknowledgements

The authors wish to thank Dominik Jeschek (University of Natural Resources and Life Sciences, Vienna,

Austria) for excellent help with differential scanning calorimetry measurements. This work was supported by the European Commission (Project INDOX FP7-KBBE-2013-7-613549, Project BIOENERGY FP7-PEOPLE-2013-ITN-607793 and Project CHEBANA FP7-PEOPLE-2010-ITN-264772), the Swedish Research Council (Vetenskapsrådet) (project 2010-5031) and the Austrian Science Fund (Fonds zur Förderung der wissenschaftlichen Forschung) (doctoral program 'BioTop – Biomolecular Technology of Proteins', FWF W1224).

Author contributions

RL, LG and CSch initiated the study, and RL, DK and KZ planned the experiments. CS produced and purified recombinant cellobiose dehydrogenases. DK and KZ performed the experiments. DK, KZ, CSch, LG and RL evaluated and analysed the data. RL and DK wrote the manuscript. All authors read, revised and approved the manuscript for submission.

References

1 Vaaje-Kolstad G, Westereng B, Horn SJ, Liu Z, Zhai H, Sørlie M & Eijsink VGH (2010) An oxidative enzyme boosting the enzymatic conversion of recalcitrant polysaccharides. *Science* **330**, 219–222.

2 Phillips CM, Beeson WT IV, Cate JH & Marletta MA (2011) Cellobiose dehydrogenase and a copper-dependent polysaccharide monooxygenase potentiate cellulose degradation by *Neurospora crassa*. *ACS Chem Biol* **6**, 1399–1406.

3 Agger JW, Isaksen T, Várnai A, Vidal-Melgosa S, Willats WGT, Ludwig R, Horn SJ, Eijsink VGH & Westereng B (2014) Discovery of LPMO activity on hemicelluloses shows the importance of oxidative processes in plant cell wall degradation. *Proc Natl Acad Sci USA* **111**, 6287–6292.

4 Isaksen T, Westereng B, Aachmann FL, Agger JW, Kracher D, Kittl R, Ludwig R, Haltrich D, Eijsink VGH & Horn SJ (2014) A C4-oxidizing lytic polysaccharide monooxygenase cleaving both cellulose and cello-oligosaccharides. *J Biol Chem* **289**, 2632–2642.

5 Vu VV, Beeson WT, Span EA, Farquhar ER & Marletta MA (2014) A family of starch-active polysaccharide monooxygenases. *Proc Natl Acad Sci USA* **111**, 13822–13827.

6 Sygmund C, Kracher D, Scheiblbrandner S, Zahma K, Felice AKG, Harreither W, Kittl R & Ludwig R (2012) Characterization of the two *Neurospora crassa* cellobiose dehydrogenases and their connection to oxidative cellulose degradation. *Appl Environ Microbiol* **78**, 6161–6171.

7 Igarashi K, Yoshida M, Matsumura H, Nakamura N, Ohno H, Samejima M & Nishino T (2005) Electron transfer chain reaction of the extracellular flavocytochrome cellobiose dehydrogenase from the basidiomycete *Phanerochaete chrysosporium*. *FEBS J* **272**, 2869–2877.

8 Harreither W, Nicholls P, Sygmund C, Gorton L & Ludwig R (2012) Investigation of the pH-dependent electron transfer mechanism of ascomycetous class II cellobiose dehydrogenases on electrodes. *Langmuir* **28**, 6714–6723.

9 Igarashi K, Momohara I, Nishino T & Samejima M (2002) Kinetics of inter-domain electron transfer in flavocytochrome cellobiose dehydrogenase from the white-rot fungus *Phanerochaete chrysosporium*. *Biochem J* **365**, 521–526.

10 Zamocky M, Ludwig R, Peterbauer C, Hallberg BM, Divne C, Nicholls P & Haltrich D (2006) Cellobiose dehydrogenase– a flavocytochrome from wood-degrading, phytopathogenic and saprotropic fungi. *Curr Protein Pept Sci* **7**, 255–280.

11 Harreither W, Sygmund C, Augustin M, Narciso M, Rabinovich ML, Gorton L, Haltrich D & Ludwig R (2011) Catalytic properties and classification of cellobiose dehydrogenases from Ascomycetes. *Appl Environ Microbiol* **77**, 1804–1815.

12 Hallberg BM, Henriksson G, Pettersson G & Divne C (2002) Crystal structure of the flavoprotein domain of the extracellular flavocytochrome cellobiose dehydrogenase. *J Mol Biol* **315**, 421–434.

13 Hallberg BM, Bergfors T, Bäckbro K, Pettersson G, Henriksson G & Divne C (2000) A new scaffold for binding haem in the cytochrome domain of the extracellular flavocytochrome cellobiose dehydrogenase. *Structure* **8**, 79–88.

14 Schulz C, Ludwig R, Micheelsen PO, Silow M, Toscano MD & Gorton L (2012) Enhancement of enzymatic activity and catalytic current of cellobiose dehydrogenase by calcium ions. *Electrochem Commun* **17**, 71–74.

15 Kulys JJ & Čénas NK (1983) Oxidation of glucose oxidase from *Penicillium vitale* by one- and two-electron acceptors. *Biochim Biophys Acta* **744**, 57–63.

16 Kovacs E, Harmat V, Tóth J, Vértessy BG, Módos K, Kardos J & Liliom K (2010) Structure and mechanism of calmodulin binding to a signaling sphingolipid reveal new aspects of lipid-protein interactions. *FASEB J* **24**, 3829–3839.

17 Busch E, Hohenester E, Timpl R, Paulsson M & Maurer P (2000) calcium affinity, cooperativity, and domain interactions of extracellular EF-hands present in BM-40. *J Biol Chem* **275**, 25508–25515.

18 Qiu X, Andresen K, Kwok LW, Lamb JS, Park HY & Pollack L (2007) Inter-DNA attraction mediated by divalent counterions. *Phys Rev Lett* **99**, 038104.

19 Kundagrami A & Muthukumar M (2008) Theory of competitive counterion adsorption on flexible polyelectrolytes: Divalent salts. *J Chem Phys* **128**, 244901.
20 Wang X, Lee SY, Miller K, Welbourn R, Stocker I, Clarke S, Casford M, Gutfreund P & Skoda MWA (2013) Cation bridging studied by specular neutron reflection. *Langmuir* **29**, 5520–5527.
21 Jiang L, Titmuss S & Klein J (2013) Interactions of hyaluronan layers with similarly charged surfaces: the effect of divalent cations. *Langmuir* **29**, 12194–12202.
22 Sobeck DC & Higgins MJ (2002) Examination of three theories for mechanisms of cation-induced bioflocculation. *Water Res* **36**, 527–538.
23 Yao N, Trakhanov S & Quiocho FA (1994) Refined 1.89 Å structure of the histidine-binding protein complexed with histidine and its relationship with many other active transport/chemosensory proteins. *Biochemistry* **33**, 4769–4779.
24 Nickitenko AV, Trakhanov S & Quiocho FA (1995) 2 Å resolution structure of DppA, a periplasmic dipeptide transport/chemosensory receptor. *Biochemistry* **34**, 16585–16595.
25 Granier T, Gallois B, Dautant A, Langlois d'Estaintot B & Précigoux G (1997) Comparison of the structures of the cubic and tetragonal forms of horse-spleen apoferritin. *Acta Crystallogr D Biol Crystallogr* **53**, 580–587.
26 Feifel SC, Kapp A, Ludwig R & Lisdat F (2014) Nanobiomolecular multiprotein clusters on electrodes for the formation of a switchable cascadic reaction scheme. *Angew Chem Int Ed Engl* **53**, 5676–5679.
27 Ludwig R, Salamon A, Varga J, Zamocky M, Peterbauer CK, Kulbe KD & Haltrich D (2004) Characterisation of cellobiose dehydrogenases from the white-rot fungi *Trametes pubescens* and *Trametes villosa*. *Appl Microbiol Biotechnol* **64**, 213–222.
28 Henriksson G, Pettersson G, Johansson G, Ruiz A & Uzcategui E (1991) Cellobiose oxidase from *Phanerochaete chrysosporium* can be cleaved by papain into two domains. *Eur J Biochem* **196**, 101–106.
29 Baminger U, Subramaniam SS, Renganathan V & Haltrich D (2001) Purification and characterization of cellobiose dehydrogenase from the plant pathogen *Sclerotium* (*Athelia*) *rolfsii*. *Appl Environ Microbiol* **67**, 1766–1774.
30 Harreither W, Sygmund C, Dunhofen E, Vicuna R, Haltrich D & Ludwig R (2009) Cellobiose dehydrogenase from the ligninolytic basidiomycete *Ceriporiopsis subvermispora*. *Appl Environ Microbiol* **75**, 2750–2757.
31 Zámocki M, Schümann C, Sygmund C, O'Callaghan J, Dobson AD, Ludwig R, Haltrich D & Peterbauer CK (2008) Cloning, sequence analysis and heterologous expression in *Pichia pastoris* of a gene encoding a thermostable cellobiose dehydrogenase from *Myriococcum thermophilum*. *Protein Expr Purif* **59**, 258–265.
32 Bradford MM (1976) Rapid and sensitive method for the quantitation of microgram quantities of protein utilizing the principle of protein–dye binding. *Anal Biochem* **72**, 248–254.
33 Arnold K, Bordoli L, Kopp J & Schwede T (2006) The SWISS-MODEL workspace: a web-based environment for protein structure homology modelling. *Bioinformatics* **22**, 195–201.
34 De Vries SJ, van Dijk M & Bonvin AMJJ (2010) The HADDOCK web server for data-driven biomolecular docking. *Nat Protoc* **5**, 883–897.

Supporting information

Additional supporting information may be found in the online version of this article at the publisher's web site:

Table S1. Influence of anions and cations (30 mM) on *Mt*CDH activity measured using cyt *c*, DCIP and 1,4-benzoquinone.

Table S2. Distances between Asp, Glu, Gln and Asn residues in the docking models.

Paper VII

ChemPubSoc Europe

DOI: 10.1002/cphc.201500112

CHEMPHYSCHEM Articles

Spectroscopic Observation of Calcium-Induced Reorientation of Cellobiose Dehydrogenase Immobilized on Electrodes and its Effect on Electrocatalytic Activity

Patrycja Kielb,[a] Murat Sezer,[a] Sagie Katz,[a] Francesca Lopez,[b] Christopher Schulz,[b] Lo Gorton,[b] Roland Ludwig,[c] Ulla Wollenberger,[d] Ingo Zebger,[a] and Inez M. Weidinger*[a]

Cellobiose dehydrogenase catalyzes the oxidation of various carbohydrates and is considered as a possible anode catalyst in biofuel cells. It has been shown that the catalytic performance of this enzyme immobilized on electrodes can be increased by presence of calcium ions. To get insight into the Ca^{2+}-induced changes in the immobilized enzyme we employ surface-enhanced vibrational (SERR and SEIRA) spectroscopy together with electrochemistry. Upon addition of Ca^{2+} ions electrochemical measurements show a shift of the catalytic turnover signal to more negative potentials while SERR measurements reveal an offset between the potential of heme reduction and catalytic current. Comparing SERR and SEIRA data we propose that binding of Ca^{2+} to the heme induces protein reorientation in a way that the electron transfer pathway of the catalytic FAD center to the electrode can bypass the heme cofactor, resulting in catalytic activity at more negative potentials.

1. Introduction

Cellobiose dehydrogenase (CDH) is an oxidoreductase that has been proposed to play a multifunctional role in the breakdown of lignocellulose.[1] The enzyme consists of a dehydrogenase domain (DH) with a FAD cofactor connected by a flexible linker with a heme-*b*-containing cytochrome domain (CYT). Cellobiose is oxidized at the catalytic FAD center to cellobionic acid, generating two excess electrons. These electrons are further donated to external one- or two-electron acceptors (e.g. benzoquinones, redox dyes) either directly[1–3] or via the second redox center (CYT domain) after an internal electron transfer (IET) process (Figure 1).[4,5] Previous crystallographic and spectroscopic studies of the cytochrome domain of CDH from *Phanerochaete chrysosporium* have shown that the heme iron is hexacoordinated by a Met and His axial ligand. The heme-propionate groups are surface exposed and, therefore, it has been proposed that they might play a role in the interdomain electron transfer (IET).[6] However, up to now neither crystallographic data nor spectroscopic studies have validated this hypothesis.

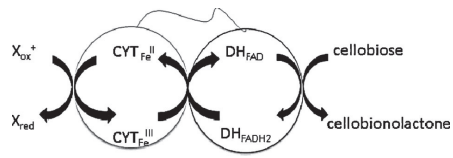

Figure 1. Catalytic cycle of CDH. The terminal acceptor (X) can be another protein like polysaccharide monooxygenase or a suitable electrode surface.

CDH is capable of oxidizing a variety of carbohydrate substrates.[1,7–9] Furthermore it has been shown to remain catalytically active when immobilized on electrodes[10–12] and thus has been involved in many applications. There are biosensors based on CDH applied to detect cellobiose[13,14] or lactose.[15–18] The most promising practical application of this enzyme is utilization as anode material in biofuel cells via catalytic oxidation of glucose, lactose or cellobiose.[19] CDH-based fuel cells were developed that use glucose in human serum as fuel[20,21] as well as CDH/pyranose dehydrogenase hybrid fuel cells that increase the coulombic efficiency by oxidizing glucose at different carbon sites respectively.[22] A variety of electrochemical measurements have been carried out on CDH/electrode systems,[10,15,20,23–28] but no spectroscopic work has been done so far that would provide additional insight into the reaction mechanism and charge transfer pathway of CDH bound to functionalized electrodes.

[a] *P. Kielb, Dr. M. Sezer, S. Katz, Dr. I. Zebger, Prof. I. M. Weidinger*
Institut für Chemie
Technische Universität Berlin
Strasse des 17. Juni 135, 10623 Berlin (Germany)
E-mail: inez.weidinger@tu-berlin.de

[b] *F. Lopez, C. Schulz, Prof. L. Gorton*
Department of Biochemistry and Structural Biology
Lund University
PO Box 124, 221 00 Lund (Sweden)

[c] *Dr. R. Ludwig*
Department of Food Science and Technology
BOKU - University of Natural Resources and Life Science
Muthgasse 18, 1190 Vienna (Austria)

[d] *Prof. U. Wollenberger*
Institüt für Biochemie und Biologie
Universität Potsdam
Karl Liebknecht Strasse 24-25, 14476 Golm (Germany)

Supporting information for this article is available on the WWW under http://dx.doi.org/10.1002/cphc.201500112.

These are not the final page numbers! ↗↗

Once a redox enzyme is immobilized on a conducting support the electrode can replace the natural electron acceptor/donor. By integrating such enzyme-coated electrodes into an electrochemical cell, oxidation or reduction of added substrate is directly transferred into an electrical current. The magnitude of electrical power generated by this process is equal to the chemical energy gained from the exothermic reaction. However, in many enzyme-based fuel cells the thermodynamically possible voltage is not achieved. The reasons for this can lie in a decreased turnover rate at the active site or in a limited electron transfer rate between catalytic center and electrode.[29] The latter can be rationalized, as the ET rate largely depends on the orientation, flexibility and distance of the catalytic center from the electrode.[30,31] In addition, adjustable parameters such as pH, ionic strength, buffer composition with various cations and anions can also modulate the ET and thus the performance of the biofuel cell.[10,15,20,23–28]

One representative of CDH is produced by the ascomycete fungus *Myriococcum thermophilum* (*Mt*CDH), a thermotolerant saprophyte.[32] It is known from previous reported investigations that *Mt*CDH can be successfully immobilized on different kinds of electrodes (graphite,[33,34] or gold[35]) while retaining good catalytic activity. In the absence of natural redox partners, electrons are believed to be transferred almost exclusively via a heme redox transition to the electrode.[36] It has been shown that CDH reaches its maximum catalytic rate at pH 5.5 after addition of 5 mM sugar (lactose, cellobiose). Moreover, increasing the ionic strength of the buffer increased the catalytic activity of immobilized *Mt*CDH.[33,37] Surprisingly, the effect was much more pronounced for the divalent cation salt $CaCl_2$ than for monovalent cation salts such as KCl.[34,37] It has been proposed that specific binding of Ca^{2+} ions either influence the intramolecular- or the heterogeneous electron transfer properties,[37] but, no final conclusions could be drawn up to now.

Vibrational spectroscopy gives detailed information about molecular structure. In Raman spectroscopy inelastic scattering of monochromatic light by the molecule is analyzed. Under resonance Raman (RR) conditions, where the frequency of the source light is close to the frequency of an electronic transition, structural changes of a chromophore are selectively probed. This approach has been widely used to study the heme cofactor in heme proteins using violet light excitation. On the other hand, infrared (IR) spectroscopy is mainly used to determine the secondary structure of proteins, which is given by the geometry of the peptide backbone.

In surface-enhanced vibrational spectroscopy locally enhanced electric fields at the surface of noble metal nanostructures are used to selectively monitor the vibrations of surface-bound molecules. In combination with electrochemistry surface-enhanced resonance Raman (SERR) and surface-enhanced infrared absorption (SEIRA) spectroscopy are powerful techniques to study structure–function relationships of enzymes on surfaces.[30] SERR and SEIRA measurements have been individually applied in the past to study the redox and catalytic properties of various enzyme/electrode systems.[38–44] In this work, we have applied both vibrational spectro-electrochemical techniques on the same enzyme to investigate the influence of monovalent Na^+ and divalent Ca^{2+} ions on the electron transfer pathway of surface-bound *Mt*CDH. SERR spectroscopy (SERRs) provides detailed insight into the structure and redox behavior of the heme located inside the cytochrome domain and its communication with the electrode, while the SEIRA signal is dominated by the vibrations of the protein backbone. Complementary SEIRA and SERR spectroscopic measurements therefore provide unique information about possible changes in the orientation of the immobilized enzyme. Finally, electrochemical measurements reveal valuable information about the overall catalytic activity of immobilized *Mt*CDH.

2. Results

2.1. Electrochemistry

Cylindrical electrodes (3 mm height and 5 mm in diameter) suitable for SERRs and electrochemistry were made of silver and prepared by polishing the solvent-exposed surface with sandpaper and subsequent electrochemical roughening via repetitive oxidative and reductive steps.[45] The electrodes were incubated in a poly(diallyldimethylammonium chloride (PDADMAC) solution for 10 min, which served as a functional coating for protein immobilization.[46] Subsequently, the electrode was rinsed with water and dried.

Enzyme attachment was achieved by incubating the coated electrode in 700 μL of a 0.33 μM *Mt*CDH in 50 mM acetate solution at pH 5.5 for 1 h at room temperature. During incubation the electrode was rotating at 360 rpm. Binding of *Mt*CDH under these conditions is expected to occur due to the electrostatic attraction of the negatively charged CYT domain and the positively charged PDADMAC.

For spectro-electrochemical measurements the silver electrode was incorporated into a three-electrode electrochemical cell as working electrode. A Pt wire functioned as counter and an Ag|AgCl (3 M KCl) electrode as reference electrode.

Cyclic voltammograms of immobilized *Mt*CDH under non-turnover and turnover conditions (10 mM lactose) were recorded at a scan rate of 2 mV s^{-1} and 100 mV s^{-1}, respectively, while the electrode was slowly rotated at 360 rpm to keep the same conditions as in the SERR experiments. Measurements were performed in different acetate buffer concentrations (50–200 mM) and in presence of $CaCl_2$ (5–50 mM). No redox peaks were recorded under non-turnover conditions although SERRs and SEIRAs measurements confirmed the presence of CDH on the electrode. However, in the presence of lactose as substrate a clear catalytic current was observed (Figure 2A). The turnover signal was fitted by a sigmoidal function taking the average values of the forward and reverse scan. This yielded an inflection point (IP) at −72 mV (Table 1), which in the following is used as a value to characterize the potential dependence of the catalytic current. Furthermore, the open-circuit potential decreased from 100 mV to 17 mV upon addition of lactose.

The size and shape of the electrochemical turnover signal showed a strong dependence on the ion concentration in solution (Figures 3A–Figure 3C). In general, upon increasing the concentration of mono- (Na^+) and di-valent (Ca^{2+}) ions in solu-

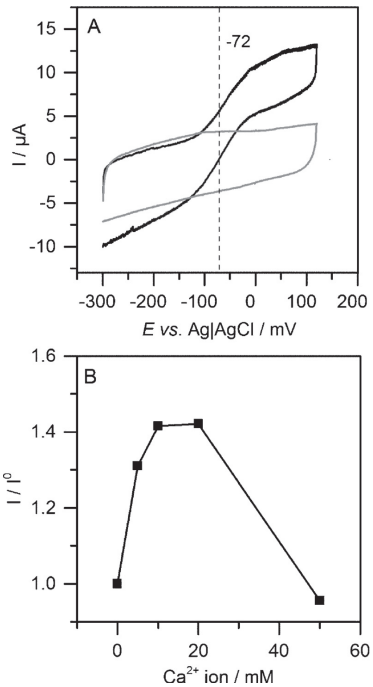

Figure 2. A) Cyclic voltammograms of *Mt*CDH recorded under non-turnover (gray) and turnover (10 mM lactose, black) conditions in 50 mM pH 5.5 acetate buffer. The inflection point potential is indicated by a dashed line. The scan rate is 2 mV s^{-1}. B) Increase in electrocatalytic current at 0 mV (vs. 3 M Ag|AgCl) of immobilized *Mt*CDH in presence of lactose as a function of Ca^{2+}-ion concentration. The current (I^0) in the absence of Ca^{2+} ions is used as reference.

tion, the catalytic current curves were shifted to more negative potentials. Mostly due to this shift, higher catalytic currents were measured for higher ion concentrations at an applied voltage of 0 V. In the case of monovalent Na^+ ions the electrocatalytic current increased by 45% upon changing the ion concentration from 50 to 200 mM. Interestingly, the same increase in catalytic activity could be reached for much lower ion concentrations if divalent Ca^{2+} ions were added to the buffer solution instead (Figure 2B). Already for Ca^{2+} concentrations below 10 mM a significant increase in catalytic current was observed, which reached a maximum at 20 mM Ca^{2+}. Higher concentrations of Ca^{2+} did not improve the catalytic performance. For 50 mM Ca^{2+} the catalytic current even fell below the value that was observed in the absence of Ca^{2+}.

Addition of either 150 mM Na^+ or 20 mM Ca^{2+} resulted in a comparable shift in the turnover signal to more negative potentials (Figures 3B,C and Table 1), yielding inflection points of −92 mV and −100 mV, respectively (dashed vertical lines in Figures 3B,C). This behavior was also reflected by a shift in the open-circuit potential to −10 mV and −55 mV, respectively.

2.2. SERR Measurements

To investigate the function of the heme cofactor in the catalytic cycle of *Mt*CDH/electrode systems, SERR measurements of *Mt*CDH illuminated with a 413 nm laser were recorded (Figure 4). The SERR spectra revealed the characteristic vibrational modes (ν_4, ν_3, ν_2, ν_{10}) of a six-coordinated low-spin *b*-type heme cofactor[47] supporting the proposed immobilization of *Mt*CDH on PDADMAC-coated electrodes via the heme domain. At positive potentials (100 mV), the oxidation-sensitive marker band (ν_4) was found at 1370 cm^{-1}, corresponding to a ferric form of the heme (Figure 4A). At an applied potential of −200 mV, the ν_4 band down-shifted to 1362 cm^{-1}, revealing complete reduction of the heme (Figure 4B). The redox transitions were found to be completely reversible (data not shown). When the substrate lactose was added at open-circuit conditions the heme became fully reduced, indicating that the protein remains catalytically active and the intra-domain electron transfer is preserved upon immobilization (Figure 4C). All spectra are in good agreement with the one presented by Cohen et al.[47]

Potential-dependent SERR measurements made it possible to determine the relative intensities of the oxidized and the reduced heme species at a given applied potential. Here complete component spectra of the ferric and ferrous form of the heme were fitted to the spectra. To transform the SERR intensities into relative concentrations the Raman cross sections for ferrous and ferric heme *b* were calculated via component analysis, as described previously.[38] This procedure yielded the molar fraction of oxidized heme (x_{ox}) as a function of potential shown in Figure 3D–Figure 3F. From the spectroscopically derived redox titration curves—fitted by the Nernst equation—the formal potential of the heme ($E^{\circ\prime}$) and the apparent number of transferred electrons could be determined. At a 50 mM buffer concentration in the absence of Ca^{2+}, $E^{\circ\prime}$ of the heme was determined to be −54.5 mV (vs. 3 M Ag|AgCl, Figure 3D and Table 1). With respect to this value, we observed a negative shift of ca.

Table 1. Redox parameters of *Mt*CDH immobilized on Ag electrodes coated with PDADMAC solution. Acetate buffer is abbreviated as ac.

Ion concentration	$E^{0\prime}$ [mV][a]	n[b]	K_{HET} [s^{-1}][c]	OCP [mV][d]	IP [mV][e]
50 mM ac.	−54.5 ± 3	0.70 ± 0.01	4.6 ± 0.7	17	−72 ± 8
200 mM ac.	−72.6 ± 6	0.86 ± 0.01	13.54	−10	−92 ± 12
50 mM ac. + 10 mM Ca^{2+}	−14.8 ± 3	0.97 ± 0.03	7.17	−55	−100 ± 14

[a] Formal heme potential (E^0). [b] Apparent number of electrons (n). [a] and [b] were determined by fitting the Nernst equation to the relative intensities of oxidized and reduced species. [c] Heterogeneous electron transfer rate (k_{HET}) between heme and electrode. [d] Open-circuit potential (OCP) in presence of lactose. [e] inflection point (IP) of the electrochemical turnover signal of *Mt*CDH

These are not the final page numbers! ↗↗

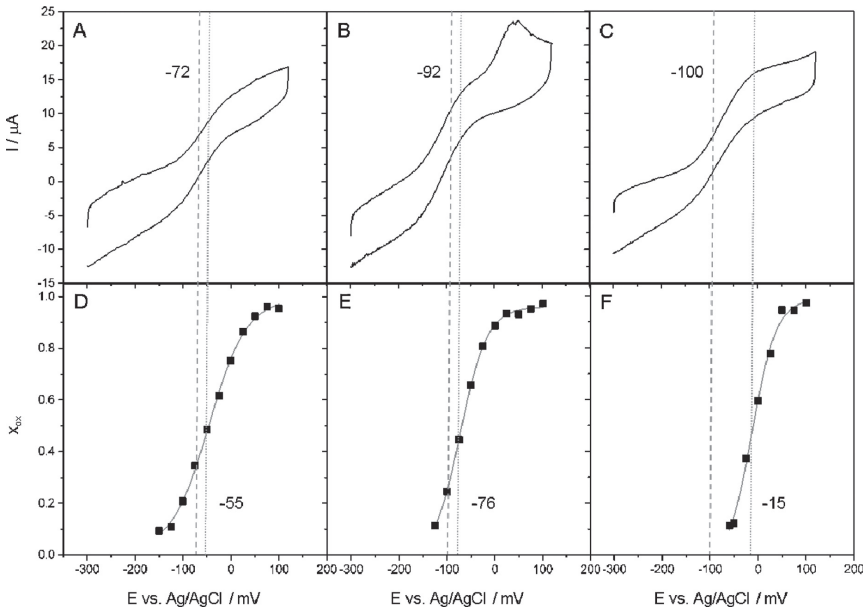

Figure 3. A)–C) Cyclic voltammograms of *Mt*CDH under turnover conditions (10 mM of lactose, scan rate 100 mVs^{-1}) Measurements were taken in A) 50 mM acetate buffer; B) 200 mM acetate buffer; C) 50 mM acetate buffer + 10 mM $CaCl_2$ buffer. Dashed lines (-----) refer to the inflection point of the curve. D)–F) Redox titration curves obtained from SERR measurements of immobilized *Mt*CDH in the absence of lactose. The line represents a Nernst fit to the data. Measurements were taken in D) 50 mM acetate buffer; E) 200 mM acetate buffer; F) 50 mM acetate buffer + 10 mM $CaCl_2$ buffer. Dotted lines (•••••) refer to the redox potential of the heme obtained from SERRs.

22 mV at higher ionic strength (200 mM) (Figure 3E and Table 1). The presence of $CaCl_2$ caused a positive shift in the $E^{\circ\prime}$ of ca. 40 mV (Figure 3F and Table 1). Furthermore, if Ca^{2+} ions were present, the SERR signal decreased significantly at potentials more negative than $E^{\circ\prime}$ (Figure 6).

Using time-resolved SERR spectroscopy,[45] the relative contributions of the oxidized and reduced species could be monitored as a function of delay time, after a change in electrode potential. Fitting the data with a mono-exponential decay formula, the heterogeneous electron transfer rate k_{HET} between the heme and the electrode was determined for potential jumps from 100 mV to the corresponding value of $E^{\circ\prime}$ (Figure S1). Under low ionic strength (50 mM) conditions, the rate constant was determined to be 4.6 s^{-1}. Increasing the ionic strength to 200 mM resulted in an almost three times faster heterogeneous electron transfer rate, whereas the presence of $CaCl_2$ only slightly increased the rate constant (Table 1).

2.3. SEIRA Measurements

Electrodes for SEIRA spectroscopy were prepared by casting a nanostructured gold island film on the flat, hydrophobic surface of an Silicon-ATR prism via chemical deposition.[48–49]

PDADMAC-coated Au working electrodes were incubated with a *Mt*CDH solution for 1 h with a total concentration of 2 µM in 1 mL. The enzyme-functionalized Au film on the silicon crystal was incorporated into a electrochemical cell as a working electrode together with a Pt and an Ag|AgCl (3 M KCl) electrode as counter and reference electrodes.

The so derived SEIRA spectrum of immobilized *Mt*CDH revealed the characteristic amide I and amide II bands of a protein (Figure 5A and S2[44]). The second-derivative analysis of spectra allowed us to assign the observed bands in the region between 1630 and 1695 cm^{-1} to the secondary structure elements of the enzyme, mainly exhibiting contributions of α-helices, β-sheets and turns (Figure S2[48]). Moreover, close to the spectral region of amide I and II vibrations we also observe a negative peak, which we assign to the aliphatic C–H bending modes of PDADMAC (Figures 5A,B and S3[50]). It has to be noted that the overlap of the amide I band with the OH bending mode deriving from water molecules fluctuating within the polymer matrix or bound to the Au surface prevents an absolute quantitative analysis of immobilized *Mt*CDH.

Upon the addition of $CaCl_2$ via buffer exchange the overall intensity of the amide I and II bands of *Mt*CDH spectra increased about 10% (Figure 5C). However, the ratio between the two amides bands remains nearly unchanged.

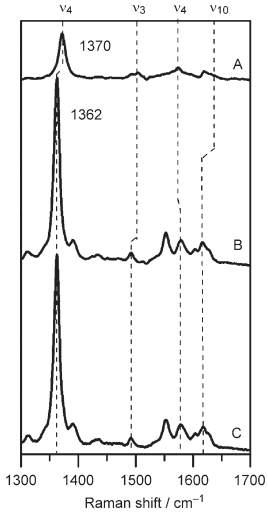

Figure 4. High-frequency SERR spectra of *Mt*CDH immobilized on silver electrodes at A) 200 mV; B) −200 mV; C) at open-circuit potential after addition of 10 mM lactose. The characteristic vibrational modes of heme are indicated by dashed lines.

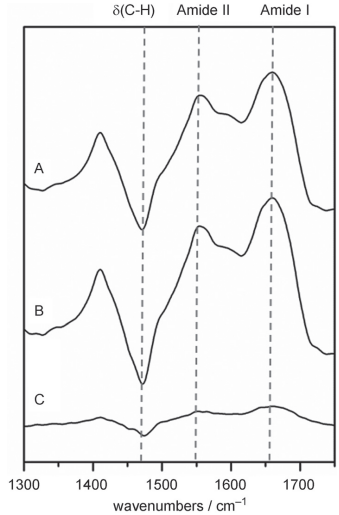

Figure 5. SEIRA spectra of immobilized *Mt*CDH on a gold electrode in: A) 50 mM acetate buffer; B) 50 mM acetate buffer + 10 mM $CaCl_2$. C) SEIRA difference spectrum of B−A. The dashed lines indicate the characteristic band positions of the aliphatic C–H bending modes of PDADMAC and the amide I and II vibrations of the protein backbone.

Characteristic bands assigned to the aliphatic C–H bending and stretching modes of PDADMAC in the SEIRA spectra decreased only slightly (< 5%) upon $CaCl_2$ addition. (Figure S3). Similar changes in forms of decreasing C–H bending intensity upon Ca^{2+} addition is observed in the (difference) spectra with immobilized *Mt*CDH (Figure 5C).

For successive potential-dependent measurements in presence of $CaCl_2$ we observed that the spectral intensity of the amide bands remains almost unchanged (variations ≤ 5%). This observation is clearly different to the one derived from SERR experiments, where the spectral intensity drastically decreased at negative potentials by up to 60% (Figure 6).

Finally the amperometric response of immobilized *Mt*CDH to the addition of lactose and calcium was tested for two different applied potentials. When the potential was set to −54.5 mV (Figure 7A), addition of lactose lead to an increase in current but subsequent addition of 10 mM $CaCl_2$ did not alter this current. Also at an applied potential of −100 mV (Figure 7B) the current increased when lactose was added. However, in this case upon subsequent calcium addition a further current increase was observed.

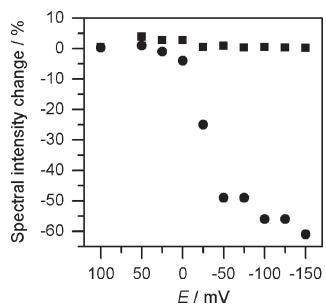

Figure 6. Potential-dependent spectral intensity changes of the heme of *Mt*CDH immobilized on a silver electrode measured with SERRs (●) and the amide I band of *Mt*CDH immobilized on a gold electrode measured with SEIRAS (■). All measurements were done in 50 mM acetate buffer + 10 mM $CaCl_2$.

3. Discussion

No noticeable spectral changes were observed between the RR spectra taken in solution and the SERR spectra obtained after protein immobilization. It is therefore concluded that immobilization of *Mt*CDH on a PDADMAC-coated silver electrode did not change the native structure of the heme environment. Furthermore, the catalytic activity of the enzyme remains intact in the immobilized state as well.

For immobilized *Mt*CDH at high ionic strength conditions $E^{\circ\prime}$ of the heme was located at ca. −76 mV, which is close to the values that have been determined previously: −81 mV for CDH from *Phanerochaete sordida* at pH 5.6, or −75 mV for CDH from *Myriococcum thermophilum* at pH 7.0 measured in a thin-

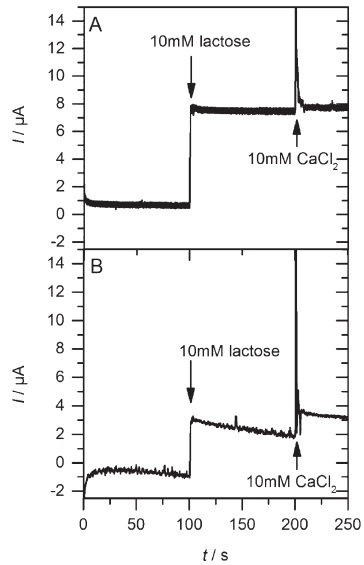

Figure 7. Current of immobilized *Mt*CDH as a response to addition of substrate and Ca^{2+} ions. During the measurement a potential of A) −54 mV and B) −100 mV was applied. The electrode was rotating during the measurement.

capillary-type spectroelectrochemical cell.[35–36] For immobilized *MtCDH*,measured under low ionic strength conditions, a slightly more positive value of $E^{\circ\prime} = -54$ mV was determined. This shift can be explained on the basis of strengthened electrostatic interactions between the positively charged polymer and the surface of the cytochrome domain. We assume that at low ionic strength, the positively charged polymer preferentially stabilizes the ferrous form of the heme, which results in upshifting of $E^{\circ\prime}$.[51] At higher ionic strength (200 mM) the electrostatic interactions of the protein with the polymer are weakened and thus $E^{\circ\prime}$ coincides with its value in solution.

This interpretation is in line with the observed increase in the heterogeneous electron transfer rate under high ionic strength conditions. The weakened electrostatic interactions between the bound protein and electrode surface may ensure a higher mobility of the cytochrome domain such that the enzyme can adopt orientations that are not favored by electrostatic interactions, but which establish a faster electron transfer pathway.[52]

It has to be noted that these observations are similar to those reported in our previous experiments on human sulfite oxidase,[38] an enzyme with a cytochrome b_5 (Cyt b_5) domain similar to CDH. In this work we observed that increasing the ionic strength of a buffer solution led to a higher flexibility of the Cyt b_5 domain on the surface resulting in an increase in $E^{\circ\prime}$, the catalytic current and the heterogeneous electron transfer rate.

The direct comparison of the cyclic voltammograms under turnover conditions and the SERR redox titration under high and low ionic strength conditions shows that in both cases the onset and rise of the catalytic current correlates with the heme redox transition. Although the inflection point of the CV turnover signal was ca. 20 mV more negative than the inflection point of the SERR redox titration (corresponding to $E^{\circ\prime}$ of the heme) it is reasonable to assume that the electron pathway from the catalytic FAD center to the electrode goes via a heme redox transition.

The presence of Ca^{2+} ions, however, had a different influence on CDH activity. Already at a concentration of 10 mM of Ca^{2+} the catalytic turnover signal of the enzyme was shifted to a more negative potential, therefore a simple increase in the enzyme's flexibility, as in the case of Na^{+}, can be ruled out as a possible explanation. Moreover, Ca^{2+} did not induce significant structural changes of the PDADMAC layer, as the overall intensity of the corresponding SEIRA spectra just slightly (< 5%) decreased after addition of Ca^{2+} (Figure S2). A possible explanation of the latter small effect is the increased permeability of the PDADMAC layer, which allows the adsorbed CDH molecules to move slightly closer to the surface without major reorientation.

Noticeable is the decrease in SERR intensity of the heme bands at potentials below $E^{\circ\prime}$ in presence of Ca^{2+}. Such a decrease can be a result of enzyme desorption. However, SERR and SEIRA intensities show a very strong distance dependence that scales roughly with the 12th or 6th power, respectively, of the molecule's distance to the electrode.[53] Therefore the observed signal decrease of the heme bands in the SERR spectra can also be attributed to protein reorientation. Protein desorption or large-scale reorientation can be excluded from the SEIRA data as in this case either a Ca^{2+} induced overall signal decrease or a change in relative intensity of the amide I and II bands should be observed. On the other hand, a slight signal increase (ca. 10%) after Ca^{2+} addition is observed with no significant changes in relative band intensities. Therefore, we suggest that a rather small reorientation of the CYT domain within *Mt*CDH takes place, which is triggered by binding of Ca^{2+} to the enzyme. This hypothesis is supported by the fact that the SERR intensity of the heme can already drastically decrease if the orientation of the heme plane becomes more parallel to the surface.[54] Such a small reorientation would hardly be visible in the SEIRA spectrum. Hence, we conclude that the overall orientation of the entire enzyme remains mostly unchanged and only the relative alignment of the heme plane to the surface is significantly altered.

In a previous study by Schulz et al.[37] a strong effect of Ca^{2+} ions on catalytic activity has been reported for *Mt*CDH modified graphite electrodes. In that work a five times higher catalytic current has been observed. It was proposed that the presence of Ca^{2+} either influences the heterogeneous electron transfer rate or that binding of Ca^{2+} to the enzyme decreases the distance between the FAD and the heme cofactor resulting in a higher intramolecular electron transfer.[37] In our experiments we observe that the heterogeneous electron transfer rate remains almost unchanged, suggesting that the increased

catalytic current of the enzyme does not originate from enhanced electron transfer between the cytochrome domain and the electrode. A change in the distance between the heme and the FAD, however, seems likely, taking into account the proposed CYT domain re-orientation.

The most striking differences between addition of monovalent Na^+ or divalent Ca^{2+} ions can be found when the potential dependence of the catalytic current, recorded by CV, is compared to the heme redox titration, measured with SERRs (Figure 3C). In the electrochemical turnover signal a negative potential shift of the catalytic current is observed upon addition of Ca^{2+}, similar to that measured for high ionic strength conditions. The $E^{\circ\prime}$ of the heme, however, shifts by ca. 30 mV to more positive values. Based on the direction of the shift and the fact that the change in $E^{\circ\prime}$ occurs already at a very low Ca^{2+} ion concentration, we propose that it is $E^{\circ\prime}$ of the heme itself that has changed and not the electrostatic interaction between the protein and the electrode. This redox shift could very likely be induced by binding of Ca^{2+} to the heme propionates that would stabilize the reduced form of the heme similar to what has been reported previously for myoglobin and Mn^{2+} ions.[55]

In the presence of Ca^{2+} the inflection point of the catalytic current is 85 mV more negative than $E^{\circ\prime}$ of the heme. Thus a closed catalytic cycle is already achieved at potentials where the heme domain stays reduced, limiting its ability to accept catalytically created electrons from FAD center. Therefore, we propose that under these conditions an electron pathway from the FAD to the electrode is created that bypasses the heme redox center. We further propose that this alternative electron transfer pathway is responsible for the more negative open-circuit potential measured in the presence of Ca^{2+}.

This hypothesis is supported by the chronoamperometric measurements under turnover conditions (Figure 7): When the applied potential is set equal to the heme redox potential (−54.5 mV) addition of Ca^{2+} ions has no effect on the recorded current as an efficient electron transfer pathway via the heme has been already established at this potential. At an applied potential of −100 mV the catalytic current is generally lower because heme reduction by the electrode competes with catalysis. However, at this potential, the presence of Ca^{2+} ions improves the catalytic performance as it opens up a new pathway for the electrons from the FAD to the electrode. In principle this increased current could also be a result of a faster intramolecular electron transfer. In this case, however, one should have observed increased currents at both potentials upon addition of calcium.

Based on our observations we propose the reaction model depicted in Figure 8. In the oxidized state of the heme, Coulomb interactions stabilize the positively charged iron with negatively charged propionate groups. In the reduced state, this interaction is weakened and the heme propionates are thought to bind the Ca^{2+} ion. The flavin domain exhibits several negatively charged amino acids at the surface that face the CYT domain.[56] One of these amino acids could additionally bind to the Ca^{2+} ion and compensate for the excess charge. Note that this binding would not occur if only monovalent

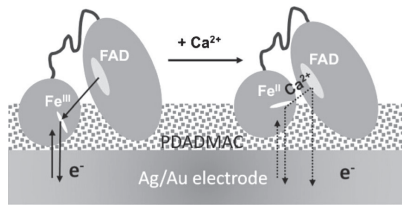

Figure 8. Schematic representation of the proposed changes in orientation and electron transfer mechanism of CDH on PDADMAC coated electrodes upon addition of Ca^{2+} ions.

Na^+ ions are present. The newly formed electrostatic bond between the two domains could alter the electron pathway from the FAD to the electrode. This might in general lead to faster internal electron transfer rate as proposed before.[37] However, the catalytic currents below −50 mV, observed in in this work, do not involve a redox transition of the heme cofactor as they occur at much more negative potentials than its $E^{\circ\prime}$ value. The negatively shifted catalytic activity in the presence of Ca^{2+} would then be attributed to the promotion of an alternative electron transfer pathway between the flavin and the PDADMAC-coated electrode triggered by the Ca^{2+}-induced reorientation. In this scenario the cytochrome domain would function as an anchor for *Mt*CDH to the electrode. Although the electron pathway bypasses the heme at more negative potentials, the presence of the cytochrome domain nevertheless stabilizes the enzyme on the surface in a desirable orientation. Such an stabilizing effect has been observed before for the membrane-bound hydrogenase (MBH) trimer on electrodes[39] where five times higher catalytic activity was observed in the presence of the cytochrome domain that was not involved in the electron transfer pathway.

4. Conclusions

Cellobiose dehydrogenase from *Myriococcum thermophilum* was successfully immobilized on PDADMAC-coated metal electrodes and showed to be catalytically active in presence of lactose as substrate. Comparison of the catalytic currents with SERR spectroscopic monitoring of the heme oxidation state confirmed that the electrocatalytic electron transfer pathway from the catalytic FAD center to the electrode involves the heme as an intermediate electron acceptor. Addition of monovalent Na^+ and divalent Ca^{2+} ions both lead to a negative shift of the catalytic turnover signal. However, the mechanistic origin of this shift was found to be quite different for both types of ions. Higher concentrations of monovalent Na^+ affected the electrostatic interaction between the enzyme and the coated electrode, resulting in a negative shift of the heme redox potential which was still involved in the ET pathway. On the other hand, complementary SERR and SEIRA measurements strongly indicate that divalent Ca^{2+} ions bind directly to the reduced heme propionate groups, leading to a positive shift of the heme redox potential and a reorientation of the

heme plane in respect to the surface. To explain the observed negative shift in the catalytic turnover we propose a scenario where a negatively charged amino acid chain of the flavin domain also binds from the other side to Ca^{2+} to compensate for the excess charge. This local reorientation establishes a new electron transfer pathway to the electrode that does not need the heme iron as intermediate electron acceptor. Electron transfer is thus not limited by the heme redox potential anymore and more negative open-circuit potentials could be achieved this way. Undoubtedly, these findings are of high interest for better understanding the parameters that control the catalytic activity of CDH on electrodes and thus can give valuable suggestions for rational design of enzymatic biofuel cells.

Experimental Section

Chemicals

Poly(diallyldimethylammonium chloride) solution (PDADMAC) was purchased from Sigma Aldrich (Steinheim, Germany). Lactose was provided by Sigma Aldrich and used as a substrate for catalysis. CDH from *Myriococcum thermophilum* was expressed and purified as described previously.[2] As measuring buffers 50 mM and 200 mM acetate at pH 5.5 were used. Since acetate has a pK_a of 4.76, the pH was further adjusted with NaOH to reach the final pH of 5.5. In the further analysis we discuss this condition as the one in presence of monovalent Na^+ ions. Optionally, $CaCl_2$ salt in a concentration between 5–50 mM was added to 50 mM acetate buffer. $CaCl_2$ was provided by Sigma Aldrich. The water used in all experiments was purified by a Millipore system (Bedford, MA, USA).

Electrochemistry and Surface-Enhanced Resonance Raman Spectroscopy

SERR and electrochemical measurements were performed with the CDH-modified silver electrode mounted in a three-electrode electrochemical cell in different buffers. During the measurement the sample was flashed with Argon and rotated constantly. Cyclic voltammograms were recorded using a CH 600E potentiostat in a potential range of −300–100 mV vs. Ag|AgCl (3 M KCl). All experiments were done at room temperature.

Chronoamperometric measurements were recorded using a CH 600E potentiostat. The electrode was rotated applying 360–1140 rpm. 250 μl of lactose and 250 μl of $CaCl_2$ solution was added to the cell to reach final concentrations of 10 mM each.

SERR measurements were performed using the 413 nm laser line of a Krypton Ion Laser (Coherent Innova 300 c). The spectra were recorded at room temperature with a confocal Raman Spectrometer (LabRam HR-800, Jobin Yvon) using 250 μW laser power for continuous wave (CW) measurements and 500 μW laser power for measurements using pulsed laser illumination (PW). CW SERR spectra were accumulated three times 10 s each and averaged, PW SERR spectra were accumulated two times 1 min each and averaged. During the measurement the electrode was rotated to avoid photoreduction.

Surface-Enhanced Infrared Absorption Spectroscopy

SEIRAs measurements were performed with a Kretschmann-ATR configuration using a Silicon crystal under an angle of incidence of 60°. The SEIRA spectra were recorded between 1000–4000 cm^{-1} with a spectral resolution of 4 cm^{-1} on a Bruker Tensor 27 spectrometer, equipped with a liquid-nitrogen-cooled photoconductive MCT detector. 400 scans were co-added for each spectrum. Electrode potentials were applied by a Metrohm PGSTAT 101 Autolab potentiostat under control of NOVA 1.9 software. All potentials in the paper are referred to the Ag|AgCl (3 M KCl) electrode (+0.21 V vs. SHE).

Acknowledgements

The authors would like to thank Uwe Kuhlmann and Peter Hildebrandt for helpful scientific discussions and support. Financial support was given by the DFG (BIG-NSE, Unicat, SFB 1078 Project A1), the "Programm zur Berliner Chancengleichheit (BCP)", the Swedish Research Council (projects 2010–5031, 2014-5908) and by the European Commission ("Chebana" FP7-PITN-GA-2010–264772 and "Bioenergy" FP7-PEOPLE-2013-ITN-607793.

Keywords: cellobiose dehydrogenase · electron transfer · enzyme catalysis · spectroelectrochemistry · surface-enhanced vibrational spectroscopy

[1] G. Henriksson, G. Johansson, G. Pettersson, *J. Biotechnol.* **2000**, *78*, 93–113.
[2] M. Zámocký, C. Schümann, C. Sygmund, J. O'Callaghan, A. D. W. Dobson, R. Ludwig, D. Haltrich, C. K. Peterbauer, *Protein Expr. Purif.* **2008**, *59*, 258–265.
[3] M. D. Cameron, S. D. Aust, *Enzyme Microb. Technol.* **2001**, *28*, 129–138.
[4] R. Ludwig, W. Harreither, F. Tasca, L. Gorton, *ChemPhysChem* **2010**, *11*, 2674–2697.
[5] M. G. Mason, P. Nicholls, M. T. Wilson, *Biochem. Soc. Trans.* **2003**, *31*, 1335–1336.
[6] B. M. Hallberg, T. Bergfors, K. Bäckbro, G. Pettersson, G. Henriksson, C. Divne, *Structure* **2000**, *8*, 79–88.
[7] A. R. Ayers, S. B. Ayers, K.-E. Eriksson, *Eur. J. Biochem.* **1978**, *90*, 171–181.
[8] F. F. Morpeth, *Biochem. J.* **1985**, *228*, 557–564.
[9] W. Bao, S. N. Usha, V. Renganathan, *Arch. Biochem. Biophys.* **1993**, *300*, 705–713.
[10] F. Tasca, L. Gorton, W. Harreither, D. Haltrich, R. Ludwig, G. Nöll, *J. Phys. Chem. C* **2008**, *112*, 9956–9961.
[11] A. Lindgren, L. Gorton, T. Ruzgas, U. Baminger, D. Haltrich, M. Schülein, *J. Electroanal. Chem.* **2001**, *496*, 76–81.
[12] A. Christenson, N. Dimcheva, E. E. Ferapontova, L. Gorton, T. Ruzgas, L. Stoica, S. Shleev, A. I. Yaropolov, D. Haltrich, R. N. F. Thorneley, S. D. Aust, *Electroanalysis* **2004**, *16*, 1074–1092.
[13] L. Hildén, L. Eng, G. Johansson, S. E. Lindqvist, G. Pettersson, *Anal. Biochem.* **2001**, *290*, 245–250.
[14] N. Cruys-Bagger, G. Ren, H. Tatsumi, M. J. Baumann, N. Spodsberg, H. D. Andersen, L. Gorton, K. Borch, P. Westh, *Biotechnol. Bioeng.* **2012**, *109*, 3199–3204.
[15] G. Safina, R. Ludwig, L. Gorton, *Electrochim. Acta* **2010**, *55*, 7690–7695.
[16] L. Stoica, R. Ludwig, D. Haltrich, L. Gorton, *Anal. Chem.* **2006**, *78*, 393–398.
[17] F. Tasca, R. Ludwig, L. Gorton, R. Antiochia, *Sens. Actuators B* **2013**, *177*, 64–69.
[18] N. Glithero, C. Clark, L. Gorton, W. Schuhmann, N. Pasco, *Anal. Bioanal. Chem.* **2013**, *405*, 3791–3799.
[19] F. Tasca, L. Gorton, W. Harreither, D. Haltrich, R. Ludwig, G. Nöll, *J. Phys. Chem. C* **2008**, *112*, 13668–13673.
[20] V. Coman, C. Vaz-Domínguez, R. Ludwig, W. Harreither, D. Haltrich, A. L. De Lacey, T. Ruzgas, L. Gorton, S. Shleev, *Phys. Chem. Chem. Phys.* **2008**, *10*, 6093–6096.

[21] V. Coman, R. Ludwig, W. Harreither, D. Haltrich, L. Gorton, T. Ruzgas, S. Shleev, *Fuel Cells* **2010**, *1*, 9 – 16.
[22] M. Shao, M. N. Zafar, M. Falk, R. Ludwig, C. Sygmund, C. K. Peterbauer, D. A. Guschin, D. MacAodha, P. Ó Conghaile, D. Leech, M. D. Toscano, S. Shleev, W. Schuhmann, L. Gorton, *ChemPhyschem* **2013**, *14*, 2260 – 2269; Conghaile, D. Leech, M. D. Toscano, S. Shleev, W. Schuhmann, L. Gorton, *ChemPhyschem* **2013**, *14*, 2260 – 2269.
[23] W. Harreither, C. Sygmund, M. Augustin, M. Narciso, M. L. Rabinovich, L. Gorton, D. Haltrich, R. Ludwig, *Appl. Environ. Microbiol.* **2011**, *77*, 1804 – 1815.
[24] T. Larsson, A. Lindgren, T. Ruzgas, S.-E. Lindquist, L. Gorton, *J. Electroanal. Chem.* **2000**, *482*, 1 – 10.
[25] F. Tasca, W. Harreither, R. Ludwig, J. J. Gooding, L. Gorton, *Anal. Chem.* **2011**, *83*, 3042 – 3049.
[26] H. Matsumura, R. Ortiz, R. Ludwig, K. Igarashi, M. Samejima, L. Gorton, *Langmuir* **2012**, *28*, 10925 – 10933.
[27] S. C. Feifel, R. Ludwig, L. Gorton, F. Lisdat, *Langmuir* **2012**, *28*, 9189 – 9194.
[28] R. Ludwig, R. Ortiz, C. Schulz, W. Harreither, C. Sygmund, L. Gorton, *Anal. Bioanal. Chem.* **2013**, *405*, 3637 – 3658.
[29] M. T. Meredith, S. D. Minteer, *Annu. Rev. Anal. Chem.* **2012**, *5*, 157 – 179.
[30] M. Sezer, D. Millo, I. M. Weidinger, I. Zebger, P. Hildebrandt, *IUBMB Life* **2012**, *64*, 455 – 464.
[31] D. Leech, P. Kavanagh, W. Schuhmann, *Electrochim. Acta* **2012**, *84*, 223 – 234.
[32] R. Maheshwari, G. Bharadwaj, M. K. Bhat, *Microbiol. Mol. Biol. Rev.* **2000**, *64*, 461 – 488.
[33] W. Harreither, V. Coman, R. Ludwig, D. Haltrich, L. Gorton, *Electroanalysis* **2007**, *19*, 172 – 180.
[34] C. Schulz, R. Ludwig, L. Gorton, *Anal. Chem.* **2014**, *86*, 4256 – 4263.
[35] V. Coman, W. Harreither, R. Ludwig, D. Haltrich, L. Gorton, *Chem. Anal.* **2007**, *52*, 945 – 960.
[36] T. Larsson, A. Lindgren, T. Ruzgas, *Bioelectrochemistry* **2001**, *53*, 243 – 249.
[37] C. Schulz, R. Ludwig, P. O. Micheelsen, M. Silow, M. D. Toscano, L. Gorton, *Electrochem. commun.* **2012**, *17*, 71 – 74.
[38] M. Sezer, R. Spricigo, T. Utesch, D. Millo, S. Leimkuehler, M. A. Mroginski, U. Wollenberger, P. Hildebrandt, I. M. Weidinger, *Phys. Chem. Chem. Phys.* **2010**, *12*, 7894 – 7903.
[39] M. Sezer, S. Frielingsdorf, D. Millo, N. Heidary, T. Utesch, M.-A. Mroginski, B. Friedrich, P. Hildebrandt, I. Zebger, I. M. Weidinger, *J. Phys. Chem. B* **2011**, *115*, 10368 – 10374.
[40] M. Sezer, A. Santos, P. Kielb, T. Pinto, L. O. Martins, S. Todorovic, *Biochemistry* **2013**, *52*, 3074 – 3084.
[41] J. Hrabakova, K. Ataka, J. Heberle, P. Hildebrandt, D. H. Murgida, *Phys. Chem. Chem. Phys.* **2006**, *8*, 759 – 766.
[42] P. A. Ash, K. A. Vincent, *Chem. Commun.* **2012**, *48*, 1400 – 1409.
[43] D. Millo, P. Hildebrandt, M.-E. Pandelia, W. Lubitz, I. Zebger, *Angew. Chem. Int. Ed.* **2011**, *50*, 2632 – 2634; *Angew. Chem.* **2011**, *123*, 2680 – 2683.
[44] N. Wisitruangsakul, O. Lenz, M. Ludwig, B. Friedrich, F. Lendzian, P. Hildebrandt, I. Zebger, *Angew. Chem. Int. Ed.* **2009**, *48*, 611 – 613; *Angew. Chem.* **2009**, *121*, 621 – 623.
[45] H. Wackerbarth, U. Klar, W. Gunther, P. Hildebrandt, *Appl. Spectrosc.* **1999**, *53*, 283 – 291.
[46] P. Knöös, C. Schulz, L. Piculell, R. Ludwig, L. Gorton, M. Wahlgren, *Int. J. Pharm.* **2014**, *468*, 121 – 132.
[47] J. D. Cohen, W. Bao, V. Renganathan, S. S. Subramaniam, T. M. Loehr, *Arch. Biochem. Biophys.* **1997**, *341*, 321 – 328.
[48] N. Wisitruangsakul, I. Zebger, K. H. Ly, D. H. Murgida, S. Ekgasit, P. Hildebrandt, *Phys. Chem. Chem. Phys.* **2008**, *10*, 5276 – 5286.
[49] H. Yue, D. H. Waldeck, J. Petrović, R. A. Clark, *J. Phys. Chem. B* **2006**, *110*, 5062 – 5072.
[50] S. Owusu-Nkwantabisah, M. Gammana, C. P. Tripp, *Langmuir* **2014**, *30*, 11696 – 11703.
[51] J. Petrović, R. A. Clark, H. Yue, D. H. Waldeck, E. F. Bowden, *Langmuir* **2005**, *21*, 6308 – 6316.
[52] D. Alvarez-Paggi, W. Meister, U. Kuhlmann, I. Weidinger, K. Tenger, L. Zimányi, G. Rákhely, P. Hildebrandt, D. H. Murgida, *J. Phys. Chem. B* **2013**, *117*, 6061 – 6068.
[53] F. Siebert, P. Hildebrandt *Vibrational Spectroscopy in Life Science*, Wiley-VCH, Weinheim, **2008**, pp. 38 – 60.
[54] A. Kranich, H. K. Ly, P. Hildebrandt, D. H. Murgida, *JACS* **2008**, *130*, 9844 – 9848.
[55] C. L. Hunter, R. Maurus, M. R. Mauk, H. Lee, E. L. Raven, H. Tong, N. Nguyen, M. Smith, G. D. Brayer, G. Mauk, *Proc. Natl. Acad. Sci. USA* **2003**, *100*, 3647 – 3652.
[56] B. M. Hallberg, G. Henriksson, G. Pettersson, C. Divne, *J. Mol. Biol.* **2002**, *315*, 421 – 34.

Received: February 9, 2015
Revised: March 12, 2015
Published online on ■■ ▮▮, 2015

*P. Kielb, M. Sezer, S. Katz, F. Lopez, C. Schulz, L. Gorton, R. Ludwig, U. Wollenberger, I. Zebger, I. M. Weidinger**

■■ – ■■

Spectroscopic Observation of Calcium-Induced Reorientation of Cellobiose Dehydrogenase Immobilized on Electrodes and its Effect on Electrocatalytic Activity

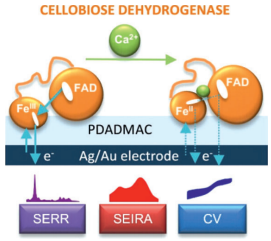

A new road: Electrochemistry combined with surface enhanced vibrational (SERR and SEIRA) spectroscopy are employed to obtain mechanistic insight into the catalytic performance of cellobiose dehydrodegane (*Mt*CDH) immobilized on noble metal electrodes in the presence of Ca^{2+} ions. The results show induced reorientation of the enzyme on the electrode, which leads to a new electron transfer pathway between the protein and the electrode.

Paper VIII

Direct Electron Transfer of Cellobiose Dehydrogenase on Positively Charged Polyethyleneimine Gold Nanoparticles

Mojtaba Tavahodi [†, ‡], Roberto Ortiz [‡], Christopher Schulz [‡], Ali Ekhtiari [‡], Roland Ludwig [§], Behzad Haghighi [†], Lo Gorton * [‡]

† Department of Chemistry, Institute for Advanced Studies in Basic Sciences, P.O. Box 45195-1159, Gava Zang, Zanjan, Iran.

‡ Department of Analytical Chemistry/Biochemistry and Structural Biology, Lund University P.O. Box 124, SE-22100 Lund, Sweden.

§ Food Biotechnology Laboratory, Department of Food Sciences and Technology, BOKU-University of Natural Resources and Life Sciences Vienna, Muthgasse 18, A-1190 Wien, Austria.

ABSTRACT

Efficient conjugation between biomolecules and electrode materials is one of the main challenges in the field of biosensors. Cellobiose dehydrogenase (CDH) is a monomeric enzyme, which carries a flavin adenine dinucleotide (FAD) containing dehydrogenase domain (DH) and a *b*-type heme containing cytochrome domain (CYT) connected by linker region. Here we report on the development of a lactose biosensor, based on direct electron transfer (DET) from CDH from *Phanerochaete sordida* (*Ps*CDH) electrostatically attached onto polyethyleneimine gold nanoparticles (PEI@AuNPs) used to cover a conventional solid gold disk electrode. PEI@AuNPs were synthesized in aqueous solution using PEI as reducing agent for the Au(III) and as stabilizer for the nanoparticles. The heterogeneous electron transfer (ET) rate (k_s) for the redox reaction of immobilized *Ps*CDH at the modified electrodes was calculated based on the Laviron theory and was found to be $39.6 \pm 2.5\ s^{-1}$. The proposed lactose biosensor exhibits good long term stability as well as high and reproducible sensitivity to lactose with a response time less than 5 s and a linear range from 1 to 100 μM.

1. Introduction

In the past decade, the establishment of efficient ET communication between redox enzymes and various electrode materials has been one of the major challenges in the field of bioelectrochemistry both for understanding the structures and mechanism of different enzymatic reactions and for developing bioelectronic devices such as biosensors and biofuel cells[1]. However, because of unfavorable orientation of the biomolecules at the surface of the electrodes, the enzyme molecules may exhibit a rather low heterogeneous electron transfer (ET) rate, k_s, although their ET rate is fast in biological systems[2].

Recently, redox enzymes such as flavocytochromes, quinohemoproteins, and multicopper oxidases have received much attention in the field of bioelectronics device, because these multidomain enzymes have both a catalytic domain and a separate ET domain containing another cofactor than the catalytic domain[3]. The ET domain can act as a built-in mediator connecting the active site of the catalytic domain with the surface of the electrodes via the ET domain. Cellobiose dehydrogenase (EC 1.1.99.18, CDH) is a monomeric enzymes, which consists of a flavin adenine dinucleotide (FAD) containing dehydrogenase domain (DH_{CDH}) and a *b*-type heme containing cytochrome domain (CYT_{CDH}) connected by a flexible linker region[4]. Depending on the origin, CDHs show varying substrate specificities, but in general, they all oxidize β-1.4-linked di- and oligosaccharides such as cellobiose, cellodextrins and lactose. In the catalytic cycle, two electrons are donated from the substrate to the oxidized FAD cofactor of DH_{CDH} and will convert FAD into its fully reduced state. In the absence of any electron acceptor, the electrons can be sequentially transferred from the FAD to the *b*-type heme cofactor in the

smaller cytochrome domain (CYT_{CDH}) by an intramolecular electron transfer (IET) reaction, which can act as a mediator between DH_{CDH} and an electrode[5].

To enhance the efficiency of direct electron transfer (DET) of redox enzymes, nanostructure materials such as various kinds of metal nanoparticles[6], single and multiwall carbon nanotubes[7] and mesoporous materials[8] were included between the redox centers of the enzyme and the electrode's surface leading to the advantage of having a large surface area for protein immobilization. The conjugation of enzymes onto surfaces modified with nanomaterials having the opposite charge of the enzyme have been shown to be helpful for the fabrication of biosensors[9]. Some of the approaches for providing cationic charges on metals and metal oxide nanoparticles, which include silica, iron oxide, silver and gold nanoparticles, typically involve surface coating with cationic polymers (e.g., polyethyleneimine, polylysine, and polyallylamine hydrochloride) through either electrostatic or covalent conjugation[10]. PEI is a synthetic polycation consisting of a high density of cationic groups such as secondary and tertiary amines, which make PEI completely miscible with water at room temperature. PEI is often used in biosensor constructions due to its positive charges at neutral pH and adhesive properties[11]. Recently, Schulz *et al.* have shown that the catalytic currents from lactose oxidation by spectroscopic graphite electrodes modified with CDH from *Myriococcum thermophilum* (*Mt*CDH) could be highly increased through modification of the electrodes with branched PEI[12]. It is suggested that the increase in the catalytic currents could be accomplished from either facilitated IET due to adjustment of distance between the CTY_{CDH} and DH_{CDH} domains through positive charges of the polycation or by increasing the surface loading as a result of premodification of surface with PEI. Matsumura *et al.* have also reported DET reaction of *Phanerochaete chrysosporium* CDH (*Pc*CDH) covalently immobilized on AuNPs electrodes.

They have shown that the catalytic current density of *Pc*CDH/AuNPs electrode was notably enhanced compared with those electrodes without modification[6d].

In this study, we report on combining our previous observations to improve the DET reaction of *Ps*CDH electrostatically attached to gold electrodes premodified with positively charged polyethyleneimine coated AuNPs. The AuNPs were synthesized in aqueous solution using PEI as reducing agent for the metal precursor and as stabilizer for the final NPs. PEI has recently been shown to be beneficial for the construction of CDH based biosensors by enhancing the surface load of CDH and possibly the rate of the IET within CDH[12]. After immobilization of *Ps*CDH, the biosensor exhibited clear, well defined redox waves of the heme *b* of CYT_{CDH}. The long term stability and catalytic current density of the proposed biosensor using lactose as substrate was drastically increased compared with unmodified solid Au electrodes.

2. Experimental Section

Reagents and Equipment. The metal precursor $HAuCl_4$, branched polyethylenimine (PEI, 50% w/v in H_2O, M_n~60 000, M_w~750 000), β-lactose, 4-morpholineethanesulfonic acid (MES) and tris(hydroxymethyl)aminomethane (TRIS) were obtained from Sigma Aldrich Chemicals (Steinheim, Germany). Acetic acid (100%) and sodium hydroxide solution (50%) were purchased from Merck (Darmstadt, Germany). All chemicals were of analytical reagent grade and were used without further purification. Milli-Q water (Millipore 18.2MΩ cm, Millipore, Bedford, MA, USA) was used in all experiments.

Cyclic voltammetry studies were performed using a electrochemical analyzer model BAS 100 (Bioanalytical Systems, West Lafayette, IN, USA) with a conventional three electrode setup, in which a *Ps*CDH/PEI@AuNPs/Au electrode, an Ag|AgCl (saturated KCl) and a platinum foil

served as the working, reference and auxiliary electrodes, respectively. The experiments were performed at a scan rate of 1 mV s^{-1} in a N_2-saturated acetate buffer solution (5 mM, pH = 4.5). For amperometric studies a wall jet cell with three electrodes connected to a potentiostat (Zäta Elektronik, Höör, Sweden) was used containing a modified Au electrode as working electrode, Ag|AgCl (0.1 M KCl) as reference electrode and a Pt wire as auxiliary electrode. 5 mM acetate buffer (pH 4.50) was used as carrier buffer with a constant flow rate of 0.5 mL min^{-1} by a peristaltic pump (Minipuls 2, Gilson, Villier-le-Bel, France). An electrically controlled six-port valve (LabPRO, Rheodyne, USA) with a 50 µl injection loop was used for the injection of analytes into the carrier flow.

The hydrodynamic radius of the AuNPs was measured using a Nano Zetasizer equipped with a He–Ne laser (λ=633 nm) and a digital autocorrelator at room temperature.

Solutions and enzymes. The protein concentration of *Ps*CDH was calculated photometrically by using an extinction coefficient of ε_{280} = 141750 M^{-1} cm^{-1} determined from the amino acid sequence (ABS45567.2). A stock solution of lactose (500 mM) was prepared using Milli-Q water and stored at 4˚C when not in use. The lactose stock solution was allowed to mutarotate for at least 24 h before use. The running buffers were 5 mM sodium acetate (pH 3.0-6.5), 5 mM MES (pH 6.0-7.0) and 5 mM TRIS (pH 6.5-9.0).

Synthesis of gold nanoparticles. 0.01 g of branched PEI was dissolved completely in 100 mL of distilled water for an hour. Then, $HAuCl_4$ was dissolved in the aqueous solution of PEI to a final concentration of 2 mM under magnetic stirring for another hour. The mixture was stirred vigorously at room temperature for 24 h for complete reduction. In this case, PEI played a role of a mild reductant so that a slow color change from yellow to red was observed, indicating the formation of AuNPs. Then, the reacted mixture was dialyzed using a membrane with a molecular

weight cut off of 12 kDa with repeated water exchanges for 1 day to eliminate remaining unreacted chemicals.

Preparation of *Ps*CDH immobilized on PEI@AuNPs modified gold electrodes. The surface of polycrystalline gold disk electrodes (BAS, West Lafayette, IN, USA, d = 0.016 cm) was mechanically polished on a Microcloth (Buehler, Lake Bluff, IL, USA) in aqueous alumina FF slurry (d=0.1 μm, Struers, Copenhagen, Denmark), then thoroughly rinsed with Milli-Q water, followed by ultrasonication for 5 min in Milli-Q water. The electrodes were electrochemically cleaned by cycling in 0.5 M H_2SO_4, with a scan rate of 100 mV s^{-1} between -300 and -1700 mV vs Ag|AgCl (saturated KCl) for 20 scans and finally rinsed with Milli-Q water[13]. To obtain AuNPs modified solid gold electrodes, a volume of 5 μl of the concentrated AuNP solution was cast on the surface of the clean gold electrode and dried at room temperature. Modification of the electrode with *Ps*CDH was made by trapping a 3 μl droplet of the enzyme solution (10 mg ml^{-1}) between the gold electrode surface and a permselective dialysis membrane (MWCO < 12 000−14 000 Da, Spectrum Laboratories, Broadwick, CA, USA). The prepared electrodes were immersed into 50 mM acetate buffer (pH 4.5) for 1 h, and then the membrane was removed, followed by rinsing with buffer.

3. Results and Discussion

Preparation and characterization of gold nanoparticles. An appealing feature of AuNPs is the possibility to change their properties by varying the size of the core as well as the surface modification with suitable functional molecules. Although the surface of AuNPs can be easily functionalized with a polymer shell by layer-by-layer assembly of certain polyelectrolytes[14], in this work we utilize a one-step synthesis method developed recently by Sun et al., who used PEI

as both the reducing agent and stabilizer to prepare PEI-capped AuNPs[9a, 10a, 15]. After directly mixing the metal precursor solution with PEI at room temperature, the color of the reaction mixture turns to dark red after 24 h, indicating the formation of AuNPs. As shown in Fig. 1a, the UV-vis absorption maximum of the resulting AuNPs appeared at 527 nm due to the surface plasmon resonance (SPR) of the AuNPs, which confirmed the formation of AuNPs-PEI[15-16]. The diameter of the prepared, spherical AuNPs-PEI was 9±2 nm measured using transmission electron microscopy (TEM) images, Fig. 1b. The hydrodynamic diameter determined by dynamic light scattering (DLS), 11±1 nm, is larger. Due to the fact that TEM images display only the metal core, it can be assumed that the AuNPs are surrounded by a polyethyleneimine shell of around 2–3 nm.

Cyclic voltammograms of Au and PEI@AuNPs/Au electrodes were recorded in 0.5 M H_2SO_4 solution at a scan rate of 100 mVs^{-1}. The CV showed (Fig. 1C) the characteristic current features for Au reduction (at 0.83 V) and Au oxide formation (at 1.3 V)[17]. The responses corresponding to the so-called surface redox reaction of gold were observed. It can be seen that the effective surface area of the PEI@AuNPs/Au electrodes is about 30 times higher than that of unmodified gold electrodes, which is due to the modification of AuNPs onto the Au electrodes, leading to the increase in surface area of the modified electrodes.

Electrochemistry of *Ps*CDH on PEI@AuNPs modified gold electrodes. To study the DET of *Ps*CDH electrostatically bound to PEI@AuNPs modified gold electrodes, we initially investigated CVs obtained for the enzyme in the absence and in the presence of the PEI-capped AuNPs. As shown in Fig. 2(A), in the presence of PEI@AuNPs, the *Ps*CDH modified electrode exhibits clear well-defined and reversible redox waves in acetate buffer (pH 4.5), corresponding to the DET communication between the CYT_{CDH} domain of immobilized *Ps*CDH and the

AuNPs[6d, 18]. No significant waves of the heme of the CYT_{CDH} were observed in the absence of the PEI@AuNPs (Fig. 1A). The presence of clear redox waves for CDH when using the PEI@AuNPs could be explained by an increased number/surface concentration of well oriented CDH molecules immobilized on the electrode surface being capable of efficient DET, as previously suggested[19]. Electrostatic interactions between the positively charged PEI@AuNPs and negatively charged *Ps*CDH (pI 4.1) at pH 4.5 may play a major role. On the other hand, the surface modification of the solid Au electrode with the NPs created a really porous structure. The effective surface area of the AuNPs modified electrode was enhanced 30 times in comparison to the geometric surface of the bare electrode estimated from CVs of Au and PEI@AuNPs/Au electrodes in 0.5 M H_2SO_4 solution (Fig. 1C). The effective immobilization of enzyme and the porosity of the AuNP coated surface are combined to assist the progress of DET communication between the heme *b* group of the enzyme and surface of the electrode. The formal potential (E°') of the heme *b* group of CYT_{CDH}, evaluated as the midpoint of the oxidation and reduction peak potentials, was approximately -25 mV vs. Ag|AgCl (sat. KCl), which is consistent with previously reported values for *Pc*CDH in solution[5b]. The peak-to-peak potential separation (ΔE_p) and the ratio of the cathodic to anodic peak currents were approximately 55 mV and 1, respectively.

Figure 2B presents typical CVs for the *Ps*CDH modified PEI@AuNPs gold electrodes in an acetate buffer solution (5 mM, pH 4.5) at different scan rates. The anodic and cathodic peak currents were linearly proportional versus the scan rate, υ, in the range of 1-300 mVs^{-1} (Fig. 2D), indicating that this was a surface controlled electrochemical behavior.

Further analysis of the CVs yields the apparent heterogeneous electron transfer rate constant (k_s) for the redox reaction of the immobilized CDH with the modified PEI@AuNPs electrode

using Laviron's theory[20]. The graph of peak potentials as a function of the logarithm of scan rate (Fig. 2C) shows a typical trumpet shape, in which at high scan rates the peak potentials separate from the E°' value with a slope of 120 mV/log unit due to limitation of charge transfer kinetics. The so determined α value was 0.55. The k_s could also be calculated based on the Laviron equation (1), which was 39.6 (± 2.5) s^{-1} (υ changed from 50 to 300 mV s^{-1}).

$$\log ks = \alpha \log(1-\alpha) + (1-\alpha)\log(RT/nFv) - \alpha(1-\alpha)nF\Delta Ep/2.3RT \quad (1)$$

The k_s at modified PEI@AuNPs electrode is higher compared with the intramolecular ET rate between the DH_{CDH} and the CYT_{CDH} domains (30 s^{-1}), which has been suggested to be the rate-limiting step in the overall *Pc*CDH reaction[21]. Thus, the maximum electrocatalytic current would be limited by the intrinsic enzymatic dehydrogenase activity on the electrodes.

Electrocatalytic behavior of *Ps*CDH modified PEI@AuNP gold electrodes. As mentioned above, CDH is a monomeric enzyme, which carries a flavin adenine dinucleotide (FAD) containing dehydrogenase domain DH_{CDH} and a *b*-type heme containing CYT_{CDH}. In the catalytic cycle, the DH_{CDH} catalyzes the dehydrogenation of cellobiose, cello-oligosaccharides, and lactose to their corresponding δ-lactones followed by intermolecular electron transfer (IET) from DH_{CDH} to CYT_{CDH}. In this work, lactose was chosen as substrate because lactose does not exhibit substrate inhibition for *Ps*CDH in contrast to the natural substrate, cellobiose[22]. Figure 3 presents the CVs of the *Ps*CDH modified PEI@AuNPs gold electrodes in acetate buffer solution containing different concentrations of lactose from 0.5 to 5 mM. In the absence of substrate, the redox peaks of the heme *b* group can be observed at around -20 mV. After addition of lactose, the catalytic currents appear at the beginning of the anodic peak of heme *b* of the CYT_{CDH}, indicating that the CYT_{CDH} is responsible for electro-chemical communication between *Ps*CDH

and the electrode so that the oxidation of lactose can be followed and registered. The electrocatalytic current density is around 10 μA cm^{-2} for 5 mM lactose in acetate buffer.

Flow injection analysis. Flow injection measurements were performed with *Ps*CDH modified PEI@AuNPs gold electrodes mounted in a flow through electrochemical cell coupled to a single line flow injection analysis (FIA) system. The applied potential for all *Ps*CDH modified electrodes was 250 mV vs. a Ag|AgCl (0.1 M KCl) reference electrode to guarantee that the ET from *Ps*CDH bound to the PEI@AuNPs modified gold electrodes is not the kinetically limiting step. The peak response is fast with around 3 s, mainly because of the good communication between the *Ps*CDH and the surface of the electrodes.

A calibration curve for the *Ps*CDH modified PEI@AuNP gold electrodes done with different concentrations of lactose in acetate buffer (5 mM, pH 4.5) is shown in Fig. 4. The calibration curve was linear in the concentration range of 1-100 μM, with a correlation coefficient (R^2) of 0.99. The detection limit was found to be 0.330 μM (S/N = 3). The relative standard deviation for repeated measurements (n = 6) for 5 mM lactose was 4.46%. As shown in Table 1, the analytical characteristics of some reported lactose biosensors are summarized and compared with those obtained in this work using *Ps*CDH/PEI@AuNPs solid gold electrode. The results confirmed that the proposed biosensor has good performing properties such as low detection limit, fast response and acceptable linear rang due to the enhancement of the electroactive surface area as well as excellent communication between the *Ps*CDH molecules and the positively charged AuNPs.

The apparent Michaelis-Menten constant (K_M^{app}) was estimated by fitting the calibration curves illustrated in Fig. 4 to the Michaelis-Menten equation. The observed K_M^{app} value of *Ps*CDH for lactose was determined to be 0.2 mM, which was smaller than that obtained when immobilized

onto aryl diazonium modified single wall carbon nanotubes deposited on a glassy carbon electrode (0.7 mM) [23,24].

Figure 5 shows the dependence of the catalytic currents gained from the oxidation of lactose by the *Ps*CDH modified PEI@AuNP gold electrodes versus the solution pH, which was determined amperometrically using the FIA system. The pH optimum was found to be at pH 4.0, which was similar to previous reported results[24].

Stability Measurements. The stability of the *Ps*CDH modified PEI@AuNP gold electrodes was measured using the amperometric flow injection analysis system by measuring the decrease in the electrocatalytic currents during successive injections of lactose. The catalytic currents decreased only by 5.3% during continuous injections for 24 h. Attractive electrostatic interactions between the negative residue of *Ps*CDH and positive shell around the PEI@AuNPs seem to prevent the release of the enzyme from the surface of PEI@AuNPs electrodes and support the long term stability of the biosensors.

Conclusion

We have developed an approach for lactose biosensing, based on DET of an electrostatically attached *Ps*CDH onto gold electrodes premodified with PEI capped gold nanoparticles synthesized in aqueous solution using PEI as reducing agent for the Au(III) and as stabilizer for the nanoparticles. Basic characterization of the AuNPs by TEM and DLS reveal a gold core particle diameter of 9 ± 2 nm capped by a polyethyleneimine shell of around 2–3 nm.

Clear, well defined redox waves due to the electrochemical communication with the CYT_{CDH} domain of *Ps*CDH was observed in CV when *Ps*CDH was electrostatically attached on the surface of the PEI@AuNP modified gold electrodes, whereas the corresponding *Ps*CDH modified polycrystalline gold electrodes lacking the PEI@AuNP did not show any redox waves.

The heterogeneous ET rate (k_s) could also be estimated based on the Laviron approach and was found to be 39.6 (± 2.5) s^{-1}.

The proposed lactose biosensor presented a number of attractive features such as a wide linear range for the detection of lactose between 1 – 100 μM, a fast current response and an excellent long term stability with only a 5% signal loss in 24h. These features can be attributed to a higher number of well oriented enzyme molecules immobilised on the PEI@AuNP modified electrode surface due to electrostatic interactions between the negatively charged *Ps*CDH molecules and the positively charged, PEI capped gold nanoparticles.

ACKNOWLEDGMENTS

The authors would like to thank Gunnel Karlsson (Lund University, Sweden) for taking the TEM pictures. The authors thank the following agencies for financial support:

Institute for Advanced Studies in Basic Sciences (IASBS, Grant Number G2014IASBS119),

1. (a) Sassolas, A.; Blum, L. J.; Leca-Bouvier, B. D., Immobilization strategies to develop enzymatic biosensors. *Biotechnology Advances* **2012,** *30* (3), 489-511; (b) Talbert, J. N.; Goddard, J. M., Enzymes on material surfaces. *Colloids and Surfaces B: Biointerfaces* **2012,** *93* (0), 8-19; (c) Willner, I.; Yan, Y. M.; Willner, B.; Tel-Vered, R., Integrated Enzyme-Based Biofuel Cells–A Review. *Fuel Cells* **2009,** *9* (1), 7-24.

2. Frew, J. E.; Hill, H. A. O., Direct and indirect electron transfer between electrodes and redox proteins. *European Journal of Biochemistry* **1988,** *172* (2), 261-269.

3. (a) Gorton, L.; Lindgren, A.; Larsson, T.; Munteanu, F. D.; Ruzgas, T.; Gazaryan, I., Direct electron transfer between heme-containing enzymes and electrodes as basis for third generation biosensors. *Analytica Chimica Acta* **1999,** *400* (1–3), 91-108; (b) Shleev, S.; Tkac, J.; Christenson, A.; Ruzgas, T.; Yaropolov, A. I.; Whittaker, J. W.; Gorton, L., Direct electron transfer between copper-containing proteins and electrodes. *Biosensors and Bioelectronics* **2005,** *20* (12), 2517-2554; (c) Cracknell, J. A.; Vincent, K. A.; Armstrong, F. A., Enzymes as Working or Inspirational Electrocatalysts for Fuel Cells and Electrolysis. *Chemical Reviews* **2008,** *108* (7), 2439-2461; (d) Stoica, L.; Dimcheva, N.; Haltrich, D.; Ruzgas, T.; Gorton, L., Electrochemical investigation of cellobiose dehydrogenase from new fungal sources on Au electrodes. *Biosensors and Bioelectronics* **2005,** *20* (10), 2010-2018.

4. (a) Henriksson, G.; Johansson, G.; Pettersson, G., A critical review of cellobiose dehydrogenases. *Journal of Biotechnology* **2000,** *78* (2), 93-113; (b) Ludwig, R.; Salamon, A.; Varga, J.; Zámocky, M.; Peterbauer, C. K.; Kulbe, K. D.; Haltrich, D., Characterisation of cellobiose dehydrogenases from the white-rot fungi Trametes pubescens and Trametes villosa. *Applied Microbiology and Biotechnology* **2004,** *64* (2), 213-222.
5. (a) Ludwig, R.; Harreither, W.; Tasca, F.; Gorton, L., Cellobiose Dehydrogenase: A Versatile Catalyst for Electrochemical Applications. *ChemPhysChem* **2010,** *11* (13), 2674-2697; (b) Stoica, L.; Ludwig, R.; Haltrich, D.; Gorton, L., Third-Generation Biosensor for Lactose Based on Newly Discovered Cellobiose Dehydrogenase. *Analytical Chemistry* **2005,** *78* (2), 393-398.
6. (a) Zayats, M.; Katz, E.; Baron, R.; Willner, I., Reconstitution of Apo-Glucose Dehydrogenase on Pyrroloquinoline Quinone-Functionalized Au Nanoparticles Yields an Electrically Contacted Biocatalyst. *Journal of the American Chemical Society* **2005,** *127* (35), 12400-12406; (b) Malel, E.; Ludwig, R.; Gorton, L.; Mandler, D., Localized Deposition of Au Nanoparticles by Direct Electron Transfer through Cellobiose Dehydrogenase. *Chemistry – A European Journal* **2010,** *16* (38), 11697-11706; (c) Lu, J.; Do, I.; Drzal, L. T.; Worden, R. M.; Lee, I., Nanometal-Decorated Exfoliated Graphite Nanoplatelet Based Glucose Biosensors with High Sensitivity and Fast Response. *ACS Nano* **2008,** *2* (9), 1825-1832; (d) Matsumura, H.; Ortiz, R.; Ludwig, R.; Igarashi, K.; Samejima, M.; Gorton, L., Direct Electrochemistry of Phanerochaete chrysosporium Cellobiose Dehydrogenase Covalently Attached onto Gold Nanoparticle Modified Solid Gold Electrodes. *Langmuir* **2012,** *28* (29), 10925-10933.
7. (a) Joshi, P. P.; Merchant, S. A.; Wang, Y.; Schmidtke, D. W., Amperometric Biosensors Based on Redox Polymer−Carbon Nanotube−Enzyme Composites. *Analytical Chemistry* **2005,** *77* (10), 3183-3188; (b) Li, W.-S.; Hou, P.-X.; Liu, C.; Sun, D.-M.; Yuan, J.; Zhao, S.-Y.; Yin, L.-C.; Cong, H.; Cheng, H.-M., High-Quality, Highly Concentrated Semiconducting Single-Wall Carbon Nanotubes for Use in Field Effect Transistors and Biosensors. *ACS Nano* **2013,** *7* (8), 6831-6839; (c) Lu, X.; Cheng, H.; Huang, P.; Yang, L.; Yu, P.; Mao, L., Hybridization of Bioelectrochemically Functional Infinite Coordination Polymer Nanoparticles with Carbon Nanotubes for Highly Sensitive and Selective In Vivo Electrochemical Monitoring. *Analytical Chemistry* **2013,** *85* (8), 4007-4013.
8. (a) Feng, J.-J.; Xu, J.-J.; Chen, H.-Y., Direct electron transfer and electrocatalysis of hemoglobin adsorbed on mesoporous carbon through layer-by-layer assembly. *Biosensors and Bioelectronics* **2007,** *22* (8), 1618-1624; (b) Asefa, T.; Duncan, C. T.; Sharma, K. K., Recent advances in nanostructured chemosensors and biosensors. *Analyst* **2009,** *134* (10), 1980-1990.
9. (a) Frasca, S.; Rojas, O.; Salewski, J.; Neumann, B.; Stiba, K.; Weidinger, I. M.; Tiersch, B.; Leimkühler, S.; Koetz, J.; Wollenberger, U., Human sulfite oxidase electrochemistry on gold nanoparticles modified electrode. *Bioelectrochemistry* **2012,** *87* (0), 33-41; (b) Oaew, S.; Charlermroj, R.; Pattarakankul, T.; Karoonuthaisiri, N., Gold nanoparticles/horseradish peroxidase encapsulated polyelectrolyte nanocapsule for signal amplification in Listeria monocytogenes detection. *Biosensors and Bioelectronics* **2012,** *34* (1), 238-243; (c) Feifel, S. C.; Ludwig, R.; Gorton, L.; Lisdat, F., Catalytically Active Silica Nanoparticle-Based Supramolecular Architectures of Two Proteins – Cellobiose Dehydrogenase and Cytochrome c on Electrodes. *Langmuir* **2012,** *28* (25), 9189-9194.
10. (a) Song, W.-J.; Du, J.-Z.; Sun, T.-M.; Zhang, P.-Z.; Wang, J., Gold Nanoparticles Capped with Polyethyleneimine for Enhanced siRNA Delivery. *Small* **2010,** *6* (2), 239-246; (b) Marsich, L.; Bonifacio, A.; Mandal, S.; Krol, S.; Beleites, C.; Sergo, V., Poly-l-lysine-Coated

Silver Nanoparticles as Positively Charged Substrates for Surface-Enhanced Raman Scattering. *Langmuir* **2012,** *28* (37), 13166-13171; (c) Schweiger, C.; Pietzonka, C.; Heverhagen, J.; Kissel, T., Novel magnetic iron oxide nanoparticles coated with poly(ethylene imine)-g-poly(ethylene glycol) for potential biomedical application: Synthesis, stability, cytotoxicity and MR imaging. *International Journal of Pharmaceutics* **2011,** *408* (1–2), 130-137; (d) Xia, T.; Kovochich, M.; Liong, M.; Meng, H.; Kabehie, S.; George, S.; Zink, J. I.; Nel, A. E., Polyethyleneimine Coating Enhances the Cellular Uptake of Mesoporous Silica Nanoparticles and Allows Safe Delivery of siRNA and DNA Constructs. *ACS Nano* **2009,** *3* (10), 3273-3286; (e) Li, Z.; Barnes, J. C.; Bosoy, A.; Stoddart, J. F.; Zink, J. I., Mesoporous silica nanoparticles in biomedical applications. *Chemical Society Reviews* **2012,** *41* (7), 2590-2605; (f) Ho Youk, J., Preparation of gold nanoparticles on poly(methyl methacrylate) nanospheres with surface-grafted poly(allylamine). *Polymer* **2003,** *44* (18), 5053-5056.

11. (a) Gorton, L.; Jonsson-Pettersson, G.; Csoregi, E.; Johansson, K.; Dominguez, E.; Marko-Varga, G., Amperometric biosensors based on an apparent direct electron transfer between electrodes and immobilized peroxidases. Plenary lecture. *Analyst* **1992,** *117* (8), 1235-1241; (b) Lojou, E.; Bianco, P., Key role of the anchoring PEI layer on the electrochemistry of redox proteins at carbon electrodes: Consequences on assemblies involving proteins and clay. *Electrochimica Acta* **2007,** *52* (25), 7307-7314; (c) Lakard, B.; Herlem, G.; Lakard, S.; Antoniou, A.; Fahys, B., Urea potentiometric biosensor based on modified electrodes with urease immobilized on polyethylenimine films. *Biosensors and Bioelectronics* **2004,** *19* (12), 1641-1647; (d) Zhang, W.; Huang, Y.; Dai, H.; Wang, X.; Fan, C.; Li, G., Tuning the redox and enzymatic activity of glucose oxidase in layered organic films and its application in glucose biosensors. *Analytical Biochemistry* **2004,** *329* (1), 85-90; (e) Campos, P. P.; Moraes, M. L.; Volpati, D.; Miranda, P. B.; Oliveira, O. N.; Ferreira, M., Amperometric Detection of Lactose Using β-Galactosidase Immobilized in Layer-by-Layer Films. *ACS Applied Materials & Interfaces* **2014,** *6* (14), 11657-11664.

12. Schulz, C.; Ludwig, R.; Gorton, L., Polyethyleneimine as a Promoter Layer for the Immobilization of Cellobiose Dehydrogenase from Myriococcum thermophilum on Graphite Electrodes. *Analytical Chemistry* **2014,** *86* (9), 4256-4263.

13. Carvalhal, R. F.; Sanches Freire, R.; Kubota, L. T., Polycrystalline Gold Electrodes: A Comparative Study of Pretreatment Procedures Used for Cleaning and Thiol Self-Assembly Monolayer Formation. *Electroanalysis* **2005,** *17* (14), 1251-1259.

14. Schneider, G.; Decher, G., Functional Core/Shell Nanoparticles via Layer-by-Layer Assembly. Investigation of the Experimental Parameters for Controlling Particle Aggregation and for Enhancing Dispersion Stability. *Langmuir* **2008,** *24* (5), 1778-1789.

15. Sun, X.; Dong, S.; Wang, E., One-step preparation of highly concentrated well-stable gold colloids by direct mix of polyelectrolyte and HAuCl4 aqueous solutions at room temperature. *Journal of Colloid and Interface Science* **2005,** *288* (1), 301-303.

16. Kim, K.; Lee, H. B.; Lee, J. W.; Park, H. K.; Shin, K. S., Self-Assembly of Poly(ethylenimine)-Capped Au Nanoparticles at a Toluene−Water Interface for Efficient Surface-Enhanced Raman Scattering. *Langmuir* **2008,** *24* (14), 7178-7183.

17. Hoare, J. P., A Cyclic Voltammetric Study of the Gold-Oxygen System. *Journal of The Electrochemical Society* **1984,** *131* (8), 1808-1815.

18. (a) Lindgren, A.; Larsson, T.; Ruzgas, T.; Gorton, L., Direct electron transfer between the heme of cellobiose dehydrogenase and thiol modified gold electrodes. *Journal of Electroanalytical Chemistry* **2000,** *494* (2), 105-113; (b) Stoica, L.; Ludwig, R.; Haltrich, D.;

Gorton, L., Third-Generation Biosensor for Lactose Based on Newly Discovered Cellobiose Dehydrogenase. *Analytical Chemistry* **2006,** *78* (2), 393-398.
19. (a) Tasca, F.; Gorton, L.; Harreither, W.; Haltrich, D.; Ludwig, R.; Nöll, G., Comparison of Direct and Mediated Electron Transfer for Cellobiose Dehydrogenase from Phanerochaete sordida. *Analytical Chemistry* **2009,** *81* (7), 2791-2798; (b) Ortiz, R.; Matsumura, H.; Tasca, F.; Zahma, K.; Samejima, M.; Igarashi, K.; Ludwig, R.; Gorton, L., Effect of Deglycosylation of Cellobiose Dehydrogenases on the Enhancement of Direct Electron Transfer with Electrodes. *Analytical Chemistry* **2012,** *84* (23), 10315-10323.
20. Laviron, E., General expression of the linear potential sweep voltammogram in the case of diffusionless electrochemical systems. *Journal of Electroanalytical Chemistry and Interfacial Electrochemistry* **1979,** *101* (1), 19-28.
21. Harreither, W.; Nicholls, P.; Sygmund, C.; Gorton, L.; Ludwig, R., Investigation of the pH-Dependent Electron Transfer Mechanism of Ascomycetous Class II Cellobiose Dehydrogenases on Electrodes. *Langmuir* **2012,** *28* (16), 6714-6723.
22. Stoica, L.; Ruzgas, T.; Gorton, L., Electrochemical evidence of self-substrate inhibition as functions regulation for cellobiose dehydrogenase from Phanerochaete chrysosporium. *Bioelectrochemistry* **2009,** *76* (1–2), 42-52.
23. Tasca, F.; Harreither, W.; Ludwig, R.; Gooding, J. J.; Gorton, L., Cellobiose Dehydrogenase Aryl Diazonium Modified Single Walled Carbon Nanotubes: Enhanced Direct Electron Transfer through a Positively Charged Surface. *Analytical Chemistry* **2011,** *83* (8), 3042-3049.
24. Tasca, F.; Ludwig, R.; Gorton, L.; Antiochia, R., Determination of lactose by a novel third generation biosensor based on a cellobiose dehydrogenase and aryl diazonium modified single wall carbon nanotubes electrode. *Sensors and Actuators B: Chemical* **2013,** *177* (0), 64-69.
25. Gürsoy, O.; Çelik, G.; Gürsoy, S. Ş., Electrochemical Biosensor Based on surfactant doped polypyrrole (PPy) matrix for lactose determination. *Journal of Applied Polymer Science* **2014,** *131* (9), n/a-n/a.
26. Conzuelo, F.; Gamella, M.; Campuzano, S.; Ruiz, M. A.; Reviejo, A. J.; Pingarrón, J. M., An Integrated Amperometric Biosensor for the Determination of Lactose in Milk and Dairy Products. *Journal of Agricultural and Food Chemistry* **2010,** *58* (12), 7141-7148.
27. Safina, G.; Ludwig, R.; Gorton, L., A simple and sensitive method for lactose detection based on direct electron transfer between immobilised cellobiose dehydrogenase and screen-printed carbon electrodes. *Electrochimica Acta* **2010,** *55* (26), 7690-7695.

Figure legends

Figure 1. (A) UV-VIS spectra of PEI@AuNPs. (B) TEM of PEI@AuNPs. (C) DLS graph of PEI@AuNPs. (D) CVs of unmodified Au electrode (dashed line) and PEI@AuNPs/Au electrode (solid line) in 0.5M H_2SO_4 solution. Scan rate: 100 mV s^{-1}.

Figure 2. (A) CVs of the *Ps*CDH/PEI@AuNPs/Au (solid line) and the *Ps*CDH/Au (dotted line) in a N_2-saturated acetate buffer solution (5 mM, pH = 4.5) at a scan rate of 1 mV s^{-1}. (B) CVs of the *Ps*CDH/PEI@AuNPs/Au in a N_2-saturated acetate buffer solution (5 mM, pH = 4.5) at various scan rates from 1 to 300 mV s^{-1}. (C) Variations of the (Ep - $E^{\circ\prime}$) versus the logarithmic scan rate (log ν) for *Ps*CDH modified electrode. (D) Plot of the peak current (Ip) versus scan rate (ν).

Figure 3. Electrocatalytic currents of *Ps*CDH electrostatically immobilized on modified PEI@AuNPs electrode in the presence of 0.0 (a), 0.5 (b), 1.0 (c) and 5.0 (d) mM lactose. The experiments were performed at a scan rate of 1 mV s^{-1} in a N_2-saturated acetate buffer solution (5 mM, pH = 4.5).

Figure 4. Calibration curve for different concentrations of lactose in buffer acetate (5 mM, pH 4.5). In the inset: the response in the low-micromolar range. Applied potential: +250 mV vs. Ag|AgCl (0.1M KCl).

Figure 5. Dependence of catalytic currents versus pH-profile. The electrodes were mounted in an electrochemical flow through cell connected to a FIA system with 50 mM NaAc, MES, or TRIS of varying pH as a running buffer. The electrocatalytic current responses to 5mM lactose were recorded at an applied potential of 250 mV vs Ag|AgCl (0.1 M KCl).

Figure 1

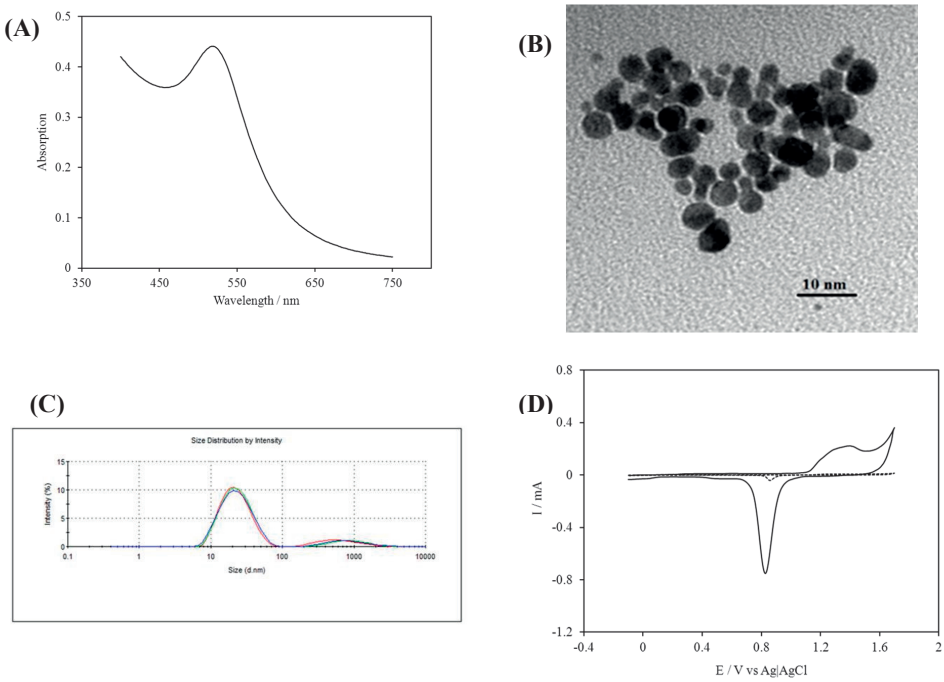
(A)
Absorption
Wavelength / nm
(B)
10 nm
(C)
Size Distribution by Intensity
Intensity (%)
Size (d.nm)
(D)
I / mA
E / V vs Ag|AgCl

Figure 2

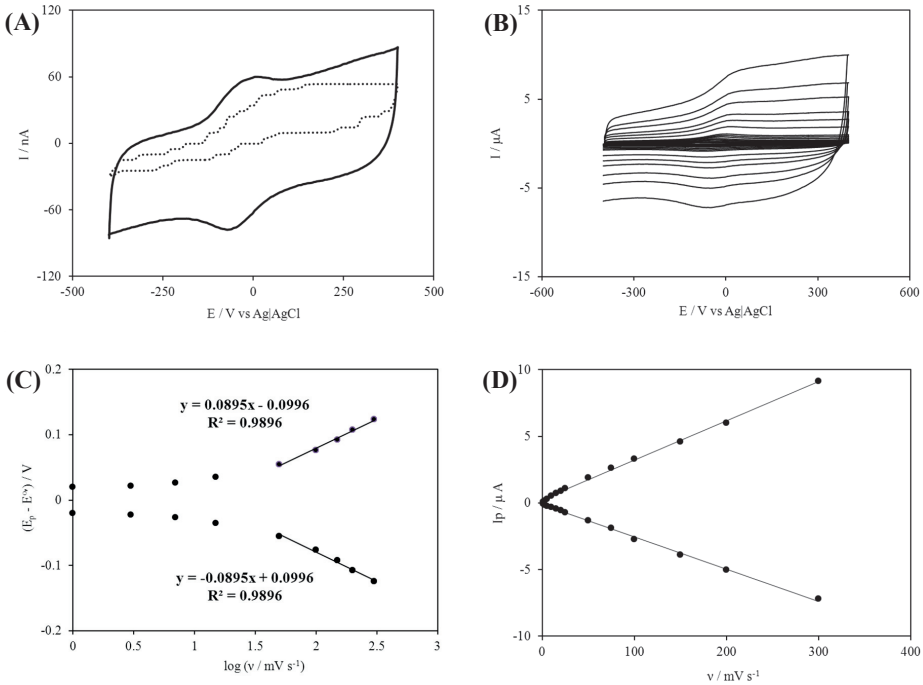
(A)
I / nA
E / V vs Ag|AgCl
(B)
I / µA
E / V vs Ag|AgCl
(C)
y = 0.0895x - 0.0996
R² = 0.9896
y = -0.0895x + 0.0996
R² = 0.9896
(Ep - E°') / V
log (v / mV s-1)
(D)
Ip / µA
v / mV s-1

Figure 3

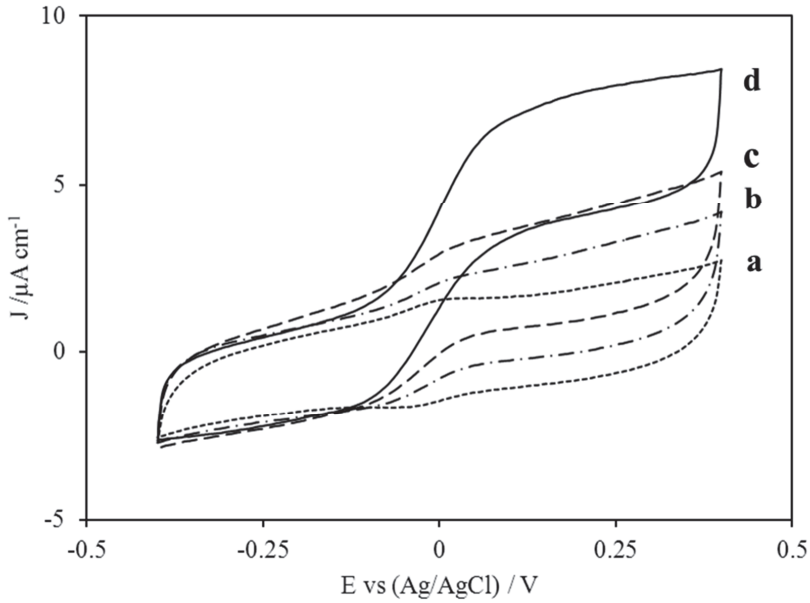

Figure 4

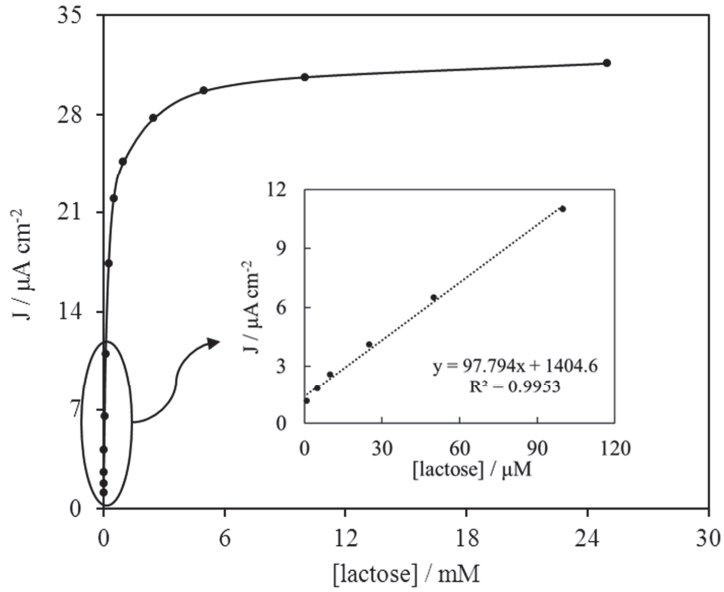
35
28
21
14
7
0
J / µA cm-2
0
6
12
18
24
30
[lactose] / mM
12
9
6
3
0
J / µA cm-2
y = 97.794x + 1404.6
R² – 0.9953
0
30
60
90
120
[lactose] / µM

Figure 5

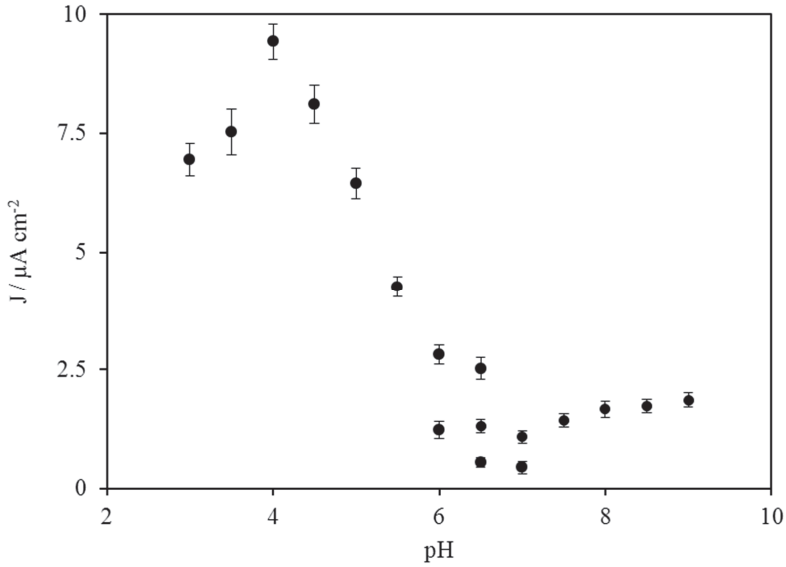

Table 1

Analytical parameters reported for some lactose biosensors.

Lactose biosensor	LDR (μM)	DL (μM)	Sensitivity ($\mu A\ mM^{-1}$)	Response Time (s)	Eapp (V)
(PEI/β-Gal)/(PEI/PVS)/PB/ITO[11e]	-	1130	0.31	-	0.04
β-Gal-GaOx/PPy/Pt[25]	300-1220	2	76	8-10	0.4
β-Gal-GOD-HRP/TTF/MPA/AuE[26]	13-1000	3.8	11	300	0.00
CDH/MWCNTs/SPCEs[27]	0.5-100	0.25	-	65	0.1
CDH/PEI@AuNPs/AuE	1-100	0.33	3.93	3	0.25

LDR, linear dynamic range; DL, detection limit; β-Gal, β-galactosidase; PVS, poly (vinyl sulfonate) ; PB, Prussian Blue; ITO, indium tin oxide; PPy, polypyrrole; GOD, glucose oxidase; HRP, horse radish peroxidase; TTF, tetrathiafulvalene; MPA, 3-mercaptopropionic acid; AuE, solid gold electrode; MWCNTs, multi wall carbon nanotubes; SPCE, screen printed carbon electrodes.

Graphical Abstract

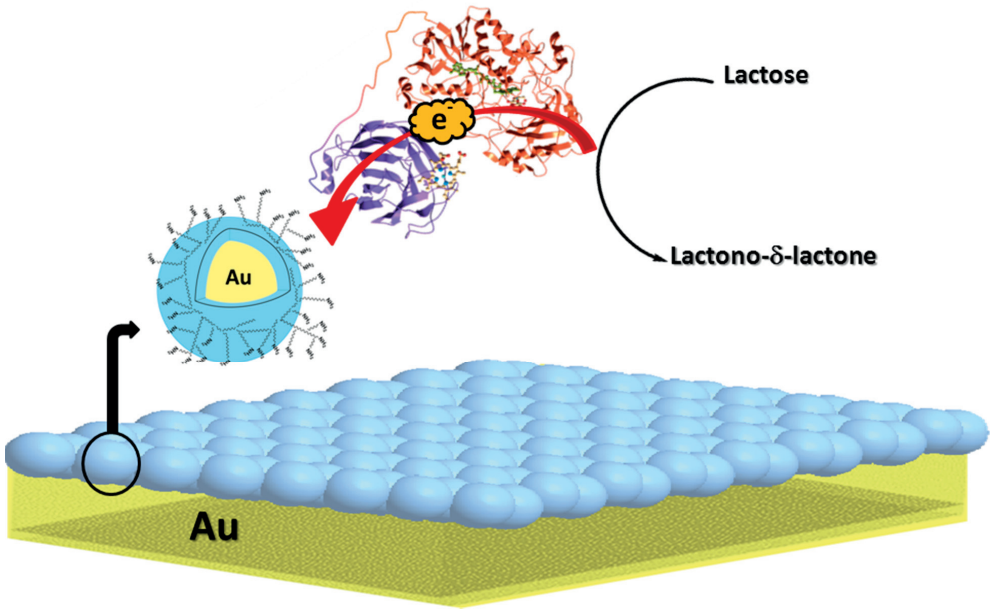
Lactose
e
Lactono-δ-lactone
Au
Au

Paper IX

Interaction of Polymer-Coated Gold Nanoparticles with Cellobiose Dehydrogenase: The Role of Surface Charges

Mojtaba Tavahodi[†], Anna Assarsson[‡], Christopher Schulz[‡], Roberto Ortiz[‡], Roland Ludwig[§], Behzad Haghighi[†], Celia Cabaleiro-Lago[‡], Lo Gorton[‡,*]

† Department of Chemistry, Institute for Advanced Studies in Basic Sciences, P.O. Box 45195-1159, Gava Zang, Zanjan, Iran

‡ Department of Analytical Chemistry/Biochemistry and Structural Biology, Lund University P.O. Box 124, SE-22100 Lund, Sweden

§ Food Biotechnology Laboratory, Department of Food Sciences and Technology, BOKU – University of Natural Resources and Life Sciences Vienna, Muthgasse 18, A-1190 Wien, Austria

ABSTRACT. Studying the interaction of functional proteins such as enzymes and nanoparticles (NPs) includes the important topic of investigating the changes of stability and function of enzymes in nanostructured environments. The effects of NPs on enzymes are governed by their physical and chemical properties such as structure, size, surface chemistry, shape and their surface charges. In this study we investigated the influence of negatively as well as positively charged polyelectrolyte gold NPs on the activity and the direct electron transfer of *Myriococcum thermophilum* cellobiose dehydrogenase (*Mt*CDH). The premodification of the *Mt*CDH electrode with positively charged AuNPs causes an alkaline pH shift of the maximum response of the electrode from pH 5.5 to 8. No change in the pH optimum was observed when the electrode was modified with negatively charged AuNPs indicating the effect of surface charge of the NPs on the properties of enzyme. The catalytic current densities of *Mt*CDH electrodes carrying AuNPs with positive charges were enhanced up to 66 times and the K_M^{app} values were increased up to 8 times. Two spectroscopic assays for measuring the enzymatic activity were performed and the beneficial influence of the positively charged AuNPs on the activity of *Mt*CDH was also present in homogeneous solution. Our results demonstrate that the electron transfer from *Mt*CDH to the electrode or the homogeneous electron acceptor was highly dependent on the type of surface charge of the NPs.

Introduction

The interaction of various types of nanoparticles (NPs) and functional proteins has been broadly studied in medicine, diagnostics, biosensors and fuel cells[1]. This interaction is controlled by the physicochemical parameters of NPs such as, shape, size, charge and surface chemistry[2]. Recent studies report that surface charge is another important parameter that affects the function of NPs in cellular uptake, drug delivery and protein interaction[3]. Layer-by-layer (LBL) deposition is a well-established method for the synthesis of coated gold nanoparticles (AuNPs) and allows the fabrication of AuNPs with negative or positive net charges by covering the NPs with polyelectrolytes containing $–SO_3^-$ or $–NH_3^+$ groups[4,5].

In studies elucidating the direct electron transfer (DET) of redox proteins with electrodes, the biocomponents were conjugated with nanomaterials to overcome the sluggish rate of heterogeneous electron transfer of deeply embedded prosthetic groups of proteins[6]. This strategy can be applied to design efficient biosensors and biofuel cells[7,8] with high current outputs.

Cellobiose dehydrogenase (EC 1.1.99.18, CDH) is one of the redox enzymes capable of facile DET, which is a result of its two domain structure[9,10]. The enzyme is composed of a catalytic FAD containing dehydrogenase domain (DH), a heme *b* containing cytochrome domain (CYT), and a flexible linker region connecting the two domains. During the catalytic oxidation of carbohydrate substrates, $2H^+/2e^-$ are donated to the FAD cofactor. These electrons are then further transferred through an intramolecular electron transfer step (IET) to the heme *b* cofactor located in CYT, which acts as a “built in” redox mediator between DH and an electrode and is executing the final DET step. Because of their cellobiose, glucose and lactose oxidizing activity, various CDHs have been employed in DET based amperometric biosensors and biofuel cells[11,12].

Our group has previously reported that the activity of class II CDH from *Myriococcum thermophilum* in solution and on the electrode could be greatly enhanced to a maximum of around five-fold when the concentration of calcium chloride in the electrolyte was increased to 50 mM.[13] The increases were suggested to arise from a calcium ion bridging effect involving the heme propionates and negatively charged amino acid residues present on the interfaces of both domains leading to a better CYT-DH interaction and a faster IET[13,14] which is otherwise the rate limiting step.[8,15] The polycation polyethyleneimine (PEI) used here as a capping agent for the AuNPs has also been shown previously to exhibit beneficial effects on the activity of immobilized *Mt*CDH. Graphite electrodes premodified with PEI were shown to increase the catalytic current output (up to 140 times at pH 8) and shift the pH optimum of *Mt*CDH for DET from pH 5.5 to pH 8. The effects were partly assigned to a higher loading of the negatively charged enzyme molecules onto the positively charged electrode surface and to an increased IET due to a screening of negatively charged amino acid residues present at the interfaces of both domains allowing a faster IET comparable to the Ca^{2+} bridging effect.[11]

In the present study, we investigate the effect of positively and negatively charged AuNPs capped with polyelectrolytes on the activity and DET properties of *Mt*CDH with the aim to increase the current density and stability of the modified electrodes. The preparation of AuNPs was carried out via the citrate reduction method[5] and then the polyelectrolytes were deposited on the surface of the NPs through electrostatic interaction. We have chosen polyethyleneimine (PEI) and poly sodium-4-styrenesulfonate (PSS) polymers for modification of AuNPs because they exhibit positive and negative charges at physiological pH. These polyelectrolytes form a shell around the AuNPs preventing their aggregation and providing a link to keep the enzyme on the electrode surface by electrostatic interactions.

Experimental Section

Reagents and Equipment. Branched polyethyleneimine (PEI) (50 % w/v in H_2O, Mn~60 000, Mw~750 000), poly(allylamine hydrochloride) (PAH) (Mw = 15 000 g mol^{-1}), β-lactose, 4-morpholineethanesulfonic acid (MES), tris(hydroxymethyl)aminomethane (TRIS), tetrachloroauric(III) acid, $HAuCl_4 \cdot 3\ H_2O$ and trisodium citrate dihydrate were obtained from Sigma Aldrich Chemicals (Steinheim, Germany). Acetic acid (100%) and sodium hydroxide solution (50%) were purchased from Merck (KGaA, Darmstadt, Germany). Poly(sodium 4-styrenesulfonate) (PSS, M_w = 13400 g mol^{-1}) was obtained from Polymer Standard Service (Mainz, Germany). All chemicals were of analytical reagent grade and were used without further purification. Milli-Q water (Millipore 18.2 MΩ cm) was used in all experiments.

Optical characterization of the AuNPs was carried out by UV−Vis−NIR spectroscopy with a Hewlett-Packard HP 8453 spectrophotometer. A Philips CM120 BioTWIN Cryo transmission electron microscope (TEM) operating at an acceleration voltage of 120 kV was used for particle size analysis. Particle drops were applied on 300 mesh formvar carbon film grids (Electron Microscopy Sciences, Hatfield, PA).

The ζ-potential of the NPs was studied using a Malvern Zetasizer Nano ZS (Malvern Instruments Ltd, UK) operating with a 633 nm laser at a 175° scattering angle in 50 mM citrate buffer (pH 7.0) at 25°C. A minimum of 5 measurements were performed for each sample using a folded capillary cell (Malvern Instruments Ltd, UK).

Flow Injection Setup. A flow amperometric wall jet cell with three electrodes, a working electrode, a reference electrode (Ag|AgCl in 0.1 M KCl), and a counter electrode made of a platinum wire, connected to a potentiostat (Zäta Elektronik, Höör, Sweden) was used. The 50

mM acetate buffer (pH 5.50) carrier flow was maintained at a constant flow rate of 1 mL min^{-1} by a peristaltic pump (Minipuls 2, Gilson, Villier-le-Bel, France). An electrically controlled six-port valve (LabPRO, Rheodyne, USA) with a 50 µL injection loop was used.

Solutions and enzymes. *Mt*CDH (GenBank identifier 164597964) was recombinantly expressed in *Pichia pastoris* and purified as explained in reference[16]. The protein concentration was determined photometrically by using an extinction coefficient of ε_{280} = 159063 M^{-1} cm^{-1} determined from the amino acid sequence (ABS45567.2). Enzyme dilutions of the enzyme stock solution (c = 37.9 mg/ml) were performed with a 50 mM acetate buffer, pH 5.5. A stock solution of lactose (500 mM) was prepared using Milli Q_water and stored at 4°C when not in use. The lactose stock solution was allowed to mutarotate at room temperature for at least 24 h before use. As measuring buffers 50 mM sodium acetate (pH 3.0-6.5), 50 mM MES (pH 6.0-7.0) and 50 mM TRIS (pH 6.5-9.0) were used.

Activity assays in solution. To study the effect of AuNPs on the activity of enzyme, two assays were used. In the first assay, the $2H^+/2e^-$ acceptor 2,6-dichloroindophenol (DCIP) was used to monitor the activity of the DH domain by measuring the time dependent change of absorption at 520 nm (ε_{520} = 6.9 mM^{-1} cm^{-1}) of a mixture of 100 µl of 3 mM DCIP, 100 µl of 300 mM lactose, 770 µl of 50 mM buffer, 10 µl of 0.50 mM AuNPs and 20 µl of the enzyme solution.[17] In a second assay the one-electron acceptor cytochrome *c* (cyt *c*) was used, which accepts the electrons only from the CYT_{CDH} domains due to steric reasons and consequently screens the activity of intact *Mt*CDH involving the IET between the two domains. The absorption was recorded at 550 nm (ε_{550} = 19.6 mM^{-1} cm^{-1}) of a mixture of 20 µl of 1 mM cyt c, 100 µl of 300 mM lactose, 850 µl of 50 mM buffer,10 µl of 0.50 mM AuNPs and 20 µl of the enzyme

solution.[17] One unit of DCIP and cyt *c* activity was defined as the amount of enzyme that reduces 1 μmol of the electron acceptor per min under the applied conditions.[17]

Synthesis and coating of gold nanoparticles. The AuNPs were synthesized with the citrate reduction method[5,18]. In short, 1% citric acid sodium salt solution was added to boiling water (to a final concentration of 34 mM) containing 1 mM tetrachloroauric(III) acid and stirred for 20 min. The negatively charged NPs were cleaned by centrifugation and redispersion before coating them with the polycation PEI (Au@PEI) or the polycation PAH followed by the polyanion PSS (Au@PSS) as described by Schneider and Decher[4]. The polyelectrolytes were deposited on the NPs by electrostatic interactions. To ensure a positive charge of the PEI the pH of the polyelectrolyte solution was decreased to pH 5 with HCl before coating. The non-coated NPs (Au@Cit) were used in addition to the polymer coated NPs. These NPs have a negative surface charge from the citrate in the synthesis process.

Fabrication of CDH modified electrodes. The surface of a spectrographic graphite electrode (GE, Ringsdorff Werke GmbH, Bonn, Germany, type RW001, diameter = 3.05 mm) was polished on wet emery paper (P1200 from Norton, Saint-Gobain Abrasives AB, Sollentuna, Sweden) then thoroughly rinsed with Milli-Q water, and finally allowed to dry. Optionally 5 μl of concentrated AuNPs solution was cast on the surface of the graphite electrode and dried at room temperature, followed by the addition of 3 μl of enzyme solution (10 mg ml^{-1}) onto the surface of the electrode, which was allowed to dry at room temperature. The prepared electrodes were stored overnight at 4 °C, and before each measurement, the electrodes were rinsed with acetate buffer to remove loosely bound enzyme molecules.

3. Result and Discussion

Characterization of gold nanoparticles

Before their intended use to study the effect on the electrochemistry of *Mt*CDH the size and charge of the formed AuNPs were characterized using TEM and zeta (ζ) potential measurements. The size of the NPs was similar with diameters of 16±4 nm for Au@PEI, 14±3 nm for Au@Cit and 17±3 nm for Au@PSS based on TEM measurements (Fig. 1). The coating was verified by a positive ζ-potential for Au@PEI (30 ± 3 mV) and a negative ζ-potential for Au@PSS(-42 ± 3 mV). The uncoated, citrate based NPs had a ζ-potential of -27 ± 2 mV.

Electrochemistry of *Mt*CDH on different AuNP modified electrode. Cyclic voltammetry was carried out in acetate buffer (50 mM, pH 5.5) to measure the electrochemical behavior of *Mt*CDH modified graphite electrodes optionally premodified with the differently charged AuNPs. As shown in Fig. 2A, no obvious redox peaks and no catalytic currents were observed for *Mt*CDH graphite electrodes lacking the AuNPs. This is expected as this type of graphite electrodes exhibits strong capacitive and pseudocapacitive background currents making the redox conversion of CDH invisible. Only more sensitive techniques as square wave voltammetry allow the visibility of electrochemistry of the heme of the CYT on this type of graphite electrodes.[19]

When using any type of the AuNPs as a premodifier on the graphite electrodes (Figs. 2B-D) clear redox waves originating from the redox conversion of the CYT are visible at pH 5.5 with catalytic currents starting at potentials around the oxidation peak potential of the CYT indicating DET between *Mt*CDH and the electrode. The midpoint potential of the oxidation and reduction peaks is around -50 mV vs. Ag|AgCl (0.1 M KCl) and corresponds well with literature values.[20] The visibility of the electrochemistry of *Mt*CDH in the presence of the NPs can be explained by

several factors. It is reasonable to assume that the introduction of NPs on the surface of the graphite electrode induces an increased surface area of the electrode leading to a higher load of enzyme. This is supported by higher apparent K_M values of *Mt*CDH in the presence of AuNPs indicating diffusion limitations of substrate to the enzyme within the highly loaded AuNP-*Mt*CDH layers (see Table 1). Since the redox electrochemistry of the CYT is visible also on the negatively charged NPs not only electrostatic interactions between enzyme and NPs are responsible for the enzyme immobilization. Negatively charged surfaces alone were shown not be able to electrostatically immobilize CDH as tested for *Pc*CDH (pI of 4.2) at pH 5 on mercaptopropionic acid modified gold electrodes, where no electrochemistry of the CYT is visible in the absence of a membrane keeping the enzyme confined on the electrode surface.[21] As reported in the literature driving forces as entropic gain due to enzyme immobilization on surfaces accompanied by a release of solvent molecules (water) or counter ions from the enzyme/surface contact area can lead to the immobilization of enzymes on surfaces bearing the same charge.[22]

Upon addition of substrate, the highest catalytic current densities were detected for the *Mt*CDH electrodes premodified with the positively charged AuNPs (Au@PEI, see Fig. 2D). Compared to *Mt*CDH electrodes modified with the negatively charged AuNPs, the current densities were around 3 times higher. The obtained results demonstrate that the surface charge of AuNPs plays a key role in the catalytic response of the *Mt*CDH modified electrodes. These increases in the catalytic current densities as a result of a premodification of the graphite electrode with positively charged AuNPs can be explained by three effects. Firstly, *Mt*CDH is an acidic enzyme with an overall isoelectric point of 3.8[9,23] with many negatively charged amino acid residues present on its surface at a pH of 5.5. An electrostatic interaction between the negative charges of

the CYT_{CDH} and the DH_{CDH} domains and the positive charges of the Au@PEI is suggested to possibly decrease the distance between the DH_{CDH} and CYT_{CDH} and consequently increase the rate of the IET comparable to the findings for *Mt*CDH immobilized on graphite electrode premodified with PEI only.[11] Secondly, based on the strong electrostatic interactions between *Mt*CDH and the Au@PEI more CDH molecules might be immobilized on Au@PEI compared to the immobilization on negatively charged AuNPs, resulting in an increase in the catalytic current densities. This is also supported by the higher apparent K_M, K_M^{app}, values obtained for *Mt*CDH immobilized on the Au@PEI compared to any other electrode modification indicating diffusion limitation of substrate to the enzyme within the highly loaded Au@PEI/CDH layer (see Table 1). Thirdly, the rate of electron transfer from the CYT domain to the surface of the electrode might have been increased due to an enhanced conductivity through the AuNPs as suggested e. g., for glucose oxidase reconstituted on FAD modified gold nanoparticles.[24]

To further investigate the effect of the charged polyelectrolyte AuNPs on the efficiency of DET of the enzyme, the catalytic current densities of *Mt*CDH electrodes with and without modification with AuNPs at varying lactose concentrations (1 µM – 50 mM) were recorded amperometrically using a flow injection analysis system (see Figs. 3 and 4). The maximal current densities, J_{max}, and K_M^{app} extracted from fitting the response data given in Figs. 3 and 4 to the Michaelis-Menten equation are summarized in Table 1.

As already observed in the cyclic voltammograms the catalytic currents are always higher when the electrodes were premodified with polyelectrolyte NPs. Compared to electrodes lacking NPs increases in catalytic current densities J_{max} of 2.1x, 3.1x and 7.3x were exhibited for the negatively charged Au@PSS, Au@Cit and the positively charged Au@PEI, respectively, at pH 5.5. At pH 8 the increases in J_{max} were comparable when the negatively charged NPs were used

(3.1x and 3.7x times) but much higher in case of the positively charged Au@PEI with increases in around 66 times highlighting the importance of the charge. The K_M^{app} values were also increased in the presence of NPs with increases in 5.7x, 3.5x and 8.0x achieved for the negatively charged Au@PSS, Au@Cit and the positively charged Au@PEI, respectively, at pH 5.5. As mentioned above, this indicates diffusion limitations of substrate to the enzyme possibly achieved by a higher enzyme load onto the electrode surface. This effect is highest for the positively charged Au@PEI due to an additional, strong electrostatic binding between oppositely charged *Mt*CDH and NPs.

As our group reported previously on the influence of Ca^{2+} on the catalytic response of *Mt*CDH[13], equivalent calibration graphs in the presence of 50 mM $CaCl_2$ have been performed as well. In the absence of any NPs a 4.8 times increase in the J_{max} was found in the presence of 50 mM $CaCl_2$ at pH 5.5, which compares well with our previous findings.[13] Divalent metal cations as Ca^{2+} were suggested to interact with both negatively charged domains of *Mt*CDH decreasing repulsion leading to an increased IET resulting in a higher J_{max}. In the presence of the Au@PEI NPs the Ca^{2+} induced increases in J_{max} are only 1.8x at pH 5.5 and 1.7 at pH 8 suggesting that PEI mimics the Ca^{2+} effect as also suggested for graphite electrodes modified with PEI and *Mt*CDH.[11] Also an electrostatic repulsion of Ca^{2+} leading to a decreased availability of Ca^{2+} in the PEI/CDH layer is plausible. The effect of Ca^{2+} on *Mt*CDH electrodes modified with the negatively charged NPs Au@Cit and Au@PSS is much greater and increases in J_{max} of up to 13.7x are achieved at pH 8 highlighting that only in a negatively charged environment Ca^{2+} can display its full, beneficial effect on the activity of *Mt*CDH.

In Fig. 5 it is shown the dependency of the catalytic current densities of *Mt*CDH modified electrodes premodified with the differently charged AuNPs on the solution pH. The pH optimum of *Mt*CDH immobilized on graphite electrodes was found to be at pH 5.5 and agrees with the literature.[15] When positively charged Au@PEI were used as a premodifier the pH optimum shifted to pH 8 and the overall catalytic current densities increased in the entire investigated pH range, which is in accordance with the findings described above (see Fig. 5A). This indicates that not only an increased enzyme load is achieved by increased electrostatic interactions between *Mt*CDH and the Au@PEI but that the polycation PEI also possibly acts on the rate limiting IET of *Mt*CDH leading to a better visibility of the catalytic turnover of the DH domain. A similar trend with increased catalytic currents and a shift in pH optimum was also described previously for *Mt*CDH immobilized on PEI modified graphite electrodes.[11] In the presence of the negatively charged nanoparticles Au@PSS and Au@Cit the catalytic currents were only slightly increased (see Table 1), however, no shift in the pH optimum was observed. This result again supports the assumption of a general, higher enzyme load onto the NP modified electrodes. When adding $CaCl_2$ to the measuring solution also in this case for the electrodes lacking NPs or modified with the negatively charged Au@PSS and Au@Cit a shift in the pH optimum to pH 8 can be observed and catalytic currents are increased with highest increases for the unmodified electrodes and the electrodes modified with the negatively charged AuNPs. As suggested above Ca^{2+} can display its tuning capability best in a negatively charged environment and PEI might partly mimic the Ca^{2+} effect.

Effect of gold nanoparticles on the activity of *Mt*CDH in solution. A cyt *c* and a DCIP assay were performed at pHs ranging between pH 3.0 and pH 9.0 to investigate the dependence of the

solution activity of *Mt*CDH on additionally present positively or negatively charged AuNPs. The electron acceptor cyt *c* only accepts electrons from the CYT domain of *Mt*CDH and monitors the activity of the entire enzyme, including the rate limiting IET from the DH to the CYT. The two electron/two proton electron acceptor DCIP accepts electrons only from the DH domain of *Mt*CDH and solely monitors the catalytic turnover of the DH domain itself. In the absence of any NPs the optimum for the cyt *c* assay for *Mt*CDH is found to be at pH 5.5. Adding positively charged Au@PEI an overall increase in the cyt *c* activity starting at around pH 4 is observed (see Fig. 6A). Two distinct pH optima, one around pH 4.5 to 5 and one around 7 to 7.5 can be identified with maximum increases in activity of around 30 times at neutral pH. Surprisingly, adding the negatively charged Au@Cit or Au@PSS similar increases in the cyt *c* activity in the acidic region but already starting at around pH 3.5 with an optimum between pH 4.5 to 5 can be observed. At pH 5.5 and above, the negatively charged AuNPs have only a minor influence on the cyt *c* activity of *Mt*CDH in solution, which compares well with the electrochemical findings of immobilized *Mt*CDH. We suggest that the comparable increases in the cyt *c* activity in the acidic region in the presence of the negatively or positively charged NPs are due to the electrostatic interactions of positively charged cyt *c* with the negatively charged Au@PSS or Au@Cit or in case of the positively charged AuNPs due to electrostatic interactions between Au@PEI and negatively charged CDH at pHs above the enzymes pI of 3.8. Both types of interactions might lead to bigger and more stabilized protein-NP complexes increasing the cyt *c* activity. However, further measurements are necessary to investigate this effect.

The second pH optimum around pH 7-7.5 only observed in the presence of the positively charged Au@PEI is suggested to arise from an interaction of the polycation PEI with the

negatively charged interfaces of CYT and DH increasing the IET in accordance with the electrochemical findings above with immobilized *Mt*CDH leading to a shifted pH optimum.

The catalytic turnover of the DH domain is also influenced by the presence of AuNPs, however, the increase in the DCIP activity is only around 50% in the presence of AuNPs, does not differ between positively and negatively charged AuNPs, and no shift in pH optimum is observed. Similar increases in activity were observed for glucose oxidase using DCIP as electron acceptor after the addition of comparable AuNPs with increases in the DCIP activity of around 44% at pH 7 as reported here.[25] It was suggested that the NPs can act as electron acceptors additionally mediating electron transfer between glucose oxidase and the electron acceptor DCIP, which might also happen here in case of *Mt*CDH. A similar mediating effect of the AuNPs might be another explanation for the observed, increased cyt *c* activities in the presence of NPs in the acidic region.

4. Conclusion

AuNPs were synthesized by citrate reduction and were further coated with either positively charged PEI or negatively charged PSS as the outer layer. The NPs had comparable sizes of 16±4 nm, 14±3 nm and 17±3 nm and zeta potentials of +30±3, -27±2 and -42±3 as determined for the Au@PEI, Au@Cit and Au@PSS particles. The particles were used to premodify graphite electrodes to investigate their influence on the electrocatalytic activity of immobilized *Mt*CDH in the absence and in the presence of the substrate lactose at different pHs as well as in the absence and in the presence of $CaCl_2$.

After modification of graphite electrodes with the positively charged Au@PEI, the catalytic current densities of *Mt*CDH electrodes significantly increased by up to 66 times and the optimal

pH shifted from 5.5 to 8 compared to electrodes lacking modification by NPs. Even on negatively charged NPs the catalytic current densities of negatively charged *Mt*CDH were slightly increased by up to 3.7 times compared to graphite electrodes only modified with *Mt*CDH, indicating that the immobilization of *Mt*CDH not only occurs via electrostatic binding but also via other interactions. On factor increasing the catalytic current densities in the presence of NPs is suggested to be a higher load of enzyme onto the NP modified surface, as indicated by elevated K_M^{app} values indicating diffusion limitations of substrate to the enzyme.

As previously reported, additional Ca^{2+} present in the buffer further enhanced the catalytic currents. This effect was previously ascribed to arise from a complexation of the Ca^{2+} by negatively charged heme propionates and amino acid residues present at both domains of *Mt*CDH leading to a decrease in repulsion and an increase in the rate limiting IET. The effect of Ca^{2+} on the activity of *Mt*CDH was less when positively charged Au@PEI NPs were used as a premodifier suggesting that PEI itself already partly acts as Ca^{2+}. The influence of Ca^{2+} was highest when the negatively charged NPs Au@PSS and Au@Cit were used as premodifier suggesting that Ca^{2+} can exhibit its full effect best in a negatively charged environment.

As also reported previously, the presence of Au@PEI as well as Ca^{2+} leads to a shift in the pH optimum of *Mt*CDH from pH 5.5 to pH 7.5-8, as proven to occur for *Mt*CDH when immobilized on the electrode surface as well as when investigated in solution. Both cationic compounds are suggested to increase the rate limiting IET making the catalytic turnover of the DH domain more visible. When investigating the effects of the charged NPs on the activity of *Mt*CDH in solution we observed further enhancements in the catalytic activities especially in the acidic region. In solution the AuNPs are suggested to also interact with the electron acceptors cyt *c* and DCIP and with *Mt*CDH leading to increased activities due to the formation of bigger protein/NP complexes

and due to an additional mediation of electron transfer between *Mt*CDH and the electron acceptor by the AuNPs. The findings are of interest for a better understanding of the enzyme mechanism as well as for increasing current outputs of potential CDH based biosensors and biofuel cell anodes operating at low voltages avoiding the oxidation of potential interferents.

ACKNOWLEDGMENTS

The authors thank the following agencies for financial support:

The European Commission ("Chebana", FP7-PEOPLE-2010-ITN-264772 and the Integrated Infrastructure Initiative N. 262348, European Soft Matter Infrastructure, ESMI) and the Institute for Advanced Studies in Basic Sciences (IASBS, Grant Number G2014IASBS119).

References

(1) Lacerda, S. H. D. P.; Park, J. J.; Meuse, C.; Pristinski, D.; Becker, M. L.; Karim, A.; Douglas, J. F. *ACS Nano* **2009**, *4*, 365-379; Elodie, S.; Julien, D.; Fernando, R.-L.; Jean-Marie, D. *J. Physics: Conference Series* **2011**, *304*, 012039; Saha, K.; Agasti, S. S.; Kim, C.; Li, X.; Rotello, V. M. *Chem. Rev.* **2012**, *112*, 2739-2779.
(2) Rivera-Gil, P.; Jimenez De Aberasturi, D.; Wulf, V.; Pelaz, B.; Del Pino, P.; Zhao, Y.; De La Fuente, J. M.; Ruiz De Larramendi, I.; Rojo, T.; Liang, X.-J.; Parak, W. J. *Acc. Chem. Res.* **2012**, *46*, 743-749.
(3) Hühn, D.; Kantner, K.; Geidel, C.; Brandholt, S.; De Cock, I.; Soenen, S. J. H.; Rivera-Gil, P.; Montenegro, J.-M.; Braeckmans, K.; Müllen, K.; Nienhaus, G. U.; Klapper, M.; Parak, W. J. *ACS Nano* **2013**, *7*, 3253-3263; Frohlich, E. *Int. J. Nanomed.* **2012**, *7*, 5577-91; Cho, E. C.; Xie, J.; Wurm, P. A.; Xia, Y. *Nano Letters* **2009**, *9*, 1080-1084.
(4) Schneider, G.; Decher, G. *Langmuir* **2008**, *24*, 1778-1789.
(5) Shin, H. J.; Hwang, I.-W.; Hwang, Y.-N.; Kim, D.; Han, S. H.; Lee, J.-S.; Cho, G. *J. Phys. Chem. B* **2003**, *107*, 4699-4704.
(6) Frasca, S.; Rojas, O.; Salewski, J.; Neumann, B.; Stiba, K.; Weidinger, I. M.; Tiersch, B.; Leimkühler, S.; Koetz, J.; Wollenberger, U. *Bioelectrochemistry* **2012**, *87*, 33-41; Oaew, S.; Charlermroj, R.; Pattarakankul, T.; Karoonuthaisiri, N. *Biosens. Bioelectron.* **2012**, *34*, 238-243; Frew, J. E.; Hill, H. A. O. *Eur. J. Biochem.* **1988**, *172*, 261-269.
(7) Yang, X.-Y.; Tian, G.; Jiang, N.; Su, B.-L. *Energy Environ. Sci.* **2012**, *5*, 5540-5563; Yan, Y.-M.; Baravik, I.; Yehezkeli, O.; Willner, I. *J. Phys. Chem. B* **2008**, *112*, 17883-17888.
(8) Matsumura, H.; Ortiz, R.; Ludwig, R.; Igarashi, K.; Samejima, M.; Gorton, L. *Langmuir* **2012**, *28*, 10925-10933.
(9) Ludwig, R.; Harreither, W.; Tasca, F.; Gorton, L. *ChemPhysChem* **2010**, *11*, 2674-2697.
(10) Ludwig, R.; Ortiz, R.; Schulz, C.; Harreither, W.; Sygmund, C.; Gorton, L. *Anal Bioanal Chem* **2013**, *405*, 3637-3658.
(11) Schulz, C.; Ludwig, R.; Gorton, L. *Anal. Chem.* **2014**, *86*, 4256-4263.
(12) Tasca, F.; Ludwig, R.; Gorton, L.; Antiochia, R. *Sens. Actuat. B* **2013**, *177*, 64-69; Yakovleva, M.; Buzas, O.; Matsumura, H.; Samejima, M.; Igarashi, K.; Larsson, P.-O.; Gorton, L.; Danielsson, B. *Biosens. Bioelectron.* **2012**, *31*, 251-256; Safina, G.; Ludwig, R.; Gorton, L. *Electrochim. Acta* **2010**, *55*, 7690-7695.
(13) Schulz, C.; Ludwig, R.; Micheelsen, P. O.; Silow, M.; Toscano, M. D.; Gorton, L. *Electrocchem Commun.* **2012**, *17*, 71-74.
(14) Kracher, D.; Zahma, K.; Schulz, C.; Sygmund, C.; Gorton, L.; Ludwig, R. *FEBS J.* **2015**.
(15) Harreither, W.; Nicholls, P.; Sygmund, C.; Gorton, L.; Ludwig, R. *Langmuir* **2012**, *28*, 6714-6723.
(16) Flitsch, A.; Prasetyo, E. N.; Sygmund, C.; Ludwig, R.; Nyanhongo, G. S.; Guebitz, G. M. *Enzyme Microbial Technol.* **2013**, *52*, 60-67.
(17) Baminger, U.; Subramaniam, S. S.; Renganathan, V.; Haltrich, D. *Appl. Environ. Microbiol.* **2001**, *67*, 1766-1774.
(18) Turkevich, J.; Stevenson, P. C.; Hillier, J. *Discussions of the Faraday Society* **1951**, *11*, 55-75.
(19) Larsson, T.; Lindgren, A.; Ruzgas, T.; Lindquist, S. E.; Gorton, L. *J. Electroanal. Chem.* **2000**, *482*, 1-10.

(20) Harreither, W.; Coman, V.; Ludwig, R.; Haltrich, D.; Gorton, L. *Electroanalysis* **2007**, *19*, 172-180.
(21) Lindgren, A.; Gorton, L.; Ruzgas, T.; Baminger, U.; Haltrich, D.; Schülein, M. *J. Electroanal. Chem.* **2001**, *496*, 76-81.
(22) Rabe, M.; Verdes, D.; Seeger, S. *Adv. Colloid Interface* **2011**, *162*, 87-106; Norde, W. *Colloid Surface B* **2008**, *61*, 1-9.
(23) Zámocký, M.; Schümann, C.; Sygmund, C.; O'Callaghan, J.; Dobson, A. D. W.; Ludwig, R.; Haltrich, D.; Peterbauer, C. K. *Protein Expres. Purif.* **2008**, *59*, 258-265.
(24) Xiao, Y.; Patolsky, F.; Katz, E.; Hainfeld, J. F.; Willner, I. *Science* **2003**, *299*, 1877-1881.
(25) Ramanaviciene, A.; Nastajute, G.; Snitka, V.; Kausaite, A.; German, N.; Barauskas-Memenas, D.; Ramanavicius, A. *Sens. Actuat. B* **2009**, *137*, 483-489.

Figure captions

Figure 1. (A) Schematic representations of the AuNPs used in the present work. TEM micrographs of (B) citrate coated; (C) PEI coated; and (D) PSS coated AuNPs.

Figure 2. Cyclic voltammograms of *Mt*CDH modified graphite electrodes in acetate buffer (50 mM, pH 5.5) at the scan rate of 1 mV s^{-1} in the absence (dashed line) and presence (solid line) of 10 mM lactose. The enzyme was cast on the surface of (A) GE, (B) PSS/AuNPs/GE, (C) Cit/AuNPs/GE and (D) PEI/AuNPs/GE, respectively.

Figure 3. Calibration curves for PEI/AuNPs/*Mt*CDH/GE (●) and *Mt*CDH/GE (▲) with lactose as substrate at pH 5.5 (left column) and pH 8 (right column) in the presence (C, D) and absence (A, B) of 50 mM $CaCl_2$. The calibration curves were recorded amperometrically with modified graphite electrodes mounted in a flow through cell connected to a FIA system. The buffer solutions were 50 mM NaAc, pH 5.5, or 50 mM TRIS, pH 8. The applied potential was 250 mV vs Ag|AgCl (0.1 M KCl).

Figure 4. Calibration curves for Cit/AuNPs/MtCDH/GE (◆), PSS/AuNPs/MtCDH/GE (○) and MtCDH/GE (▲) with lactose as substrate at pH 5.5 (left column) and pH 8 (right column) in the presence (C, D) and absence (A, B) of 50 mM $CaCl_2$. The buffer solutions were 50 mM NaAc, pH 5.5, or 50 mM TRIS, pH 8. The applied potential was 250 mV vs Ag|AgCl (0.1 M KCl).

Figure 5. (A)Dependence of the catalytic current densities of PEI/AuNPs/*Mt*CDH/GE (●), (B) Cit/AuNPs/*Mt*CDH/GE (◆), PSS/AuNPs/*Mt*CDH/GE (○) and *Mt*CDH/GE (▲) on the pH determined in the absence and presence (C) of 50 mM $CaCl_2$. The running buffers were 50 mM NaAc (pH 3.0-6.5), 50 mM MES (pH 6.0-7.0) and 50 mM TRIS (pH 6.5-9.0) for 10 mM lactose as substrate. The applied potential was +250 mV vs Ag|AgCl (0.1 M KCl).

Figure 6. Dependence of the cyt *c* (A) and DCIP (B) activities of *Mt*CDH (▲) on the pH in the presence of PEI/AuNPs (●), Cit/AuNPs (◆), PSS/AuNPs (○) in the measuring buffer determined with *Mt*CDH in solution with 30 mM lactose as substrate. The running buffers: 50 mM NaAc (pH 3.0-6.5), 50 mM MES (pH 6.0-7.0) and 50 mM TRIS (pH 6.5-9.0).

Figure 1.

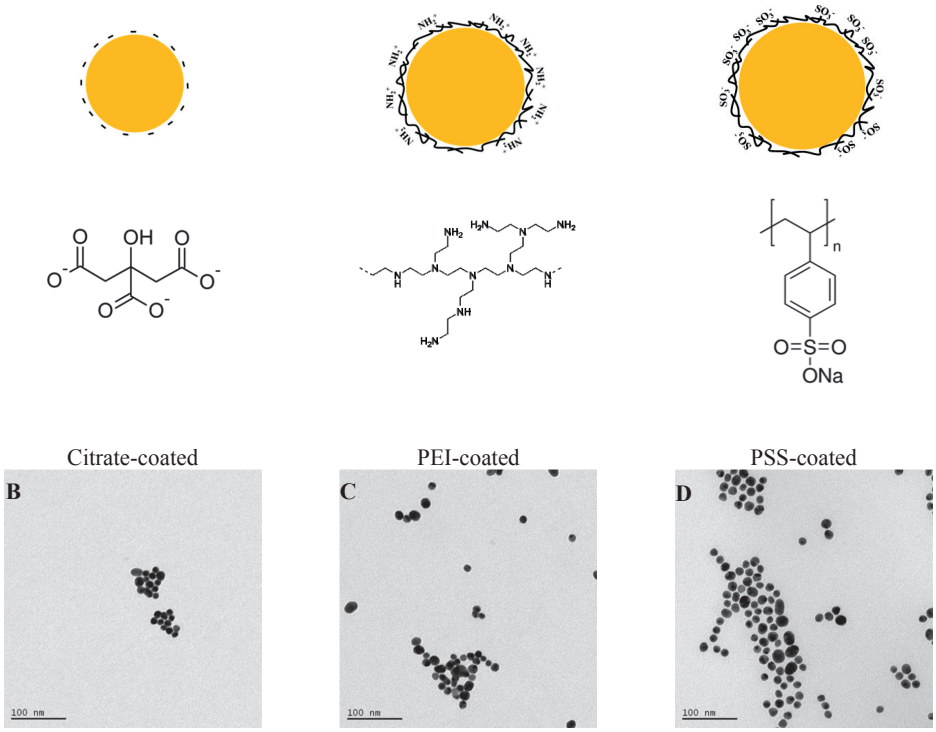

Figure 2.

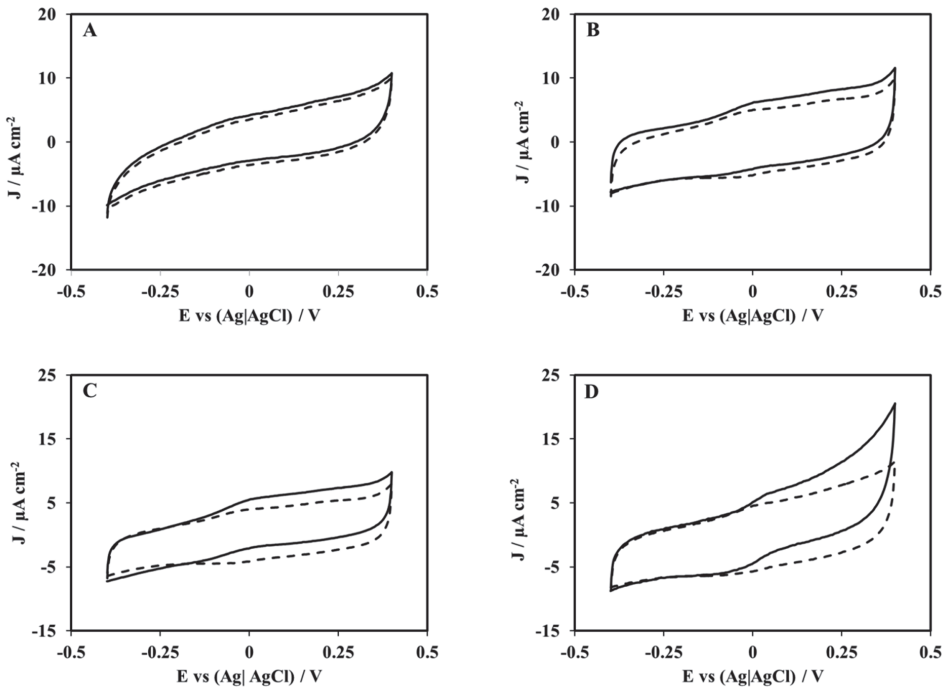
A
B
C
D
J / µA cm-2
E vs (Ag|AgCl) / V
E vs (Ag| AgCl) / V
20
10
0
-10
-20
25
15
5
-5
-15
-0.5
-0.25
0
0.25
0.5

Figure 3.

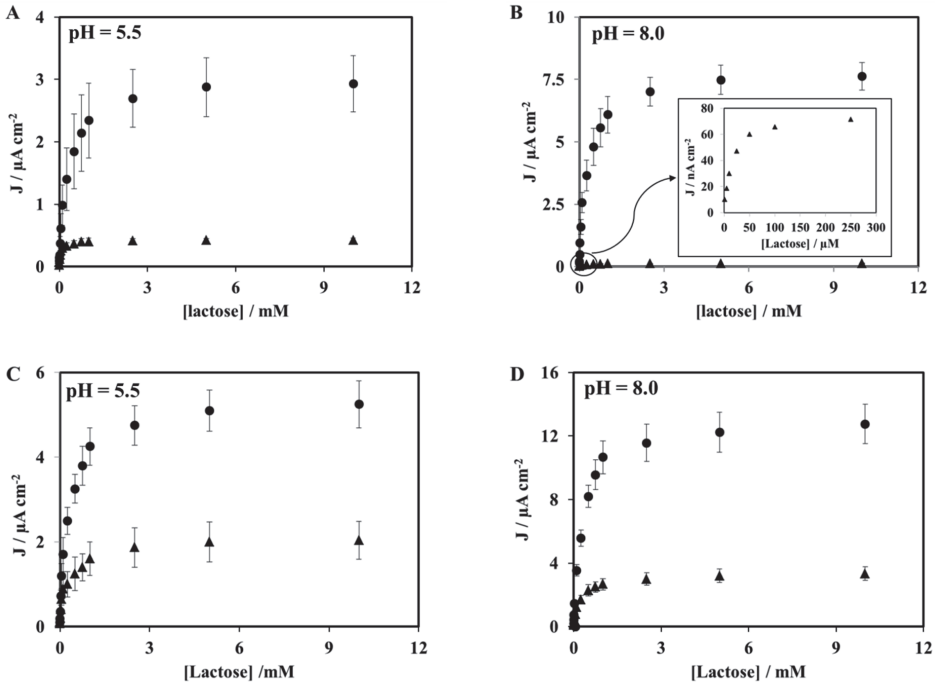
A
pH = 5.5
J / µA cm-2
[lactose] / mM
B
pH = 8.0
J / µA cm-2
[lactose] / mM
J / nA cm-2
[Lactose] / µM
C
pH = 5.5
J / µA cm-2
[Lactose] /mM
D
pH = 8.0
J / µA cm-2
[Lactose] / mM

Figure 4.

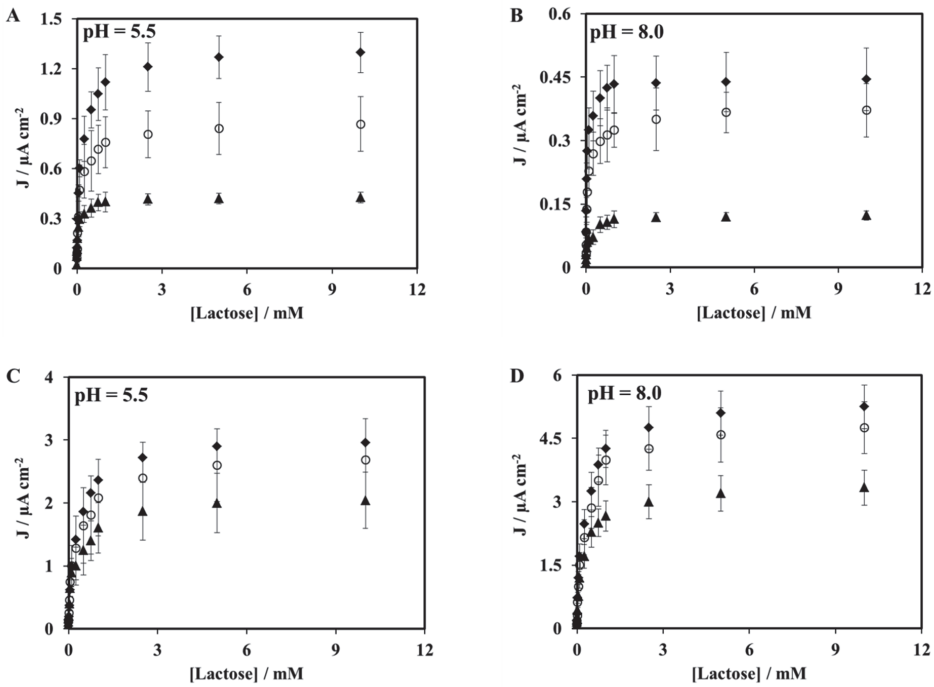
A
pH = 5.5
J / µA cm-2
[Lactose] / mM
B
pH = 8.0
J / µA cm-2
[Lactose] / mM
C
pH = 5.5
J / µA cm-2
[Lactose] / mM
D
pH = 8.0
J / µA cm-2
[Lactose] / mM

Figure 5.

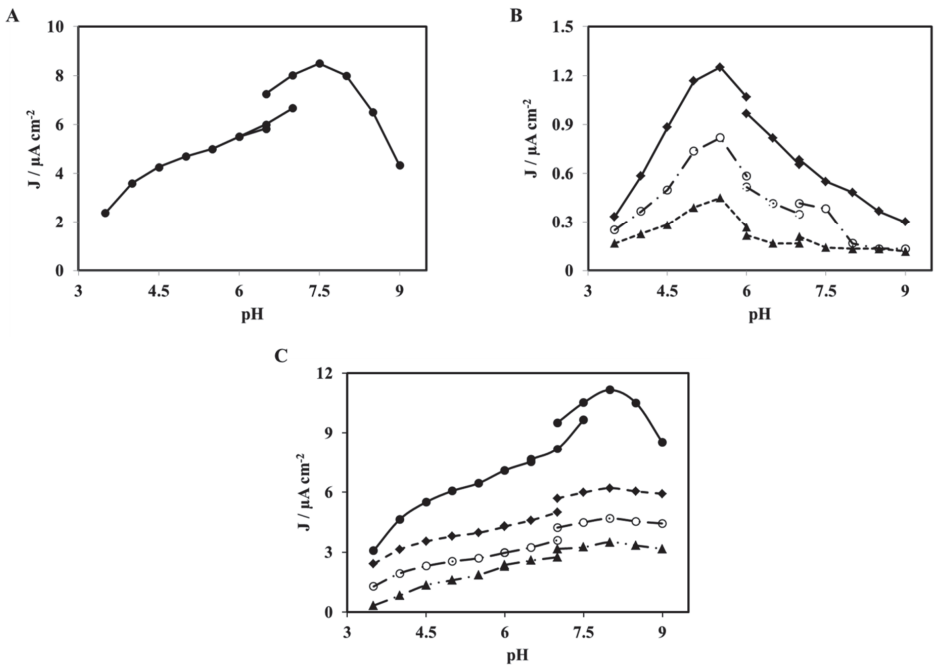

Figure 6.

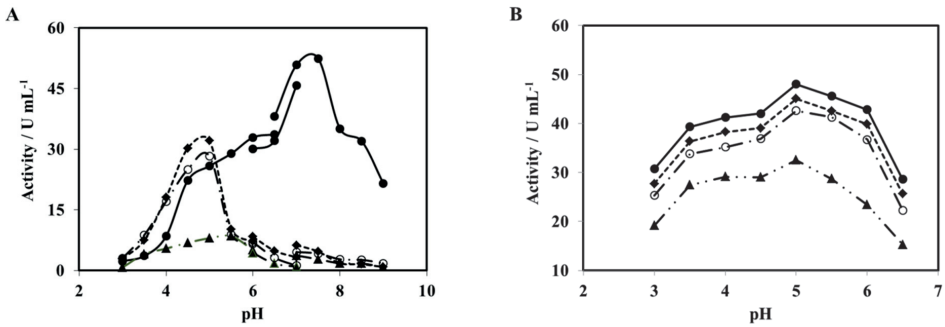

Table 1. J_{max}, and K_M^{app} for *Mt*CDH immobilized on graphite electrodes or on graphite electrodes premodified with positively (PEI) or negatively (Cit, PSS) charged AuNPs with lactose as substrate at pH 5.5 and pH 8 in the presence and in the absence of 50 mM $CaCl_2$.

Graphite electrode +	Buffer: pH ± $CaCl_2$	J_{max} ± SD / nA cm^{-2}	K_M^{app} ± SD / µM
PEI/AuNPs/*MtCDH*	5.5	3063 ± 470	271 ± 14
	5.5 + $CaCl_2$	5411 ± 514	273 ± 24
	8	7702 ± 515	252 ± 17
	8 + $CaCl_2$	13409 ± 689	284 ± 16
Cit/AuNPs/*MtCDH*	5.5	1282 ± 127	120 ± 15
	5.5 + $CaCl_2$	2993 ± 550	153 ± 19
	8	438 ± 70	38 ± 10
	8 + $CaCl_2$	5306 ± 513	160 ± 21
PSS/AuNPs/*MtCDH*	5.5	852 ± 157	193 ± 12
	5.5 + $CaCl_2$	2670 ± 521	236 ± 35
	8	357 ± 57	150 ± 17
	8 + $CaCl_2$	4876 ± 574	278 ± 24
MtCDH	5.5	415 ± 35	34 ± 4
	5.5 + $CaCl_2$	1998 ± 420	81 ± 18
	8	117 ± 12	56 ± 11
	8 + $CaCl_2$	3367 ± 465	93 ± 23

Paper X

Direct electron transfer from the FAD of cellobiose dehydrogenase to electrodes

Christopher Schulz[a], Roman Kittl[b], Roland Ludwig[b], Lo Gorton[a]
[a] Department of Biochemistry and Structural Biology, Lund University, SE-22100 Lund, Sweden
[b] Department of Food Sciences and Technology, Food Biotechnology Laboratory, BOKU-University of Natural Resources and Life Sciences, Muthgasse 18, A-1190 Vienna, Austria

Abstract
Cellobiose dehydrogenase (CDH) is an interesting candidate for the construction of biosensors and biofuel cell anodes. The flavin adenine dinucleotide (FAD) containing, catalytic domain of the enzyme oxidizes carbohydrates, while the cytochrome *b* containing, electron mediating domain, shuttles the electrons to the electrode. Here we report for the first time in an unequivocal manner on the possibility of a direct electric communication between the FAD containing catalytic domain and electrodes by showing clear non-turnover voltammetric waves in the absence and turnover waves in the presence of substrate by using cyclic voltammetry and square wave voltammetry. Results were obtained by entrapping CDH under a dialysis membrane on alkanethiol modified, polycrystalline gold electrodes. Direct electron transfer (DET) from the FAD cofactor occurs at potentials roughly 130 mV more negative than the previously reported and established DET from the electron mediating, cytochrome *b* containing domain to electrodes. However, direct electrochemistry was only observed for two types of basidiomycete class I CDHs from *Trametes villosa* and *Phanerochaete sordida* and at pH values below 5 and not for some ascomycete class II CDHs investigated under the same experimental conditions. The present findings are of high interest for the development of biosensors and biofuel cells, since a lower substrate oxidation potential decreases the occurrence of interfering reactions and potentially increases the cell voltage in biofuel cells. Furthermore, these findings may also be transferrable to structurally related enzymes such as glucose oxidase and glucose dehydrogenase.

Introduction
Cellobiose dehydrogenase (CDH, EC number: 1.1.99.18) is a monomeric oxidoreductase consisting of two domains secreted by wood degrading fungi. The catalytic dehydrogenase domain (DH) contains one flavin adenine dinucleotide (FAD) molecule as cofactor and is connected via a flexible linker to an electron mediating cytochrome domain (CYT) featuring a *b*-type heme cofactor. CDH is involved in the degradation process of cellulose, during which it oxidizes cellobiose formed as product of the cleavage of cellulose by cellulases. The oxidation of the substrate by CDH leads to the full reduction of the FAD cofactor to $FADH_2$ located in the DH domain.[1-4] Those two electrons can be donated from the DH domain to various 2-electron/2-proton and 1-electron/no-proton acceptors/mediators such as 1,4-benzoquinone, 2,6-dichlorophenolindophenol, or osmium redox polymers, but have never been unequivocally proven to be donated directly by DH to electrode surfaces in a true mediatorless fashion.[2-6] Instead a direct electrical communication between CDH and electrodes was always found to rely on the presence of the CYT domain.[2, 7] To achieve this, the electrons stored in the reduced DH domain are transferred via an internal electron transfer step (IET) to the CYT domain leading to the reduction of the heme *b* cofactor. In a final direct electron transfer (DET) step the electrons are transferred, one by one, directly to an electrode surface leading to a reoxidized CYT domain. In nature the final electron acceptors were found to be copper dependent, lytic polysaccharide monooxygenases (LPMOs, CAZY AA9).[8-9] The reduced LPMOs were suggested to react with molecular oxygen to form reactive oxygen radicals assisting in the decomposition of the lignocellulose matrix.
CDH is produced by the fungi of the phyla Ascomycota and Basidiomycota, represented by a phylogenetic classification of class II and class I CDHs respectively.[3] A third class of CDHs has been suggested based on sequenced genomes but the secretion of any class III CDH has not yet been confirmed.[10-11] The natural substrates for CDH are breakdown products of cellulose, viz. cellodextrins including cellobiose. The structurally similar molecule lactose is also efficiently oxidized by all class I

and II CDHs as well. Class I CDHs have shorter amino acid sequences and pH optima in the acidic pH range. Class II CDHs can have pH optima also in the human physiological pH range and some are able to also oxidize glucose and other mono- and disaccharides although with lower efficiencies.[1, 12-13]
Recently, we gained more insight into how positive charges definitely affect the performance of CDH in solution as well as when immobilized on an electrode surface increasing the registered catalytic current. Most CDHs have isoelectric points in the acidic range between pH 3 and 5.[1, 3] Divalent cations as Ca^{2+} or Mg^{2+} were found to increase the IET of some CDHs possibly by screening negative, repulsing charges present at the interface of the CYT and DH domains decreasing the distance the electrons need surpass from the DH domain to the CYT domain leading to an increased rate of the IET.[14 FEBS] These effects were highest in the neutral/alkaline pH range, where both domains of CDH are highly negatively charged. Similar, beneficial effects were also observed when positively charged polycations such as polyethylenimine (PEI) or polydiallyldimethyl ammonium chloride (PDADMAC) were used as immobilization matrices for CDH onto gold or graphite surfaces.[15-17] In both cases, using Ca^{2+} and polycations, catalytic currents were increased by up to 140 times being advantageous in both biosensor and biofuel cell applications.
CDH has been used to construct a variety of biosensors for the detection of e. g., lactose and glucose but also ATP and pollutants such as phenolic compounds.[16-20] Biofuel cell anodes based on CDH using lactose and glucose as fuel were shown to be promising applications as well.[2, 19, 21-23] For both applications, biosensors and biofuel cell anodes, not only a high catalytic current but also a low electric potential, at which the electric communication with CDH occurs, is preferable to minimize the oxidation of possibly interfering compounds and to increase the cell voltage when developing biofuel cells.
In the present paper the possibility of electrically communicating directly with the sugar oxidizing DH domain at an unprecedented low potential is presented. The distance between the FAD located in the DH domain to the surface of the enzyme is about 12-15 Å[24], theoretically allowing DET by electron tunneling.[25] Indications of the possibility of directly communicating with the DH domain of CDH have been presented already in 2000, 2005 and 2007 by Lindgren et al., Stoica et al. and Coman et al. respectively, and later by others but has never been proven unequivocally.[26-30] Clear, indisputable proofs of DET with the bound flavin cofactor of sugar oxidizing enzymes, showing both, a non-catalytic/non-turnover wave and a coinciding catalytic wave in the presence of substrate are rare, not to say absent applying the above criteria rigorously. Indications for a direct electric communication with the FAD cofactor of a sugar oxidizing enzyme were shown by Courjean et al. for glucose oxidase (GOx) immobilized on a glassy carbon electrode with a catalytic current visible at potentials as low as -420 mV vs. Ag | AgCl at pH 7.4[31], which is close to the potential of the FAD bound in GOx.[32] Holland et al. immobilized GOx site-specifically onto gold nanoparticles and showed promising onsets of catalytic currents at potentials around the enzyme bound FAD.[33] Further enzymes where DET for the FAD cofactor might have been achieved are pyranose dehydrogenase (PDH) immobilized on graphite electrodes[34-35] and FAD dependent glucose dehydrogenase (GDH) immobilized on gold electrodes modified with gold nanoparticles.[36] However, no *coinciding,* non-catalytic waves originating from the electrochemistry of the FAD cofactor located *in* the enzyme were presented in any case. In the cases of GOx[31] and PDH, DET was only possible after (partial) deglycosylation of the respective enzyme, indicating the insulating and electron transfer distance increasing properties of the glycans present on the surface of the enzymes.[31, 34] In the present paper we present for the first time clear proofs of direct electric communication between a glycosylated, FAD containing domain of a sugar oxidizing enzyme and an electrode showing non-catalytic waves and coinciding catalytic waves obtained from cyclic voltammetric measurements.

Experimental

Chemicals

Sodium acetate (NaAc), 3-(N-morpholino)propansulfonic acid (MOPS), hydrogen peroxide, sulfuric acid, lactose, glucose, poly(diallyldimethylammonium chloride) solution (20% wt, PDADMAC), 6-mercapto-1-hexanol (97% purity), 11-mercapto-1-undecanol (MUDOH, 97% and 99% purity), flavin adenine dinucleotide disodium salt (FAD), and riboflavin were obtained from Sigma-Aldrich (St. Louis, MO, USA). Sodium hydroxide was obtained from Scharlau Chemie S. A. (Barcelona, Spain) and calcium chloride was obtained from Merck KgaA (Darmstadt, Germany). The thiol N-(5-mercapto) pentylpyridinium (MPP) was similarly synthesized as described here[37]. All chemicals were of analytical grade if not stated differently.

Enzymes and buffers

The various CDHs investigated were either recombinantly expressed in *Pichia pastoris* (referred to as rec*Xx*CDH) or produced by the respective fungus and purified (referred to as *Xx*CDH). The recombinant expression in *Pichia pastoris* is known to glycosylate CDH to a greater extent than the naturally produced one.[38-39] Class I CDHs investigated were CDHs from *Trametes villosa* (*Tv*CDH[40] and rec*Tv*CDH) and *Phanerochaete sordida* (*Ps*CDH[40-41]). Class II CDHs investigated were CDHs from *Myriococcum thermophilum* (rec*Mt*CDH[42]), *Corynascus thermophilus*, (syn. *Chaetomidium thermophilum*, ana. *Myceliophthora fergusii*) (rec*Ct*CDH[43]) and a mutant of rec*Ct*CDH with enhanced glucose turnover (rec*Ct*CDHC291Y[44]). The concentrations of the enzymes were determined photometrically using the absorption at 280 nm and a molar extinction coefficient calculated from the amino acid sequence using a web-based calculator (http://www.biomol.net/en/tools/proteinextinction.htm). The concentrations of the enzyme stock solutions are given in Supplementary Information Table S1.

As buffers 50 mM NaAc and 50 mM MOPS were used. The pH was adjusted using concentrated sodium hydroxide or hydrochloric acid solutions.

Isolation and expression of TvCDH

For the isolation of the full-length cDNA for *Trametes villosa* CDH the fungal mycelium was squeezed dry between filter papers and homogenized with the Precellys 24 homogenizer (Peqlab Biotechnologie GmbH, Erlangen, GER) using 0.5 mm glass beads and 700 µl of the breaking buffer of the Spektrum Plant Total RNA Kit (Sigma, Steinheim, GER). The RNA was reverse transcribed with the High Capacity cDNA Reverse Transcription Kit (Applied Biosystems, Foster City, CA, USA) using the Anchor2 primer (Supplemental Table S2). The reaction was incubated for 10 min at 25°C (annealing), 120 min at 37°C (elongation), and 20 s at 85°C (reverse transcriptase inactivation). Restriction enzymes and T4 ligase were obtained from Fermentas (St. Leon-Rot, Germany) and used as recommended. Nucleic acid amplifications were done using Phusion proof-reading polymerase (New England Biolabs, Beverly, MA, USA), dNTP mix, oligonucleotide- primers (VBC Biotech, Vienna, Austria) and a Biometra TRIO thermocycler (Biometra, Göttingen, Germany). The primer annealing temperature was 55°C. The translated amino acid sequence of the obtained cDNA was analyzed using the program SignalP 3.0 at http://www.cbs.dtu.dk/services/SignalP/ (Nielsen et al. 1997, Bendtsen et al. 2004).

For expression with the native signal sequence the cDNA (Supplemental Table S2) was amplified with the primer pair 5TVBstB1 and 3ECV, digested and cloned into the equally cut vectors pPICZαA. Thereby the α–factor sequence of the vector was removed and the start codon of the CDH gene was placed on the position of the α–factor ATG. The resulting plasmid was linearized and transformed into *Pichia pastoris* X33. For secreted expression of the CDH cDNA with the native signal sequence in *Pichia pastori*s the cDNA was amplified with the primer pair 5TVBstB1 and 3ECV, digested with the restriction enzymes BstBI and XbaI and cloned into the equally cut expression vector pPICZαA (Invitrogen, Carlsbad, CA, USA). The ligation mixture was transformed into chemically competent *E. coli* DH5α (Invitrogen). The presence of the correctly inserted PCR product was confirmed by restriction enzyme digestion and sequencing. The confirmed plasmid was linearized with XmaJI at 37°C for 3 h and transformed into the *Pichia pastoris* strain X33. Electrocompetent *P. pastoris* cells

were prepared and transformed following the protocol of Cregg and Russell.[45] The selective plates were incubated at 30°C for 3 days. Positive transformants were selected in a deep-well microtiter plate screening using in BMM (100 mM potassium phosphate buffer, pH 6.0, 13.4 g/l yeast nitrogen base without amino acids and ammonium sulfate (Amresco, Solon, OH, USA), 1% ammonium sulfate, 400 µg/l biotin, 0.5% methanol). CDH activity was detected by the DCIP assay.[40] The most productive clone was employed in a fed-batch fermentation following the *Pichia* fermentation process guidelines (Invitrogen) using a Multifors fermenter (Infors, Wetzikon, Switzerland). The temperature was set to 28°C, the pH to 5.0 and the fed-batch medium was 100% methanol with trace elements. The supernatant of the fermentation was dialyzed and applied to an AIEX column equilibrated with a 50 mM sodium-MES buffer, pH 6.5 and eluted with a gradient with a 50 mM sodium-MES buffer, pH 6.5, 0.5 M NaCl. The second step was a hydrophobic interaction chromatography with a 100 mM NaAc buffer, pH 5.0, 20% $(NH_4)_2SO_4$ and 0.2 M NaCl. Elution was done with 50 mM NaAc buffer, pH 5.0.

Electrochemical measurements

Polycrystalline gold electrodes (diameter=1.6 mm, BASi, West Lafayette, IN, USA) were incubated in a Piranha solution for 2 min (3:1 conc. sulfuric acid and conc. hydrogen peroxide). ***Careful, hydrogen peroxide and sulfuric acid react violently and highly exothermic with each other***. The gold electrodes were rinsed with water and polished on polishing cloth with deagglomerated alumina slurry with particle diameters of first 1 µm and then 0.1 µm. In between and after polishing the electrodes were sonicated for 5 min in ultrapure water. This was followed by an electrochemical cleaning step by cycling between 0.1 and 1.7 V vs. a saturated calomel reference electrodes (SCE, 244 mV vs. SHE) for 30 times at a speed of 300 mV/s in 0.5 M sulfuric acid. Afterwards the electrodes were rinsed with ultrapure water, dried with nitrogen and incubated in a 10 mM ethanolic solution of the respective thiol overnight at room temperature. The electrodes were rinsed with ultrapure water, excess liquid was shaken off, then a drop of 1.5 µl of enzyme solution was spread on the electrode surface and entrapped under a pre-soaked dialysis membrane (Spectrapor, MWCO 12-14 kDa, Spectrum Medical Industries, CA, USA), which was fixed with a rubber O-ring and Parafilm (Bemis, Neenah, WI, USA). Electrochemical measurements were done in a glass vessel filled with 50 ml of buffer solution, which was degassed with nitrogen for 20 min prior to measurements. For cyclic voltammetry an Autolab PGSTAT30 (Metrohm Autolab B.V., Utrecht, The Netherlands) was used. For square wave voltammetry a Palmsens EmStat2 (PalmSens BV, Utrecht, The Netherlands) was used with the following parameters: Amplitude of 10 mV, step potential of 1 mV, frequency of 1 Hz. For all experiments a SCE and a platinum flag counter electrode were used. Potential values below are given vs. SCE.

Results and Discussion

Electrochemistry of wild-type TvCDH and PsCDH

In Figure 1, we show direct electrochemistry of the class I *Trametes villosa* CDH (*Tv*CDH, harvested and purified from the fungal culture) entrapped under a dialysis membrane fixed onto a MUDOH modified gold electrode measured at pH 3.0. As expected from previous investigations[7, 28], two well defined waves originating from the oxidation and reduction of the heme *b* located in the CYT are clearly visible forming one redox wave with a midpoint potential of -40 mV. In addition, a well-defined, more narrow oxidation peak and a less defined reduction peak are visible forming a second voltammetric wave with a midpoint potential of -162 mV originating from the bound FAD cofactor. The addition of lactose induces a clear catalytic wave in the voltammogram with catalytic currents being visible already at the potential of the oxidation peak of the bound FAD. This suggests that the observed electrochemistry of FAD originates from FAD located in the DH and qualifies for the claim of true DET between the DH domain and the electrode. To exclude free FAD being responsible for

mediating the electron transfer between the DH and the electrode the more sensitive technique square wave voltammetry was used instead of cyclic voltammetry and a ten-fold stoichiometric excess of FAD over CDH was added to the measuring solution in a pH range between pH 3.0 and 6.0. As shown in Fig. 2, free FAD has a much lower midpoint potential (-316±1 mV at pH 4.5) than FAD located in the DH (-221±3 mV at pH 4.5), which is true for the whole investigated pH range. The midpoint potential of free FAD shifted with 64±3 mV/pH, reflecting 2 e^- and 2 H^+ being involved in the reaction. The obtained values for free FAD agree well with midpoint potentials estimated and recalculated from the literature ranging between -310 to -344 mV for gold, mercury, titanium and graphite electrodes.[46-49] Adding lactose inducing a catalytic current leads to a catalytic wave starting at the potential of the FAD located in the DH domain. The additionally added, free FAD does not affect the DET from DH and can therefore be excluded as a possible redox mediator.

When increasing the scan rate the oxidation peak of the DH domain and the CYT domain cannot be discriminated any more at scan rates higher than 50 mV/s (at pH 3.0, Fig. 1). The electrochemistry of the CYT domain is visible even up to the highest tested scan rate of 1000 mV/s. This indicates that the rate of electron transfer rate between the electrode and the DH domain is slower than that via the CYT domain. This is also supported by the peak width at half height, which theoretically should be 45 mV for a 2 e^- and 90 mV for a 1 e^- transfer process. The obtained values of 56 mV for DH and 88 mV for CYT (see Supplementary Information Table S3) support a probably kinetically limited 2 e^- transfer process originating from the FAD cofactor and a 1 e^- transfer process originating from the heme *b* located in the CYT domain.

A further class I CDH, *Ps*CDH, was tested, which was also harvested and purified from the fungal culture. As shown in Supplementary Information Fig. S4 also here direct electrochemistry with both domains is possible exhibiting similar pH and scan rate dependencies as *Tv*CDH (see Supplementary Information Table S3). *Ps*CDH was previously shown to be a very efficient CDH for DET[50] and has been used for the measurement of e. g. lactose in real samples as milk[18] and for at-line monitoring of lactose in a dairy processing plant[51].

Electrochemistry of recombinantly expressed TvCDH

The over-expression of proteins as CDH in expression systems as *Pichia pastoris* leads to much higher protein yields enabling more in depths investigations of the protein of interest. However, the expression of proteins in *Pichia pastoris* is also known to potentially over-glycosylate them[38-39] hindering the electron transfer between redox enzymes and electrode surfaces.[31, 34] Thus, we also investigated the electron transfer from class I rec*Tv*CDH, which was recombinantly over-expressed in *Pichia pastoris*.

As shown in Fig 3, DET from the DH of rec*Tv*CDH is possible as well. The electrochemistry of both, the CYT and the DH are best visible at pH 3 with midpoint potentials of -28 mV and -144 mV respectively (see Figs. 3 and 4). Also, the addition of lactose induces a catalytic wave starting at the oxidation potential of the FAD cofactor located in the DH. As shown in the insets of Fig. 4 (and more clear in Supplementary Figure S5) the catalytic currents decrease with increasing pH and are kinetically limited by the electron transfer from the DH and CYT to the electrode.

The midpoint potentials of the CYT and the DH domains of rec*Tv*CDH were slightly more positive (12 mV and 18 mV respectively, see Supplementary Information Table S3) compared to the ones of *Tv*CDH. Possibly a higher degree of glycosylation due to the expression in *Pichia pastoris* affects the midpoint potentials of both domains and thus the electric communication with rec*Tv*CDH. The higher peak separation observed for the DH peak of rec*Tv*CDH (ΔE_p=91 mV) compared to *Tv*CDH (ΔE_p=36 mV) indicates kinetic restrictions of the DET reaction possibly due to its more heavily glycosylated surface.

The electrochemistry of the DH domain of rec*Tv*CDH is maximal at the lowest investigated pH of 3.0 and visible up to pH 5.0 (Fig. 4 and Supplementary Information Table S3). Similar pH dependencies were observed for *Ps*CDH and *Tv*CDH (Fig. 1, Supplementary Information Table S3, and Supplementary Information Figure S4). DET from the DH domain is only possible at acidic pHs.

However, catalytic currents are visible even at pH values above pH 5 via DET of the CYT meaning that the DH domain is still catalytically active, only DET is not possible (Fig. 4 and Supplementary Information Fig. S5).
We can exclude changes in the secondary structure of rec*Tv*CDH when changing the pH from 3 to 4.5 and 6, since no pH induced differences in the circular dichroism spectra in the UV range were observed (see Supplementary Information Fig. S6)

One hypothesis to explain DET from DH being possible only at acidic pHs is that at pH values below the isoelectric point of the enzyme (Supplementary Information Table S1) the interacting surfaces of the DH and CYT domains are positively charged[52] so that both domains might repel each other sufficiently so that the DH domain is more accessible for DET. However, this is valid also at pH values well above the pI of the enzyme but no DET from any DH was observed at neutral or alkaline pHs up to pH 8.0. The replacement of uncharged MUDOH by MPP, carrying a positively charged, quaternary ammonium group to attract the negatively charged DH domain at pH 8.0 also did not enable DET of DH. Hence as for MUDOH, at pH 3.0 DET of DH was visible for rec*Tv*CDH on positively charged MPP (Supplementary Information Fig. S7). Assuming a neutral to slight positive charge for the DH at pH 3 this indicates that rather the CYT-DH interaction (or non-interaction) than the electrode-CDH interaction is determining the possibility of DET from DH.
Another hypothesis for the breakdown of DET from DH at pH > 5 might be a strong interaction of the heme propionate of CYT with an arginine residue present at the substrate tunnel of DH (at position 586 for class I *Pc*CDH; PDB accession code: 1KDG) at pH values above pH 3.5. Negatively charged heme propionate groups (pK_a around 3.5[53]) are known to form strong electrostatic interactions with arginines (positively charged at pH <12).[54] A strong propionate-arginine interaction at elevated pH values might hinder a DET from the DH. Such an ionic propionate-arginine interaction was also observed for the recently chrystallized, full length *Mt*CDH.[55] Whether the CYT-DH domain interaction is the crucial factor in determining the possibility of DET from DH is planned to be tested in the future with a separately expressed DH domain of rec*Tv*CDH, lacking the CYT domain.
Very interesting is also the presence of aromatic amino acids around the substrate tunnel of the DH in conjunction with a glutamic acid residue within this patch (at position 70 for class I CDH *Pc*CDH; structure code 1KDG). The aromatic amino acids might play a role in the DET from the DH to the electrode since aromatic amino acids are known to facilitate electron transfer.[56-58] A deprotonated glutamic acid residue (solution pK_a of 4.2[59]) at elevated pH might hinder the transport of charges from the DH along the aromatic amino acid patch to the electrode. The suggested amino acid pattern of interest (FExxFxxxxxxWWxxxxxxF) is conserved and present in many class I CDHs as *Pc*CDH and the here investigated *Tv*CDH. Single point mutations at position 70 might support its crucial influence on the DET of DH and are planned to be executed in the future.
The contribution of protonable groups with a pK_a in the acidic region to the possibility of DET from DH is also highlighted by the following observation. The dependency of the oxidation peak potentials of DH on the pH is greater at lower pHs. Between pH 3 to 4 an averaged shift 48±1 mV/pH was observed. Between pH 4 to 5 a shift of 22 ± 16 mV/pH was observed (Supplementary Information Table S3, values averaged from all class I CDHs). Assuming a two electron oxidation of the FAD this points to the involvement of rather 2 protons between pH 3 and 4 ($FAD + 2e^- + 2H^+ \rightleftharpoons FADH_2$) compared to rather 1 or no proton at pH values above pH 4 ($FAD + 2e^- + H^+ \rightleftharpoons FADH^-$) during the full redox reaction of the FAD cofactor located in the DH domain. Contrary, free FAD exhibits a shift of the midpoint potential of 64±2 mV/pH even up to a pH of 6 as experimentally determined and discussed below, indicating a $2H^+/2e^-$ redox mechanism. This reflects further involvement of protonable groups, most likely amino acids, in the redox conversion of the enzyme bound FAD.
Vogt et al. found for FAD dependent GOx from *Aspergillus niger* a dependence of the midpoint potential by a change of 57 mV/pH in the region between pH 4.5 to 7.4, suggesting a $2H^+/2e^-$ redox mechanism of the FAD cofactor.[46] At pH values between pH 7.6 and 8.5 the slope decreased to 27 mV/pH, indicating a $1H^+/2e^-$ redox mechanism of FAD. Apparently, the switch from a $2H^+/2e^-$ to a

$1H^+/2e^-$ redox conversion of FAD happens at much lower pHs in the case of CDH, indicating structural differences of the catalytic site in spite of many similarities, since both, CDH and GOx belong to the same glucose-methanol-choline oxidoreductase family (GMC).[24] In CDH the catalytic site located at the *re*-face of the flavin ring includes two conserved residues, asparagine and histidine. Contrary, in GOx there are two histidines instead.[60] The asparagine in CDH is suggested to further facilitate the proton abstraction from the substrate by the histidine residue.[60] This might contribute to a catalytic activity of CDH in a rather proton rich, acidic environment.

A further interesting observation is the larger size of the oxidation peak of the DH domain compared to its reduction peak (see Figs. 1, 3, 4). Together with the restricted visibility of the DET of the DH domain limited to only acidic pH values this again highlights the importance of protons being involved in the redox reaction of the FAD. Possibly the non-catalytic re-protonation of the flavin cofactor during its reduction (by the electrode) is limited by the availability of protons making it the rate limiting step at increasing pH values.[30] Similar observations have been made for FAD dependent GOx from *Aspergillus niger,* which shares a very similar active site as CDH.[24] At pH values below pH 5 the reduction of the FAD (by glucose) was found to be the rate limiting step.[61]

The effect of the length of the thiol on the DET of recTvCDH

Insights into the dependence of the rate of the electrochemistry of the DH domain on the distance was gained when rec*Tv*CDH was investigated also on gold electrodes modified with the shorter MHOH (see Fig. 5 and compare with Fig. 3). The ΔE_p between the oxidation and reduction peaks of the DH domain was decreased from 91 mV on MUDOH to 40 mV on MHOH, whereas the E°'s did no vary significantly (see Supplementary Information Table S3). The oxidation peak of DH was distinguishable up to 100 mV/s from the oxidation peak of CYT when MHOH was used instead of MUDOH (see Fig. 5), suggesting a faster rate of electron transfer on the MHOH modified surface. However, the pH dependency of DET between the electrode and the DH domain was similar, above pH 5 no DET from the DH is visible even on the shorter MHOH (see Supplementary Information Fig. S8). This suggests that both, distance and pH, are crucial but independent parameters influencing the electrochemistry between the electrode and DH.

Comparison of class I and class II CDHs

The investigated class II CDHs, viz. rec*Mt*CDH, rec*Ct*CDH and rec*Ct*CDHC291Y, did not allow a direct electric communication with the DH domain at any pH (see Fig. 6 and Supplementary Information Fig. S4). Class II CDHs were tested on electrodes modified with MUDOH and MHOH, but also with the polycation PDADMAC[17], at low scan rates as low as to 2 mV/s, in the presence of $CaCl_2$[14] and at pH values as high as pH 8 (data not shown). The electrochemistry of the CYT of the class II CDHs were comparable to the ones of class I CDHs (see Supplementary Information Table S3) but in no case DET from the DH was observed. Indications for a possible DET of DH at pH 5.5 were recently found for *Mt*CDH immobilized on gold and silver electrodes modified with the polycation polydiallyldimethylammonium chloride in the presence of 10 mM $CaCl_2$ investigated with cyclic voltammetry, surface enhanced resonance Raman and surface enhanced infrared spectroscopy.[29] However, in the present investigation we have not observed DET from DH on PDADMAC modified electrodes neither in the absence nor in the presence of $CaCl_2$.

All tested class I CDHs exhibit DET from the DH, but none of the tested class II CDHs do. However, the number of CDHs tested is certainly not enough to derive a secure class difference here. If the hints of a class difference were to be reasoned, one might focus on the amino acids forming the substrate channel assuming that they might assists in the electron transfer pathway from the DH to the electrode. The above mentioned amino acid pattern consisting of aromatic amino acids and one glutamic acid (FExxFxxxxxxWWxxxxxxF) is only present in class I CDHs and might be used to further investigate a potential class difference with respect to the possibility of DET from DH.

Conclusions

To the best of our knowledge we have shown in an unequivocal manner that DET from the FAD containing catalytic domain of CDH to a gold electrode modified with only the alkanethiol MUDOH or MHOH is possible. DET from DH was observed for the tested class I CDHs at pH values below 5 and at scan rates of up to 100 mV/s. The DET from DH occurs at potentials roughly 130 mV more negative than the usually observed DET of CYT. No DET from DH of class II CDHs could yet be achieved. The findings are of both fundamental interest to shed further light into biological charge transfer reactions as well as for the construction of biosensors and biofuel cell anodes, since lower potentials prevent the oxidation of interfering compounds and increase the overall obtained cell voltage when applied to biofuel cell anodes. Furthermore, the results give more insights into the electron transfer mechanism of CDH stressing once more the differences between class I and class II CDHs.

Acknowledgements

We kindly acknowledge Dr. Olegas Eicher-Lorka for the sample of MPP (Department of Organic Chemistry, Center for Physical Sciences and Technology, Vilnius, Lithuania), Dr. Sebastian Rämisch for performing circular dichroism spectroscopy measurements and discussing biochemical aspects of CDH (Lund University, Lund, Sweden) and Dr. Roberto Ortiz for constructive discussions about the ET of CDH (Technical University of Denmark, Kungens Lyngby, Denmark). We want to acknowledge the following institutions for financial support: The Swedish Research Council (grants 2010-5031 and 2014-5908) and the European Commission ("Chebana" FP7-PEOPLE-2010-ITN-264772, "Bioenergy" FP7-PEOPLE-2013-ITN-607793).

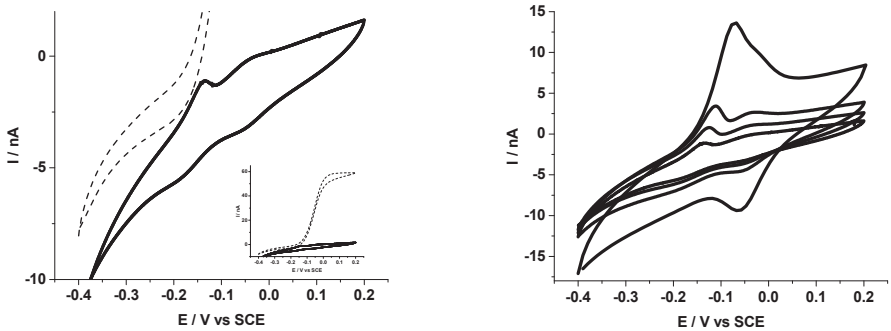

Figure 1. Cyclic voltammograms of *Tv*CDH on MUDOH modified gold electrodes at pH 3.0 at a scan rate of 5 mV/s (left) in the absence (solid line) and in the presence of 1 mM lactose (dashed line) with the full extent of the catalytic curve as inset and (right) at scan rates of 5, 10, 20 and 50 mV/s from inner to outer curve.

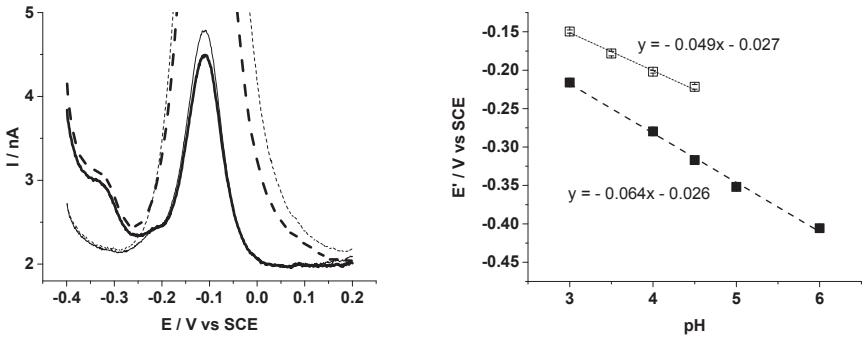

Figure 2. (Left part) Square wave voltammograms of *Tv*CDH on MUDOH modified gold electrodes at pH 4.5 in the absence (thin lines) and in the presence of additional 1.4 mM FAD (thick lines) without (solid lines) and with 1 mM lactose as substrate (dashed lines). (Right part) Plot of the midpoint potential of free FAD (filled squares) and the DH (empty squares) versus pH extracted from square wave voltammograms with the equation from the linear fit of the data points (R^2 = 1 and 0.99 respectively).

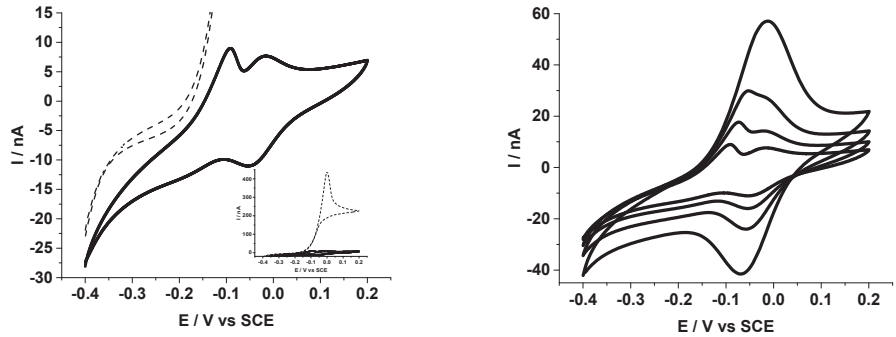

Figure 3. Cyclic voltammograms of rec*Tv*CDH on MUDOH modified gold electrodes at pH 3.0 at a scan rate of 5 mV/s (left) in the absence (solid line) and in the presence of 1 mM lactose (dashed line) and (right) at scan rates of 5, 10, 20 and 50 mV/s from inner to outer curve. The insert in the left part shows the entire catalytic wave.

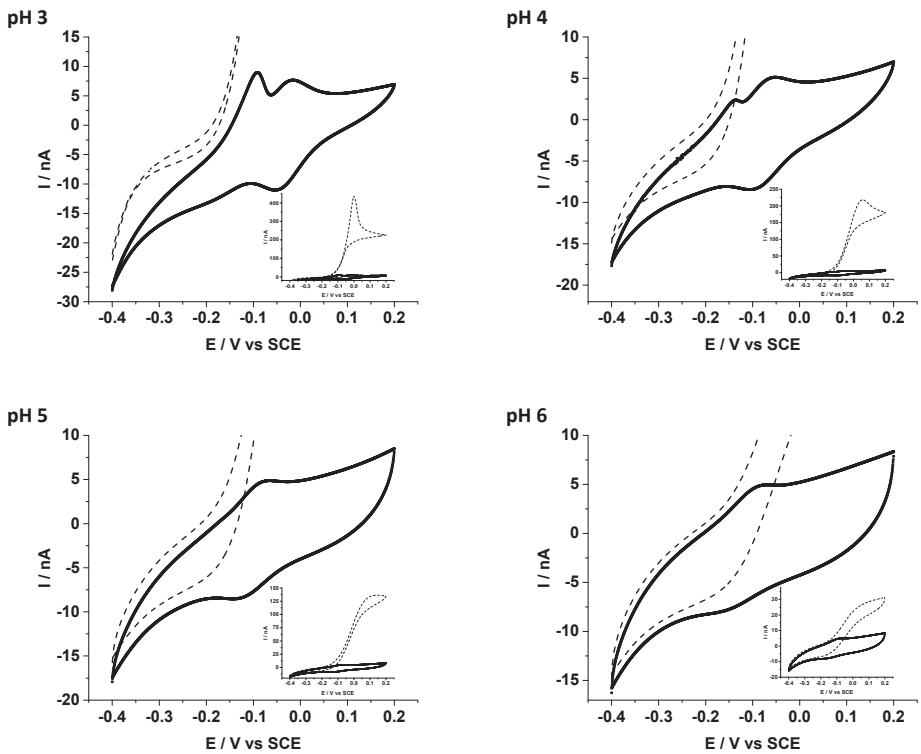

Figure 4. Cyclic voltammograms of rec*Tv*CDH on MUDOH modified gold electrodes at varying pHs at a scan rate of 5 mV/s in the absence (solid line) and in the presence of 1 mM lactose (dashed line) with insets showing the whole extend of the catalytic current.

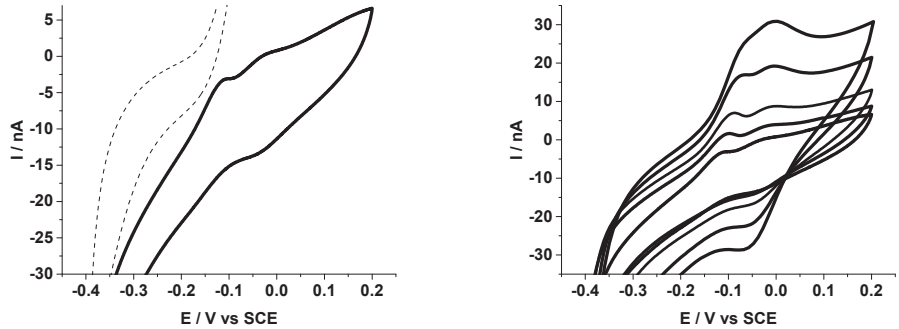

Figure 5. Cyclic voltammograms of rec*Tv*CDH on MHOH modified gold electrodes at pH 3.0 at a scan rate of 5 mV/s (left) in the absence (solid line) and in the presence of 1 mM lactose (dashed line) and (right) at scan rates of 5, 10, 20, 50 and 100 mV/s from inner to outer curve.

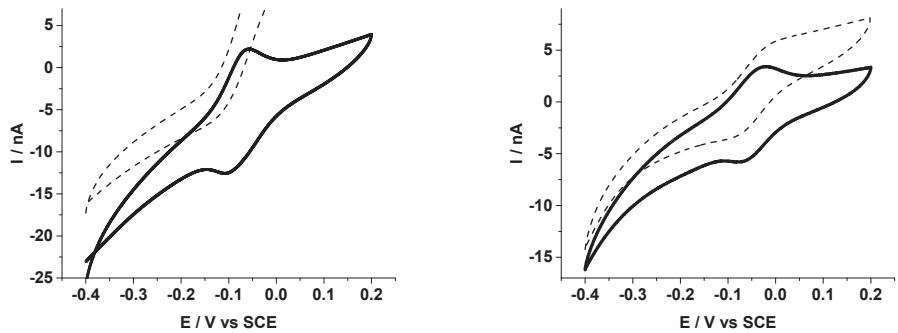

Figure 6. Cyclic voltammograms of class II CDHs (left) rec*Ct*CDH and (right) rec*Mt*CDH on MUDOH modified gold electrodes at pH 3 at a scan rate of 5 mV/s in the absence (solid line) and in the presence of 1 mM lactose (dashed line)

Supplementary Information

Control experiments

To exclude remaining contaminations as nanoparticles or nanotubes being present from previous experiments carried out in the same laboratory and being responsible for the DET of DH, newly ordered gold electrodes were used as well. The response of rec*Tv*CDH on thiol modified, newly ordered gold electrodes was qualitatively similar to the ones obtained with used electrodes (see Supplementary Information Fig. S7). The lower purity of the 97% thiol mercaptoundecanol used for the electrode modification also did not affect the measured DET from DH (see Supplementary Information Fig. S7).

Table S1. Overview of the investigated CDHs including their isoelectric points (pI).

species	class	Concentration / mg ml^{-1}	pI	Sequence length / amino acids
rec*Ct*CDH	II	10	3.8	787
rec*Ct*CDhC291Y	II	28	3.8	787
rec*Mt*CDH	II	9	3.8	828
*Tv*CDH	I	11	4.2	768
rec*Tv*CDH	I	25	4.2	768
rec*Ps*CDH	I	63	4	sequence unknown

Table S2: Primers for amplification and heterologous expression of the CDH gene of *Tv*CDH

Anchor2	GCTGTCAACGATACGCTACGTAACGGCATGACAGTGTTTTTTTTTTTTTTTTT
UniversalA	GCTGTCAACGATACGCTACGTAACG
UniversalB	CGCTACGTAACGGCATGACAGTG
5CDHc1	GGCTATTTCTCGCACTACCG
5CDHc2	ACGGTGAGCGCAACATTACG
3ECV	AATTCTAGATCAAGGCCCCCCGGCGAGCG
5TVBstB1	TTATTCGAAACGATGAAGTTTAAGAGCCTGCTG

Table S3: Electrochemical parameters determined from cyclic voltammetric experiments for various CDHs on either MUDOH or MHOH modified gold electrodes at varying pHs. E'_x = midpoint potential, ΔEP_x = peak separation between oxidation and reduction peak potentials, $Epox_x$ = oxidation peak potential, $w_{1/2(x)}$ = oxidation peak width at half height. x=DH refers to the dehydrogenase domain and x=CYT refers to the cytochrome domain of CDH. The second value in each line indicates the standard deviation obtained from the measurements of three equally modified electrodes. If a parameter could not be determined at least three times, the number in brackets refers to the amount of values used to calculate the given parameter. If no value is given, the parameter could not be determined at all.

CDH (SAM)	class	pH	E'_{DH} / V	ΔEP_{DH} / V	$Epox_{DH}$ / V	$w_{1/2(DH)}$ / V	E'_{CYT} / V	ΔEP_{CYT} / V	$Epox_{CYT}$ / V	$w_{1/2(CYT)}$ / V
*Tv*CDH (MUDOH)	I	3	-0.162 (2)	0.036	-0.144 0.001	0.056 0.006	-0.040 0.003	0.015 0.006	-0.032 0.006	0.088 0.004
		4			-0.194 0.002	0.039 0.007	-0.065 0.003	0.014 0.017	-0.081 0.016	0.101 0.016
		4.5			-0.210 0.003	0.045 0.003	-0.105 0.004	0.023 0.016	-0.094 0.011	0.104 0.013
		5			-0.221 (2)	0.052 (2)	0.115 (2)	0.030 (2)	-0.102 0.006	0.102 (2)
		6					-0.135 0.006	0.031 0.008	-0.119 0.005	
rec*Tv*CDH (MUDOH)	I	3	-0.144 0.003	0.091 0.012	-0.099 0.008		-0.028 0.001	0.020 0.005	-0.017 0.003	0.079 0.001
		4	-0.190 (2)	0.088 (2)	-0.146 0.005		-0.074 0.001	0.022 0.007	-0.063 0.005	0.086 0.002
		5			-0.187 (2)		-0.102 0.003	0.030 0.004	-0.087 0.005	0.099 0.007
		6					-0.121 0.005	0.056 0.012	-0.093 0.002	0.112 0.008
rec*Tv*CDH (MHOH)		3	-0.150 0.003	0.040 0.009	-0.130 0.007	0.055 0.004	-0.025 0.002	0.020 0.022	-0.015 0.013	0.084 0.014
		4			-0.174 0.004	0.055 (2)	-0.071 0.005	0.021 0.003	-0.060 0.006	0.092 0.004
		5			-0.189 (1)		-0.085 0.006	0.039 0.008	-0.065 0.009	0.095 0.014
		6					-0.116 (1)		-0.097 0.034	
*Ps*CDH (MUDOH)	I	3	-0.136 (2)	0.090 (2)	-0.099 0.040	0.058 (2)	-0.025 0.002	0.019 0.004	-0.015 0.002	0.074 0.018
		4			-0.147 0.031	0.056 0.013	-0.067 0.001	0.015 0.003	-0.059 0.002	0.096 0.028
		5			-0.151 (2)		-0.077 0.007	0.039 0.011	-0.058 0.013	0.091 0.029
		6					-0.095 0.011	0.045 0.027	-0.072 0.016	0.127 0.020
rec*Mt*CDH (MUDOH)	II	3					-0.042 0.003	0.020 0.008	-0.032 0.002	0.138 0.012
		4					-0.086 0.005	0.022 0.011	-0.075 0.006	0.126 0.031
		5					-0.108 0.008	0.056 0.012	-0.080 0.014	0.123 (1)
rec*Ct*CDH (MUDOH)	II	3					-0.071 0.007	0.022 0.008	-0.060 0.003	0.110 0.015
		4					-0.116 0.010	0.025 0.001	-0.104 0.010	0.122 0.018
		5					-0.121 0.047	-0.027 0.093	-0.135 0.007	0.124 0.022

		6					-0.150 (2)	0.045 0.012	-0.126 0.009	0.124 0.008
rec*Ct*CDH C291Y (MUDOH)	II	3					-0.065 0.004	0.024 0.003	-0.053 0.004	0.114 (2)
		4					-0.108 0.002	0.022 0.005	-0.097 0.001	0.120 (2)
		5					-0.135 0.004	0.036 0.007	-0.117 0.000	0.135 (1)
		6					-0.152 0.002	0.052 0.007	-0.126 0.004	0.144 (1)

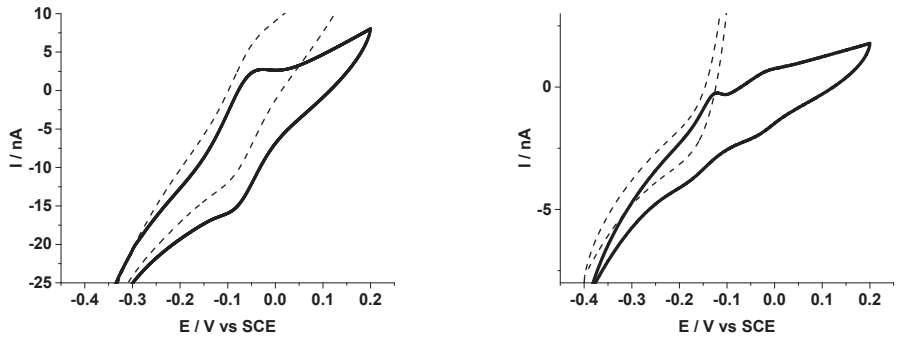

Figure S4. (Left) Cyclic voltammograms of class II CDH rec*Ct*CDHC291Y and (Right) class I CDH *Ps*CDH on MUDOH modified gold electrodes at pH 3 at a scan rate of 5 mV/s in the absence (solid line) and in the presence of 1 mM lactose (dashed line).

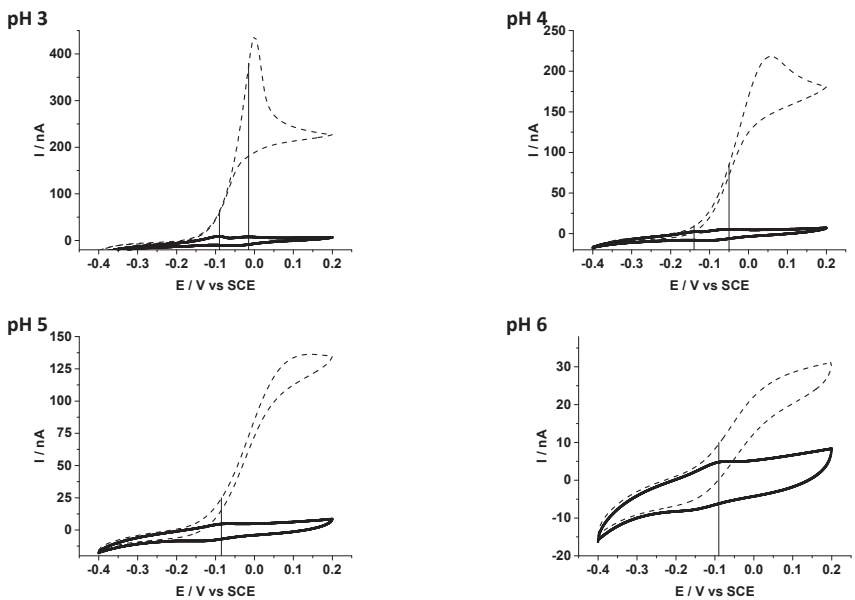

Figure S5. Cyclic voltammograms of rec*Tv*CDH on MUDOH modified gold electrodes at varying pHs at a scan rate of 5 mV/s in the absence (solid line) and in the presence of 1 mM lactose (dashed line) showing the whole extent of the catalytic currents as shown as insets in Figure 4 with marked positions of the oxidation peaks of DH and CYT (if visible).

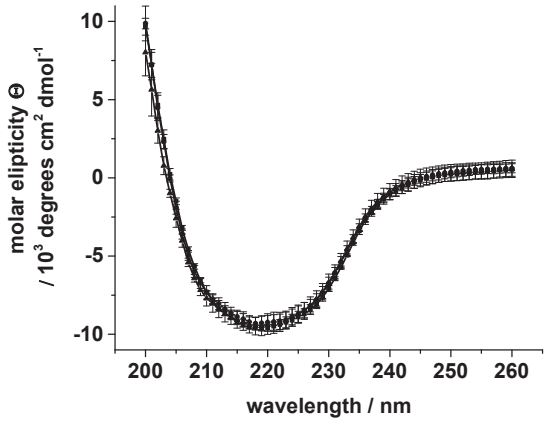

Figure S6. Circular dichroism spectra of 0.2 mg/ml rec*Tv*CDH in 50 mM NaAc at pH 3 (square), pH 4.5 (circle) and pH 6 (triangle). Each spectrum represents the average of three independently measured samples with the standard deviation shown as error bars.

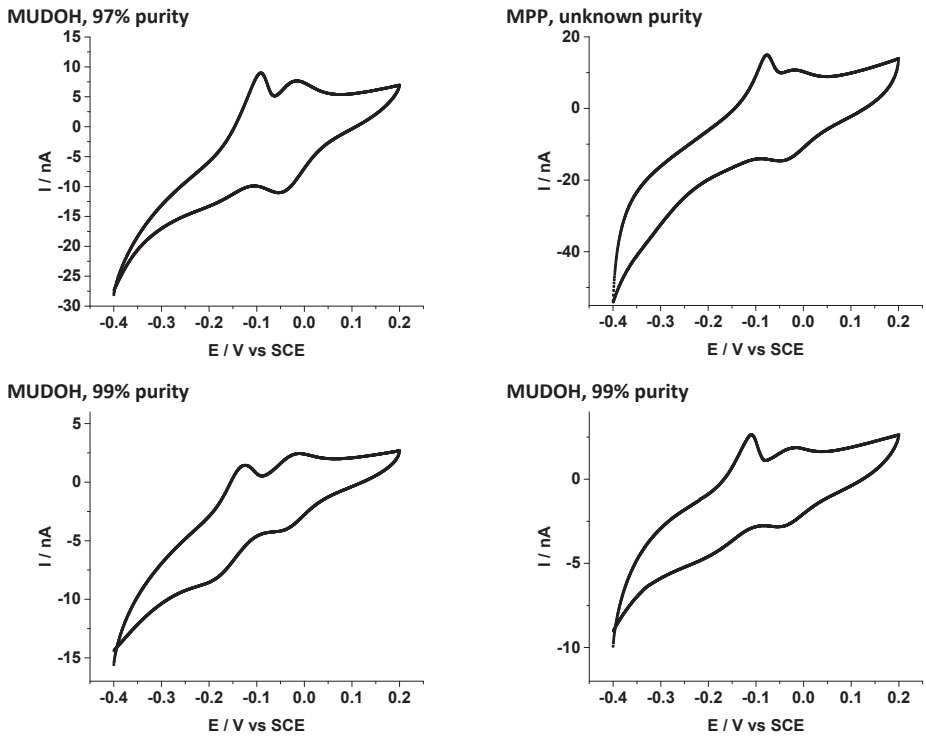

Figure S7. Cyclic voltammograms of class I CDH rec*Tv*CDH (left) on already used or (right) newly ordered gold electrodes modified with different thiols of different purity at pH 3 at scan rate of 5 mV/s.

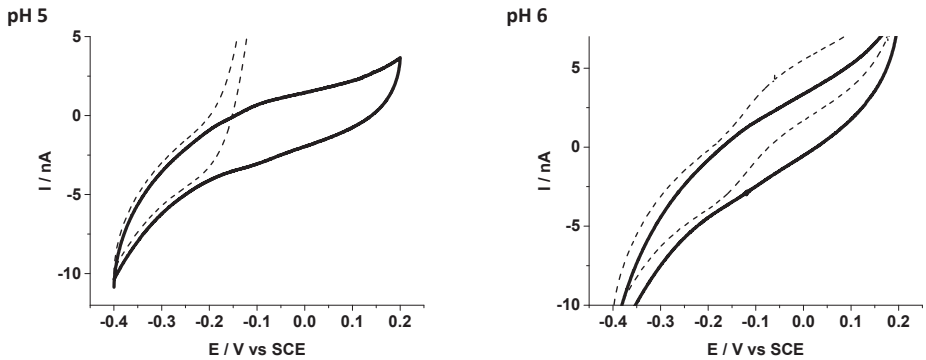

Figure S8. Cyclic voltammograms of class I CDH rec*Tv*CDH on MHOH modified gold electrodes at a scan rate of 5 mV/s in the absence (solid line) and in the presence of 1 mM lactose (dashed line)

References

1. Ludwig, R.; Harreither, W.; Tasca, F.; Gorton, L. Cellobiose dehydrogenase: A versatile catalyst for electrochemical applications. *ChemPhysChem* **2010,** *11* (13), 2674-2697.
2. Ludwig, R.; Ortiz, R.; Schulz, C.; Harreither, W.; Sygmund, C.; Gorton, L. Cellobiose dehydrogenase modified electrodes: Advances by materials science and biochemical engineering. *Anal. Bioanal. Chem.* **2013,** *405* (11), 3637-3658.
3. Zamocky, M.; Ludwig, R.; Peterbauer, C.; Hallberg, B. M.; Divne, C.; Nicholls, P.; Haltrich, D. Cellobiose dehydrogenase - a flavocytochrome from wood-degrading, phytopathogenic and saprotropic fungi. *Current Protein & Peptide Science* **2006,** *7* (3), 255-280.
4. Henriksson, G.; Johansson, G.; Pettersson, G. A critical review of cellobiose dehydrogenases. *J Biotechnol* **2000,** *78* (2), 93-113.
5. Elmgren, M.; Lindquist, S. E.; Henriksson, G. Cellobiose oxidase crosslinked in a redox polymer matrix at an electrode surface-a new biosensor. *J. Electroanal. Chem.* **1992,** *341* (1-2), 257-273.
6. Guschin, D.; Castillo, J.; Dimcheva, N.; Schuhmann, W. Redox electrodeposition polymers: Adaptation of the redox potential of polymer-bound os complexes for bioanalytical applications. *Anal. Bioanal. Chem.* **2010,** *398* (4), 1661-1673.
7. Stoica, L.; Dimcheva, N.; Haltrich, D.; Ruzgas, T.; Gorton, L. Electrochemical investigation of cellobiose dehydrogenase from new fungal sources on au electrodes. *Biosens. Bioelectron.* **2005,** (20), 2010-2018.
8. Phillips, C. M.; Beeson, W. T.; Cate, J. H.; Marletta, M. A. Cellobiose dehydrogenase and a copper-dependent polysaccharide monooxygenase potentiate cellulose degradation by *neurospora crassa*. *ACS Chem. Biol.* **2011,** *6* (12), 1399-1406.
9. Sygmund, C.; Kracher, D.; Scheiblbrandner, S.; Zahma, K.; Felice, A. K. G.; Harreither, W.; Kittl, R.; Ludwig, R. Characterization of the two *neurospora crassa* cellobiose dehydrogenases and their connection to oxidative cellulose degradation. *Appl. Environ. Microbiol.* **2012,** *78* (17), 6161-6171.
10. Harreither, W.; Sygmund, C.; Augustin, M.; Narciso, M.; Rabinovich, M. L.; Gorton, L.; Haltrich, D.; Ludwig, R. Catalytic properties and classification of cellobiose dehydrogenases from ascomycetes. *Appl Environ Microb* **2011,** *77* (5), 1804-1815.
11. Zamocky, M.; Schumann, C.; Sygmund, C.; O'Callaghan, J.; Dobson, A. D. W.; Ludwig, R.; Haltrich, D.; Peterbauer, C. K. Cloning, sequence analysis and heterologous expression in *pichia pastoris* of a gene encoding a thermostable cellobiose dehydrogenase from *myriococcum thermophilum*. *Protein Expres. Purif.* **2008,** *59* (2), 258-265.
12. Harreither, W.; Coman, V.; Ludwig, R.; Haltrich, D.; Gorton, L. Investigation of graphite electrodes modified with cellobiose dehydrogenase from the ascomycete *myriococcum thermophilum*. *Electroanalysis* **2007,** *19* (2-3), 172-180.
13. Kovacs, G.; Ortiz, R.; Coman, V.; Harreither, W.; Popescu, I. C.; Ludwig, R.; Gorton, L. Graphite electrodes modified with *neurospora crassa* cellobiose dehydrogenase: Comparative electrochemical characterization under direct and mediated electron transfer. *Bioelectrochemistry* **2012,** *88* (0), 84-91.
14. Schulz, C.; Ludwig, R.; Micheelsen, P. O.; Silow, M.; Toscano, M. D.; Gorton, L. Enhancement of enzymatic activity and catalytic current of cellobiose dehydrogenase by calcium ions. *Electrochem. Commun.* **2012,** *17* (0), 71-74.
15. Schulz, C.; Ludwig, R.; Gorton, L. Polyethyleneimine as a promoter layer for the immobilization of cellobiose dehydrogenase from *myriococcum thermophilum* on graphite electrodes. *Anal. Chem.* **2014,** *86* (9), 4256-4263.
16. Yarman, A.; Schulz, C.; Sygmund, C.; Ludwig, R.; Gorton, L.; Wollenberger, U.; Scheller, F. W. Third generation atp sensor with enzymatic analyte recycling. *Electroanalysis* **2014,** *26* (9), 2043-2048.

17. Knöös, P.; Schulz, C.; Piculell, L.; Ludwig, R.; Gorton, L.; Wahlgren, M. Quantifying the release of lactose from polymer matrix tablets with an amperometric biosensor utilizing cellobiose dehydrogenase. *Int. J. Pharmaceut.* **2014,** *468* (1–2), 121-132.
18. Safina, G.; Ludwig, R.; Gorton, L. A simple and sensitive method for lactose detection based on direct electron transfer between immobilised cellobiose dehydrogenase and screen-printed carbon electrodes. *Electrochim Acta* **2010,** *55* (26), 7690-7695.
19. Harreither, W.; Felice, A. K. G.; Paukner, R.; Gorton, L.; Ludwig, R.; Sygmund, C. Recombinantly produced cellobiose dehydrogenase from *corynascus thermophilus* for glucose biosensors and biofuel cells. *Biotechnol J* **2012,** *7* (11), 1359-1366.
20. Lindgren, A.; Stoica, L.; Ruzgas, T.; Ciucu, A.; Gorton, L. Development of a cellobiose dehydrogenase modified electrode for amperometric detection of diphenols. *Analyst* **1999,** *124* (4), 527-532.
21. Wang, X.; Falk, M.; Ortiz, R.; Matsumura, H.; Bobacka, J.; Ludwig, R.; Bergelin, M.; Gorton, L.; Shleev, S. Mediatorless sugar/oxygen enzymatic fuel cells based on gold nanoparticle-modified electrodes. *Biosens. Bioelectron.* **2012,** *31* (1), 219-225.
22. Falk, M.; Alcalde, M.; Bartlett, P. N.; De Lacey, A. L.; Gorton, L.; Gutierrez-Sanchez, C.; Haddad, R.; Kilburn, J.; Leech, D.; Ludwig, R.; Magner, E.; Mate, D. M.; Ó Conghaile, P.; Ortiz, R.; Pita, M.; Pöller, S.; Ruzgas, T.; Salaj-Kosla, U.; Schuhmann, W.; Sebelius, F. Self-powered wireless carbohydrate/oxygen sensitive biodevice based on radio signal transmission. *Plos One* **2014,** *9* (10), e109104.
23. Ortiz, R.; Ludwig, R.; Gorton, L. Highly efficient membraneless glucose bioanode based on *corynascus thermophilus* cellobiose dehydrogenase on aryl diazonium-activated single-walled carbon nanotubes. *ChemElectroChem* **2014,** *1* (11), 1948-1956.
24. Hallberg, M. B.; Henriksson, G.; Pettersson, G.; Divne, C. Crystal structure of the flavoprotein domain of the extracellular flavocytochrome cellobiose dehydrogenase. *J. Mol. Biol.* **2002,** *315* (3), 421-434.
25. Gray, H. B.; Winkler, J. R.; Halpern, J. Long-range electron transfer. *Proceedings of the National Academy of Sciences* **2005,** *102* (10), 3534-3539.
26. Stoica, L.; Dimcheva, N.; Haltrich, D.; Ruzgas, T.; Gorton, L. Electrochemical investigation of cellobiose dehydrogenase from new fungal sources on au electrodes. *Biosens. Bioelectron.* **2005,** *20* (10), 2010-2018.
27. Ortiz, R. Improving the biocatalyst. Engineering of fungal oxidoreductases and thin-film electrodes for improvement of membraneless biofuel cells and carbohydrate biosensors. Doctoral Thesis, Lund University, 2013.
28. Lindgren, A.; Larsson, T.; Ruzgas, T.; Gorton, L. Direct electron transfer between the heme of cellobiose dehydrogenase and thiol modified gold electrodes. *J. Electroanal. Chem.* **2000,** *494* (2), 105-113.
29. Kielb, P.; Sezer, M.; Katz, S.; Lopez, F.; Schulz, C.; Gorton, L.; Ludwig, R.; Wollenberger, U.; Zebger, I.; Weidinger, I. M. Spectroscopic observation of calcium-induced reorientation of cellobiose dehydrogenase immobilized on electrodes and its effect on electrocatalytic activity. *ChemPhysChem* **2015,** *16* (9), 1960-1968.
30. Coman, V.; Harreither, W.; Ludwig, R.; Haltrich, D.; Gorton, L. Investigation of electron transfer between cellobiose dehydrogenase from myriococcum thermophilum and gold electrodes. *Chem Anal-Warsaw* **2007,** *52* (6), 945-960.
31. Courjean, O.; Gao, F.; Mano, N. Deglycosylation of glucose oxidase for direct and efficient glucose electrooxidation on a glassy carbon electrode. *Angew. Chem., Int. Ed.* **2009,** *48*, 5897-5899.
32. Stankovich, M. T.; Schopfer, L. M.; Massey, V. Determination of glucose oxidase oxidation-reduction potentials and the oxygen reactivity of fully reduced and semiquinoid forms. *J. Biol. Chem.* **1978,** *253* (14), 4971-4979.

33. Holland, J. T.; Lau, C.; Brozik, S.; Atanassov, P.; Banta, S. Engineering of glucose oxidase for direct electron transfer via site-specific gold nanoparticle conjugation. *Journal of the American Chemical Society* **2011,** *133* (48), 19262-19265.
34. Yakovleva, M. E.; Killyéni, A.; Ortiz, R.; Schulz, C.; MacAodha, D.; Ó Conghaile, P.; Leech, D.; Popescu, I. C.; Gonaus, C.; Peterbauer, C. K.; Gorton, L. Recombinant pyranose dehydrogenase—a versatile enzyme possessing both mediated and direct electron transfer. *Electrochem. Commun.* **2012,** *24* (0), 120-122.
35. Yakovleva, M. E.; Gonaus, C.; Schropp, K.; Ó Conghaile, P.; Leech, D.; Peterbauer, C. K.; Gorton, L. Engineering of pyranose dehydrogenase for application to enzymatic anodes in biofuel cells. *Phys Chem Chem Phys* **2015,** *17*, 9074-9081.
36. Yehezkeli, O.; Tel-Vered, R.; Raichlin, S.; Willner, I. Nano-engineered flavin-dependent glucose dehydrogenase/gold nanoparticle-modified electrodes for glucose sensing and biofuel cell applications. *ACS Nano* **2011,** *5* (3), 2385-2391.
37. Krikstolaityte, V.; Lamberg, P.; Toscano, M. D.; Silow, M.; Eicher-Lorka, O.; Ramanavicius, A.; Niaura, G.; Abariute, L.; Ruzgas, T.; Shleev, S. Mediatorless carbohydrate/oxygen biofuel cells with improved cellobiose dehydrogenase based bioanode. *Fuel Cells* **2014,** *14* (6), 792-800.
38. Letourneur, O.; Gervasi, G.; Gaïa, S.; Pagès, J.; Watelet, B.; Jolivet, M. Characterization of *toxoplasma gondii* surface antigen 1 (sag1) secreted from *pichia pastoris*: Evidence of hyper o-glycosylation. *Biotechnol Appl Bioc* **2001,** *33* (1), 35-45.
39. Sygmund, C.; Kracher, D.; Scheiblbrandner, S.; Zahma, K.; Felice, A. K.; Harreither, W.; Kittl, R.; Ludwig, R. Characterization of the two neurospora crassa cellobiose dehydrogenases and their connection to oxidative cellulose degradation. *Appl Environ Microb* **2012,** *78* (17), 6161-6171.
40. Ludwig, R.; Salamon, A.; Varga, J.; ZÃ¡mocky, M.; Peterbauer, C. K.; Kulbe, K. D.; Haltrich, D. Characterisation of cellobiose dehydrogenases from the white-rot fungi trametes pubescens and trametes villosa. *Appl Microbiol Biot* **2004,** *64* (2), 213-222.
41. Tasca, F.; Gorton, L.; Harreither, W.; Haltrich, D.; Ludwig, R.; Nöll, G. Direct electron transfer at cellobiose dehydrogenase modified anodes for biofuel cells. *J Phys Chem C* **2008,** *112* (26), 9956-9961.
42. Flitsch, A.; Prasetyo, E. N.; Sygmund, C.; Ludwig, R.; Nyanhongo, G. S.; Guebitz, G. M. Cellulose oxidation and bleaching processes based on recombinant *myriococcum thermophilum* cellobiose dehydrogenase. *Enzyme Microb Tech* **2013,** *52* (1), 60-67.
43. Harreither, W.; Felice, A. K. G.; Paukner, R.; Gorton, L.; Ludwig, R.; Sygmund, C. Recombinantly produced cellobiose dehydrogenase from corynascus thermophilus for glucose biosensors and biofuel cells. *Biotechnol J* **2012,** (7), 1359-1366.
44. Ludwig, R.; Sygmund, C.; Harreither, W.; Kittl, R.; Felice, A. Mutated cellobiose dehydrogenase with increased substrate specificity. 2013.
45. Cregg, J. M.; Russell, K. A. Transformation. In *Pichia protocols*, Higgins, D. R.; Cregg, J. M., Eds. Humana Press: Totowa, 1998; Vol. 103, pp 27-39.
46. Vogt, S.; Schneider, M.; Schäfer-Eberwein, H.; Nöll, G. Determination of the ph dependent redox potential of glucose oxidase by spectroelectrochemistry. *Anal. Chem.* **2014,** *86* (15), 7530-7535.
47. Kamal, M. M.; Elzanowska, H.; Gaur, M.; Kim, D.; Birss, V. I. Electrochemistry of adsorbed flavin adenine dinucleotide in acidic solutions. *J. Electroanal. Chem.* **1991,** *318* (1–2), 349-367.
48. Garjonyte, R.; Malinauskas, A.; Gorton, L. Investigation of electrochemical properties of fmn and fad adsorbed on titanium electrode. *Bioelectrochemistry* **2003,** *61* (1–2), 39-49.
49. Gorton, L.; Johansson, G. Cyclic voltammetry of fad adsorbed on graphite, glassy carbon, platinum and gold electrodes. *J. Electroanal. Chem.* **1980,** *113* (1), 151-158.
50. Tasca, F.; Gorton, L.; Harreither, W.; Haltrich, D.; Ludwig, R.; Nöll, G. Comparison of direct and mediated electron transfer for cellobiose dehydrogenase from *phanerochaete sordida*. *Anal. Chem.* **2009,** *81* (7), 2791-2798.

51. Glithero, N.; Clark, C.; Gorton, L.; Schuhmann, W.; Pasco, N. At-line measurement of lactose in dairy-processing plants. *Anal. Bioanal. Chem.* **2013,** *405* (11), 3791-3799.
52. Kracher, D.; Zahma, K.; Schulz, C.; Sygmund, C.; Gorton, L.; Ludwig, R. Interdomain electron transfer in cellobiose dehydrogenase: Modulation by ph and divalent cations. *Federation of the Societies of Biochemistry and Molecular Biology* **2015**.
53. Das, D. K.; Medhi, O. K. The role of heme propionate in controlling the redox potential of heme: Square wave voltammetry of protoporphyrinato ix iron(iii) in aqueous surfactant micelles. *Journal of Inorganic Biochemistry* **1998,** *70* (2), 83-90.
54. Schneider, S.; Marles-Wright, J.; Sharp, K. H.; Paoli, M. Diversity and conservation of interactions for binding heme in b-type heme proteins. *Natural Product Reports* **2007,** *24* (3), 621-630.
55. Tan, T.-C.; Kracher, D.; Gandini, R.; Sygmund, C.; Kittl, R.; Haltrich, D.; Hallberg, B. M.; Ludwig, R.; Divne, C. Structural basis for cellobiose dehydrogenase action during oxidative cellulose degradation. *Nature Communications* **2015,** *6*.
56. Giese, B.; Graber, M.; Cordes, M. Electron transfer in peptides and proteins. *Curr. Opin. Chem. Biol.* **2008,** *12* (6), 755-759.
57. Giese, B.; Wang, M.; Gao, J.; Stoltz, M.; Müller, P.; Graber, M. Electron relay race in peptides. *J. Org. Chem.* **2009,** *74* (10), 3621-3625.
58. Page, C. C.; Moser, C. C.; Dutton, P. L. Mechanism for electron transfer within and between proteins. *Curr. Opin. Chem. Biol.* **2003,** *7* (5), 551-556.
59. Haynes, W. M. *Crc handbook of chemistry and physics*. CRC Press: Boca Raton, Fla., 2014.
60. Hallberg, B. M.; Henriksson, G.; Pettersson, G.; Vasella, A.; Divne, C. Mechanism of the reductive half-reaction in cellobiose dehydrogenase. *The Journal of Biological Chemistry* **2003,** *278* (9), 7160-7166.
61. Weibel, M. K.; Bright, H. J. The glucose oxidase mechanism: Interpretation of the ph dependence. *J. Biol. Chem.* **1971,** *246* (9), 2734-2744.

Paper XI

A novel Bio-Electronic Tongue using cellobiose dehydrogenase from different origins to resolve mixtures of various sugars and interfering analytes.

Andrea Cipri*[1]; Christopher Schulz*[2]; Roland Ludwig[3]; Lo Gorton[2]; Manel del Valle[1];

[1]Sensor & Biosensor Group, Chemistry Department, Universitat Autònoma de Barcelona, Barcelona, Spain;

[2]Department of Analytical Chemistry/Biochemistry and Structural Biology, Lund University, Lund, Sweden;

[3]Department of Food Science and Technology BOKU University of Natural Resources and Life Science, Muthgasse 18, 1190 Vienna, Austria

*Both authors contributed equally to this work

Abstract

A novel application of cellobiose dehydrogenase (CDH) as sensing element for an electronic tongue (ET) system has been tested. In this work CDH from different origins and substrate specificities are used to discriminate between various sugars (lactose and glucose) plus interfering analytes (Ca^{2+}) in mixtures working in a direct electron transfer mode at low potentials. The work exploits the advantage of an ET system with practically zero pre-treatment of samples and operation at low voltages in a direct electron transfer mode. The Artificial Neural Network (ANN) used in the ET system to treat the voltammetric data was able to give a good prediction of the concentrations of the analytes considered, showing high correlation coefficients especially for lactose and Ca^{2+}, R^2 of respectively 0.975 and 0.945. This application has a high potential especially in the food and dairy industries and also, in a future miniaturized system, for in situ food analysis.

1. Introduction

Electronic tongues (ETs) constitute a relatively new approach to solve problems in Analytical Chemistry. Today it has become increasingly more difficult to find cheap and highly selective sensors or biosensors, considering this fact the ETs can come in our help. ETs are multi-sensor systems with cross-response that can process the signal using advanced mathematical methods based on pattern recognition and/or multivariate data analysis. These characteristics of the ET system are an advantage due to the possibility to make further interpretation of complex compositions of analytes, to solve mixtures, to differentiate primary species from interfering components or even to distinguish between false responses and true ones (del Valle 2010). ETs can be exploited to quantify a wide variety of compounds in different fields as food and beverage analysis (Cetó et al. 2013a), environment (Nunez et al. 2013; Raud and Kikas 2013) and medical fields (Lvova et al. 2009). They have also been applied in food industry to solve qualitative problems (Bagnasco et al. 2014; Cetó et al. 2013b). As it is possible to understand from the wide field of use of the ET systems a variety of sensors can be used in the sensor array: for instance *"in bulk"* biosensors, where the enzymes or other biomolecules are inside the bulk of the electrode, *"inorganic"* sensors, as classic bare electrodes like glassy carbon, graphite or gold etc. and electrodes modified with metal nanoparticles, ion selective sensors (ISEs) covered with a PVC membrane or electrodes with catalysts (Cetó et al. 2012; Gutierrez et al. 2008; Wilson et al. 2015). In the range of surface modified electrodes the possibilities are almost infinite, from nanomaterials to biomolecules, e.g., carbon nanotubes, nanoparticles, enzymes, aptamers and a combination of these modifiers citing just a few (Cipri and del Valle 2014; Ocaña et al. 2014; Pacios et al. 2009). Most of such materials have been exploitable for ETs systems. Due to the nature of the ET there is no need for high selectivity. The key point is a good stability of the sensor response at least through a set of samples but also ideally through days. Also enzymes have been used as a detection element in ETs. Glucose oxidase was used for glucose determination in the presence of common interferents of the enzyme (A.Gutés 2006). Urease (and creatinine deiminase) was used for the determination of urea (or urea plus creatinine) in kidney related samples (Gutes et al. 2005; Gutierrez et al. 2007). Tyrosinase, peroxidases (Sapelnikova et al. 2003; Solna et al. 2005; Tønning et al. 2005) and also laccase were applied for resolution of phenol mixtures (Cetó et al. 2013a; Cetó et al. 2012). Acetylcholinesterases (Tønning et al. 2005) and cholinesterase (Sapelnikova et al. 2003; Solna et al. 2005) were applied to discriminate between different pesticides in their inhibition reaction

(Valdes-Ramirez et al. 2009). Such ET systems using biomolecules as enzymes for the detection have received the name Bioelectronic Tongues (BioETs) (Tønning et al. 2005) and were most recently reviewed by Peris and Escuder-Gilabert (Peris and Escuder-Gilabert 2013) and Ha and co-workers (Ha et al. 2015). It is known that enzymes are advantageous due to their inherent, higher specificity and the reduction of the activation energy necessary to drive a desired chemical reaction compared with non-enzymatically catalysed reactions (Berg et al. 2002). Both factors decrease (but do not abolish) the risk of interfering analytes being detected. Recently, there has been a lot of interest in redox enzymes and their applications for electrochemical biosensors, biofuel cells and bioelectrosynthesis (Katz and Willner 2004; Meredith and Minteer 2012; Osman et al. 2011; Rabaey and Rozendal 2010). One focus lies on the establishment of a direct electronic communication between electrodes and enzymes called direct electron transfer (DET) enabling biosensors or biofuel cell electrodes to operate at low or no overpotential with respect to the redox potential of the enzyme leading to increased cell voltages when applied to biofuel cells and when applied to biosensors, to mediator-less, third generation biosensors with decreased problems of interfering species being non-enzymatically detected. Furthermore often toxic and diffusive redox mediators shuttling electrons between enzymes and electrodes can be avoided when working with DET (Leech et al. 2012; Wang 2008). One of the enzymes for which a lot of interest has been shown in the field of biosensors and biofuel cells is cellobiose dehydrogenase (CDH) as it has been shown DET for a variety of substrates including analytically relevant sugars as glucose and lactose (Ludwig et al. 2013a).

CDH is an extracellular oxidoreductase secreted by wood degrading fungi. It is involved in the degradation process of cellulose being a structural part of wood. The natural substrate is cellobiose, which is a decomposition product from cellulose. (Henriksson et al. 2000; Ludwig et al. 2010; Zamocky et al. 2006) CDH oxidises cellobiose and reduces lytic polysaccharide monooxygenases (LPMOs), which in its reduced form aid in the decomposition of cellulose as was recently found out (Beeson et al. 2011; Eibinger et al. 2014; Langston et al. 2011; Phillips et al. 2011).

CDH consists of two separate domains connected by a flexible polypeptide linker. These two domains consist of a larger, flavin adenine dinucleotide (FAD) containing flavodehydrogenase domain (DH_{CDH}) (Hallberg et al. 2002) and a smaller heme *b* containing cytochrome domain (CYT_{CDH}) (Hallberg et al. 2000). DH_{CDH} is catalytically active and responsible for the oxidation of the substrate leading to a fully reduced

FAD cofactor located in the DH_{CDH} (Jones and Wilson 1988). The electrons can be transferred by an internal electron transfer pathway (IET) to the CYT_{CDH} reducing the heme *b* cofactor (Igarashi et al. 2002). The CYT_{CDH} acts as an electron transfer protein between DH_{CDH} and the natural electron acceptor (LPMOs, see above) or an electrode surface (Ludwig et al. 2013a). CDHs are expressed by fungi from the dikaryotic phyla of Basidiomycota and Ascomycota and were phylogenetically classified into class I and class II respectively (Zamocky et al. 2006). Depending on the origin the biochemical properties, as size (usually between 80-100 kDA), isoelectric point (usually below pH 5) substrate spectrum and pH optimum, of CDHs can vary (Ludwig et al. 2010). All CDHs have a preferred selectivity for cellodextrines as cellobiose but also its epimer lactose (Zamocky et al. 2006) as substrate, but some class II CDHs also show activity for glucose (Harreither et al. 2011; Henriksson et al. 1998; Zamocky et al. 2006). Next to differences in substrate specificities recently we found out that the activity of especially class II CDHs also depends on the presence of cations. Especially divalent cations as Ca^{2+} at millimolar concentrations were found to enhance the activity of CDH possibly by enhancing the rate limiting IET by screening negative charges being present at the interfaces of both domains decreasing the distance between the two domains. The activity of *Mt*CDH (class II) was found to be tunable most by Ca^{2+} with increases of around 5 times of its original activity at its optimal pH 5.5 when adding 50 mM Ca^{2+} (Kielb et al. 2015; Kracher et al. 2015; Larsson et al. 2000; Schulz et al. 2012).

The origin dependent different preferences for the substrate (lactose vs. glucose) and the varying dependence of the activity of CDH on cations make CDH a good candidate to build a sensor array to be exploited for a BioET system. CDH has already been applied in a BioET like setup, however in a rather selective manner using other enzymes as cholinesterase, tyrosinase and peroxidase to detect pesticides and phenols with low extend of cross-responses between the electrodes (Solna et al. 2005). However, the use of additional, unmodified electrodes and the rather high selectivity make both terms, Bio and ET questionable in this context. This work aims to show the feasibility of BioET using CDHs from different origins as recognition elements. To make this possible we took advantage of the power of data analysis in ETs systems and the sensing and DET properties of CDH. To show how the system works two sugars (lactose and glucose) and one enzyme regulating cation (Ca^{2+}) were chosen as targets. A system like this can be potentially interesting for applications in the food and dairy industry, detecting levels of lactose in e. g. milk or lactose free milk.

The Ca^{2+} and glucose content of milk might be of interest to detect possible adulteration of milk (Walstra et al. 2014). In previous studies third-generation biosensors based on CDH to detect lactose in milk and in a dairy processing plant were shown to reliably measure levels of lactose with only dilution necessary as a sample preparation step (Glithero et al. 2013; Safina et al. 2010; Stoica et al. 2006; Yakovleva et al. 2012). Another advantage of this e-tongue system is the non pre-treatment of the samples, giving an advantage for the producers to have a real time or in production line analysis.

2. Experimental

2.1 Reagents and Instruments

Sodium chloride (NaCl), 3-(N-morpholino)propanesulfonic acid (MOPS), lactose, D-glucose, ethanol (EtOH), sulphuric acid (H_2SO_4), hydrogen peroxide (H_2O_2) and 6-mercapto-1-hexanol 97% were purchased from Sigma Aldrich (St. Louis, MO, USA), calcium chloride ($CaCl_2$) was purchased from Merck KgaA (Darmstadt, Germany), dialysis membranes (Spectrapor, MWCO 12-14 kDA) were purchased from Spectrum Medical Industries (CA, USA). CDH from *Myriococcum thermophilum* (*Mt*CDH) (Zamocky et al. 2008) and a mutant of CDH from *Corynascus thermophilus* with enhanced activity for glucose (*Ct*CDHC291Y) (Harreither et al. 2012; Ludwig et al. 2013b) were recombinantly expressed in *Pichia pastoris*. CDH from *Neurospora crassa* (*Nc*CDH) was harvested and purified from the fungus culture (Harreither et al. 2011). The CDH preparations were used directly without further dilution and had concentrations of 7 mg/ml for *Mt*CDH, 18.8 mg/ml for *Ct*CDHC291Y and 8.4 mg/ml for *Nc*CDH. The concentrations of the enzymes were determined photometrically converting the absorption measured at 280 nm to a protein concentration by using the calculated absorption coefficients based on the amino acid sequences. The buffer used to perform the experiments was a 50 mM MOPS pH 6.7 adjusted to an ionic strength of 63 mM with NaCl. A pH of 6.7 and an ionic strength of 63 mM were chosen to potentially mimic the conditions present in cow's milk (Walstra et al. 2014).

The voltammetric analyses were performed with an EmStat2 PalmSens potentiostat using three modified gold electrodes as working electrodes (WE), a saturated calomel electrode (SCE) as a reference electrode and a platinum flag as an auxiliary electrode.

2.2 Preparation of the different CDH-biosensors

Polycrystalline gold electrodes (diameter=1.6 mm, BASi, West Lafayette, IN, USA) were cleaned by incubation in Piranha solution for 2 min (1:3 mixture of conc. H_2O_2 with H_2SO_4. (**Careful, the compounds react violently and highly exothermic with each other**), polished on polishing cloths with deagglomerated alumina slurry of a diameter of 1 µm (Struers, Ballerup, Danmark), sonicated in ultrapure water for 5 min and electrochemically cleaned in 0.5 M H_2SO_4 by cycling 30 times between 0.1 V and 1.7 V vs. SCE at a scan rate of 300 mV/s. The sensors were modified with a self-assembled monolayer (SAM) by immediately after rinsing with water, immersing the electrodes in a 10 mM ethanolic solution of 6-mercapto-1-hexanol overnight at room temperature. The electrodes were gently rinsed with ultrapure water and excess liquid was shaken off. On each of the three electrodes forming the ET 5 µL of a CDH solution, either *Mt*CDH, *Nc*CDH or *Ct*CDHC291Y was dropped on the SAM modified gold electrode surface and entrapped by covering it with a pre-soaked dialysis membrane, which was fixed with a rubber O-ring and Parafilm (Bemis, Neenah, WI, USA) as described by Haladjian and coworkers (Haladjian et al. 1994) and as shown in Fig. S1 (Supplementary material).

2.3 Measurement procedure

The voltammetric cell contained the three working electrodes (WEs) forming the sensor array, a reference and an auxiliary electrode. Each WE of the sensor array was measured independently and successively after each other connecting them to the single channel potentiostat. Stock solutions of lactose (5 mM), glucose (5 mM) and $CaCl_2$ (10 mM) were diluted with 50 mM MOPS/NaCl buffer, pH 6.7, to obtain solutions with varying concentrations of lactose, glucose and $CaCl_2$. For the characterisation and identification of the linear ranges of each of the biosensors used in the array calibration curves with concentrations between 0 and 7 mM for lactose, 0 and 7 mM for glucose and 0 and 50 mM for $CaCl_2$ were used. The concentrations for training and testing the ANN ranged from 0 to 250 µM for lactose and glucose and from 0 to 10 mM for

Ca^{2+}. 27 samples were distributed in a simple 3-level factorial design[1] for training and 10 samples were randomly distributed along the experimental domain[2] for external test (Fig. 1).

The cyclic voltammetric measurements were performed under nitrogen atmosphere at room temperature with samples being degased for 10 min with nitrogen prior to the measurement. The working potential was swept between -0.3 V and 0.15 V *vs.* SCE at a scan rate of 20 mV/s and a step potential of 2 mV.

2.4 Building the ANN model

The data analysis of the measurements was carried out using a multivariate calibration process. This process was based on an Artificial Neural Network (ANN) as response model. As explained in Section 2.2 a batch of 37 samples was prepared and divided in two groups (27+10), this division was made to train the model using the group of 27 and to test it with the group of 10. The test samples are useful to determine the prediction ability of the ANN. The samples were distributed randomly during the measurements to avoid any history effect.

The architecture definition of the ANN was configured and optimised based on our group's previous experience with ETs formed by amperometric sensors (Fig. 2). The optimisation included the number of neurons in the hidden layer in a range between 4 and 12, the number of output neurons was fixed to 3 (the number of target molecules) and 4 transfer functions (*logsig*: log-sigmoidal, *tansig*: hyperbolic tangent sigmoid, *purelin*: linear and *satlins*: saturated-linear) were assayed for each layer (input and output). Another optimisation step was provided from the pre-processing of the voltammetric data. The voltammograms were used in their full size unfolding them and joining the signals from every sensor to a "single-sensor-like" signal per every sample. Since this has generated tens of thousands of data points a pre-processing step consisting of wavelet compression was used. The pre-processing/compression step allowed the decrease of data to be managed from the software from 48 600 to 186 values, with a Daubechies wavelet function (*db4*) and a compression level of 3.

To evaluate the goodness of the fit of the ANN model the smallest value obtained from the test samples with an MSE (mean squared error) function was taken. The prediction abilities, instead, were evaluated through

[1] A 3-level factorial design is a design with points of interest organized in a cube 3x3x3.

[2] The experimental domain is the range of concentrations used to train the ANN and the test has to stay inside the domain otherwise they would be insignificant.

the linear regression of the comparison graphs of obtained (y) vs. expected (x) concentrations with slope of 1 and correlation coefficient close to 1 for the three target molecules.

2.5 Software

The voltammetric data were acquired by using PSTrace 4.4 (PalmSens, Utrecht, The Netherlands) software. Neural Network processing was developed by the authors by MATLAB 7.0 (Mathworks, Natick, MA, USA), using its Neural Network Toolbox (v. 3.0). The graphs were made with Sigma Plot 12 (Systat Software Inc., California, USA).

3. Results and discussion

3.1 Characterisation of each CDH biosensor

The sensor array used for the ET consisted of three different CDH modified gold/SAM electrodes – one was modified with *Mt*CDH, one with *Nc*CDH, and one with *Ct*CDHC291Y, expecting different substrate specificities depending on the enzyme origin. Before developing the ET application, the integrity and linear ranges for each of the biosensors versus each of the three analytes of interest, lactose, glucose and Ca^{2+} were determined. In Fig. 3 the cyclic voltammograms of the gold/SAM electrodes modified with either *Mt*CDH, *Nc*CDH or *Ct*CDHC291Y are shown. In the absence of substrate, clear redox waves originating from the oxidation and reduction of the heme *b* cofactor located in the CYT_{CDH} is visible. The midpoint potentials range between -153 mV vs. SCE for *Mt*CDH, -144 mV vs. SCE for *Nc*CDH and -148 mV vs. SCE for *Ct*CDHC291Y, which are close to literature values (Coman et al. 2007; Harreither et al. 2012; Sygmund et al. 2012). The additional oxidative redox wave present for *Nc*CDH at -210 mV vs. SCE might originate from the oxidation of the FAD cofactor located in the DH_{CDH} as found out to be possible recently (Schulz et al., in manuscript). The peak separations between the anodic and cathodic peak potentials vary between 42 mV and 52 mV and thus lie between a solution and a surface confined redox process typical for thin layer protein electrochemistry (Haladjian et al. 1994; Laviron 1979). When lactose as the standard substrate is added clear catalytic waves can be seen for all CDH modified electrodes proving they are catalytically active. For *Mt*CDH and *Ct*CDHC291Y, the catalytic waves start at potentials around the oxidation peak potential the

CYT_{CDH} peak indicating DET from the CYT_{CDH} domain. For *Nc*CDH it seems that there are traces of catalysis at potentials already below the oxidation potential of the CYT_{CDH} peak indicating a potential DET from the DH_{CDH} as found out to be possible recently (Schulz et al., in manuscript; I will fill in the complete reference when we get the paper accepted). To determine the linear measuring ranges, the response of each CDH biosensor to varying analyte concentrations of lactose, glucose and Ca^{2+} was determined, as shown in Fig. 4. The investigation with Ca^{2+} as analyte was performed in the presence of 7 mM lactose, since Ca^{2+} is not a substrate for CDH but only potentially increases the existing catalytic currents as described in the Introduction. As shown in Fig. 4 all CDH biosensors tested respond to lactose. The best responding biosensors are the ones modified with *Nc*CDH and *Ct*CDHC291Y, possibly because their pH optima for DET of 5.5 (Kovacs et al. 2012) and 7.5 (Harreither et al. 2012) respectively are close to the investigated pH of 6.7. The pH optimum for DET of *Mt*CDH is also at pH 5.5 (Harreither et al. 2007) but its decline of activity with increasing pH is steeper compared to that of *Nc*CDH (Harreither et al. 2007; Kovacs et al. 2012) possibly explaining the comparable low response of the *Mt*CDH biosensor to lactose. The linear measuring range for lactose can be estimated to reach up to around 500 µM.

When looking into glucose as substrate (Fig. 4, middle row) clearly the *Ct*CDHC291Y mutant designed for high activity with glucose responds best to glucose with a linear measuring range to up to 260 µM. When looking into Ca^{2+} as analyte the *Ct*CDHC291Y and *Mt*CDH modified biosensors are sensitive to additional Ca^{2+}. The absolute currents are higher for *Ct*CDHC291Y, since its activity in the absence of Ca^{2+} is already higher than that for *Mt*CDH. However, looking into the relative increases of the catalytic currents in the presence of 50 mM Ca^{2+} increases of around 6.3 times for *Ct*CDHC291Y and 4.5 times for *Mt*CDH show similar dependencies for both enzymes on additional concentrations of Ca^{2+}. The dependency of the activity of *Mt*CDH on additional [Ca^{2+}] is comparable to what has been found in other studies done at pH 5.5 and 7.5 (Kracher et al. 2015; Schulz et al. 2012). The activity of the glucose mutant, *Ct*CDHC291Y, has not been studied before in the presence of Ca^{2+} but when comparing its activity with that of the wildtype *Ct*CDH in solution with cytochrome *c* as electron acceptor, the Ca^{2+} induced activity increase found here is around twice as high (Kracher et al. 2015). The nearly independence of the activity of *Nc*CDH on additional [Ca^{2+}] compares well with the literature, where no increase for *Nc*CDH was found when investigated in solution

with cytochrome *c* as electron acceptor (Kracher et al. 2015). The linear ranges found here for the detection of Ca^{2+} range up to around 10 mM.

Summarising, each investigated biosensor responds differently to the investigated analytes, a desired departure point for any ET design. This cross-response pattern will be used below to create a BioET with the help of an artificial neural network to resolve mixtures of all three analytes containing varying concentrations of lactose and glucose between 0 and 250 µM and between 0 and 10 mM for Ca^{2+}. The BioET contained the three biosensors modified with *Mt*CDH, *Nc*CDH, or *Ct*CDHC291Y and an auxiliary and a reference electrode. The response of the ET to a set of 27 training samples and 10 test samples containing all three analytes was determined an analysed as input data for building the response model.

3.2 ANN response model

The training method used in the Artificial Neural Network was described in Section 2.4. To define the best architecture 144 different configurations were evaluated (product of the number of neurons in the hidden layer, the tested transfer functions in the hidden layer and the transfer functions in the output layer). The best result was as follows: 9 neurons in the hidden layer with the transform function *"logsig"* and 3 neurons in the output layer with a *"purelin"* as transform function. With this configuration the responses of the 10 test samples with known concentrations of lactose, glucose, and Ca^{2+} were then used to compare their calculated concentrations according to the ANN with their real concentrations. The correlations between predicted (by the ANN) and expected concentrations for all analytes are shown in Fig. 5, in this case for the external test set, the samples not intervening for the training process. Considering that the samples are mixtures of similar and/or interfering compounds and the typology of the sensors used satisfactory R^2 values were calculated especially for lactose (0.975) and Ca^{2+} (0.945). For glucose a rather low R^2 of 0.726 was obtained. Despite the R^2 value for glucose being rather low, the presence of the data related to glucose in the model supports the prediction of the other two targets, lactose and Ca^{2+}. This behaviour could be explained considering that in the array there is only one biosensor to detect glucose, which can lead to a little less accurate detection; moreover for the *Ct*CDH291Y modified electrodes, the enzyme is involved also in the conversion of lactose resulting in that the active site of the enzyme is partly occupied by the preferred substrate, giving a little

lower sensitivity for glucose. To demonstrate how keeping the data related to glucose supported the prediction of lactose and Ca^{2+}, a few tests were run using 2 neurons for the output layer (data not shown), to predict only lactose and Ca^{2+} while keeping the rest of the configuration as it was for the original ANN. This resulted in significantly lower regression values showing that the ANN was less able to make a good prediction for lactose and Ca^{2+} when excluding the glucose related data. Also the prediction was completely random, being different every time the software was run. This behaviour of the ANN led us to the conclusion that even if the glucose concentration predictions were poor, those data were essential for the complete prediction of the three analytes. As an example of the goodness of the prediction model the samples, used as external test to verify the ANN, are grouped in Table 1 showing the expected and predicted concentrations. The deviations between predicted and expected concentrations are on average +6.9% for lactose, +4.8% for Ca^{2+} and +12.3% for glucose, a highly valuable result, derived in this case from the different specificities shown by the different CDH enzymes used.

4. Conclusions

In this work we show the feasibility of a novel BioET system integrating bioinformatics for data treatment and bioelectrochemistry for smart analyte detection. In the present system we utilize the cross response of CDHs from different origins to the substrates lactose and glucose and the interfering compound Ca^{2+} to resolve mixtures of these analytes. The system operates in a DET mode allowing analyte detection at reduced potentials. After data treatment with an artificial neural network the BioET was able to successfully predict the concentrations especially for lactose and Ca^{2+} in artificial samples with an R^2 value of 0.975 and 0.945 respectively and a low deviation from the expected concentration values of +6.9% for lactose and +4.8% for Ca^{2+}. A BioET system like this, using the DET capabilities of CDH from different origins as sensor modifiers is a complete novelty. The great variety of CDHs may allow the system to be tailored to detect also other analytically relevant sugars as e.g. maltose or cellobiose. The findings are of potential interest for new biosensor applications for the food and dairy industry.

Acknowledgment

This research was supported by the Research Executive Agency (REA) of the European Union under Grant Agreement number PITN-GA-2010-264772 (ITN CHEBANA), by the Catalonia Program ICREA Academia 2010, and by The Swedish Research Council (projects 2010-5031 and 2014-5908).

References and Notes

A.Gutés, A.B.I., M. del Valle, F. Céspedes, 2006. Electroanalysis 18, 82-88.

Bagnasco, L., Cosulich, M.E., Speranza, G., Medini, L., Oliveri, P., Lanteri, S., 2014. Food Chemistry 157, 421-428.

Beeson, W.T., Phillips, C.M., Cate, J.H.D., Marletta, M.A., 2011. Journal of the American Chemical Society 134, 890-892.

Berg, J.M., Tymoczko, J.L., Stryer, L., 2002. Biochemistry, Fifth Edition. W.H. Freeman, New York.

Cetó, X., Cespedes, F., del Valle, M., 2013a. Electroanalysis 25, 68-76.

Cetó, X., Cespedes, F., Pividori, M.I., Gutierrez, J.M., del Valle, M., 2012. Analyst 137, 349-356.

Cetó, X., Gutierrez-Capitan, M., Calvo, D., del Valle, M., 2013b. Food Chemistry 141, 2533-2540.

Cipri, A., del Valle, M., 2014. Journal of Nanoscience and Nanotechnology 14, 6692-6698.

Coman, V., Harreither, W., Ludwig, R., Haltrich, D., Gorton, L., 2007. Chemia Analityczna 52, 945-960.

del Valle, M., 2010. Electroanalysis 22, 1539-1555.

Eibinger, M., Ganner, T., Bubner, P., Rošker, S., Kracher, D., Haltrich, D., Ludwig, R., Plank, H., Nidetzky, B., 2014. Journal of Biological Chemistry 289, 35929-35938.

Glithero, N., Clark, C., Gorton, L., Schuhmann, W., Pasco, N., 2013. Analytical and Bioanalytical Chemistry 405, 3791-3799.

Gutes, A., Cespedes, F., Alegret, S., del Valle, M., 2005. Biosensors & Bioelectronics 20, 1668-1673.

Gutierrez, M., Alegret, S., del Valle, M., 2007. Biosensors & Bioelectronics 22, 2171-2178.

Gutierrez, M., Alegret, S., del Valle, M., 2008. Biosensors & Bioelectronics 23, 795-802.

Ha, D., Sun, Q., Su, K., Wan, H., Li, H., Xu, N., Sun, F., Zhuang, L., Hu, N., Wang, P., 2015. Sensors and Actuators B-Chemical 207, 1136-1146.

Haladjian, J., Bianco, P., Nunzi, F., Bruschi, M., 1994. Anal. Chim. Acta 289, 15-20.

Hallberg, B.M., Bergfors, T., Backbro, K., Pettersson, G., Henriksson, G., Divne, C., 2000. Structure 8, 79-88.

Hallberg, M.B., Henriksson, G., Pettersson, G., Divne, C., 2002. J. Mol. Biol. 315, 421-434.

Harreither, W., Coman, V., Ludwig, R., Haltrich, D., Gorton, L., 2007. Electroanalysis 19, 172-180.

Harreither, W., Felice, A.K.G., Paukner, R., Gorton, L., Ludwig, R., Sygmund, C., 2012. Biotechnology Journal 7, 1359-1366.

Harreither, W., Sygmund, C., Augustin, M., Narciso, M., Rabinovich, M.L., Gorton, L., Haltrich, D., Ludwig, R., 2011. Applied and Environmental Microbiology 77, 1804-1815.

Henriksson, G., Johansson, G., Pettersson, G., 2000. J. Biotechnol. 78, 93-113.

Henriksson, G., Sild, V., Szabo, I.J., Pettersson, G., Johansson, G., 1998. Biochim. Biophys. Acta 1383, 48-54.

Igarashi, K., Momohara, I., Nishino, T., Samejima, M., 2002. Biochem. J. 365, 521-526.

Jones, G.D., Wilson, M.T., 1988. Biochem. J. 256, 713-718.

Katz, E., Willner, I., 2004. Chemphyschem : a European journal of chemical physics and physical chemistry 5, 1084-1104.

Kielb, P., Sezer, M., Katz, S., Lopez, F., Schulz, C., Gorton, L., Ludwig, R., Wollenberger, U., Zebger, I., Weidinger, I.M., 2015. Chemphyschem 16, 1960-1968.

Kovacs, G., Ortiz, R., Coman, V., Harreither, W., Popescu, I.C., Ludwig, R., Gorton, L., 2012. Bioelectrochemistry 88, 84-91.

Kracher, D., Zahma, K., Schulz, C., Sygmund, C., Gorton, L., Ludwig, R., 2015. Febs Journal, in press; DOI: 10.1111/febs.13310.

Langston, J.A., Shaghasi, T., Abbate, E., Xu, F., Vlasenko, E., Sweeney, M.D., 2011. Applied and Environmental Microbiology 77, 7007-7015.

Larsson, T., Lindgren, A., Ruzgas, T., Lindquist, S.E., Gorton, L., 2000. J. Electroanal. Chem. 482, 1-10.

Laviron, E., 1979. Journal of Electroanalytical Chemistry 101, 19-28.

Leech, D., Kavanagh, P., Schuhmann, W., 2012. Electrochimica Acta 84, 223-234.

Ludwig, R., Harreither, W., Tasca, F., Gorton, L., 2010. Chemphyschem 11, 2674-2697.

Ludwig, R., Ortiz, R., Schulz, C., Harreither, W., Sygmund, C., Gorton, L., 2013a. Anal Bioanal Chem 405, 3637-3658.

Ludwig, R., Sygmund, C., Harreither, W., Kittl, R., Felice, A., 2013b. Mutated cellobiose dehydrogenase with increased substrate specificity. Google Patents.

Lvova, L., Martinelli, E., Dini, F., Bergamini, A., Paolesse, R., Di Natale, C., D'Amico, A., 2009. Talanta 77, 1097-1104.
Meredith, M.T., Minteer, S.D., 2012. Annual Review of Analytical Chemistry, Vol 5 5, 157-179.
Nunez, L., Ceto, X., Pividori, M.I., Zanoni, M.V.B., del Valle, M., 2013. Microchemical Journal 110, 273-279.
Ocaña, C., Arcay, E., del Valle, M., 2014. Sensors and Actuators B: Chemical 191, 860-865.
Osman, M.H., Shah, A.A., Walsh, F.C., 2011. Biosensors & Bioelectronics 26, 3087-3102.
Pacios, M., del Valle, M., Bartroli, J., Esplandiu, M.J., 2009. Journal of Nanoscience and Nanotechnology 9, 6132-6138.
Peris, M., Escuder-Gilabert, L., 2013. Analytica Chimica Acta 804, 29-36.
Phillips, C.M., Beeson, W.T., Cate, J.H., Marletta, M.A., 2011. Acs Chemical Biology 6, 1399-1406.
Rabaey, K., Rozendal, R.A., 2010. Nature Reviews Microbiology 8, 706-716.
Raud, M., Kikas, T., 2013. Water Research 47, 2555-2562.
Safina, G., Ludwig, R., Gorton, L., 2010. Electrochimica Acta 55, 7690-7695.
Sapelnikova, S., Dock, E., Solna, R., Skladal, P., Ruzgas, T., Emnéus, J., 2003. Analytical and Bioanalytical Chemistry 376, 1098-1103.
Schulz, C., Ludwig, R., Micheelsen, P.O., Silow, M., Toscano, M.D., Gorton, L., 2012. Electrochemistry Communications 17, 71-74.
Solna, R., Dock, E., Christenson, A., Winther-Nielsen, M., Carlsson, C., Emnéus, J., Ruzgas, T., Skladal, P., 2005. Analytica Chimica Acta 528, 9-19.
Stoica, L., Ludwig, R., Haltrich, D., Gorton, L., 2006. Analytical Chemistry 78, 393-398.
Sygmund, C., Kracher, D., Scheiblbrandner, S., Zahma, K., Felice, A.K., Harreither, W., Kittl, R., Ludwig, R., 2012. Applied and Environmental Microbiology 78, 6161-6171.
Tønning, E., Sapelnikova, S., Christensen, J., Carlsson, C., Winther-Nielsen, M., Dock, E., Solna, R., Skladal, P., Nørgaard, L., Ruzgas, T., Emnéus, J., 2005. Biosensors & Bioelectronics 21, 608-617.
Valdes-Ramirez, G., Gutierrez, M., del Valle, M., Ramirez-Silva, M.T., Fournier, D., Marty, J.L., 2009. Biosensors & Bioelectronics 24, 1103-1108.
Walstra, P., Wouters, J.T., Geurts, T.J., 2014. Dairy science and technology. CRC press, Boca Raton (FL).
Wang, J., 2008. Chemical Reviews 108, 814-825.
Wilson, D., Alegret, S., del Valle, M., 2015. Electroanalysis 27, 336-342.
Yakovleva, M., Buzas, O., Matsumura, H., Samejima, M., Igarashi, K., Larsson, P.-O., Gorton, L., Danielsson, B., 2012. Biosensors and Bioelectronics 31, 251-256.
Zamocky, M., Ludwig, R., Peterbauer, C., Hallberg, B.M., Divne, C., Nicholls, P., Haltrich, D., 2006. Current Protein & Peptide Science 7, 255-280.
Zamocky, M., Schumann, C., Sygmund, C., O'Callaghan, J., Dobson, A.D.W., Ludwig, R., Haltrich, D., Peterbauer, C.K., 2008. Protein Expression and Purification 59, 258-265.

Table 1. Comparison of expected and predicted concentrations of the external test samples for the three analytes.

Lactose (µM)		**Glucose (µM)**		**Ca^{2+} (mM)**	
Expected	*Predicted*	*Expected*	*Predicted*	*Expected*	*Predicted*
2.03E+02	2.25E+02	9.69E+01	6.57E+01	3.83E+03	4.85E+03
5.81E+01	7.40E+01	1.12E+02	1.81E+02	1.89E+03	1.53E+03
2.14E+02	2.25E+02	2.43E+02	2.53E+02	7.24E+03	8.11E+03
1.13E+02	1.05E+02	5.97E+01	4.01E+01	7.93E+03	8.98E+03
5.86E+01	6.49E+01	8.75E+01	1.43E+02	4.14E+03	5.73E+03
4.14E+01	6.22E+01	9.82E+01	1.54E+02	2.67E+03	3.72E+03
4.00E+01	7.00E+01	1.95E+02	2.90E+02	4.70E+02	1.18E+03
1.87E+02	2.22E+02	6.47E+01	2.35E+01	9.42E+03	9.68E+03
2.19E+02	2.33E+02	1.88E+02	1.76E+02	6.01E+03	5.41E+03

Figures and captions

Fig. 1. Distribution of the training (blue) and test (red) concentrations of lactose, glucose, and Ca^{2+} used to train and test the Artificial Neural Network (ANN).

Fig. 2. Scheme of the ANN architecture used. The numbers surrounded by the red circles are the numbers of neurons used in each layer.

Fig. 3. Cyclic voltammetric characterisation of the enzyme modified electrodes used for the construction of the electronic tongue. CDH was entrapped under a dialysis membrane on mercaptohexanol modified gold electrodes. From top to bottom it is possible to see the behaviour of *Mt*CDH, *Ct*CDHC291Y and *Nc*CDH in a 50 mM MOPS buffer solution at pH 6.7 in the absence (solid line) and in the presence of 250 µM lactose (dashed line). All experiments were performed at a scan rate of 20 mV/s with a SCE reference electrode and a Pt flag as counter electrode.

Fig. 4. Calibration graphs of the *Mt*CDH, *Ct*CDHC291Y and *Nc*CDH based biosensors obtained for the three analytes lactose (top), glucose (middle) and Ca^{2+} (bottom). In the left column the fully investigated concentration ranges are shown, in the right column only the linear concentration ranges are shown.

Fig. 5. Comparison graphics of the "expected vs. predicted" concentrations for the target analytes; lactose, glucose, and Ca^{2+} calculated by the ANN using the external test set samples with known, expected concentrations.

Fig. S1. 3D representation of the sensor configuration used in the electronic tongue system (ET). On the left a side view, on the right a top view.

Fig. 1

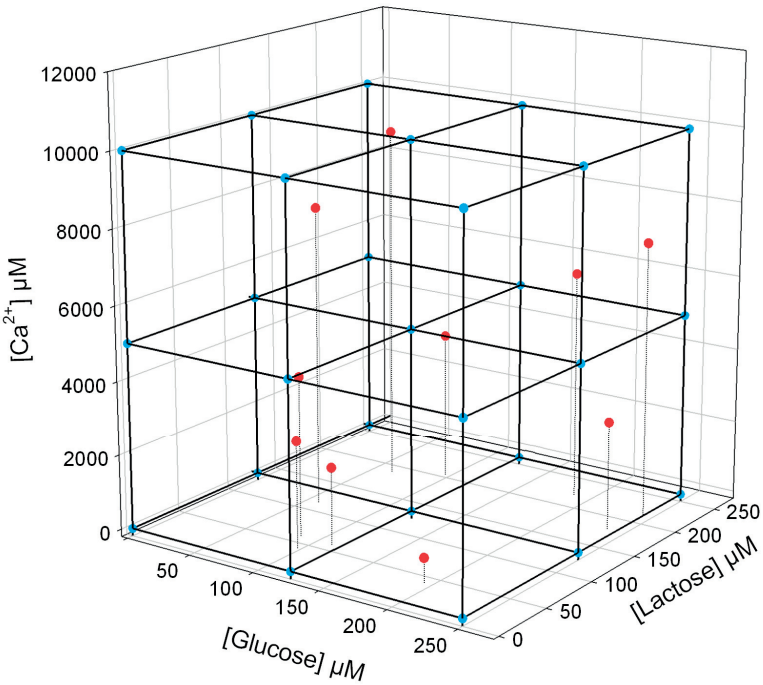
12000
10000
8000
6000
4000
2000
0
[Ca2+] µM
50
100
150
200
250
[Glucose] µM
0
50
100
150
200
250
[Lactose] µM

Fig. 2

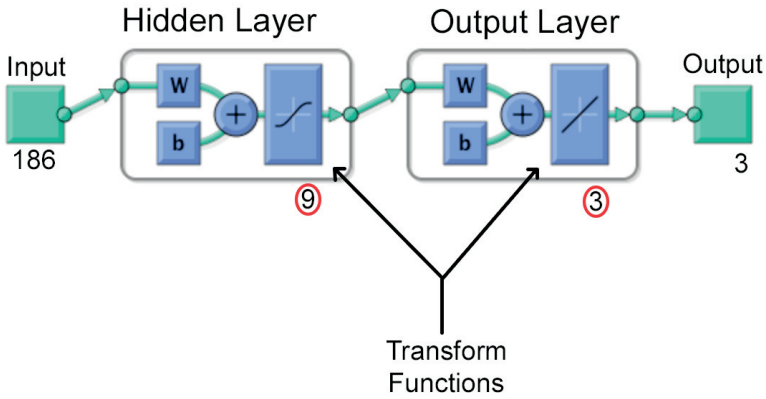
Hidden Layer
Output Layer
Input
186
W
b
W
b
Output
3
9
3
Transform
Functions

Fig. 3

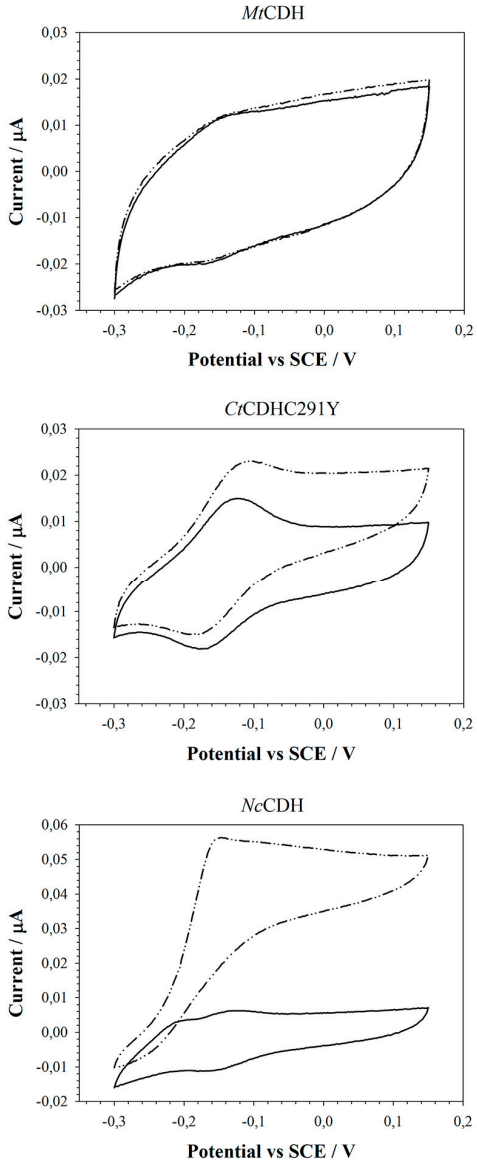
*Mt*CDH
Current / µA
0,03
0,02
0,01
0,00
-0,01
-0,02
-0,03
-0,3
-0,2
-0,1
0,0
0,1
0,2
Potential vs SCE / V
*Ct*CDHC291Y
Current / µA
0,03
0,02
0,01
0,00
-0,01
-0,02
-0,03
-0,3
-0,2
-0,1
0,0
0,1
0,2
Potential vs SCE / V
*Nc*CDH
Current / µA
0,06
0,05
0,04
0,03
0,02
0,01
0,00
-0,01
-0,02
-0,3
-0,2
-0,1
0,0
0,1
0,2
Potential vs SCE / V

Fig. 4

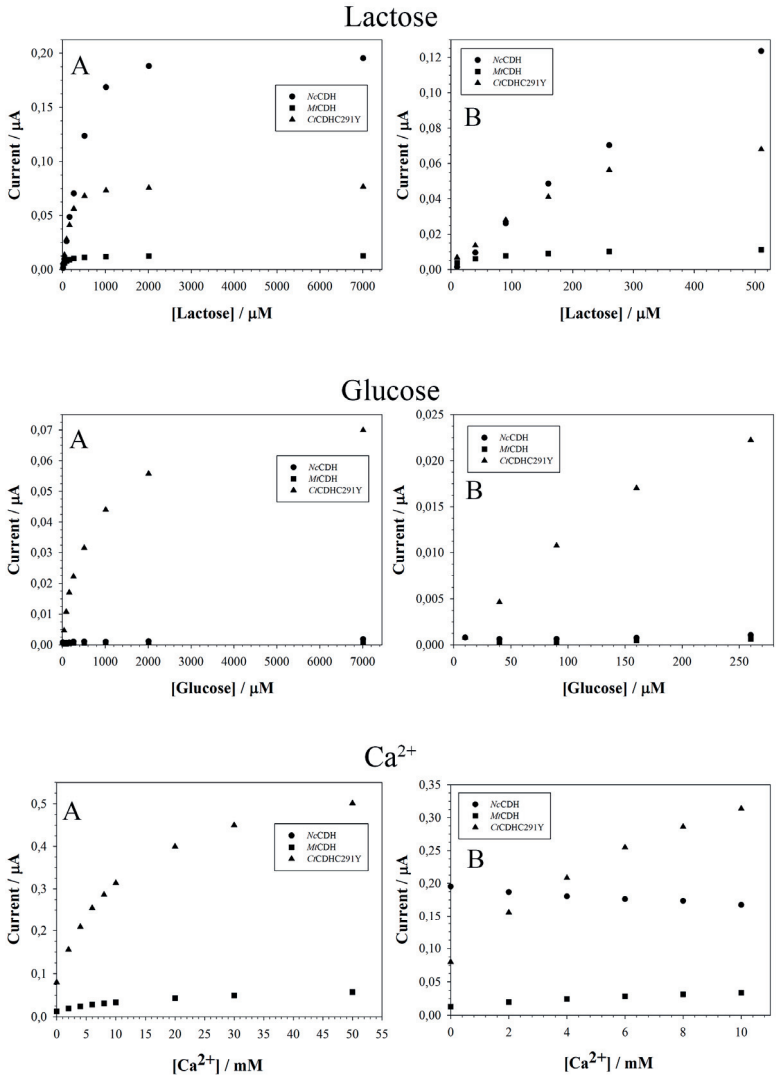
Lactose
A
B
NcCDH
MfCDH
CfCDHC291Y
Current / µA
[Lactose] / µM
Glucose
[Glucose] / µM
Ca2+
[Ca2+] / mM

Fig. 5

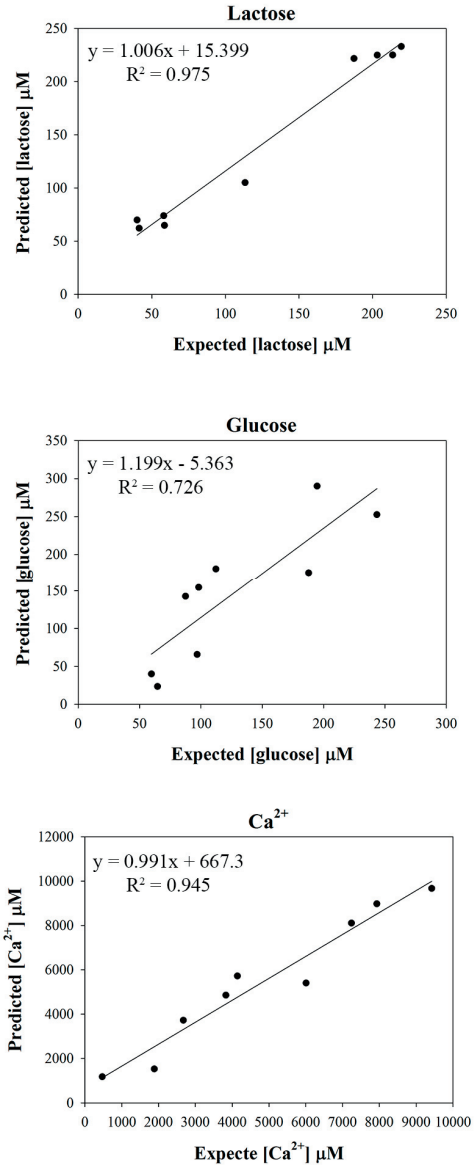
Lactose
y = 1.006x + 15.399
R² = 0.975
Predicted [lactose] µM
Expected [lactose] µM
0
50
100
150
200
250
Glucose
y = 1.199x - 5.363
R² = 0.726
Predicted [glucose] µM
Expected [glucose] µM
0
50
100
150
200
250
300
350
Ca2+
y = 0.991x + 667.3
R² = 0.945
Predicted [Ca2+] µM
Expecte [Ca2+] µM
0
2000
4000
6000
8000
10000
12000
1000
3000
5000
7000
9000

Fig. S1